SRI International

SRI Project P22157

Federal Agency: U.S. Department of Energy
National Energy Technology Center
3600 Collins Ferry Road
Morgantown, WV 26505

Cooperative Agreement No. DE-FE0012959

Title: Development of Mixed-Salt Technology for CO_2 Capture from Coal Power Plants

FINAL REPORT

Principal Investigator:
Dr. Indira S. Jayaweera
Sr. Staff Scientist and CO_2 Program Leader
Materials Research Laboratory
SRI International
333 Ravenswood Avenue
Menlo Park, CA 94025-3493
Telephone: (650) 859-4042
Fax: (650) 859-2111
Email: indira.jayaweera@sri.com

Submission Date: May 22, 2018

DUNS Number: 009232752

Project Period: 10/01/2014–04/28/2018

Reporting Period End Date: April 28, 2018

Report Term or Frequency: One Final Report

Submitted by: Indira Jayaweera

Indira Jayaweera

SRI International

May 22, 2018

DEVELOPMENT OF MIXED-SALT TECHNOLOGY FOR CO_2 CAPTURE FROM COAL POWER PLANTS

Final Report

Covering the period October 1, 2013 through February 28, 2018

SRI Project P22157

Cooperative Agreement No. DE-FE0012959

Contributors:	Dr. Indira Jayaweera (PI), Dr. Palitha Jayaweera (SRI); Dr. Kaj Thomsen (ASApS), Dr. G. Valenti (PoliMi) & Dr. D. Bonalumi; Dr. Prodip Kundu (OLI Systems), Dr. A. Anderko (OLI Systems); and Mr. C. Kang (Stanford University)
Prime Contractor:	SRI International 333 Ravenswood Avenue Menlo Park, CA 94025
Subcontractors:	Stanford University; OLI Systems; Polytecnico De Milano (PoliMi); and Aqueous Systems Aps (ASApS);
Prepared for:	U.S. Department of Energy National Energy Technology Center 3600 Collins Ferry Road Morgantown, WV 26505
DOE Project Manager:	Mr. Steven Mascaro

Technical Point of Contact:

Dr. Indira Jayaweera
Senior Staff Scientist
Materials Research Laboratory
SRI International
333 Ravenswood Avenue
Menlo Park, CA 94025
Tel: (650) 859-4042
Fax: (650) 859-2111
Email: indira.jayaweera@sri.com

Administrative Point of Contact:

Ms. V. Rene Harmount
Sr. Contracts Officer
SRI International
333 Ravenswood Avenue
Menlo Park, CA 94025
Tel: (650) 859-4284
Fax: (650) 859-6009
Email: rene.harmount@sri.com

DISCLAIMER

This report was prepared as an account of work sponsored by an agency of the United States Government. Neither the United States Government nor any agency thereof, nor any of their employees, makes any warranty, express or implied, or assumes any legal liability or responsibility for the accuracy, completeness, or usefulness of any information, apparatus, product, or process disclosed, or represents that its use would not infringe privately owned rights. Reference herein to any specific commercial product, process, or service by trade name, trademark, manufacturer, or otherwise does not necessarily constitute or imply endorsement, recommendation, or favoring by the United States Government or any agency thereof. The views and opinions of authors expressed herein do not necessarily state or reflect those of the United States Government or any agency thereof.

CONTENTS

LIST OF TABLES

LIST OF ILLUSTRATIONS

1. EXECUTIVE SUMMARY

SRI International (SRI), in collaboration with Stanford University, OLI Systems (OLI), Politecnico de Milano (PoliMi), and Aqueous Systems Aps (ASApS) performed a 45-month effort to develop a promising Mixed-Salt Process (MSP) for carbon dioxide capture. The MSP combines existing ammonia and potassium-carbonate technologies with improved absorption steps for rate enhancement and ammonia emission reduction and a novel selective regeneration process with a high-pressure CO_2 product to introduce a new and advanced transformational solvent-based technology. The striking advantages of the SRI MSP include: low heat of reaction, high loading of CO_2, high-pressure regeneration of > 99% pure dry CO_2, low sensitivity to impurities, low process cost, use of a non-degradable low-cost solvent with a very low carbon footprint for its production, low emissions, and reduced water use compared to the state-of-the-art ammonia-based and amine technologies.

The overall objective of the project was to develop and test a *solvent-based* CO_2 capture technology that can capture CO_2 from existing or new pulverized coal (PC) power plants at low cost. Our specific goal was to test SRI's newly developed MSP at the large bench-scale level to demonstrate that the process could capture CO_2 at high efficiency (> 90%) with very high CO_2 loading (> 10 wt.%), require less than 2 GJ/tonne for solvent regeneration, and produce a CO_2 stream at high pressure with a purity > 95 vol.%. This 45-month MSP development program was designed to conduct (1) extensive test campaigns with different process flowsheet variants, and (2) detailed thermodynamic, kinetic, and process modeling. These tests and models were very important to identify any issues associated with the process in the early stages and then resolve them before moving into the next scale-up (> 1 MWe scale) testing. The technology development plan consisted of balanced experimental and process modeling activities as shown in Figure i. Such an approach reduces the risks associated with the process operability at large scales and provides capital and operating expenditure (CAPEX/OPEX) predictions with improved accuracies. Under the MSP development program at SRI, we performed an aggressive testing campaign with individual subsystems as well as integrated CO_2 capture and regeneration system to identify the best operating conditions. The project was carried out in two budget periods (BP1 & BP2), and the research activities were performed under nine tasks.

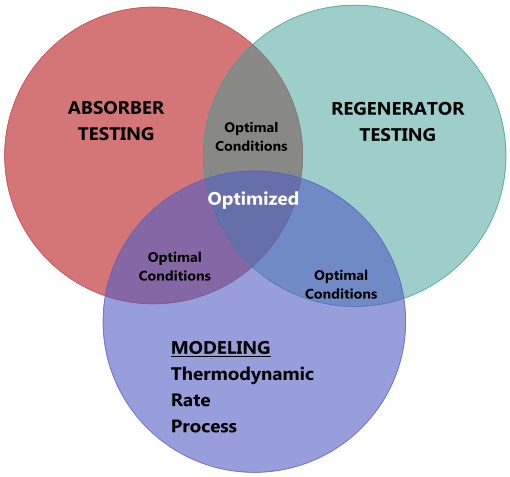

Figure i. Mixed-Salt Process optimization with experimental and modeling approach.

1.1 Objectives and Goals for Budget Period 1 (BP1)

The specific objective of BP1 was to demonstrate the absorber and regenerator operation as individual units with high efficiency, low NH_3 emissions, and reduced water use compared to the state-of-the-art ammonia-based technologies. The absorber was operated near ambient temperature, and the regenerator was operated up to 160°C. We demonstrated the stated program goals, and a summary of the work carried out in BP1 is given below.

1.2 Summary of the Work Completed in BP1

Work scope: The work completed in BP1 included individual absorber and regenerator testing in a semi-continuous mode (Task 2), preliminary process modeling, technoeconomic analysis (Task 3), and preparation of continuation application for BP2 based on the findings in BP1 (Task 4). Task 2 work included (1) design, procurement, and installation of the absorber system; (2) testing of the performance of the absorber; (3) modification of an existing high-pressure reactor system to operate and test conditions relevant to the mixed-salt regeneration process; and (4) use this modified system as a small, semi-continuous regenerator (25 scfm) to obtain data required for designing the larger regenerator (REG-BP2) that matches the absorber system (100-250 scfm). Process modeling in Task 3 included (1) development of extended UNIQAC thermodynamic model for the K_2CO_3-NH_3-H_2O-CO_2 system (ASApS); (2) development of the preliminary process layout for flue gas cleaning in the absorber-regenerator and compression units (SRI and PoliMi); (3) baseline calibration of the PoliMi's in-house power cycle modeling program to match the simulations executed by DOE-NETL (see note below) for DOE Cases 11 and 12 (PoliMi); (4) establishment of rate-based model using SRI kinetic data from small bench-scale testing (OLI Systems); (5) assessment of optional process stream extraction for the mixed-salt carbon capture unit for the retrofit application; and (6) preparation of a preliminary techno-economic analysis (TEA).

Results from absorber testing: The absorber system was designed to test many options such as the relationship between CO_2 capture efficiency and the gas flow rate, liquid-to-gas (L/G) ratio, packing type, salt composition, operating temperature, and ammonia emissions. In BP1, the absorber system was tested with gas compositions that contain 15% CO_2, and flow rates up to 25 scfm (standard cubic feet per minute). The absorber system has two absorber columns (8-in diameter) that are designed to operate independently with different absorption solutions, and the gas stream passes through them in series. Temperature, flow rate, gas composition, and pressure are monitored at various points in the system, providing the operator a convenient visual indication of all sensor readings. In this system, solution composition, solution flows, flow routing, and other operating conditions can be easily changed to perform a full range of experiments and obtain data necessary for optimization and scale up. Figure ii shows a photograph of the complete mixed-salt absorber system, instrumentation rack, and the control station.

Note: *The DOE guidelines for modeling are given in two reports, "Cost and Performance Baseline for Fossil Energy Plants – Volume 1: Bituminous Coal and Natural Gas to Electricity" (refer to Case 11 and Case 12), and "Quality Guidelines for Energy System Studies," which contain the numerical models of two pulverized-coal steam supercritical power plants, one without and one with carbon dioxide capture. These guidelines are included in the Project Management Plan (PMP).*

Figure ii. Photograph of the installed 8-in mixed-salt absorber system (*left*) and close-up view of the two absorber columns (*right*).

Four test series were conducted with the absorbers:

- Test series 1: Runs 1-3 (system response with varying conditions such as different gas feed rates compositions, liquid recycle rates, cooling water flow rates, etc.)
- Test series 2: Runs 4-10 (testing 20 wt.% mixed salt with 15 vol.% CO_2)
- Test series 3: Runs 11-18 (testing 20 wt.% mixed salt with 5-15 vol.% CO_2)
- Test series 4: Run 19 (high CO_2 loading with 20 wt.% mixed-salt)

In the MSP testing, the dual-absorber system was used as shown in Figure ii with a high ammonia/potassium ratio solution in the first absorber, and low ammonia/potassium ratio solution in the second absorber. The tests conducted clearly indicated this operation can be easily performed and the ammonia vapor pressure in the scrubbed flue gas can be greatly reduced by such flow arrangement. Figure iii shows the observed ammonia vapor pressure of the absorber 1 and absorber 2 exit gas streams. When a combination of high ammonium/ potassium and low ammonia/potassium ratio solutions were used in the tandem absorber system, ammonia loss from the absorbent solution was drastically reduced compared with a single solution approach.

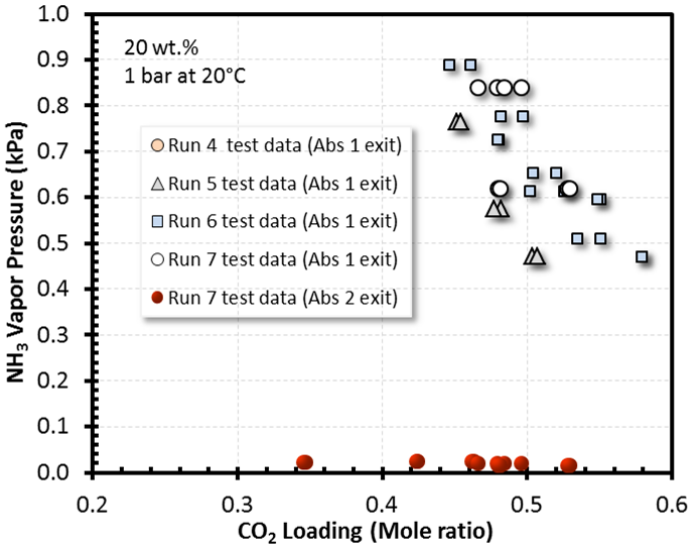

Figure iii. Measured ammonia vapor pressure at various CO_2 loadings for tests conducted with a single absorber (Runs 4, 5, and 6) and for the test conducted with the dual absorber (Run 7).

The data from the mixed-salt systems testing also demonstrated that it was possible to reach > 90% CO_2 capture even using a solution that has fairly high CO_2 loadings (e.g., CO_2 loadings in the 0.4 to 0.6 range) as predicted by the preliminary modeling. Figure iv shows the absorption efficiency data from a test conducted with mixed-salt solutions having CO_2 loading in the range 0.42 (at the start) to 0.57 (at 60 min). The data from these tests were used to determine the conditions for steady-state operation in BP2 with the integrated system. As an example, a 90% CO_2 capture efficiency can be achieved at CO_2 loadings > 0.45 with absorber 1 and absorber 2 operating at 80 and 60% efficiency, respectively.

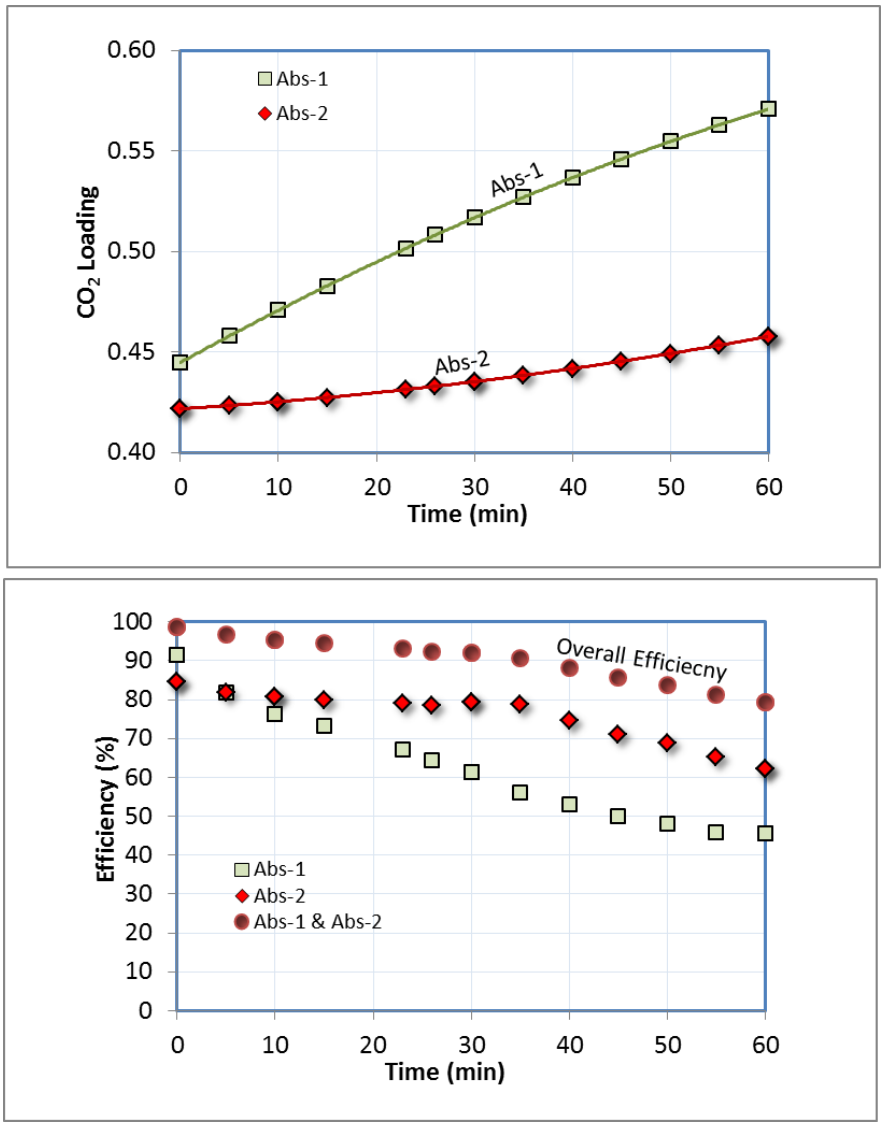

Figure iv. Measured CO_2 capture efficiency in absorber 1 and 2 at varying CO_2 loadings.

The observed efficiency data (similar to above) were used to calculate the specific gas transfer coefficient, K_g (mol s^{-1} m^{-3} Pa) for CO_2 absorption with 20 wt.% mixed-salt solutions. Figure v shows the measured gas transfer coefficient (for Runs 4 through 10). The observed overall rates for CO_2 absorption are in the same order of magnitude as monoethanalomine (MEA)-based systems and about a factor of 5-7 higher than that with chilled ammonia systems. Runs 4 and 5 were conducted at an optimal gas/liquid recycle flow rate for the column to study the temperature effect, and the observed data shows the rate of CO_2 absorption into the MSP can be enhanced by operating the absorber at room temperature (RT) or slightly above the ambient.

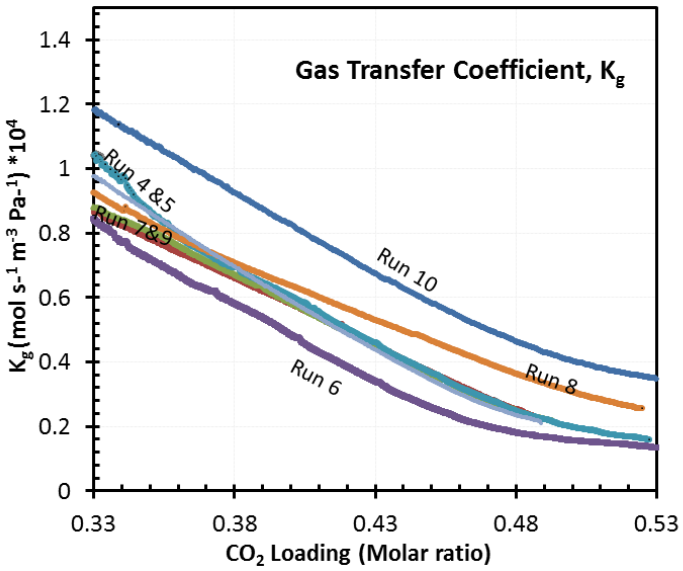

Figure v. Gas-transfer coefficient calculated from test data for varying test conditions. Gas flow rates were 8-17 cfm with a constant L/G ratio.

Results from small-scale regenerator testing. We performed parametric testing of the regenerator to identify the operational issues that can be implemented in the continuous flow regenerator with two stages. Regenerator tests were performed with 20 and 30 wt.% mixed-salt compositions in a semi-continuous mode. Figure vi shows the regenerator data for the rich solution from the absorber test series 1.We estimated the heat requirement for stripping volatile species by using the data shown in Figure vi to be 45± 5 kJ/mol. The method used was similar to the isosteric heat of adsorption of CO_2 estimated from the experimental adsorption isotherms using the Clausius-Clapeyron equation. However, application of the Clausius-Clapeyron equation for calculating enthalpy is only valid for the evaporation of ideal gases from non-reactive systems and has its limitations for reactive systems. Nevertheless, these estimated numbers are the upper limit of the heat enthalpy for volatilization of gaseous. Our team member, Dr. Kaj Thomsen, also calculated the heat of absorption of CO_2 in the mixture using the "bubble-template" in the extended UNIQUAC model and found that results agree well with the experimental observations.

One of the key requirements of the MSP regenerator is the ability to generate two lean streams with high ammonia/potassium and low ammonia/potassium ratios. To generate the low ammonia/potassium stream, ammonia has to be stripped off from a portion of the lean solution from the regenerator. Figure vii shows the number of moles of ammonia stripped from a 38-wt.% mixed-salt solution (0.6 CO_2 loading) at 5, 10, and 20 bar. This data shows that almost all the ammonia can be stripped at 5 bar at 150 °C. Based on these results, a design point for the bottom regenerator for a specific ammonia-stripping value can be selected for a given absorber operating condition.

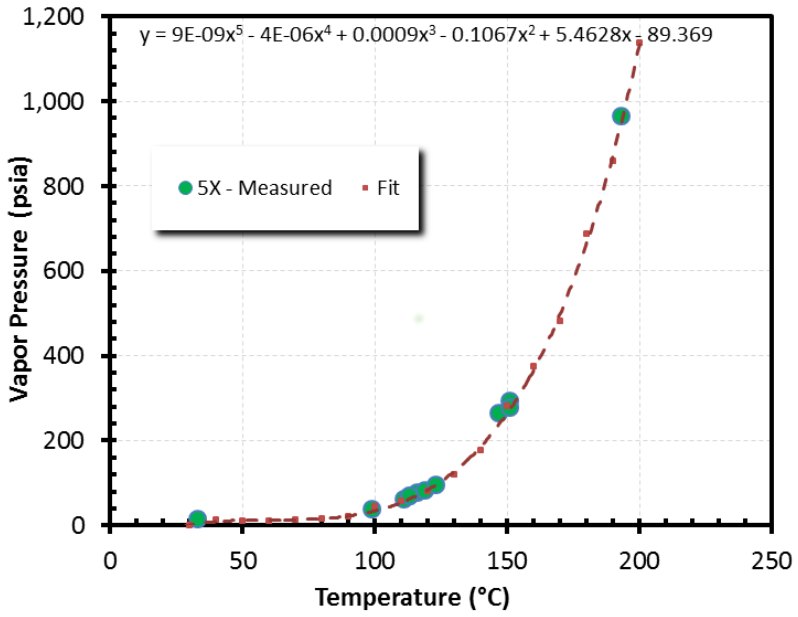

Figure vi. Vapor pressure with temperature curve for rich solution from absorber test series (composition 5X).

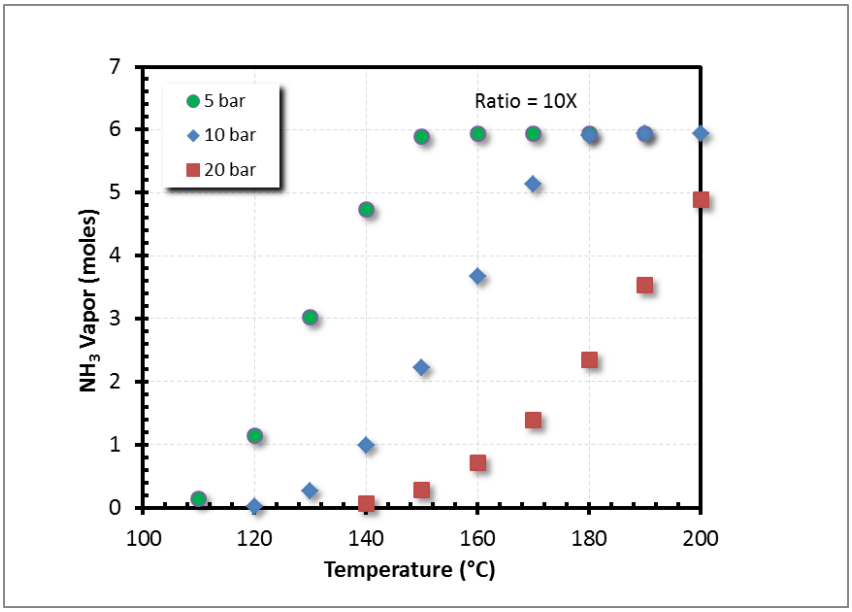

Figure vii. The NH_3 stripping potentials at various pressures and temperatures are shown for the 38-wt.% mixed-salt solution with a 0.6 loading.

The MSP regenerator system was designed to reduce water stripping. First, the operation of the regenerator at a higher pressure reduces the water stripping from the solution. In addition, a temperature gradient along the height of the column was maintained to further reduce the water vapor pressure at the regenerator exit, thus making the water stripping energy penalty negligible. This design also reduced the ammonia vapor pressure in the exiting gas. We used a split flow

inlet feed arrangement to maintain the lower temperature at the top of the regenerator. We performed number of parametric tests with variations of the split flow ratio, regeneration temperature, and pressure. Figure viii shows the number of moles of CO_2 stripped in a series of runs in the pressure ranges of 6-7 and 11-12 bar in the temperature range of 120 to 160 °C for 20-wt% mixed salt solutions. As expected, CO_2 stripping increased with increasing temperature and decreasing pressure. In these test we also observed that lean loading of 0.2 can be obtained in the MSP regenerator. These tests helped us to collect information for the design of the regenerator in BP2, and also to gain experience for operating the integrated system in BP2. Most importantly, we did not see any process issues that would arise in the scale-up process.

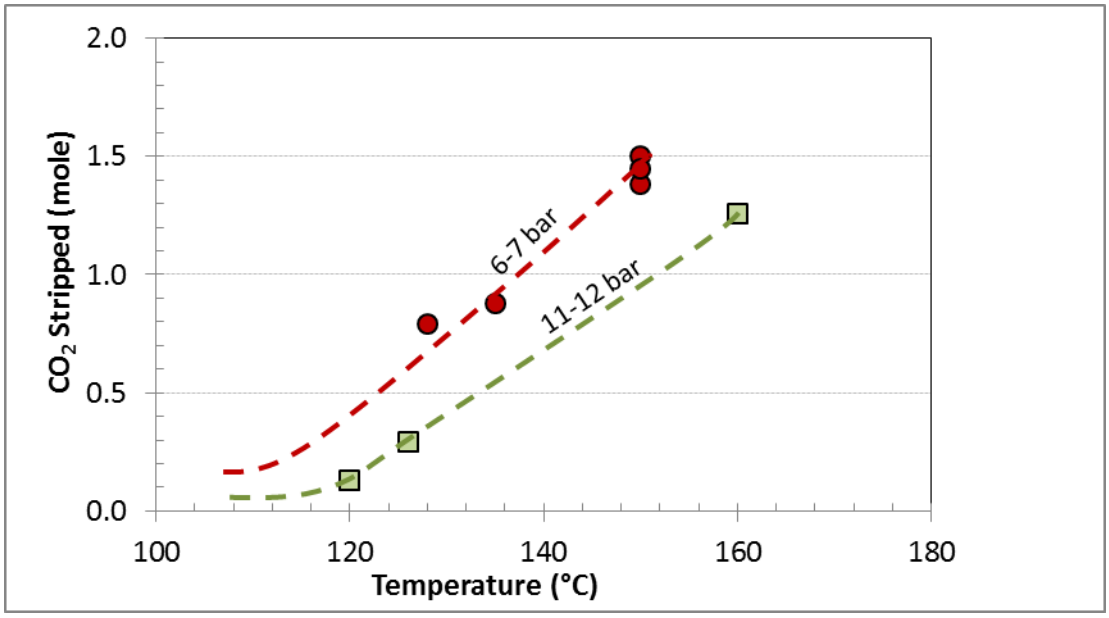

Figure viii. CO_2 stripping as a function of regenerator temperature and pressure.

Results from the preliminary process modeling. Since there were some disagreements in the data obtained from e-NRTL model that was built in ASPEN® for ammonia-based systems at high temperature and pressure, we selected two experts in thermodynamic modeling of electrolytes at very high electrolyte concentrations to perform the modeling work (Dr. Kaj Thomsen, ASApS, and Dr. Prodip Kundu and Dr. Andre Anderko, OLI Systems). ASApS compiled the latest experimental data available from the literature for the CO_2-K_2CO_3-H_2O system, and this was combined with the existing data bases of CO_2-K_2CO_3-H_2O and NH_3-CO_2-H_2O systems to generate an input file in a readable form of ASPEN® Plus. PoliMi and ASApS successfully integrated the extended UNIQAC model developed by ASApS in ASPEN® and conducted the evaluation of mass and heat balance for the preliminary process layout to simulate the mixed-salt system in their power plant model. The numerical models were prepared and executed with the PoliMi in-house code named GS, which has been developed to simulate power

cycles and energy systems. The majority of the assumptions defined by DOE-NETL were transferred as is into the GS models. The results showed no more than about 2% difference between DOE-NETL and PoliMi simulated flow rates and temperatures of relevant streams of the power cycle, both with and without CO_2 capture. Moreover, the compositions of the gaseous streams entering and leaving the flue gas desulfurization (FGD) unit were closely matched. Finally, power balances and other plant performance values were also very accurately replicated. The developed models were adapted to be used in the next stages of the project to assess the integration of the mixed-salt technology with the power generation.

1.3 Objectives and Goals for Budget Period 2 (BP2)

The specific objective of BP2 was to demonstrate the continuous, integrated absorber-regenerator operation with high efficiency, perform process modeling, and complete the techno-economic analysis. In the BP2 program, additional flowsheet variants were included to further reduce ammonia emission and water use. We demonstrated the stated program goals, and a summary of the work carried out in BP2 is given below.

1.4 Summary of Work Completed in BP2

Work scope: The work completed in BP2 included testing of the bench-scale integrated system testing (Task 5), process modeling, completion of the TEA, an environmental health and safety (EH&S) risk assessment (Task 6), integrated testing with the variant 1 flowsheet (Task 7) and variant 2 flowsheet (Task 8), high-capacity runs and modeling (Task 9), and regenerator steam measurements (Task 10). Sub-tasks in Task 5 included designing, building, and installing the large bench-scale regenerator, which is matched with the absorber system, software development for the regenerator control and data acquisition, and parametric testing of the integrated system. Task 6 included rate-based model development and validation and incorporating the latest data in the process model. Tasks 7 and 8 included modifications to the flowsheet arrangement of the MSP process to achieve lower ammonia emission and water use. The major results of these tasks are summarized below.

Results from integrated testing: As part of the integrated system testing task, we designed the regenerator and the process integration layout with the absorber system. Figure ix shows the simplified process flow diagram of the integrated Mixed-Salt process. Figure x is a photograph of the large bench-scale regenerator showing solution inlets, outlets, and heat exchangers. The rich liquid flow from absorber 1 (rich liquid 1) was split and pumped into the column at two stages with ~ 20% going to an upper stage. The rich solution from absorber 2 (rich liquid 2), was cooled to ~ 15°C and pumped to the top stage of the regenerator column to reduce the ammonia emission from the regenerator. As a polishing step, the high-pressure water wash was mounted at the very top of the regenerator such that the emitted CO_2 gas has less than 10 ppm ammonia content. The lean stream with high ammonia/potassium ratio for absorber 1 was drawn from a lower middle stage of the regenerator column, which was at ~ 130°C. The lean solution with low

ammonia/potassium ratio for absorber 2 was drawn from the bottom stage of the regenerator column, and the temperature of this stage was about 160 °C. The regenerator was operated under isobaric conditions with a temperature gradient, ~ 30-50 °C at the top and 155-160 °C at the bottom. Two main heat exchangers recovered the sensible heat from the regenerated solution to heat the incoming rich solution. The outgoing lean streams from heat exchangers were ~ 40 °C, and thus they needed to be cooled to about 15-20 °C before they were fed to the absorber columns. For the continuous operation of the regenerator, the input rich-solution flows and exit lean-solution flows were balanced, and the liquid levels of draw stages were carefully controlled to avoid flooding or dry-up of regenerator stages.

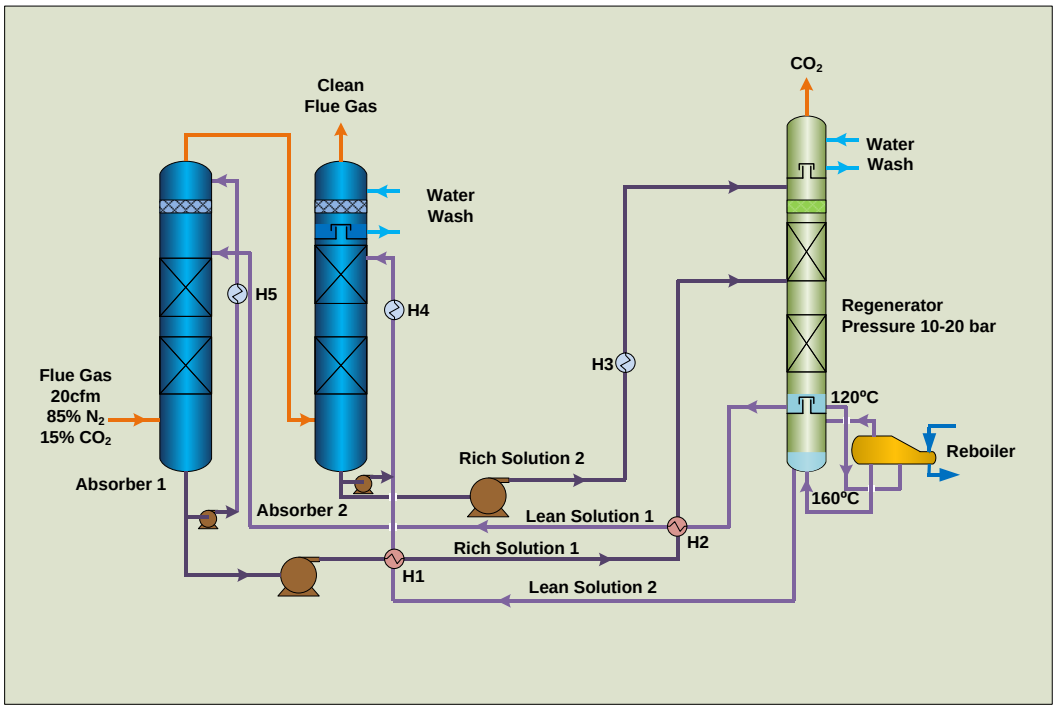

Figure ix. Schematic of the integrated system for testing the mixed-salt process in BP2 as built.

Figure xi shows representative test results from a run displaying the regenerated CO_2 flow output with time for a total of 300 slpm simulated flue gas (15% CO_2) stream in the absorber. We demonstrated the operation of integrated CO_2 capture and regeneration system with the MSP in this test. Figure xii shows the average total feed gas flow rate, CO_2 feed gas flow rate, and the generated CO_2 gas flow rates over the course of a 60-hour test campaign. The integrated system performed as designed with excellent absorption and regeneration cycles. The system controls autonomously maintained the flow rate balance in and out of the regenerator, and most of the other system controls were also automated so that the integrated system could be operated by one person.

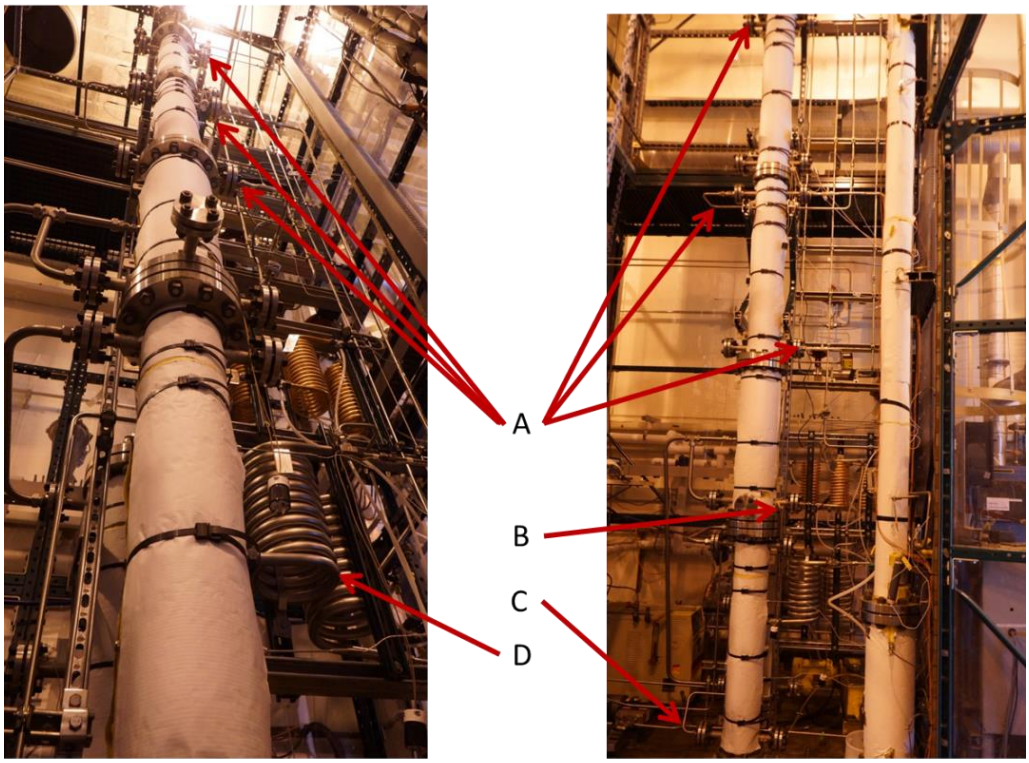

Figure x. A photograph of the completed regenerator column. The picture to the right shows both the two-stage regenerator and the single-stage regenerator built in BP2 and BP1, respectively.

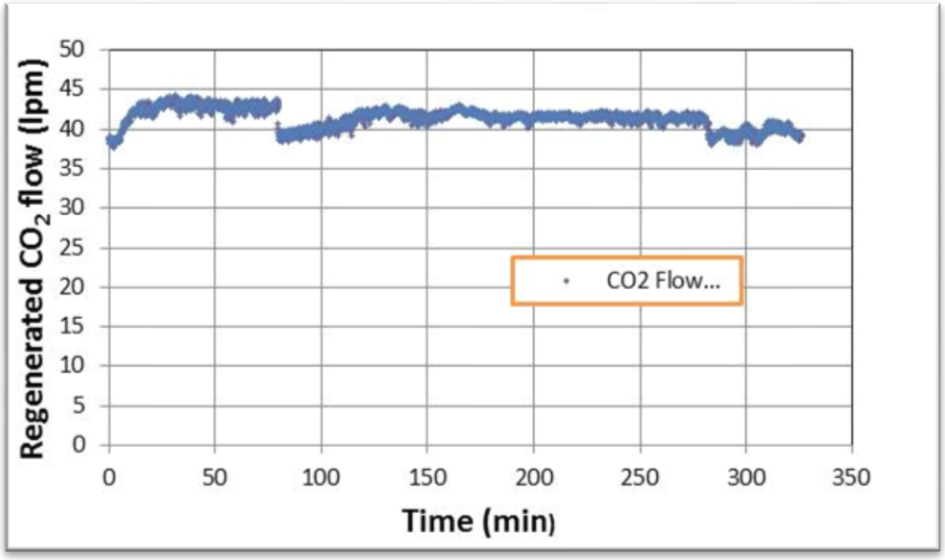

Figure xi. Observed 90% capture efficiency and regeneration with cyclic loading of ~ 0.7 M/M of ammonia.

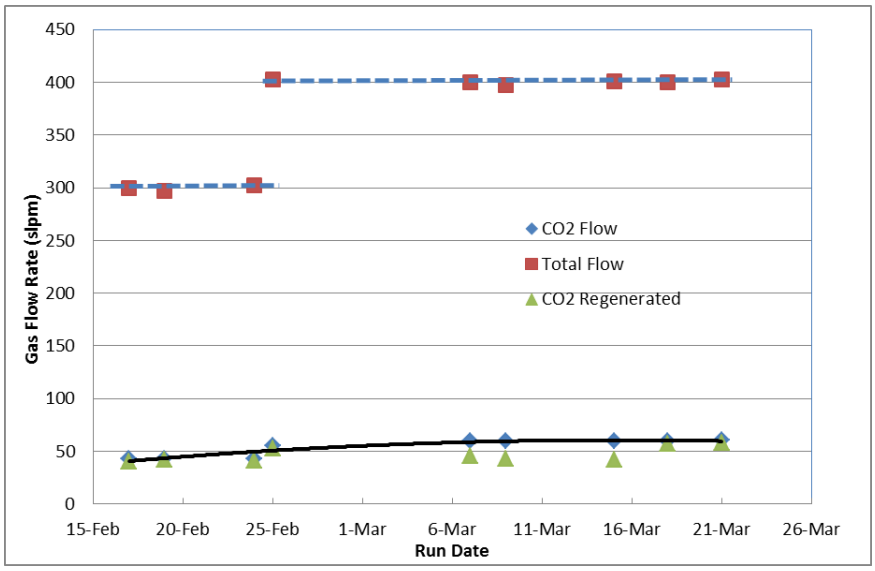

Figure xii. The average gas flow rates for the feed gas and the recovered CO_2 during the first 60-hour run campaign.

Results from process modeling: A rate-based model for detailed mass-balance and heat-balance calculations for a flue gas feed equivalent to a 550-MWe flue gas stream was developed and validated in OLI's Environmental Simulation Program (ESP). Initially, OLI conducted the mass and heat balance determination for various regenerator options. The reboiler duty requirement for the best layout with 0.2 to 0.5 cyclic CO_2 loading operation was 1.8 MJ/kg-CO_2. The mass balance and the energy balance from OLI were confirmed by PoliMi as well. We performed the absorber-regenerator system optimization to reduce water use and operate the system with < 10 ppm NH_3 in the absorber exhaust gas and regenerated CO_2 stream. Using the updated rate-based model, OLI determined the complete mass and energy balance for a full-scale system operating with the mixed-salt CO_2 capture system (a configuration similar to the current bench scale is used). The technology was modeled for the carbon dioxide recovery (CDR) facility, in which 90% percent of the CO_2 from the flue gas was captured from a supercritical PC plant with a nominal net output of 550 MW (DOE Case 11). The other fixed parameters were regeneration of high-pressure CO_2 at 99% purity and ammonia release from the absorber less than 10 ppm. The MSP was compared with Fluor Econamine FG Plus^{SM} technology (DOE Case 12). SRI's MSP can strip CO_2 at high pressure because the stripper for rich-solvent regeneration is operated at higher pressure than the Econamine FG Plus^{SM}. Thus, the electrical power required for compressing CO_2 to delivery pressures (> 130 atm) is greatly reduced in the MSP compared to other solvent-based technologies operating with lower-pressure regenerations. The MSP requires a relatively smaller recycle for cooling purposes, and the overall cooling water recycled was 71% less in SRI's MSP compared to the baseline case. As such, the auxiliary power required for SRI's MSP CDR unit was 60% less than the baseline case. The heat duty for SRI's MSP was calculated to be ~2.0 MJ/Kg of CO_2 recovered (in the stripper reboiler). This accounts

for a 44% decrease in the heat duty requirement in the MSP compared to the baseline case. Therefore, SRI's MSP can capture CO_2 at high pressure and can meet present DOE targets of CO_2 capture and pipeline purity requirements. The study showed the technology offers much lower energy penalty than Fluor Econamine FG Plus^{SM} technology and/or conventional MEA-based technology for post-combustion CO_2 capture. The technology can easily be scaled up with use of conventional process equipment.

Results from techno-economic analysis: The economic analysis for MSP post-combustion carbon capture plant applied on a super-critical PC steam cycle was conducted by the GECOS group of PoliMi. The analysis aimed to compare the economic results against the DOE reference Case 12B proposed by NETL in the report entitled, "Cost and Performance Baseline for Fossil Energy Plants (July 6, 2015)". The methodology applied for the economic analysis strictly follows the NETL guidelines provided in this report.

The cost of electricity (COE) is the most important index in evaluating the cost-effective solution for carbon capture. The COE presented by NETL for Case 12B is 142.8 $/MWh against the 126.1 $/MWh found in the PoliMi analysis of the mixed-salt technology, yielding a COE reduction of 11.7%. The comparisons between the different components of the COE show that the main contributors to the decrease of the COE in the MSP are related to the reduction of the total plant cost. Lastly, the optimization of the MSP can further improve the COE reduction. A comparison between MSP and DOE baseline case is summarized in Table i.

Table i. Comparison of MSP with the DOE baseline case.

Performance Factors	Econamine Baseline	SRI's Mixed-Salt Technology*
CO_2 capture, %	90.2	90.3
CO_2 purity (before compression), %	99.61	> 99.0
Stripper pressure, atm	1.0	10.0
Raw water recycle, gpm	~325,000	<100,000
Auxiliary power, KWe	20,600	3,581
Heat duty, MJ/kg of CO_2	3.56	2.0

Process Modeling: OLI, IHI and POLIMI
Cyclic loading: 0.18 to 0.58
Reboiler duty: 2.0 (OLI); 2.3 MJ/kg-CO_2 (POLIMI); 2.1 to 2.3 MJ/kg-CO_2 (IHI Measured)
Ammonia emission < 10 ppm
Cost of CO_2 Captured (Excluding T&S): ~$38/tonne-$CO_2$ for Mixed-Salt; $54/tonne-$CO_2$ for Case 12B

Results from EH&S risk assessment: We assessed the EH&S risk of the MSP in accordance with the DOE document entitled "Basis for Technology EH&S Risk Assessment" and the report is included in the PMP for the project. The EH&S report was prepared for the

optimized process configuration, and a hazard and operability (HAZOP) analysis was conducted to review the piping and instrumentation diagrams (P&IDs) of the current system in January 2016. The risk factors associated with the MSP are typical of that of a power plant. Additionally, precautions and safe handling are needed for large volumes of ammonia solutions, and these guidelines are well established in the chemical industry.

Results from MSP variant flowsheet testing: We tested two variants of the MSP to further decrease the ammonia loss and water usage. In variant 1, the length of absorber 2 was increased and solvent flow recirculation was slightly modified. Also, we installed a water wash with larger surface area and recirculation than the original MSP design. These changes reduced the ammonia in the absorber exit from ~ 3000 ppm to ~ 1000 ppm and the ammonia in the water wash exit to < 50 ppm. In the variant 2 configuration, we did not see any improvements from the original configuration. In fact, system operation was difficult with variant 2, and thus it was not pursued for more detailed testing. IHI Corp. also independently tested this configuration and found it to be inferior to other MSP flow sheet configurations.

Results from system operation during high-capacity testing and modeling: We performed equilibrium modeling to conduct a speciation analysis with high mixed-salt compositions and system testing, determined the system energy and mass balance, and updated the TEA. The updated rate-based model developed in BP1 and data from BP2 testing were used in process modeling to estimate the heat and mass balance for new flow sheets. The TEA prepared in Subtask 6.2 was also updated. With the bench-scale system, we performed several test runs with high loading conditions. The system operation was completely satisfactory under these conditions, and we did not encounter any operational issues. However, the CO_2 capture efficiency was reduced to about 70% under the high-capacity test conditions. Most importantly, we observed that the system operation can be easily and dynamically adjusted to the required capture efficiency and/or energy demand of the integrated system. This feature provides a greater flexibility to the plant operator for time-based CO_2 capture control.

1.6 Technology Development Timeline

Figure xiii shows the technology scale-up progress up to the BP2 work and the anticipated engineering-scale demonstrations. SRI, Technology Centre Mongstad, Norway (TCM), and the commercial partners are currently working on the engineering-scale development plan with expected DOE funding.

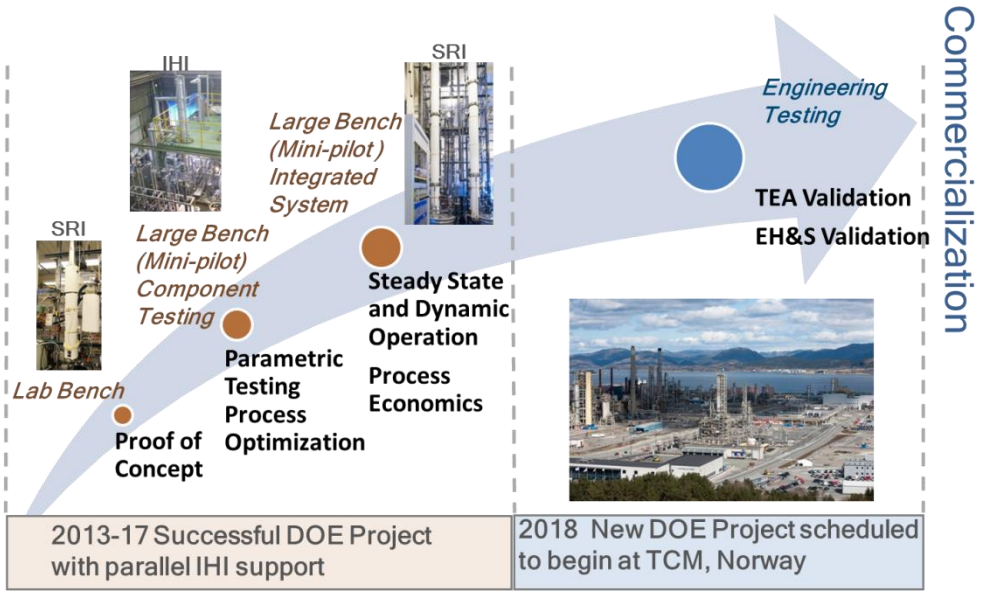

Figure xiii. Technology development timeline.

1.8 Concluding Remarks

Leveraging on the experience and knowledge of current, state-of-the-art ammonia-based and potassium-based processes, we have demonstrated a novel, highly efficient MSP in a large bench-scale system. The MSP combines existing ammonia and potassium-carbonate technologies with improved absorption steps for rate enhancement and ammonia emission reduction, and a novel selective regeneration process with a high-pressure CO_2 product to introduce a new and advanced transformational solvent-based technology. Results from bench-scale tests show the technology can capture > 99% of CO_2 and has a very high cyclic CO_2 loading capacity. Traditional CO_2 capture processes utilizing conventional amine solvents are very energy intensive and are also susceptible to solvent degradation by oxygen, SO_x, and NO_x in coal-fired flue gas, resulting in high operating costs. SRI's MSP is immune to the oxygen and trace levels of NO_x, and SO_x thus providing opportunities for reducing operational cost. Additionally, the low heat of reaction (35-50 kJ/mol) and lower reboiler duty (< 2 MJ/kg of CO_2) for regeneration reduce the energy penalty and allow opportunities for better heat integration between the CO_2 capture unit and the power plant.

The following is a list of research goals have been achieved under the DOE funded program for MSP testing at large bench scale:

- Developed comprehensive data base for both equilibrium and rate-based modeling of the H_2O-CO_2-NH_3-K_2CO_3 system used in MSP. Modeled the MSP integration with a supercritical coal power

plant (DOE case 11) and demonstrated the capture cost is less than \$40/ton-CO_2. Modeled and tested two process flowsheets to reduce both the process water use and NH_3 emissions (<10 ppmv).

- Demonstrated the operation of the MSP absorber at high temperature (20° – 40°C) without solvent chilling and reduction of ammonia emissions using the two-stage absorber approach.
- Demonstrated high cyclic CO_2 loading capacity (10 wt%) and high throughput using high-concentration solvent (~ 9 molal) without solid formation.
- Demonstrated longer-term operation of the integrated system and regeneration of the high NH_3/K and low NH_3/K lean solutions and 90% CO_2 capture with regeneration of > 99% purity CO_2.
- Measured the process steam use and demonstrated the process regeneration energy ~2 MJ/kg-CO_2 by modeling and by testing at both SRI and IHI.
- Identified technology gaps to reduce the overall process energy requirements that can be addressed at the engineering-scale testing. The integrated system has been tested over 2.5 years.

The MSP shows great promise for low cost carbon capture and is ready for a pilot scale demonstration. Upon successful completion of a large pilot scale demonstration, it can be commercially implemented starting with small scale industrial applications and advancing to large scale power plant applications as the technology reaches the maturity.

2. INTRODUCTION

Cost-effective capture of CO_2 emissions from coal-powered plants is of critical strategic importance to further enable the use of coal, an abundant natural resource in the U.S., without increasing greenhouse gas (GHG) emissions. In addition, using the captured CO_2 for enhanced oil recovery (EOR) can facilitate the U.S.'s long-term goal of becoming independent of foreign oil as EOR could potentially produce an additional 67 billion barrels of oil from economically recoverable sources [1]. The need for cost-effective supplies of CO_2 for expansion of EOR has been increasing rapidly due to the growing recognition of very large sinks in which CO_2 can be utilized to produce incremental oil and accrue incidental storage. SRI International's (SRI's) mixed-salt process (MSP) has the potential to provide CO_2 to the EOR market at a competitive price by using the captured CO_2 from coal-fired power plants and help pave the way toward U.S. energy independence.

The MSP combines existing ammonia and potassium-carbonate technologies with improved absorption steps for rate enhancement and ammonia emission reduction, and a novel selective regeneration process with a high-pressure CO_2 product to introduce a new and advanced transformational solvent-based technology. The striking advantages of the SRI process include: low heat of reaction, high loading of CO_2, high-pressure regeneration of > 99% pure dry CO_2, low sensitivity to impurities, low process cost, use of a non-degradable low-cost solvent with a very low carbon footprint for its production, low emissions, and reduced water use compared to the state-of-the-art ammonia-based and amine technologies.

SRI, in collaboration with Stanford University, OLI Systems, Aqueous Solutions Aps (ASAps), and Politecnico di Milano (PoliMi) performed a 45-month research project to develop this promising mixed-salt technology. The overall objective of the project was to advance and test a low cost solvent-based CO_2 capture technology that can capture CO_2 from existing or new pulverized coal (PC) power plants. Our goal was to test SRI's newly developed ammonia-based mixed-salt technology (MSP) at the bench-scale level to demonstrate that the process can capture CO_2 at high efficiency (> 90%) with very high CO_2 loading (> 10 wt.%) and require less than 2 GJ/tonne for solvent regeneration.

The project-specific objectives were:

- **Budget Period 1 (BP1):** Demonstrate the absorber and regenerator processes individually with high efficiency, low NH_3 emission, and reduced water use compared to the state-of-the-art ammonia-based technologies.
- **Budget Period 2 (BP2):** Demonstrate the high-pressure regeneration and integration of the absorber and the regenerator and the complete CO_2 capture system with low-cost production of CO_2 stream, optimize the system operation, and collect data to perform a detailed techno-economic analysis (TEA) of the CO_2 capture process integration to a full-scale power plant. Testing of two MSP configuration variants to further improve reboiler duty and reduce water usage.

The complete development program consisted of 10 tasks that included four new tasks added with the expansion of project work scope.

Task 1: Project Management and Planning.

Task 2: Individual Absorber and Regenerator Testing in a Semi-Continuous Mode.

Task 3: Preliminary Process Modeling and Techno-Economic Analysis

Task 4: Budget Period 2 Continuation Application

Task 5: Bench-Scale Integrated System Testing

Task 6: Process Modeling, Techno-Economic Analysis, and Technology EH&S Risk Assessment

Task 7: Integrated System Testing with Variant 1 Flowsheet

Task 8: Integrated System Testing with Variant 2 Flowsheet

Task 9: High-Capacity Runs and Modeling Update

Task 10: Regenerator Steam Use Measurement and Modeling

3. TECHNOLOGY BACKGROUND

3.1 Process Description

A simple schematic describing the concept that uses chemical absorption and regeneration mechanisms pertinent to the CO_2 capture process (CCP) is given in Figure 1. It can be integrated downstream of a flue-gas desulfurization (FGD) system in a PC power plant. The mechanism of CO_2 capture by chemical absorption using various chemical formulations has been studied extensively [2-6]. In the MSP, CO_2 is captured by a chemical absorption that involves series of ionic chemical reactions among CO_2, NH_3, K_2CO_3, and H_2O. The MSP chemistry comprises gas/liquid-phase mass transfer followed by chemical reactions in the liquid phase. Selected key reactions associated with the MSP and the speciation of K_2CO_3-NH_3-H_2O-CO_2 system are given below.

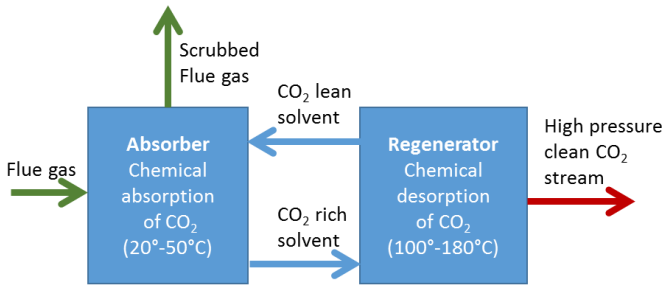

Figure 1. A simple schematic showing the concept of CO_2 absorption by chemical sorbent and regeneration of the solvent.

$$CO_2\ (g) \leftrightarrow CO_2\ (aq) \qquad \text{Eq. (1)}$$

$$NH_3(aq) + CO_2\ (aq) + H_2O\ (liq) \leftrightarrow (NH_4)HCO_3\ (aq) \qquad \text{Eq. (2)}$$

$$(NH_4)_2CO_3 + 2CO_2\ (aq) + H_2O\ (liq) \leftrightarrow 2(NH_4)HCO_3\ (aq) \qquad \text{Eq. (3)}$$

$$2NH_3(aq) + CO_2(aq) \leftrightarrow (NH_4)NH_2CO_2 \qquad \text{Eq. (4)}$$

$$(NH_4)NH_2CO_2\ (aq) + CO_2\ (aq) + 2\ H_2O(liq) \leftrightarrow 2(NH_4)HCO_3\ (aq) \qquad \text{Eq. (5)}$$

$$K_2CO_3\ (aq) + CO_2\ (aq) + H_2O(liq) + Catalyst \leftrightarrow 2KHCO_3(aq)) + Catalyst \qquad \text{Eq. (6)}$$

Speciation of the K_2CO_3-NH_3-CO_2-H_2O system includes H_2O $CO_2(g)$, $H_2O(g)$, $NH_3(g)$, $CO_2(aq)$, $NH_3(aq)$, CO_3^{-2} , HCO_3^-, H^+, K^+, $NH_2CO_2^-$, NH_4^+, OH^-, $K_2CO_3(s)$, $KHCO_3(s)$, $(NH_4)_4H_2(CO_3)_3(s)$, $NH_4HCO_3(s)$, and $K_2CO_3.1.5H_2O$. Solid species will not be present in the mixed-salt system as it is designed to operate below the solid formations concentration thresholds.

All chemical reactions in the ammonia-based process are reversible, and their direction depends on pressure, temperature, and concentration in the system. At low temperature, Equations 1 to 6 are exothermic reactions, proceed from a left-to-right direction, and require removal of heat from the process in order to maintain the desired absorption temperature. At high temperature, Equations 1 to 6 are endothermic reactions, proceed from a right-to-left direction, and require energy to release gaseous CO_2. The heat of reaction for the process can be tuned

depending on the composition of the mixture (potassium and ammonium salt ratio). SRI tested salt mixtures with 40-50 kJ/mole heat of reaction in bench-scale testing.

3.2 MSP CO_2 Capture System

The simplified schematic of the MSP CO_2 capture system is shown in Figure 2. The MSP system comprises two isothermal absorbers, a selective regenerator, and auxiliary equipment. Absorber 1 operates with high NH_3/K solvent, and absorber 2 operates with low NH_3/K solvent. The absorber system is designed to integrate downstream of a FGD unit in a PC power plant. Flue gas, after cooling to 30°-40°C in the FGD, enters absorber 1, where 60-80% of the CO_2 in the gas stream gets absorbed. The remaining CO_2 in the flue gas is absorbed in absorber 2 while reducing the ammonia carry over. The bottom stage operates with liquid recycle and cooling to keep the solution at just above cooling water temperature (30°C-40°C) and to maintain the absorber at relatively uniform temperature. Absorber 2 operates with the highest CO_2 loading in the range of 0.6-0.7 mole of CO_2 per mole of ammonia and about 0.7-0.8 mole of CO_2 per mole of potassium. Both absorbers operate with liquid recycle using heat exchangers to remove the heat of reaction and keep the solution at the optimum temperature for efficient absorption and minimum ammonia slip. The CO_2-rich solutions from the absorbers are sent to the regenerator for regeneration.

The MSP uses a novel selective regenerator to regenerate two CO_2-lean salt streams: (1) a high NH_3/K ratio mixed salt for use in the absorber 1; and (2) a low NH_3/K ratio mixed-salt stream for absorber 2. These streams are drawn from a lower-middle stage and the bottom stage of the regenerator. The regenerator is operated at high-pressure, isobaric conditions (10-20 bar) and has a temperature gradient along the height of the column (top ~30°-60°C, and bottom > 120°C). At high temperature, the NH_3 at the bottom of the regenerator is vaporized along with water and CO_2 making a lean, low-NH_3/K ratio solution to be used in absorber 2. Vaporized NH_3 and water get reabsorbed as the vapor moves up the regenerator column, thereby creating a high-NH_3/K ratio solution in the mid-section of the regenerator for use in absorber 1. The key advantage of the MSP design is to capture the latent heat within the regenerator before the stream exits the vessel, thus generating almost dry CO_2 stream (H_2O_{vap}/CO_2 <0.2) at high pressure. The benefits are twofold: reduction in the CO_2 compression cost to pipeline pressure (OPEX reduction), and the removal of the expensive first compression stage (CAPEX reduction).

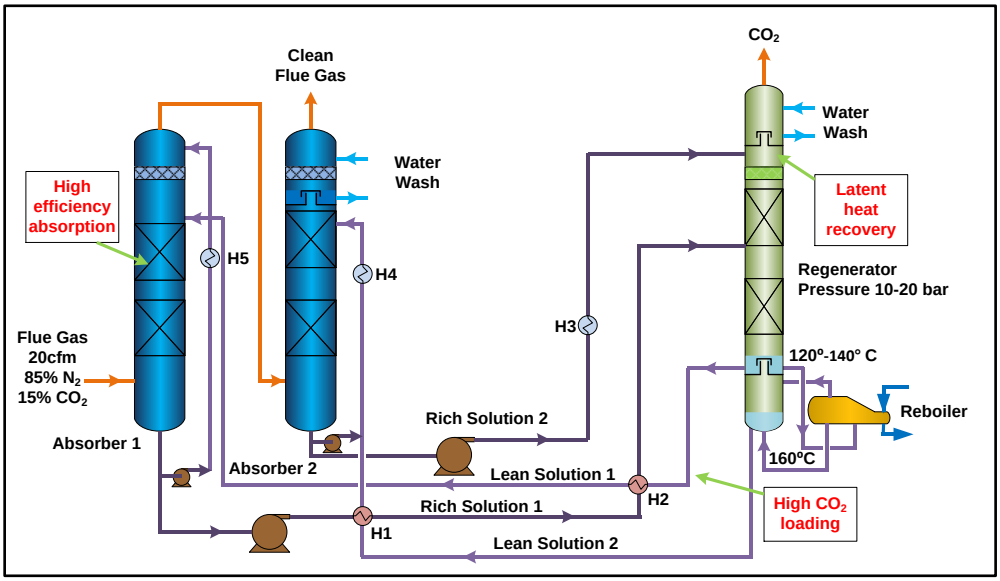

Figure 2. Simplified schematic process flow diagram for the mixed-salt process.
Note: SRI's design for the large bench-scale testing is shown in the section in which the process techno-economic analysis is discussed.

The MSP has been advanced from the proof-of-concept, to small bench-scale, and to the current large bench-scale testing and process evaluation at SRI with excellent results. Each stage of testing was conducted to demonstrate the process efficiency and allow comparison with other technologies (e.g., chilled ammonia process [CAP], precipitating K_2CO_3, or conventional monoethanolamine [MEA]). The MSP has been modeled extensively by OLI, ASAps, PoliMi, Stanford University, and IHI Corporation using ASPEN Plus® and other in-house software packages; the modeling results have confirmed the potential of the process and shown agreement with the field test results [7-10]. SRI was granted the patent for the MSP technology in 2016 [11]. The MSP concept and the results of experimental and modeling work were presented at multiple national and international conferences and NETL review meetings, and described in peer-reviewed journals and book chapters. [7-8, 11-14].

3.3 Proof of Concept and Lab-Scale Testing

In the lab-scale tests at SRI, a 12 vol.% CO_2 (~ 0.5 to 5 acfm gas flow rate) simulated flue gas stream was used to demonstrate the process. Initial tests showed that mixed-salt process has a higher CO_2 absorption rate compared to the state-of-the-art potassium carbonate process. Tests were conducted at varying starting CO_2 loadings. Tests with neat (pure) 3 m K_2CO_3 (~ 41 wt.%) loading were also conducted to compare the rate enhancement in the mixed-salt process. The data from testing at 30°C measured at 1 bar with a 38% mixed-salt solution and neat K_2CO_3 is given in Figure 3. Figure 4 compares the measured working capacity for K_2CO_3 with a mixed-salt system that has 3x the CO_2 loading capacity as neat K_2CO_3 systems.

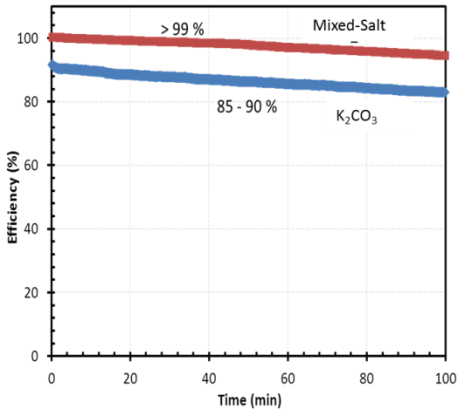

Figure 3. Comparison of CO_2 absorption efficiency of the mixed-salt process with neat K_2CO_3. The tests were conducted at 30°C and at 1 bar.

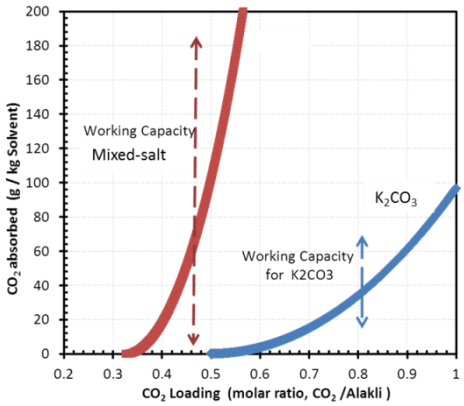

Figure 4. Measured CO_2 loadings for 38 wt.% mixed salt and ~ 40 wt.% neat K_2CO_3.

The undissociated ammonia present in the mixed salt solution has a very high diffusion rate within the aqueous solution compared to other dissolved species (ionized and undissociated) such as carbonate, bicarbonate, or dissolved carbon dioxide (Figure 5), leading to greatly improved CO_2 absorption performance. The NH_3(g) reacts with CO_2(g) at the gas/liquid interface and forms a transient complex that is dissociated by several pathways: (1) NH_3CO_2* + NH_3(g) → $NH_2CO_2^-$ + NH_4^+ and (2) NH_3CO_2* + H_2O (l) → HCO_3^- + NH_4^+. In addition, the complex — NH3CO2* — can dissociate back to NH_3(aq) and CO_2(aq). The net result is an increase in dissolved CO_2(aq). The key feature of the process is the in-situ formation of an ammonia-based inorganic moiety that has a higher diffusion coefficient and enhances the gas/liquid mass transport for increasing the rate of CO_2 capture. In summary, in the mixed-salt process, the rate of CO_2 absorption is enhanced by having ammonia act as a promoter that shuttles the CO_2 to the carbonate ion in the solution across the gas/liquid interface and increases the partial pressure of CO_2 in the dissolved phase. This increases the rate of CO_2 collision with carbonate ion and results in an increase in the rate of CO_2 absorption.

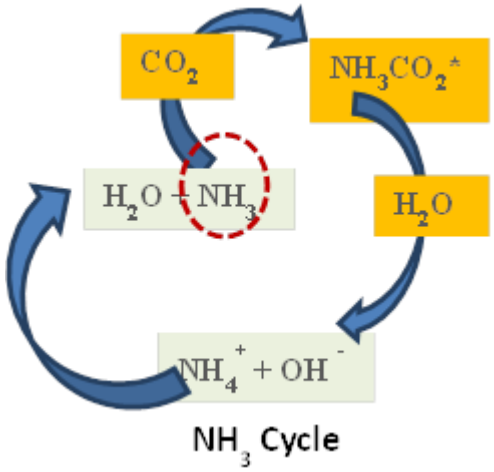

Figure 5. NH3 cycle at the gas-liquid boundary.

3.4 Effect of Temperature on the Rate of CO_2 Absorption

The rate of CO_2 absorption can be increased by increasing the temperature as long as the absorbent solvent volatility is sufficiently low and the Gibbs free energy for the reaction is negative. The experimental data for the ammonia-based system measured at SRI for a 4 m ammonia solution is shown in Figure 6. This data was obtained by measuring the CO_2 rate using a static absorber. The CO_2 absorption at 1 bar was measured at varying temperatures and CO_2 loadings as shown. Also shown in Figure 6 is the extrapolation of the expected rates to lower temperature region for each CO_2 loading. As expected, equilibrium is established very quickly with increasing temperature, and the reverse reactions become important. At lower temperatures, the rates of reactions are low, and thus the system equilibrium is slowly established.

However, ammonia processes such as chilled-ammonia and aqueous-ammonia must be operated at lower temperatures to avoid unacceptable ammonia evaporation hindering the process operation in a more desirable temperature range (25-45°C). SRI's mixed-salt process is designed to operate in the desirable temperature range 25-40°C, taking the full advantage of reaction kinetics. The CO_2 absorption kinetics in the mixed-salt process is about 5x higher than that in the chilled-ammonia process.

We used a 4-inch diameter absorber column in the lab-scale system, and performed parametric test campaigns with 7, 15, and 20 wt.% mixed salt with 15 vol.% CO_2 at 20-30°C and an ~ 5 scfm gas flow rate. The data showed that the CO_2 capture efficiency of the mixed-salt system can be similar or higher than that of MEA at the 20 wt.% level (mixed salt at 25°C and MEA at 40°C). During this test campaign, we also conducted tests with 4-6 m ammonia at 5°C to demonstrate that the mixed-salt process has a much higher CO_2 capture rate compared with currently practiced chilled ammonia-based process. These data are shown in Figure 7. The data shown for the mixed-salt process are for 7 and 20 wt. % salt concentrations.

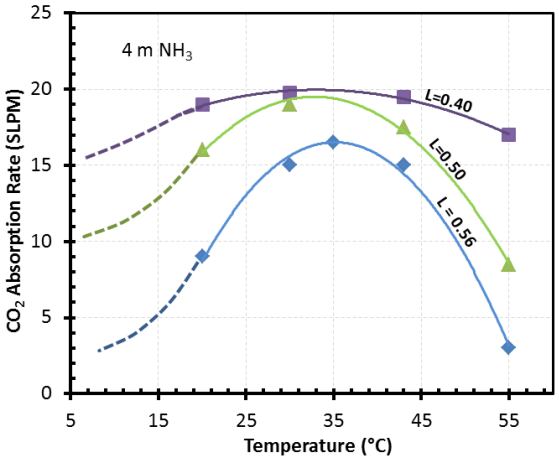

Figure 6. Effect of temperature on CO_2 capture rate at varying CO_2 loadings for ammonia based systems. L = CO_2 loading.

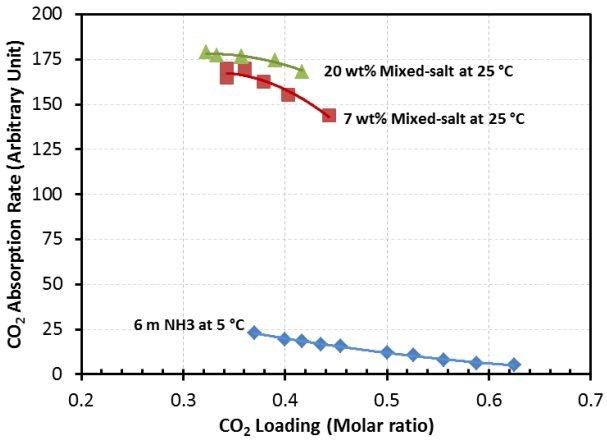

Figure 7. Comparison of CO_2 absorption efficiency of the mixed-salt process with ammonia.

4. KEY PROCESS BENEFITS

4.1 Large Reduction in Reboiler Heat Duty

CO_2 stripping and solvent regeneration are the main power consumers of solvent-based CO_2 capture systems. The required energy value for solvent regeneration comprises three major components: (1) ΔH_{sen} - sensible heat for heating the solvent; (2) ΔH_{des} - the reaction heat; and (3) ΔH_{vap} - steam evaporation. It may also include heat of dissolution of solids if any solids are formed during the absorption process. In the mixed-salt process, ΔH_{sen} is 70% lower than that of MEA-based technology because the MSP is operated with very high CO_2 loading and lean regeneration, thus a lower volume of solvent is required to carry the CO_2. Unlike in amine-based systems, there is no solvent degradation with high-temperature regeneration in the MSP, making it possible to regenerate leaner solutions with CO_2 loadings less than 0.2, which improves cyclic loading capacity. In addition, since the regenerator operates at a higher pressure in the mixed-salt process, the reflux ratio is very low ($H_2O/CO_2 < 0.01$). Therefore, the ΔH_{vap} for the MSP is insignificant. The heat of reaction, ΔH_{des}, is considerably lower for mixed salt compared to amine processes, leading to further reduction in reboiler heat duty. Another key difference in the mixed-salt process is that, unlike chilled-ammonia or neat potassium-carbonate-based processes, the MSP is designed to operate without solids in the absorber. Therefore, there is no additional heat requirement for solid dissolution in the regenerator or heat exchangers in the MSP, which can be as high as 1 MJ/kg of CO_2.

Taking into consideration the key advantages discussed above, the regenerator energy requirement for the mixed-salt process is estimated using the base data from known amine and potassium carbonate reboiler heat duties. For MEA (30 wt.% solution), the heat of CO_2 desorption, sensible heat, and the water stripping heat requirement are 1.4 to 1.8, 1.45, and 1.19

MJ/kg, respectively. Therefore, the total heat requirement is 4.04-4.44 MJ/kg. Pure potassium carbonate (~ 69 wt.% or 4 m $KHCO_3$) has a very high water stripping energy requirement (CO_2 to H_2O ratio ~ 2.6) and an additional heat requirement for solid dissolution (~ 1 MJ/kg). Figure 8 shows the comparison of heat duty of the mixed-salt process with MEA and K_2CO_3, clearly indicating the significant reduction in regenerator heat requirement for the mixed-salt process (< 1000 Btu/lb. of CO_2) [15, 16].

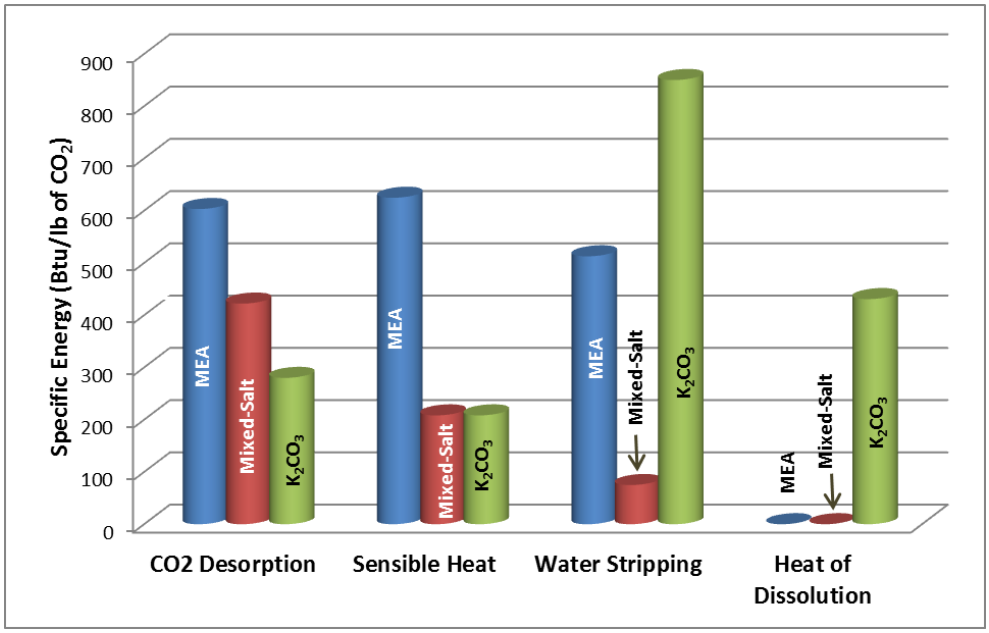

Figure 8. Estimated regenerator heat requirement for mixed-salt system with 0.2 to 0.6 cyclic loading of CO_2 (1 Btu/lb = 2.32 kJ/kg).

4.2 Reduced Energy for CO_2 Compression

CO_2 is transported or stored at high pressure, and thus in the overall CO_2 capture energy must include CO_2 compression energy. It is advantageous to strip CO_2 at high pressure if the process permits as it reduces the compressor stages and electrical demand. We have demonstrated the high-pressure regeneration potential of CO_2-loaded mixed salts solvents in tests performed at SRI. Figure 9 shows the observed static pressure when a 30 wt.% mixed-salt solution (0.6 loading) is heated from 30°C to 180°C, demonstrating that even at 130°C greater than 20 atm pressure can be achieved. Because the process can release a pressurized stream of CO_2, the electrical power required for compressing CO_2 to delivery pressures (> 130 atm) is greatly reduced compared to other solvent-based technologies operating with lower-pressure regenerations (e.g., amines, neat K_2CO_3). Figure 10 shows the energy requirement for compressing CO_2 to up to 130 atm as a function of pressure. For MEA, the energy requirement for compressing 1.5 to 135 atm is ~ 11.5 kJ/mol, while for the mixed-salt process the energy numbers are 3.5 and 4.7 kJ/mol for 30-130 atm and 20-130 atm, respectively. The minimum

isothermal compression energy requirement at 30°C (W_{comp}) is calculated by: $W_{comp} = RT \ln P_2/P_1$ where P_2/P_1 is the compression factor.

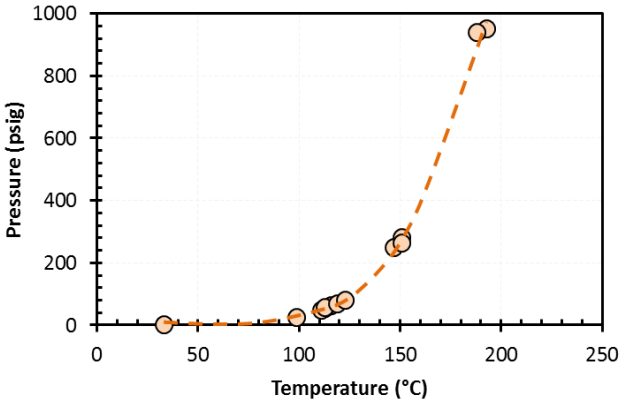

Figure 9. Attainable CO_2 pressure during solvent regeneration: Mixed-salt process with CO_2 loading value of 0.5 CO_2/alkali (20 wt.% solution).

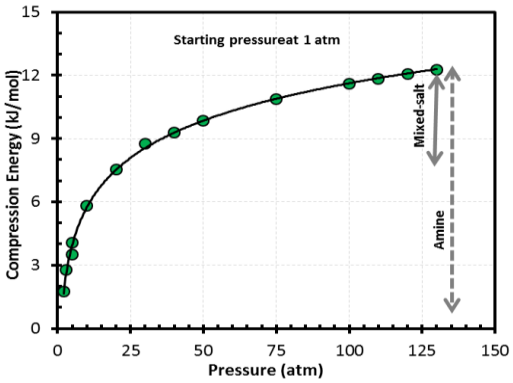

Figure 10. Comparison of CO_2 compression energy requirement for CO_2 stream from mixed-salt and amine-based regeneration processes.

4.3 Relevance and Impact

Globally, coal-based power plants are forecasted to be the largest source of electricity generation until 2040 at 29% [17]. However, environmental concerns have been raised regarding CO2 emissions. The amount of CO2 attributed to the U.S. electric power sector is expected to remain above 1.5 billion metric tons per year [18]. Thus, carbon capture and storage (CCS) integration to power generation is critical to reduce domestic and global CO2 emissions. Technical and economic challenges of integrating CCS with coal-fired power generation at commercial scale must be overcome before it can be widely implemented [19-23].

4.4 State Point Data Table

Table 1 shows the state-point data table for mixed-salt technologies**.** Heat of desorption data are estimated from experimental heat of reaction and vapor-liquid equilibrium (V-L-E) thermodynamic modeling of H_2O-CO_2-NH_3-K_2CO_3 system at 20 bar at >120°C. Physical properties of the working solution were also estimated from the thermodynamic simulation package provided by OLI.

Table 1. State-point data for the solvent-based mixed-salt system.

	Units	Measured/Estimated Performance	Projected Performance
Pure Solvent			
Molecular weight	mol^{-1}	18	18
Normal boiling point	°C	100	100
Normal freezing point	°C	0	0
Vapor pressure @ 15 °C	bar	0.17	.17
Working Solution			
Concentration	kg/kg	0.27 - 0.35	0.35
Specific gravity (15 °C/15 °C)	-	1.1-1.3	1.1-1.3
Specific heat capacity @ STP	kJ/kg·K	3.0-4.0	3.0-4.0
Viscosity @ 15°C	cP	1.6	1.6
Surface tension @ STP	dyn/cm	*73.4*	73.4
Absorption			
Pressure	bar	1	1
Temperature	°C	20 - 40	25 - 40
Equilibrium CO_2 loading	gmol CO_2/kg	1.6 - 4.3	3.8
Heat of absorption	kJ/kg CO_2	795 - 1136	< 1100
Solution viscosity	cP	1.5 - 1.8	< 1.9
Desorption			
Pressure	bar	> 10	20
Temperature	°C	120 - 170	120 - 170
Equilibrium CO_2 loading	gmol CO_2/kg	0.7 - 1.5	1.2
Heat of desorption	kJ/kg CO_2	1800 - 2200	< 2000

5. WORK PERFORMED

Below, we present the activities performed by SRI and the other team members during the total project performance period.

5.1 Task 1: Program Management and Planning

This task included management of technical, budgetary, and scheduling activities. SRI provided all required periodic reports to the U.S. Department of Energy – National Energy Technology Laboratory (DOE/NETL) as well as managed informal correspondence and collaboration. SRI prepared the continuation report at the end of BP1 and submitted it to DOE/NETL for approval and continuation to BP2. SRI also made technical briefings to DOE/NETL and presented project results jointly with other project partners at several industry- and DOE-sponsored conferences. The partners provided input to SRI on technical and financial progress reports as well as the respective final report sections. SRI monitored the project progress against the plan, reviewed and updated the project management plan on a frequent basis, and reported on budget and schedule variances to the DOE. All significant issues arising from the review were documented and discussed with DOE/NETL, and appropriate remedial actions were taken for successful completion of the project.

5.2 Task 2: Individual Absorber and Regenerator Testing in a Semi-Continuous Mode

Design, installation, and testing of the large bench-scale absorber system. The activities of this task involved: (1) completion of the design of the 8-in absorber system, procurement and installation; (2) system shakedown testing; and (3) initiation of the parametric testing.

Lab-scale 4-in absorber. For the design of the 8-in absorber system, SRI used the data collected from SRI's 4-in absorber system. This system, shown schematically in Figure 11, consisted of a 4-in diameter absorber column, reflux chamber, tanks, and a circulating pump. The column height was 8 ft. The absorber was a stainless steel shell, and the system was operated under atmospheric pressure. A metering pump at the bottom of the sump circulated the solution between the column sump and the absorber column. The flue gas from the absorber exit was directed through the reflux chamber to knock down the water and ammonia. The exhaust from the reflux chamber was further scrubbed with water wash to remove the ammonia levels below 3 ppm such that it could be vented to exhaust. The compositions of the feed solution and the bleed solution were determined by chemical analysis. Absorber inlet and outlet CO_2 composition were determined using in-line Horiba gas analyzers to evaluate the process efficiency.

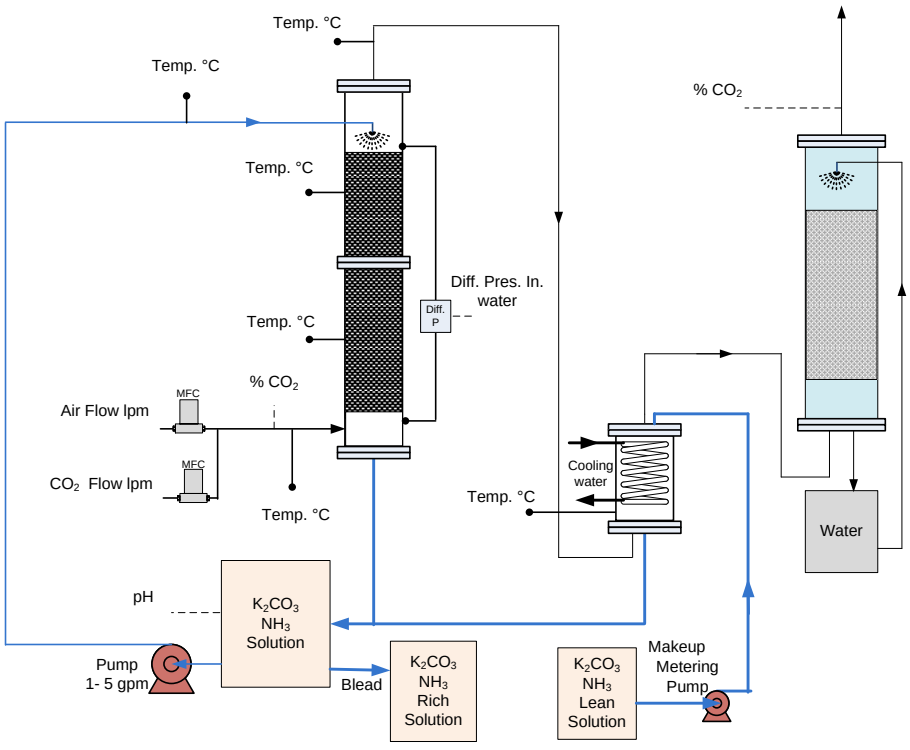

Figure 11. Schematic diagram of the 4-in lab-scale absorber.

The 4-in column was packed with Flexipac 1YHC, a commercial 316 SS stripper packing materials procured from Koch-Glitsch. The Flexipac 1YHC packing combines excellent capacity and efficiency characteristics along with a lower pressure drop per theoretical stage and is

suitable for use in vacuum distillation applications. It has a surface area of 420 m^2/m^3 and a rated height equivalent to theoretical plate (HETP) of 10 inches per stage. A select number of tests with 7 to 20 wt.% mixed salt were performed to finalize the design basis for the design of the 8-in absorber.

Large 8-in system design, fabrication, and installation. Based on the data from SRI's 4-in absorber system, we designed the 8-in mixed-salt absorber system to accommodate for processing a 100-scfm gas flow containing 15% CO_2. The liquid flow rates were selected to maintain a constant liquid-to-gas (L/G - by mass) ratio to understand the effect of the L/G ratio on the absorber performance. Initial testing of the system was conducted using 10- to 25-scfm gas flows, as the regenerator was not integrated to the absorber during Budget Period 1. The liquid recycle within each section of the absorbers was selected to maintain minimum of 5% liquid loading.

During the 2rd quarter (January 1 –March 30, 2014), we completed absorber fabrication. The absorber system was fabricated by Johansing Iron Works, Oakland, CA and installed by SRI technicians in SRI high-bay facility. The system has two absorber columns that the gas stream passes through in series. The first column, absorber 1, designed to operate with ammonia-rich absorber solution, is shown in Figure 12. Absorber 1 is packed with 450 m^2/m^3 and 350 m^2/m^3 packing material (Sulzer MellaPakPlus®) as indicated in the diagram. Figure 13 shows the schematic diagram of absorber 2. Absorber 2 is packed with 350 m^2/m^3 and 250 m^2/m^3 packing material (Sulzer MellaPakPlus®) as shown in Figure 13. MellaPakPlus® packing combines excellent capacity and efficiency characteristics along with a low pressure drop per theoretical stage and is suitable for use in similar applications. The bottom part of the column is designed to operate with potassium-rich absorber solution. The top part of the column can be operated either as a water wash or an extension of the bottom part, i.e., with potassium-rich solution. The solution flows and flow routing can be changed by closing and opening appropriate valves to perform a full range of experiments in the test matrix and obtain data necessary for optimization and scale up. For the absorber testing in BP1, we used appropriate absorber solutions recirculated from 55-gal storage tanks. Temperature, flow rate, gas composition, and pressure were monitored at various points in the system as indicated in Figures 12 and 13. Figure 14 shows the schematic diagram of complete absorber system, which we used as the background picture for the active desktop of the software interface, providing the operator convenient visual indication of all sensor readings and their locations. Figure 15 shows a photograph of complete mixed-salt absorber system.

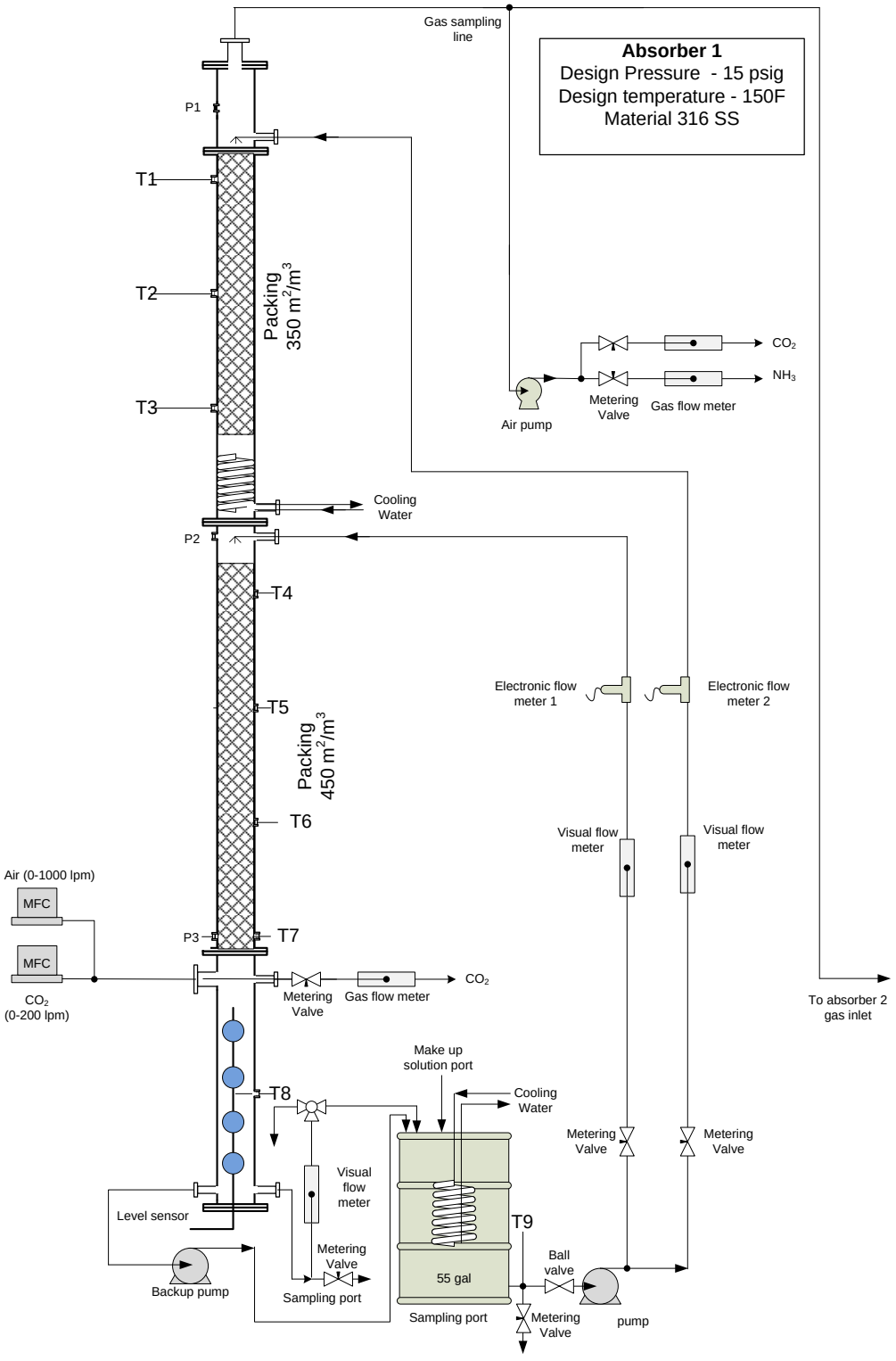

Figure 12. Schematic of the absorber 1 with 450 and 350 m^2/m^3 Sulzer MellaPakPlus® packing.

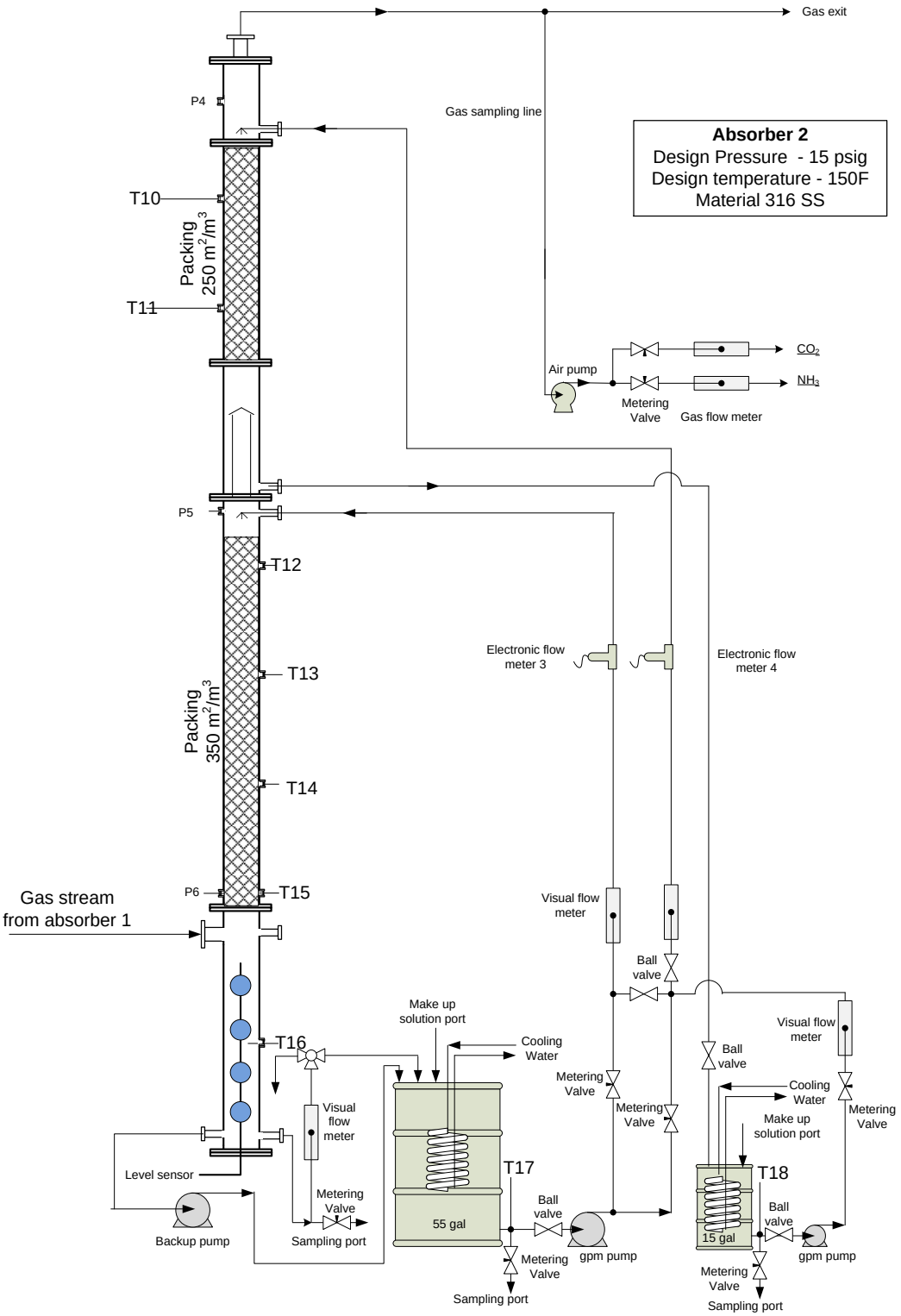

Figure 13. Schematic of the absorber 2 with 350 and 250 m^2/m^3 Sulzer MellaPakPlus® packing.

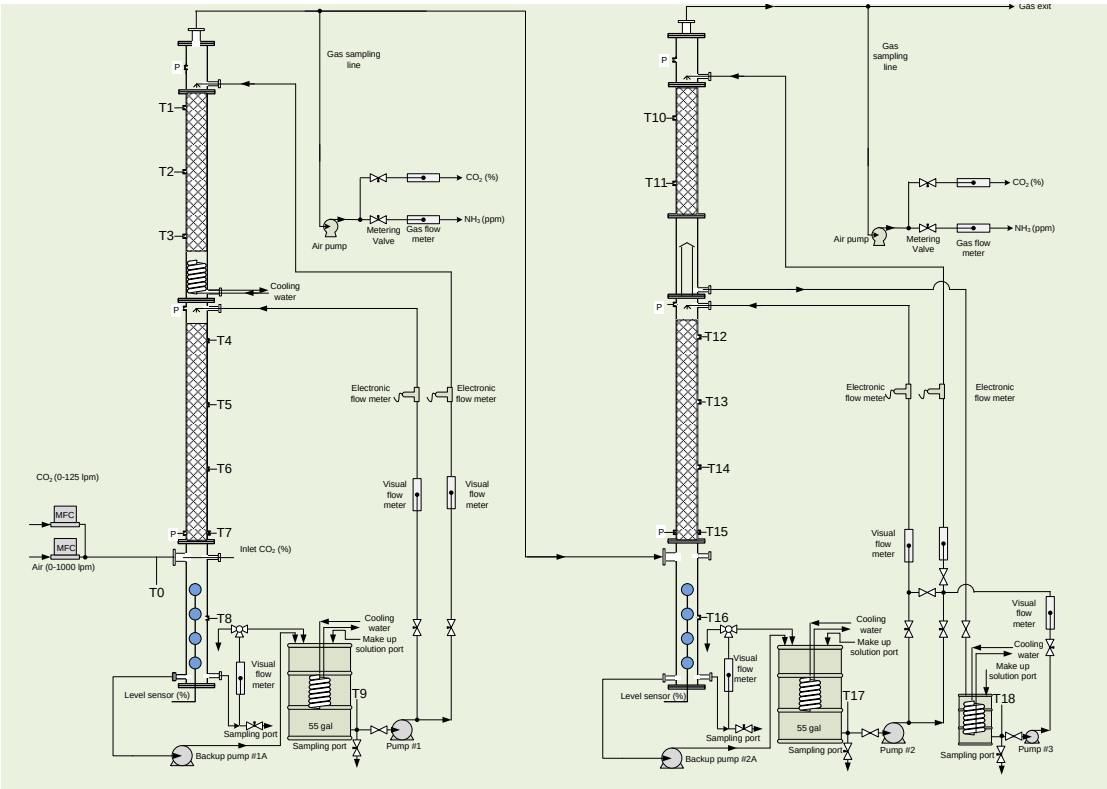

Figure 14. A schematic diagram of complete system that was used as the background picture for the active desktop of the data acquisition and control program.

Figure 15. Photograph of the installed mixed salt absorber system (*left*) and close up of two absorber columns (*right*).

We completed the necessary hardware and software for the data acquisition and control system in Q3 of BP1. Figure 16 shows the gas analyzer instrumentation rack and control computer system. We use Horiba® analyzers for CO_2 detection and Emerson® analyzers for ammonia detection. Figure 16 also shows the hardware interface that routes all temperature sensors, flow meters, pressure sensors, mass flow controllers, liquid level sensors, and gas analyzers to the computer. We used a National Instruments® multi-function data acquisition unit for the computer interface. We wrote a customized computer program for data acquisition and control with Microsoft Visual Studio®. Figure 17 shows the control program screenshots. Any sensor data can be displayed graphically in real time to visualize trends and make decisions during a run. We used two computer monitors to have a large desk top area for displaying plots and main program windows. Data are collected from 42 sensor inputs every 3 seconds and recorded to a data file, which can be directly imported to Excel for post analysis, plotting, and reporting.

Figure 16. Photograph of gas analyzer instrumentation rack, and data acquisition and control computer system (*left*) and sensor and control hardware interface for the absorber system (*right*).

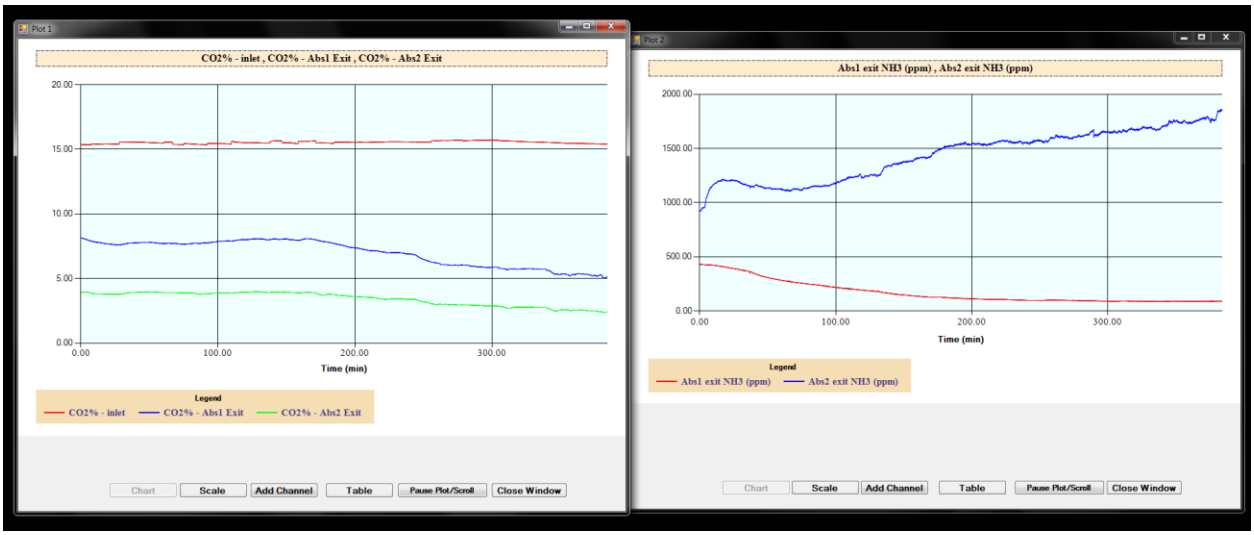

Figure 17. Screenshots of data acquisition station monitors.

Test Conditions, Data Analysis, and Results of Individual Absorber and Regenerator Testing in a Semi-Continuous Mode

Results from individual absorber and regenerator units testing are described in this section. The tests were performed in a semi-continuous mode such that it was easier to determine operational parameters and isolate any process issues. The following test series were performed and focused on specific objectives as stated.

- Test series 1 (Runs 1-3): System shakedown testing (300, 400 and 500 slpm gas flow)
- Test series 2 (Runs 4-10): Effect of gas flow rate and liquid recycle rate on absorption was tested
- Test series 3 (Runs 11-15): effect of absorber packing
- Test series 4 (Runs starting at 15): Preparation of rich solution for regenerator tests

For Test Series 1, 2, and 3, 20 wt.% mixed salt was used. We also planned to run 30 wt.% mixed salt solutions (Test Series 4) under different parametric conditions as in previous test series. The absorber test was performed in parallel to simulate the operation of absorber and regenerator with a rich solution storage option.

Test Series 1 (System shakedown testing)

Extensive system shakedown tests were conducted with water and also with low-concentration mixed-salt solution to test the section of the absorber system with full ranges of gas flow rates and liquid recycle rates. The main purpose of the shakedown testing was to identify any issues with the system such as liquid leaks, liquid drain problems, column flooding, liquid and gas sampling, and the proper operation of sensors and controls. System response time was also measured by operating the system with water and by changing the CO_2 inlet concentration and measuring the CO_2 outlet concentration at absorber 1 and absorber 2 exits.

Figures 18, 19, and 20 show CO_2 absorption efficiency vs. CO_2 loading for 300 (Run 3), 400 (Run 4), and 500 (Run 5) slpm gas flow rates, respectively. The CO_2 concentration was 15%. These test runs were performed in batch mode using only the absorber 1 column as the absorber. The absorption solution of 100 liters with 21 wt.% mixed salt (NH_3/K ratio ~ 5) and a starting CO_2 loading of 0.3 was circulated in the absorption column. The L/G ratio was maintained at a constant value for all three runs. The temperature of the operation was ~ 20°C. The top section of absorber 2 was used as the water wash to remove ammonia from the exit gas stream before sending it to the building exhaust/scrubber system.

Process mass balance was evaluated using both gas-side and liquid-side data. Gas-side data were obtained from the combinations of in-line gas feed mass flow meters, Horiba CO_2 detectors, and the ammonia detectors. Liquid-side compositions were obtained from analyzing liquid samples collected periodically with a time stamp so the results could be correlated with gas-side analysis. Liquid titrations were performed using an automatic titrator. Figure 21 shows a

liquid analysis titration curve for mixed-salt composition 5X ratio test solution loaded with 1.1 moles/kg CO_2. The typical pH curve for mixed-salt system shows two inflection points that are used to determine the bicarbonate and total carbonate concentrations. Figure 20 shows excellent agreement for the amount of CO_2 absorbed by independent gas-side and liquid-side analyses.

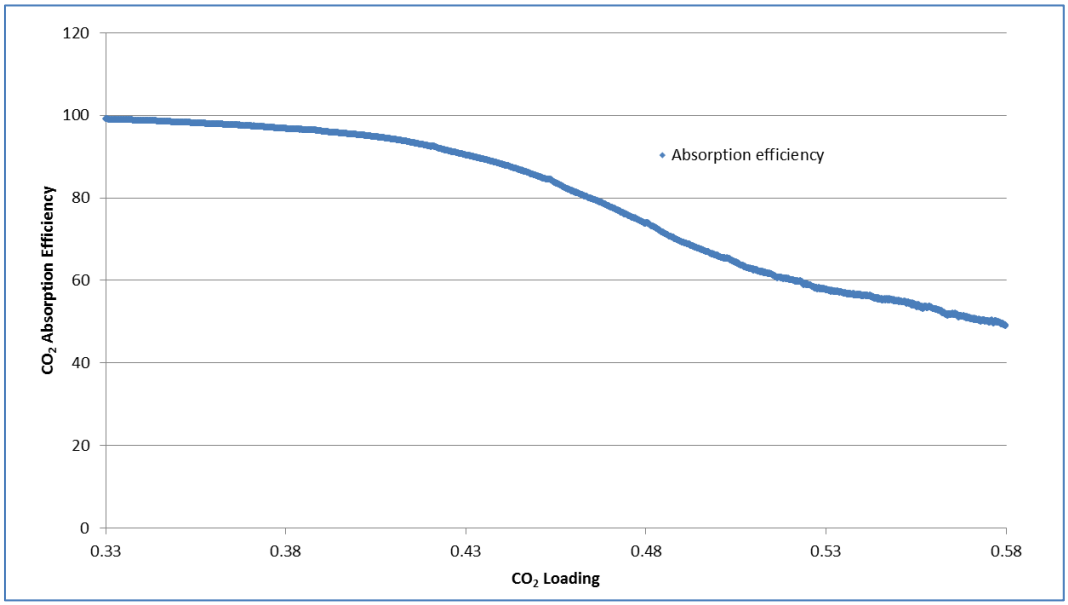

Figure 18. Absorption efficiency vs. CO_2 loading at 300 slpm total gas flow rate.

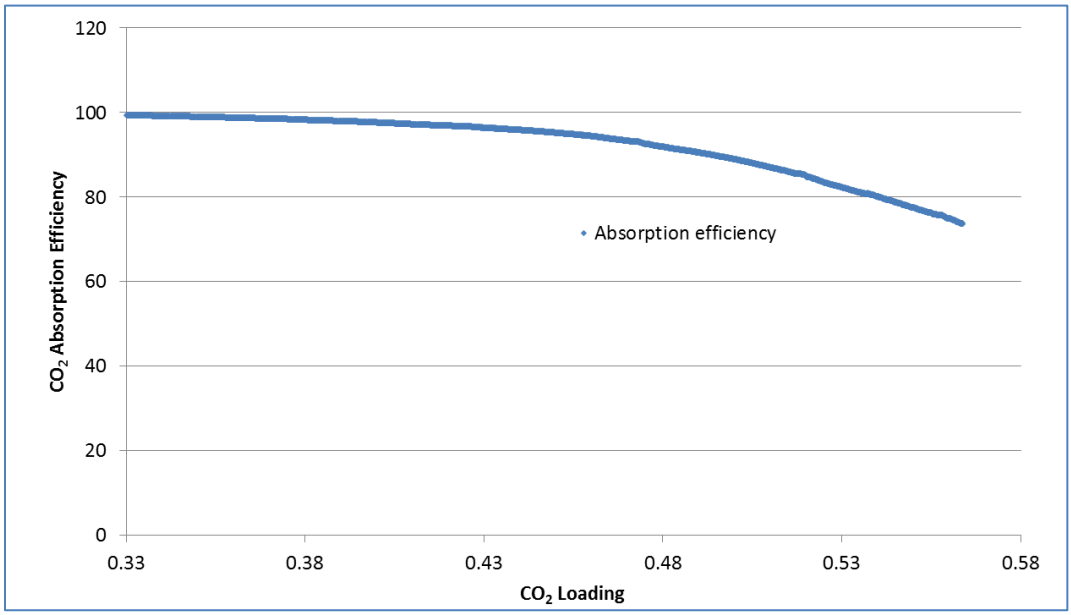

Figure 19. Absorption efficiency vs. CO_2 loading at 400 slpm total gas flow rate.

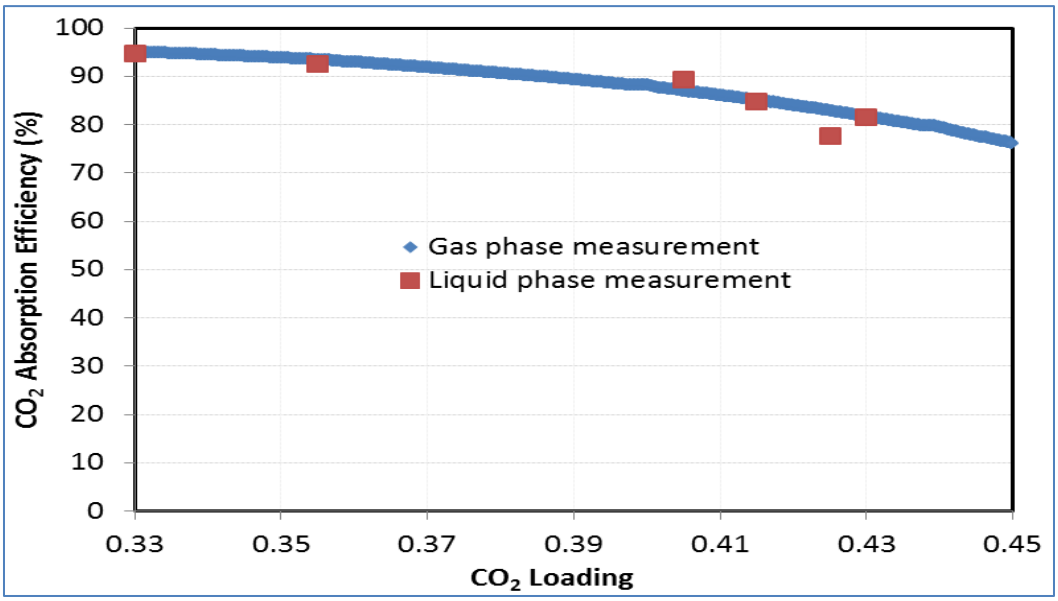

Figure 20. Absorption efficiency vs. CO_2 loading at 500 slpm total gas flow rate.

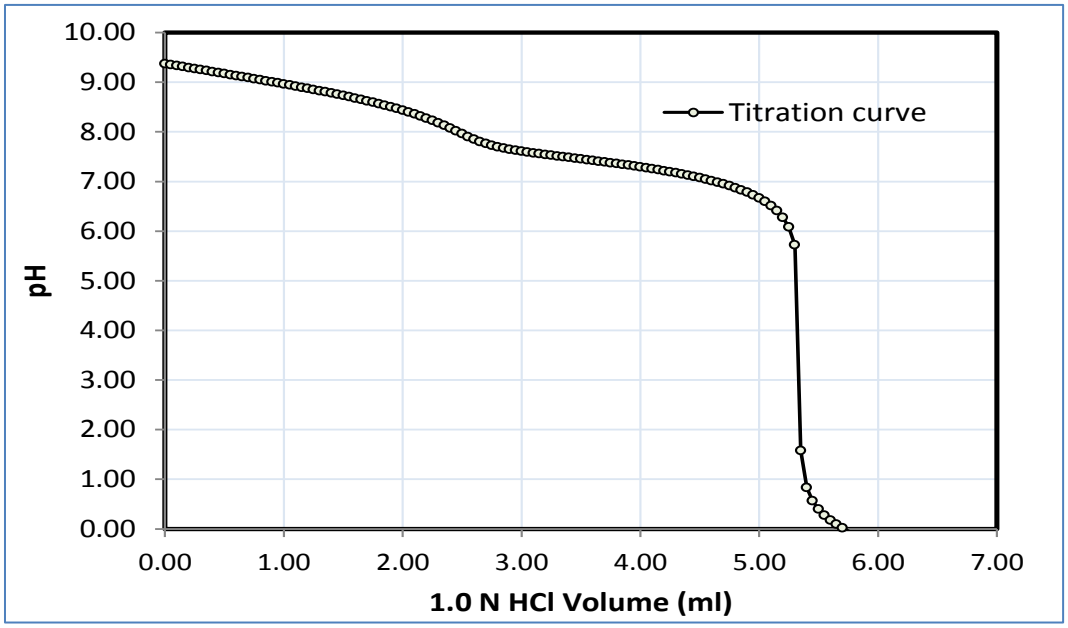

Figure 21. Typical pH titration curve for determining total ammonia and potassium content.

System pressure drop. The pressure drop of the packed column 1 was less than 3-in H_2O for the highest gas flow rate that we tested (500 slpm). Figure 22 shows the temperature profile along the absorber 1 column, indicating only a 2-3 degree temperature difference from the top and the bottom. The column temperature was maintained by manually controlling the cooling water flow to the heat exchanger coil in the 55-gal reservoir, and to the heat exchanger coil in the

middle of absorber 1. The temperature difference became smaller as the run progressed due to lower reaction heat. In some runs, the temperature profile fluctuated, as it was difficult to manually control the cooling water flow through the large thermal mass system.

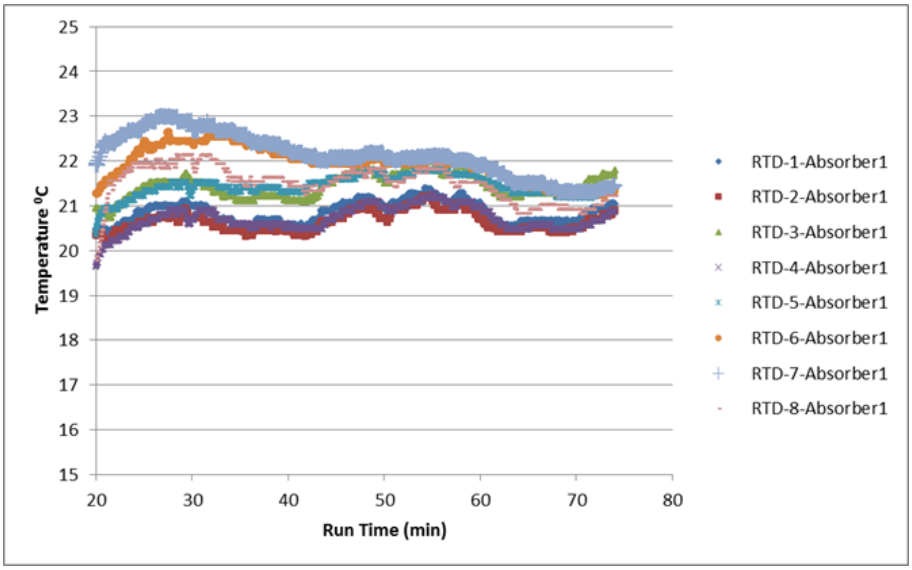

Figure 22. Temperature profiles (from top to bottom) of absorber 1 column during a run.

Accuracy of analytical and measurement methods. All the analyzers used for gas and liquid analysis were calibrated according to vendors' specifications. The CO_2 analyzers were calibrated each week with a Matheson 15 vol.% calibration gas. The accuracy of various sensors and instruments used in the absorber test system is given in Table 2.

Table 2. Accuracy of sensors and analytical instruments.

Sensor/Instrument	Measurement Range	Accuracy (%full scale)
Pressure Sensor	0 – 50psi	±0.25%
Resistance Temperature Detectors (RTDs)	-50 - 150°C	± 0.25%
Mass Flow controller (CO_2)	0 - 150 lpm	±1.5%
Mass flow controller (Air)	0 - 1000 lpm	±1.5%
CO_2 Detector (inlet)	0 - 20% v/v	±1%
CO_2 detector (outlet)	0 - 20% v/v	±1%
NH_3 analyzer	10,000 ppmv	±1%

Mass Balance

Figure 23 shows the simplified diagram that includes the process liquid and gas flows. We calculated the process mass balance in two ways. *Method 1*. The mass balance was calculated for the carbon balance using the measured gas-side data (CO_2 mass flow rate reading,

CO_2 readings from the Horiba analyzers) and liquid-side data (dissolved CO_2 from the liquid analysis of the bleed sample). Analyzer accuracies are shown above (Table 2). *Method 2*. The overall mass balance was calculated following the nitrogen balance using total liquid mass flow in and out, ammonia gas flow out, and liquid analysis.

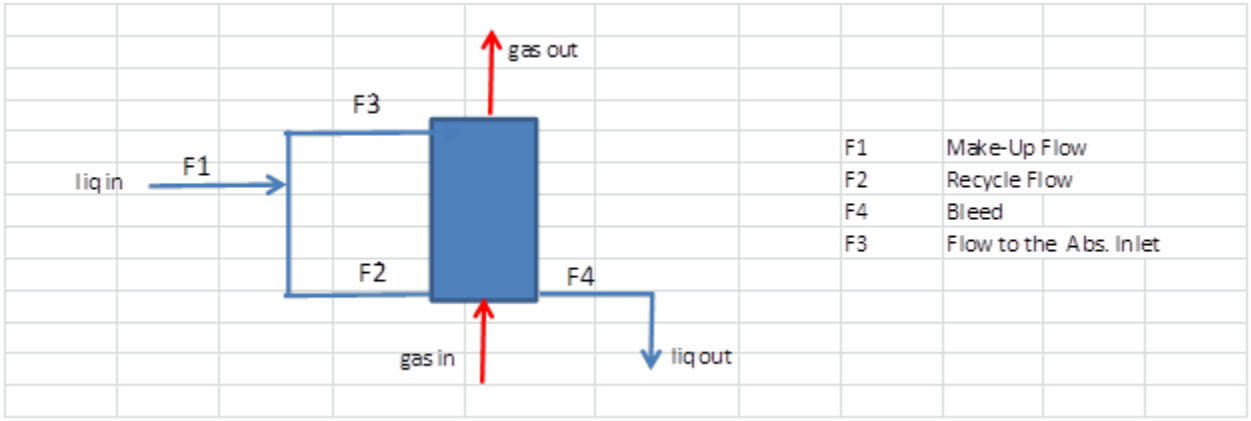

Figure 23. Mass balance calculation.

Test Series 2

Test Series 2 was conducted to test 20-21 wt.% mixed-salt solution for capturing a 15 vol. % CO_2 gas stream at a 300 to 500 slpm gas flow rate. Table 3 shows the detailed list of test parameters.

Table 3. Run log for Test Series 2.

Run #	ABS-1 Concentration (wt. %)	ABS-1 N/K Ratio	CO2 Flow Rate (LPM)	Air Flow Rate (LPM)	Total flow Rate (LPM)	ABS1 Liquid Recycle Rate (LPM)	ABS2 Liquid Recycle Rate (LPM)
4	21	5x	60	340	400	24	0
5	21	5x	75	425	500	30	0
6	21	5x	45	255	300	18	0
7	21	5x	45	255	300	18	18
8	21	2x	75	425	500	18	0
9	21	2x	75	425	500	30	0
10	21	2x	60	340	400	24	0

The data from each test run was analyzed to determine the effects of gas flow rate and the liquid recycle on the CO_2 absorption rate at 20 °C. The effect of the second absorber [potassium-rich section] was also tested.

In the mixed-salt system, a dual-absorber system is used with a high ammonia/potassium ratio in the first, and low ammonia/potassium ratio in the second absorber. The tests conducted clearly indicated that such operations can be easily performed with a significant reduction of ammonia vapor pressure in the scrubbed gas. Ammonia emissions from selected runs are shown

in Figure 24. Run 7 data shows that the ammonia in the exit gas is greatly reduced by the potassium-rich solution used in absorber 2. As an example, at a CO_2 loading of 0.45, the ammonia emission from absorber 1 is about 0.6 – 0.7 vol.% (Run 7), and that has been reduced to about 0.02 % after scrubbing the stream from absorber 1 with the potassium-rich solution in absorber 2. Figure 25 shows the measured ammonia vapor pressure with run time for a run conducted with single absorber (6) and for a test conducted with the dual absorber (Run 7).

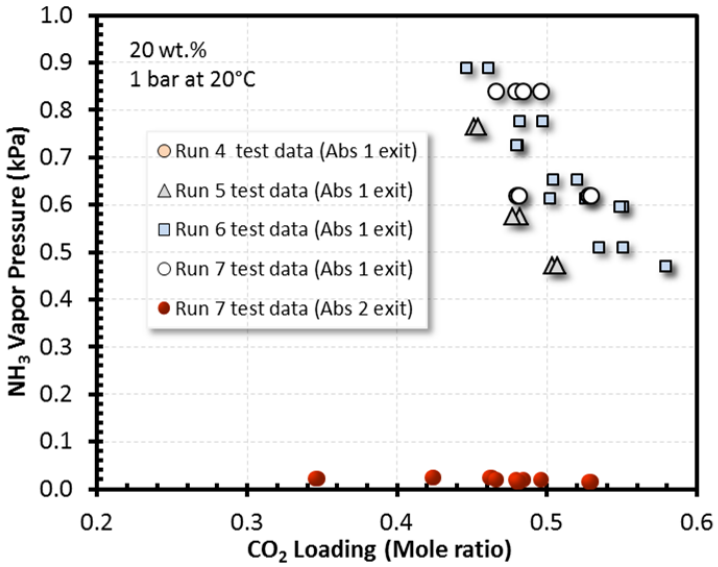

Figure 24. Measured ammonia vapor pressure at various CO_2 loadings for runs conducted with single absorber (Runs 4, 5, and 6) and for a test conducted with the dual absorber (Run 7).

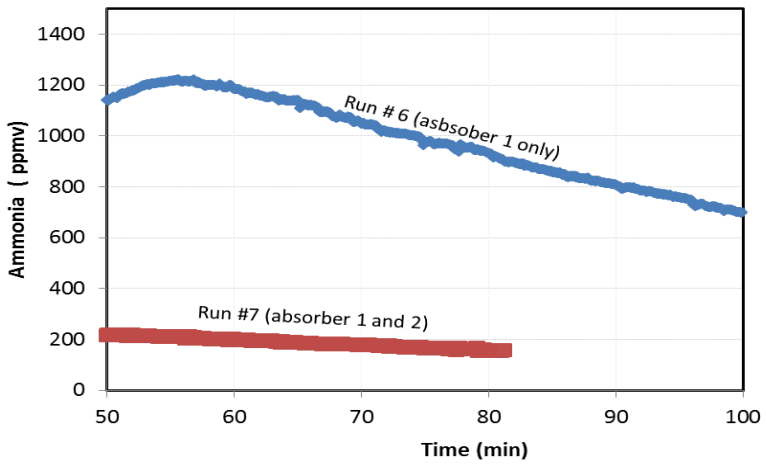

Figure 25. Measured ammonia vapor pressure with run time for a run conducted with a single absorber (Run 6) and for a test conducted with the dual absorber (Run 7).

For each run, the measure CO_2 absorption efficiency data was used to calculate the specific gas transfer coefficient, K_g (mol s^{-1} m^{-3} Pa). Figure 26 shows the measured gas transfer

coefficient for Runs 4 through 10. These values (0.4 to 1 mol s^{-1} m^{-3} Pa at CO_2 loading of 0.4) are in the same order as MEA-based systems and about factor of 5-7 higher than chilled-ammonia systems. The curves show that the K_g value decreases with loading as expected. In addition, kg values are a function of temperature (Run 4 at ~17°C and Run 10 at ~ 24°C, see Table 3 above for run conditions).

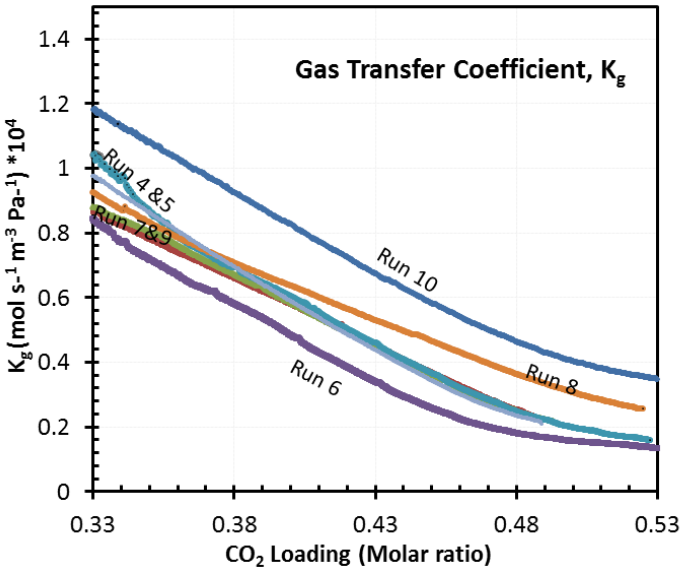

Figure 26. Gas-transfer coefficient calculated from test data for varying test conditions. Gas flow rates of 8-17 cfm with a constant L/G ratio

Effect of gas flow rate. Figure 27 shows the CO_2 absorption rate vs. total gas flow rate under various CO_2-loading level conditions. The green line at the top of the profiles shows almost 100% absorption of CO_2 from the 15% CO_2 feed stream at 300 and 400 slpm gas flow rates, and about 96% absorption at the 500 slpm gas flow rate. The linear velocities for 300, 400, and 500 slpm are 0.01, 0.02, and 0.038 m/s, respectively. As expected, with the increase of loading level, absorption rate decreases. The drops are more prominent at 300 and 500 slpm flow rates compared with a flow rate of 400 slpm. There is a higher capture rate and efficiency at higher gas velocity due to the increase in turbulence when the gas velocity is increased. At the same time, higher gas velocity shortens gas residence time so there is an optimal level after which the increased gas velocity has a diminishing return and shortening of the gas residence time becomes more dominant. We have seen the same phenomena in the FGD (open spray towers) in which higher gas velocity improved SO_2 capture up to an optimal level, and then it declined.

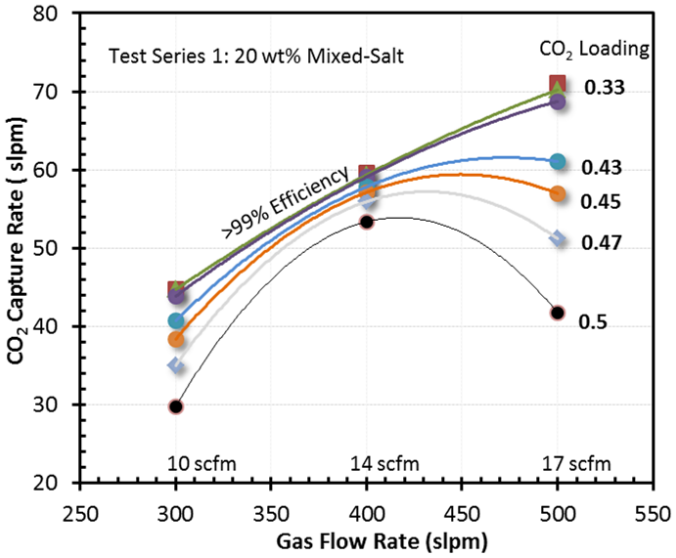

Figure 27. Variation of CO_2 absorption rate with gas flow rate under various CO_2 loading conditions.

Figure 28 shows the variation of ammonia vapor pressure with feed gas flow rate for Test Series 1 runs (corresponding CO_2 capture rates are shown in Figure 27). As predicted, ammonia vapor pressure in the system is a strong function of CO_2 loading at a given temperature and pressure. However, it is independent of the feed gas flow rate in the testing range of feed gas flow rate and the L/G ratios in Series 1. This is indeed good news, as it indicates that the ammonia dissolution is fast and equilibrium is reached quickly at a given CO_2 loading. We compared the measured NH_3 vapor pressure data from our tests with the V-L-E data generated from the OLI Systems computer program. Generated V-L-E data for NH_3 vapor pressure agree well with the experimentally measured values as seen in Figure 29. The experimental data shown in the figure are for Run 8.

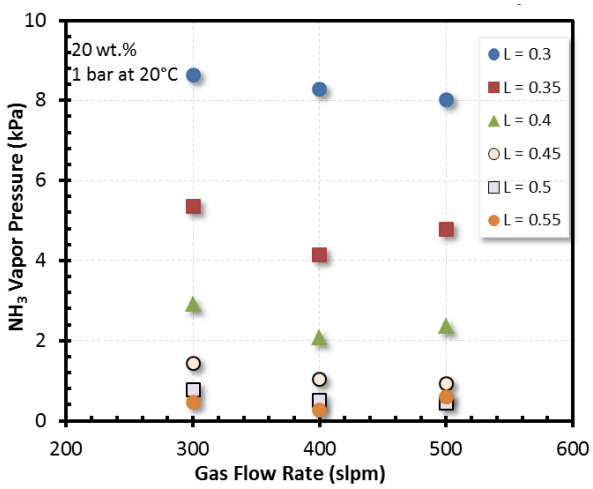

Figure 28. Variation of NH_3 vapor pressure with gas flow rate under various CO_2 loading conditions.

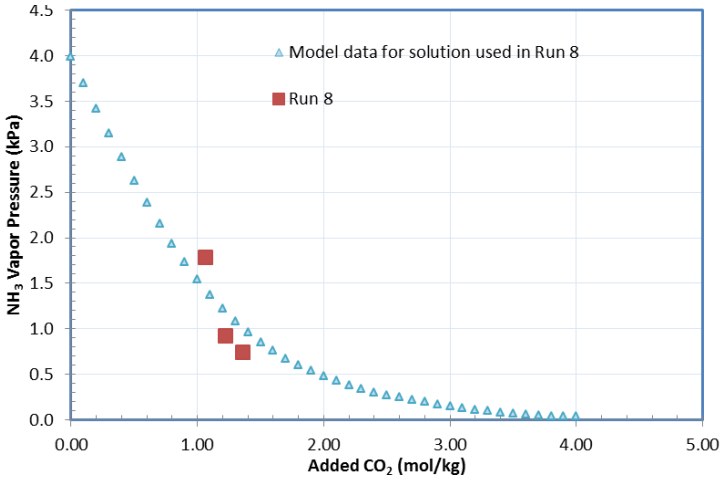

Figure 29. Comparison of ammonia vapor pressure measured and the predicted from V-L-E modeling (experimental data for Run 8 is shown).

Figures 30 and 31 show the data comparing the effect of gas flow rate and the liquid recycle rate. The data shown are the measured CO_2 vapor pressure of the gas exiting absorber 1 compared with the predicted equilibrium vapor pressure of CO_2 for 20 wt.% mixed-salt solution at 20°C and 1 atm at varying CO_2 loadings. The system operates close to equilibrium line when the CO_2 loading is below 0.4 as shown in Figure 30. The data (e.g., 18 scfm operating curve) clearly indicate CO_2 capture of greater than 90, 95, and 99% of CO_2 with regenerated lean mixed-salt solutions and CO_2 loadings of 0.4, 0.35, and 0.3, respectively. Figure 31 shows the shift of operating lines with liquid loading. Because the columns were operated well below the flooding level, there is significant room for using much higher gas flow rates and capturing > 90% CO_2. The equilibrium data for the K_2CO_3-NH_3-CO_2-H_2O system shown in Figures 30 and 31 were calculated from the VLE model developed by Dr. Kaj Thomsen (Aqueous Solutions Aps) for SRI's mixed-salt project (DOE Cooperative Agreement No. DE-FE0012959).

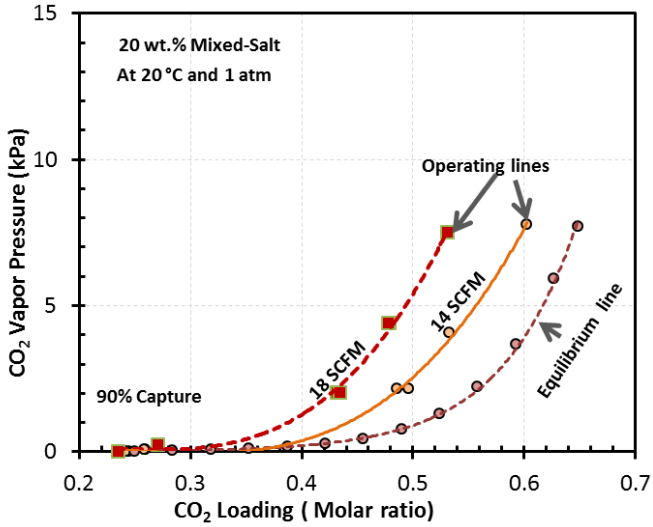

Figure 30. Test data with different gas flow rates and thermodynamic modeling of a 30 wt.% with 14 vol.% CO_2 at 20°C and at 1 atm.

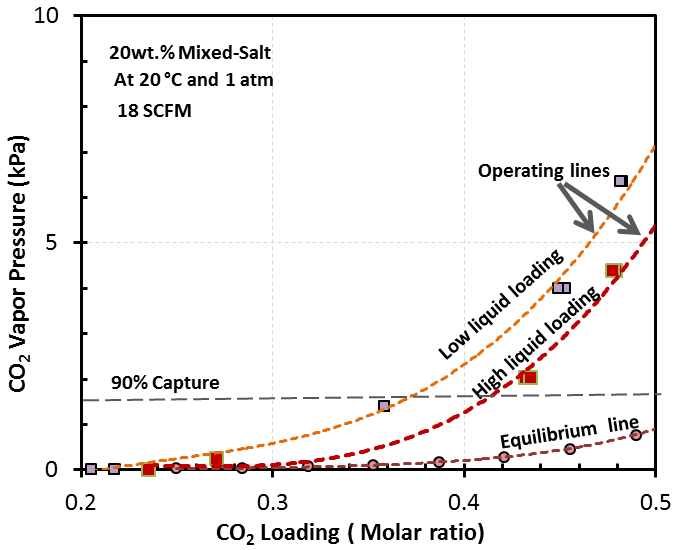

Figure 31. Test data with different liquid loading and thermodynamic modeling of a 30 wt.% mixed salt with 14 vol.% CO_2 at 20°C and at 1 atm.

Absorber run profiles for Runs 4 through 10 are given in Figures 32 through 38. They are as follows: (1) the temperature profile along the absorber column height for the run when the CO_2 loading was 0.4; (2) the temperature profile for (a) the solvent feed tank (b) the top section of the absorber, and (c) the bottom section of the absorber 1 at various CO_2 loadings; (3) the profile of CO_2 inlet and outlet concentrations over time; and (4) the measured CO_2 capture efficiency calculated based on both in-line gas analysis and sampled liquid analysis.

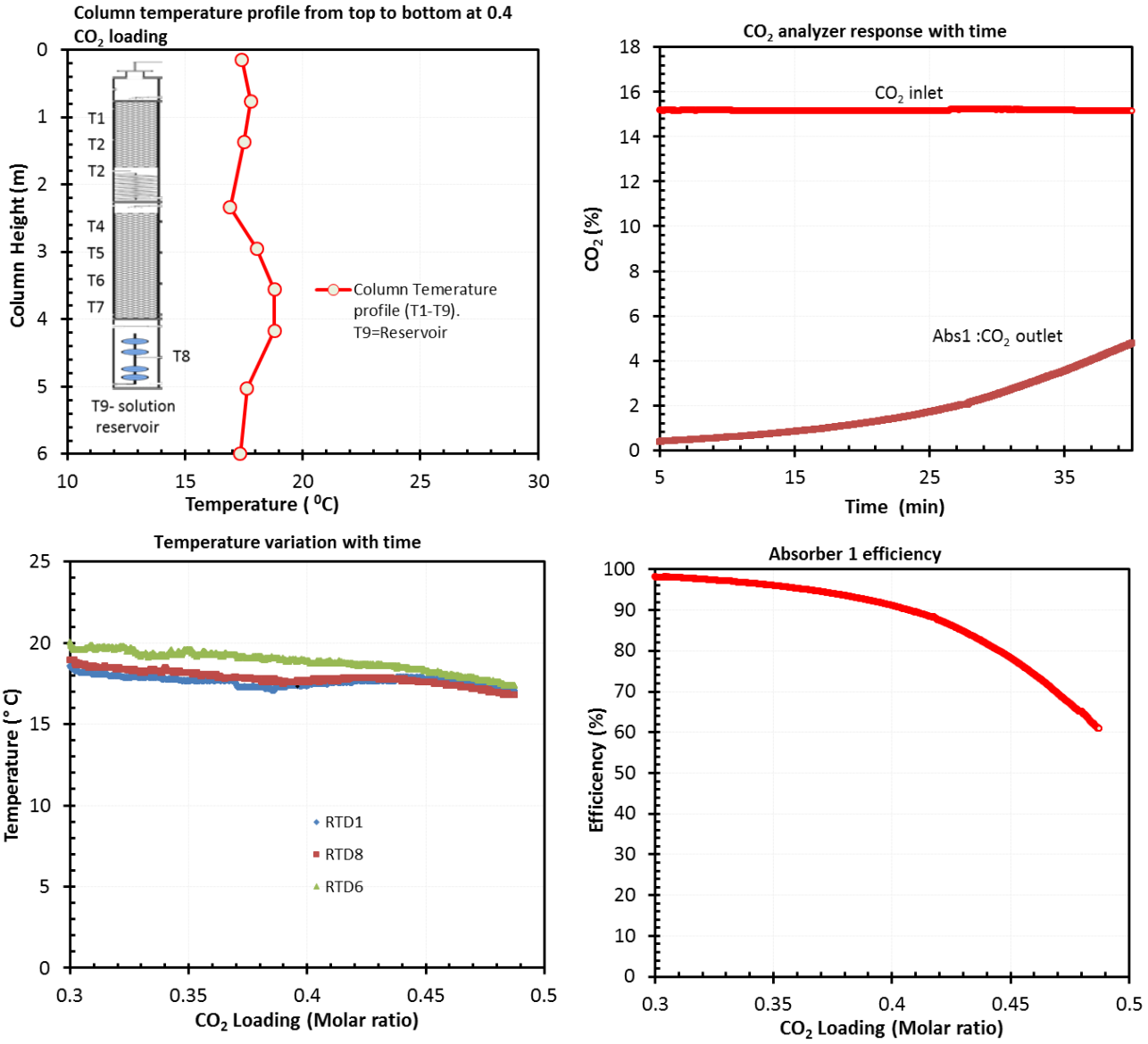

Figure 32. Profiles for Run 4: (CO_2 = 15 vol.%; gas flow rate = 400 slpm; ABS1 only; mixed-salt composition 5X).

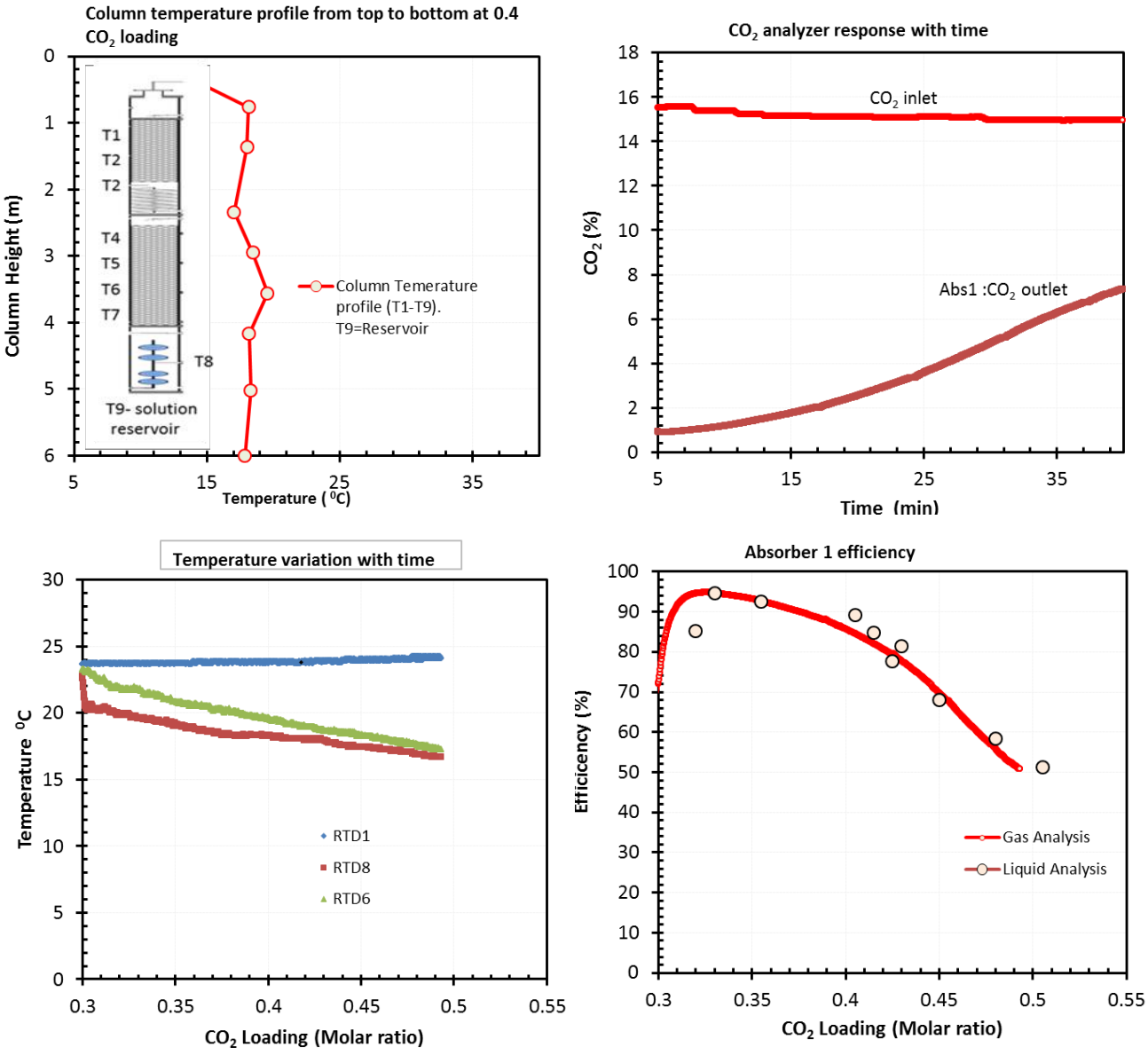

Figure 33. Profiles for Run 5: (CO_2 = 15 vol.%; gas flow rate = 500 slpm; ABS1 only; mixed-salt composition 5X).

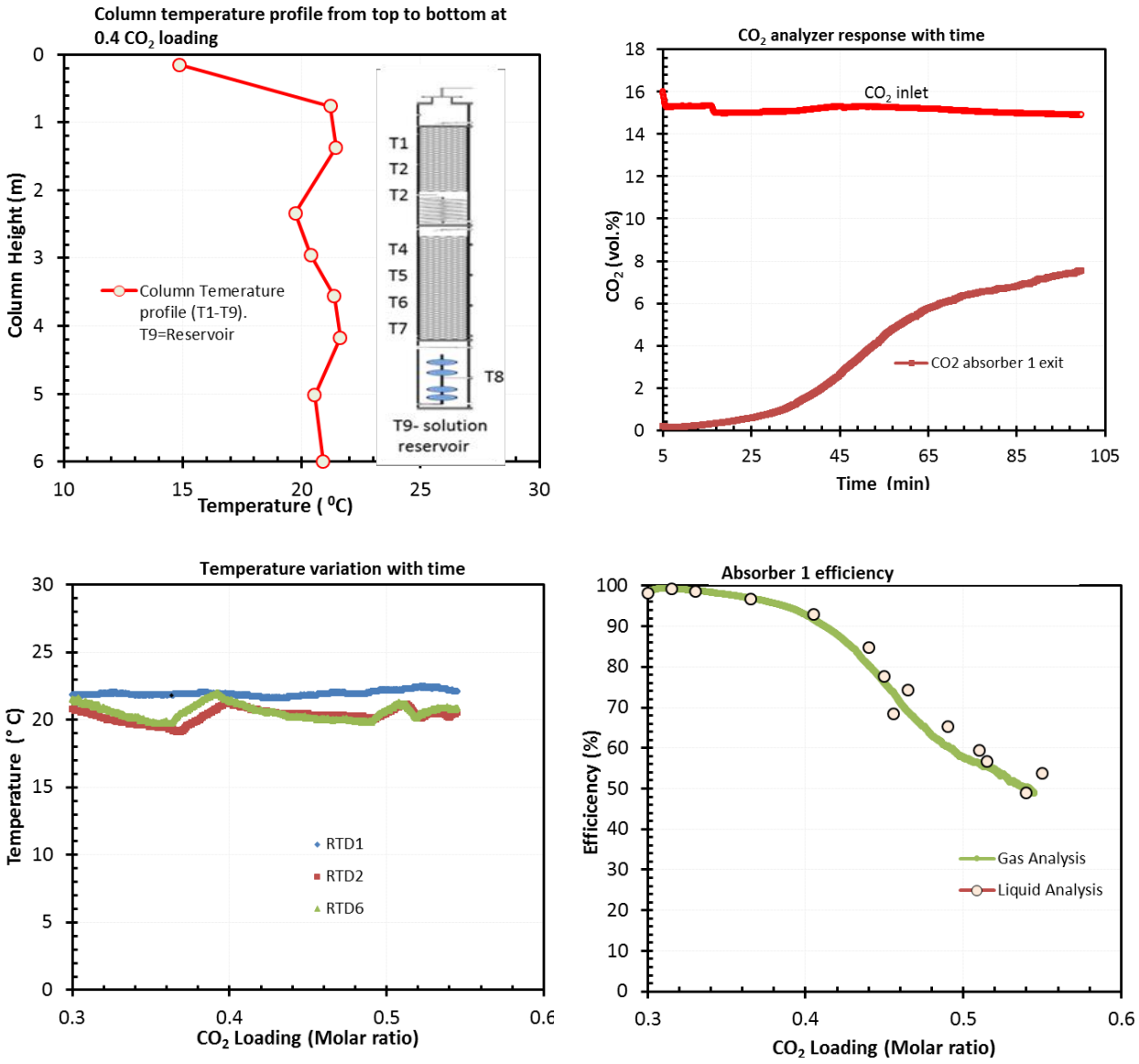

Figure 34. Profiles for Run 6: (CO_2 = 15 vol.%; gas flow rate = 300 slpm; ABS1 only; mixed-salt composition 5X).

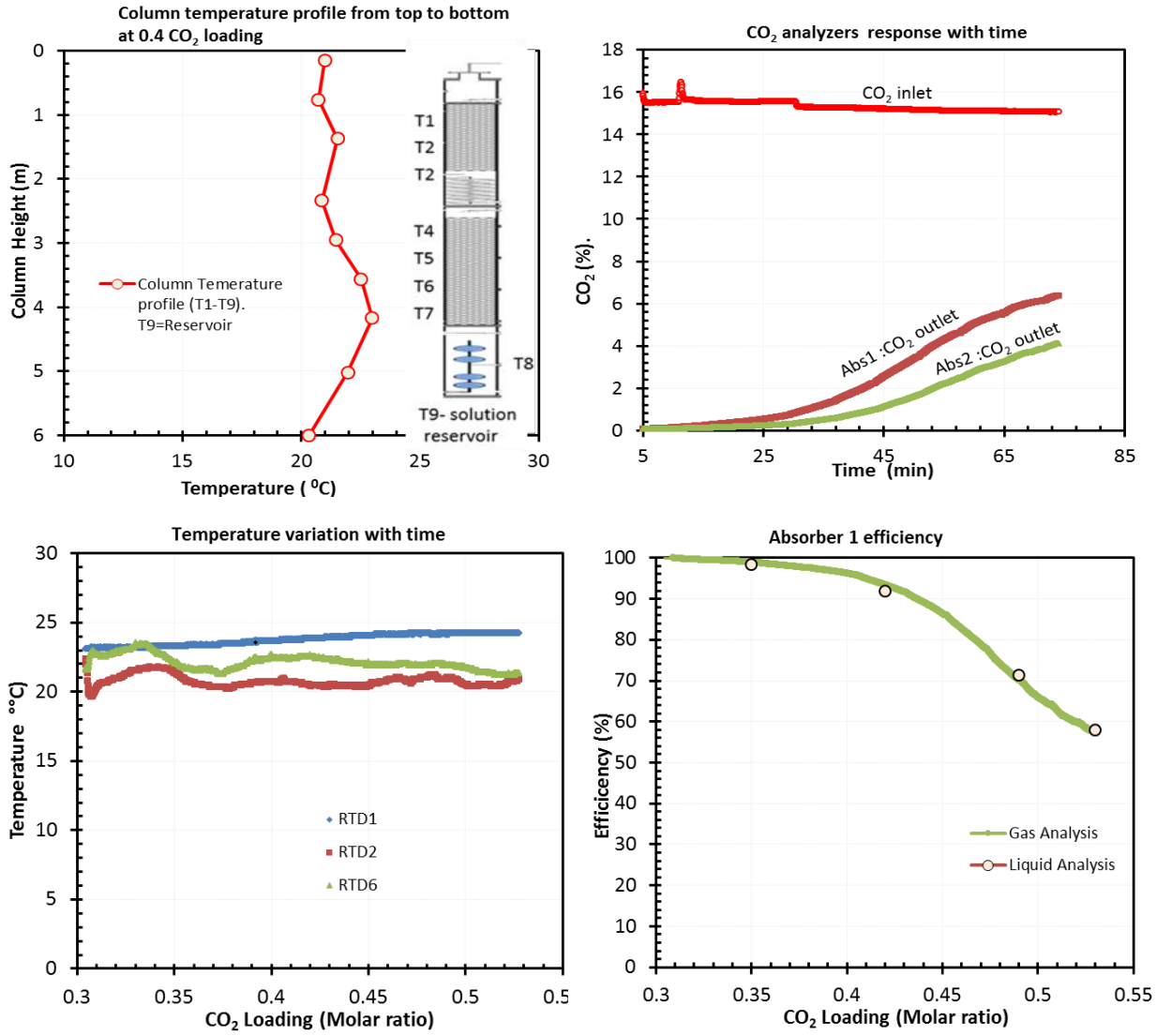

Figure 35. Profiles for Run 7: (CO_2 = 15 vol.%; gas flow rate = 300 slpm; ABS1 & ABS2; mixed-salt composition 5X).

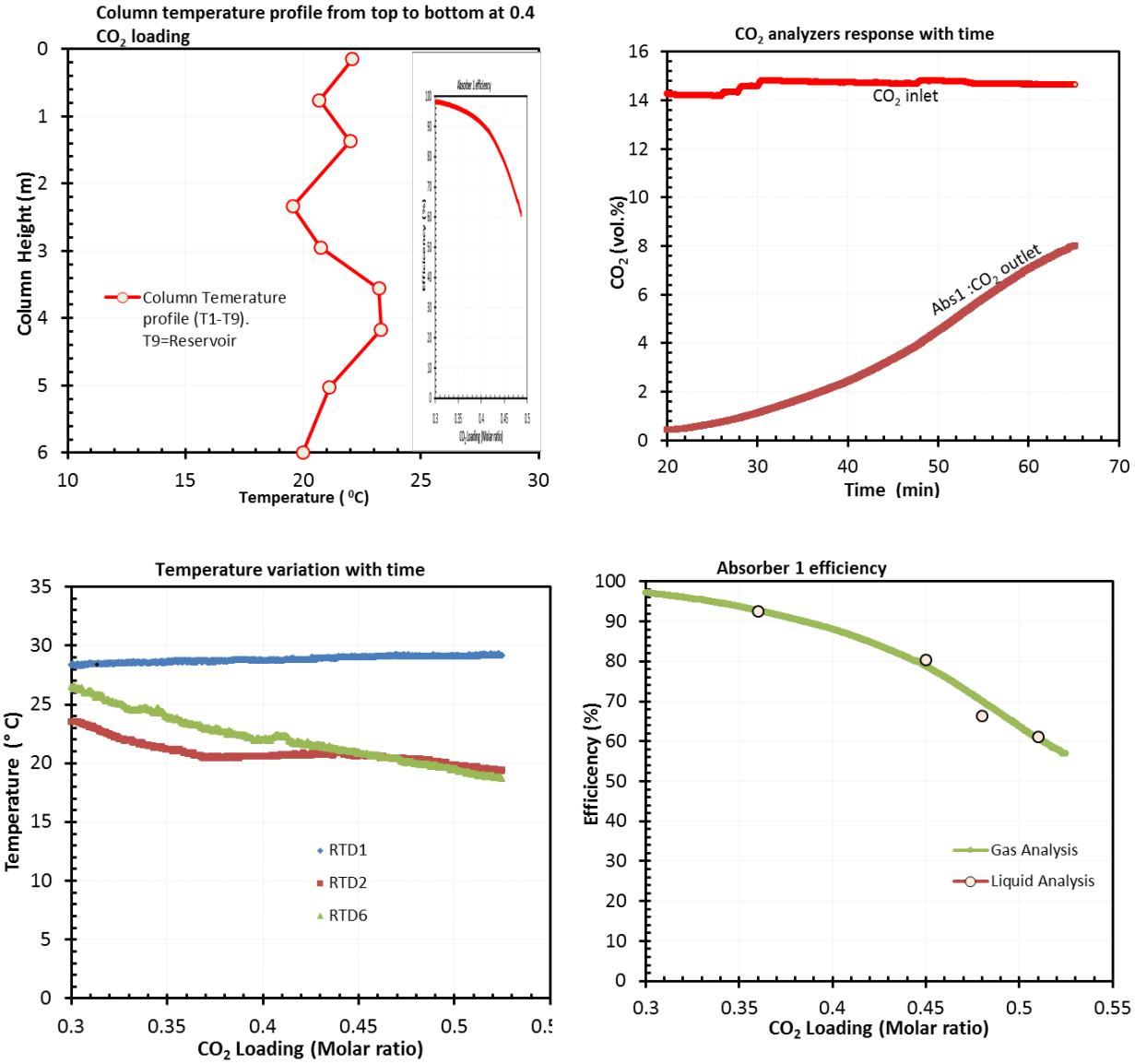

Figure 36. Profiles for Run 8: (CO_2 = 15 vol.%; gas flow rate = 500 slpm; ABS1 only; low liquid loading; mixed-salt composition 2X).

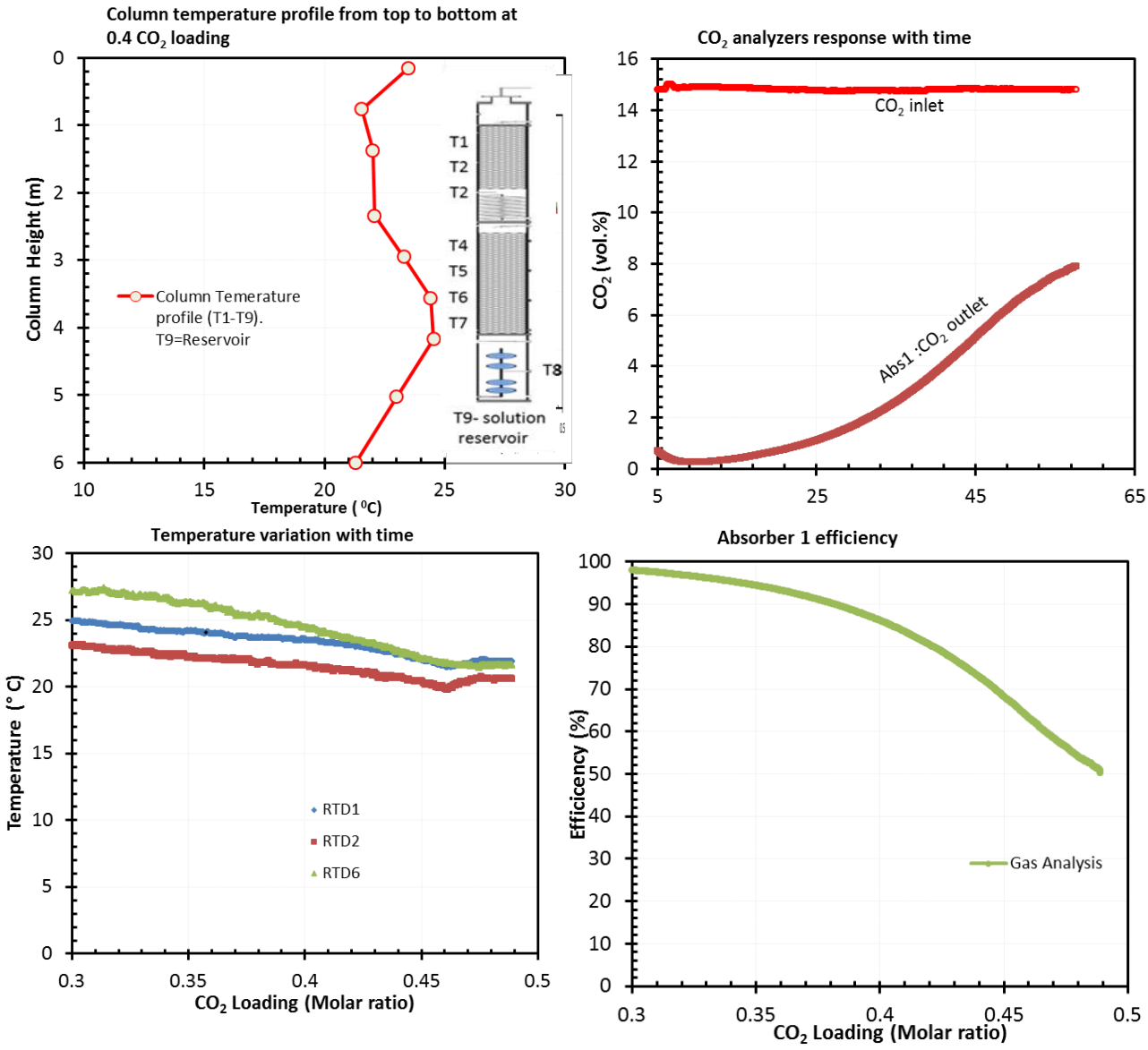

Figure 37. Profiles for Run 9: (CO_2 = 15 vol.%; gas flow rate = 500 slpm; ABS1 only; high liquid loading; mixed-salt composition 2X).

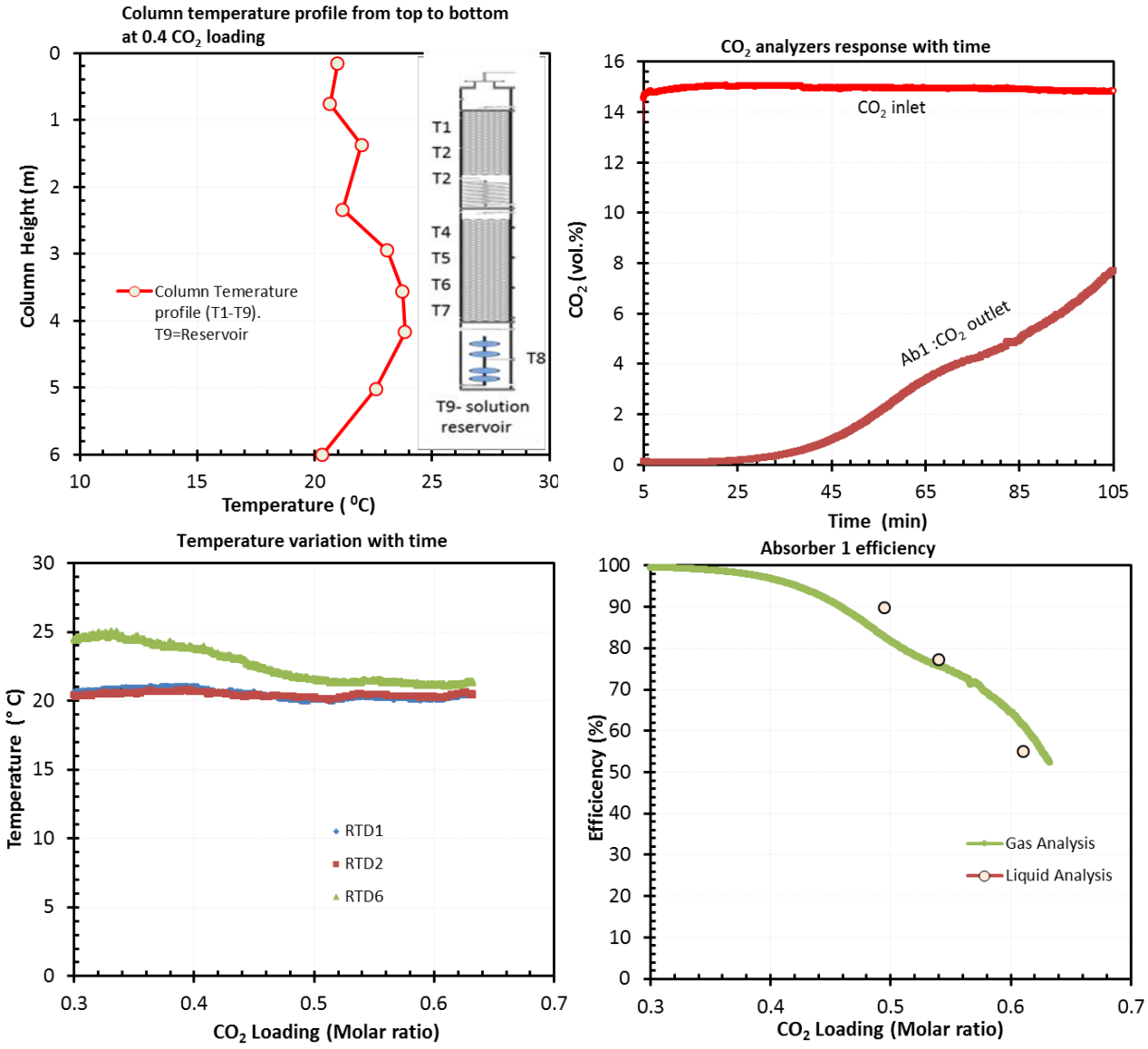

Figure 38. Profiles for Run 10: (CO_2 = 15 vol.%; gas flow rate = 400 slpm; BS1 only; mixed-salt composition 2X).

Test Series 3

Table 4 shows the run log for Test Series 3. In this test series, we studied the effect of packing type on the CO_2 absorption rate. The absorber 1 lower section (7 ft.) is packed with (Sulzer MellaPakPlus®) 450 m^2/m^3 and the absorber 2 lower section (7 ft.) is packed with 350 m^2/m^3 packing material. Since the columns can be operated independently, we can perform a direct comparison of absorption rates on each packing type when we run the tests under identical conditions.

Table 4. Run log table for Test Series 3.

Run #	ABS-1 Concentration (wt. %)	ABS-1 N/K Ratio	CO2 Flow Rate (LPM)	Air Flow Rate (LPM)	Total Gas Flow Rate (LPM)	ABS1 Liquid Recycle Rate (LPM) Top feed	ABS1 Liquid Recycle Rate (LPM) Middle Feed	ABS2 Liquid Recycle Rate (LPM)
11	21	2x	5	380	40	0	0	24
12	21	2x	10	360	40	0	0	24
13	21	2x	15	340	40	0	0	24
14	21	2x	5	380	40	0	24	
15	21	2x	10	360	40	0	24	
16	21	2x	15	340	40	0	24	
17	21	2x	5	380	40	0	24	
18	21	2x	5	380	40	0		24

We also conducted tests to determine solution composition and loading to reach 90% CO_2 capture for a given gas flow rate. Figure 39 shows data for Run 19 conducted with mixed-salt solution with high CO_2 loadings (0.42 – 0.46 in absorber 2 and 0.45 to 0.57 in absorber 1). Test parameters were as follows: 15 vol.% CO_2; 400 scfm gas flow; 20 °C; 21 wt.% mixed salt. The graph at the top shows the CO_2 loading of the mixed-salt solution at the top of each column, and the graph at the bottom section shows the corresponding efficiency. The data showed that even with highly CO_2-loaded solutions (0.4 to 0.6 range), an overall 90% CO_2 capture was achieved in the current system with only an 11-ft column height in absorber 1 (ammonia rich) and a 7-ft column in absorber 2 (potassium rich).

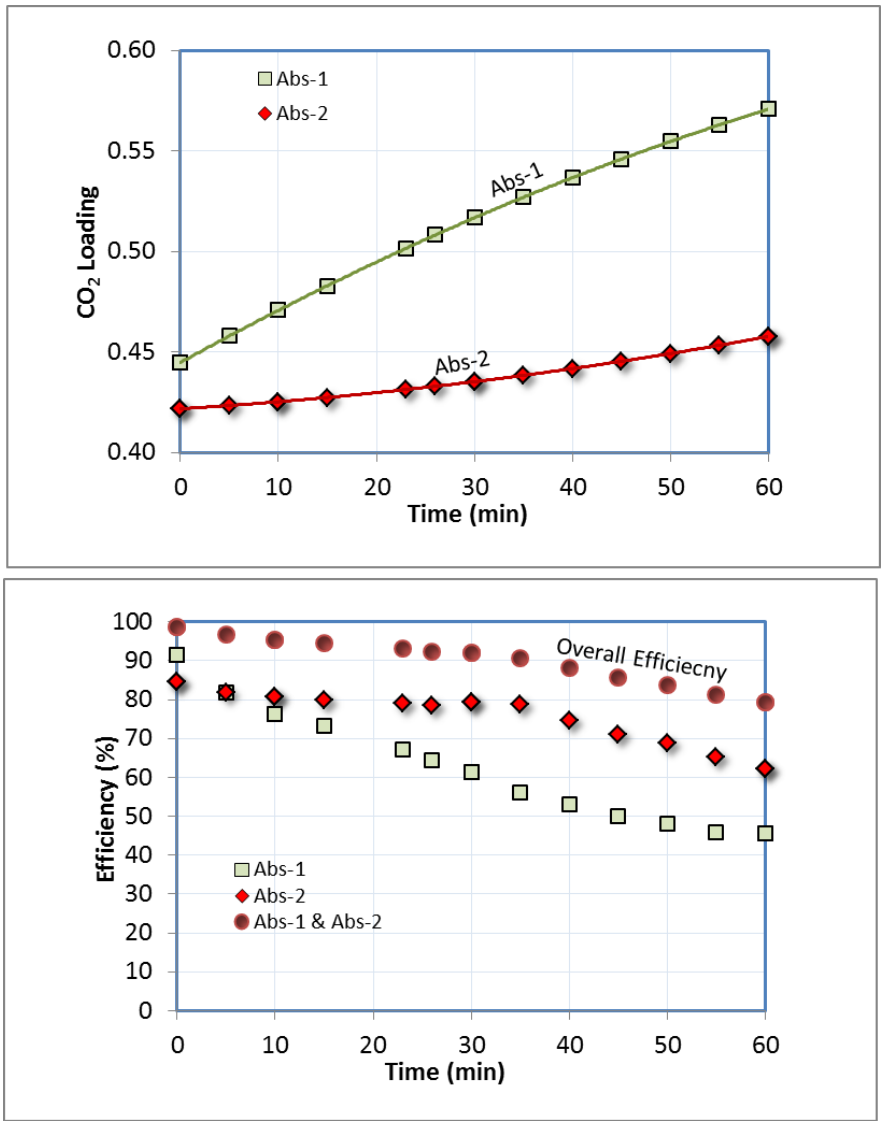

Figure 39. Measured CO_2 capture efficiency in absorber 1 and 2 at varying CO_2 loadings.

Regenerator System

Design, installation, and testing of the BP1 regenerator system. The regenerator unit for BP1 is a semi-continuous bench-scale unit (a modified version of an existing batch system); a simplistic schematic proposed in the proposal is shown in Figure 40. This regenerator was built by modifying an existing column that was used for the high-pressure absorption system. The design for the regeneration system modification was completed in Q2. The finalization of the regenerator modification was completed in Q3. The testing of the BP1 regenerator was started after completion of the Series 1 and 2 (21 wt.% salt) of the absorber testing.

This small BP1 regenerator served two purposes: (1) regenerating feed solutions for batch mode absorber operation; and (2) producing data for vapor phase compositions of CO_2, H_2O, and NH_3 under isothermal and isobaric conditions for designing a dual-stage regenerator for integrated testing in BP2. The plan was to operate (ongoing) the semi-continuous regenerator in the temperature range of 120° to 170°C and a pressure range from 10 to 30 bar and collect as many data points as possible during BP1. This data would then be used to determine the rate of desorption of CO_2 at elevated temperatures and pressures.

In the BP1 regenerator, we used an electrical heating system that circulates a heat transfer fluid through a heat exchanger coil in the bottom of the reactor. Solutions that have been loaded with CO_2 from absorber testing or synthetically prepared by dissolving mixed-salt solutions with appropriate concentrations were used as the feed. The rich solution was introduced continuously from the top of the regenerator over the packed bed. The solution drips down the packing, and it is heated to the regeneration temperature at the bottom with the heating coils. The solution, as it drips down through the packing, is also heated by the hot CO_2 leaving the boiler section of the regenerator, steam generated in the boiler, and by the absorption of ammonia. This arrangement simulates a packed column with a reboiler.

The lean solution was withdrawn from the bottom of the reactor through a pressure let-down valve. The temperature and pressure inside the regenerator can be varied to determine the extent of regeneration of the feed solution as a function of pressure and temperature. The flow rates of CO_2 were monitored continuously. Samples of the solution were withdrawn periodically to determine changes in its composition and to confirm the mass balance calculated from the gas flow rate data.

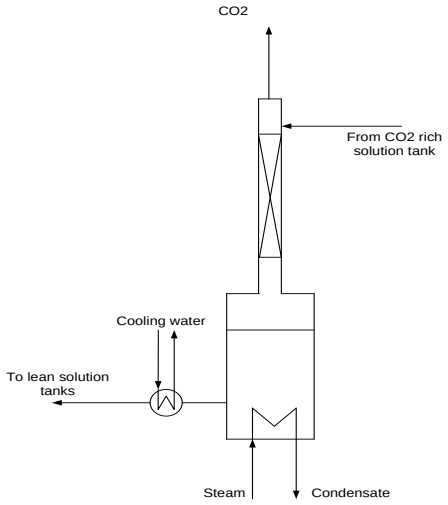

Figure 40. Simplified schematic of a semi continuous batch regenerator system.

Figure 41 shows the schematic of the actual system installed at SRI. Some of the features of the older design were left unchanged as they would be useful in expanded parametric studies. The following is the list of features of this regenerator.

- Static, semi-continuous or continuous operation.
- Operation with two rich feed streams at two different temperatures (and liquid flow rates) to simulate the rich-warm split.
- This system was originally built and commissioned in February 2014 as a high-pressure absorber for capturing CO_2 from syngas at elevated temperatures (40-100°C) and pressures (10 to 30 bar) with L/G up to 10 for 200 slpm gas flow rate (25% CO_2,

50%H_2, and 25% N_2). For this system, a second high-pressure liquid feed pump was added to match the process of rich solution from a 25-acfm absorber with 90% CO_2 capture capacity.

- The system can still operate as a high-pressure absorber or a regenerator. These options are useful in the mixed-salt process, as the volatile species stripped from the bottom regenerator are reabsorbed at the top regenerator. This allowed us to simulate the process in two stages without having an actual two-stage regenerator to get data for design of the dual-stage regenerator in BP2.

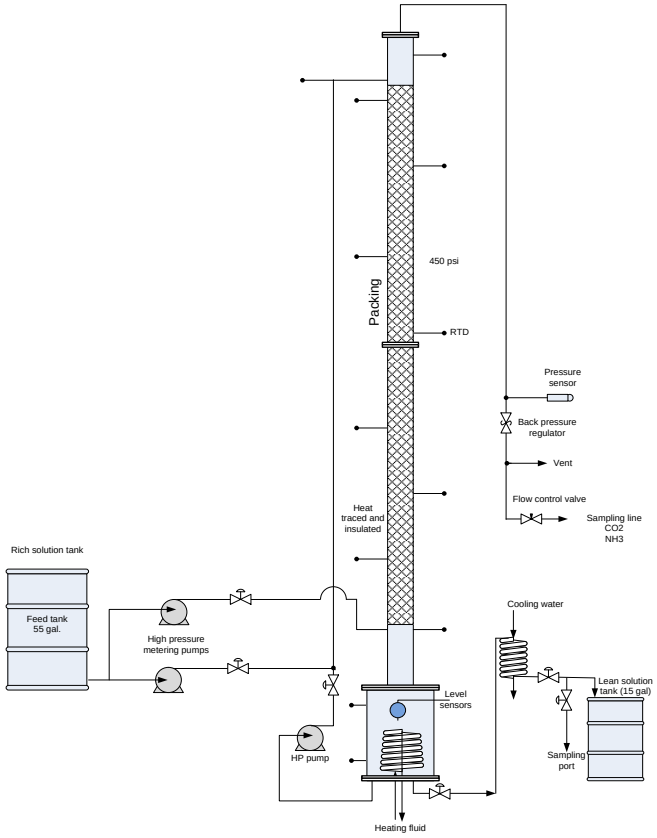

Figure 41. Continuous flow/batch regenerator system for mixed-salt system as built in BP1.

Figure 42 shows a series of photographs of the top section of the regenerator being assembled and installed. Figure 43 shows a photograph of the completed regenerator system. The stripper column, solution feed, and stripped CO_2 scrubbed gas exit lines are insulated and heat traced. The heat tracing system is controlled by five temperature controllers. The two high-pressure pumps are of connected to deliver rich solution at a 2-liter per minute rate. The top section of the stripper is packed with elements of Sulzer packing 316 SS BX+ for the 50.8-mm diameter column (surface area = 480 m^2/m^3).

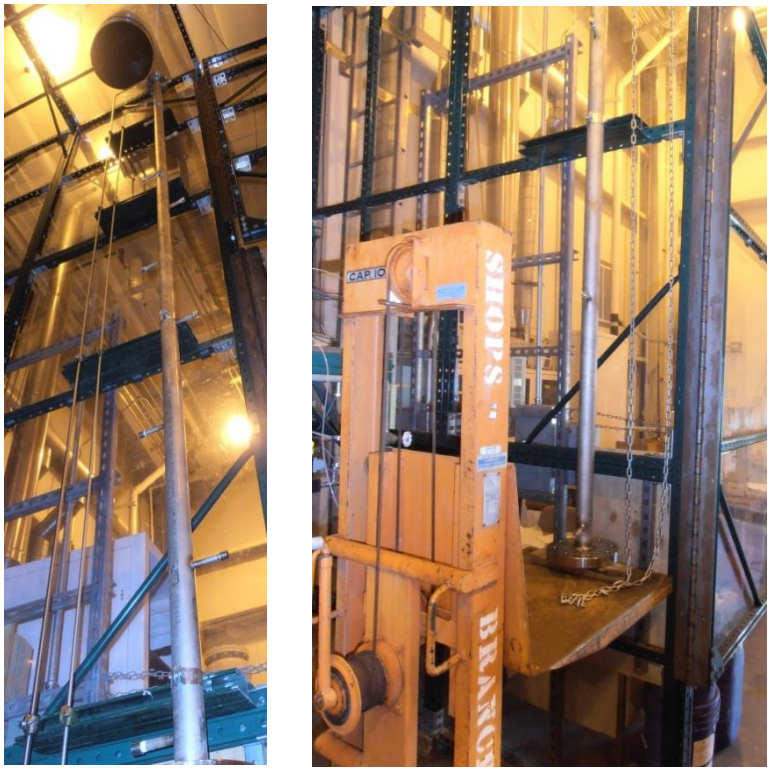

Figure 42. Column assembly and installation.

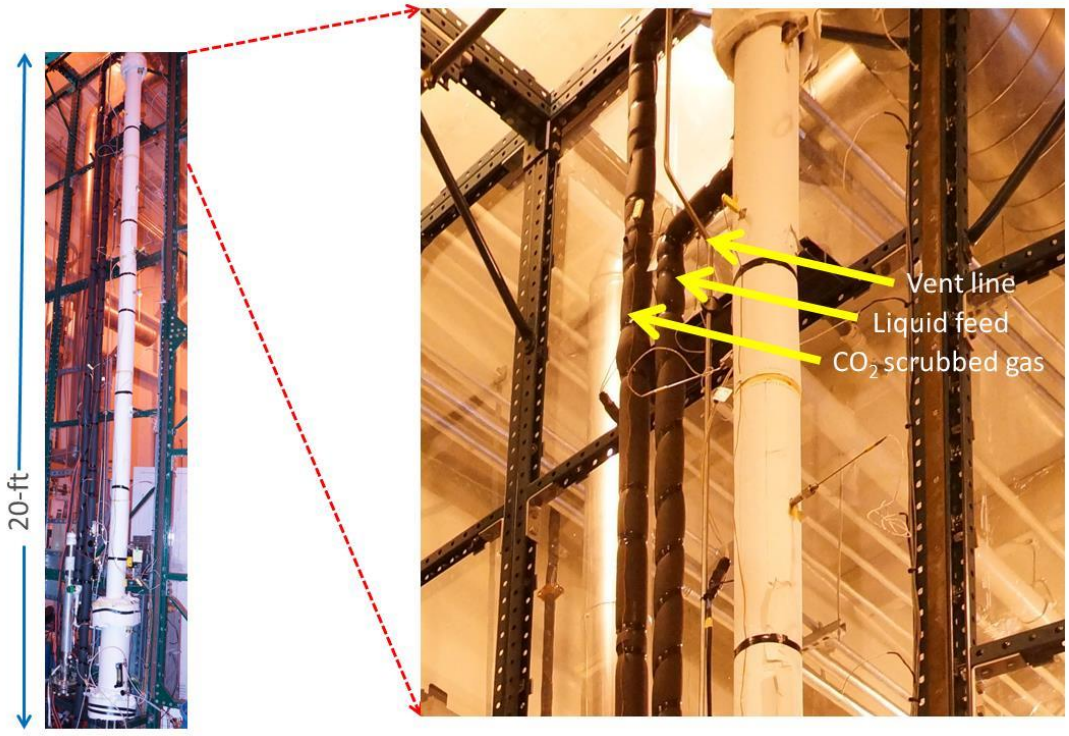

Figure 43. Photographs of absorber column and column details.

Results from regenerator testing. A semi-continuous smaller regenerator (25 scfm) was built to collect data to design the larger regenerator (REG-BP2) required to match the current absorber (100 scfm). We have completed the initial screening testing of the regenerator to identify the operational issues that can be addressed in the continuous flow regenerator with two stages. We continued regenerator tests with 20 and 30 wt.% mixed-salt compositions. We conducted the majority of the parametric testing of the regenerator during the October – December 30 2014 period. Figure 44 shows the regenerator data for rich solution from absorber test series 1.

We attempted to estimate the heat requirement for stripping volatile species by using the data shown in Figure 44. The method use is similar to the isosteric heat of adsorption of CO_2 estimated from the experimental adsorption isotherms by making use of the Clausius-Clapeyron equation: $Q_{st} = -R_g [\ln P/(1/T)]_n$ where Q_{st} is the isosteric heat of adsorption at an adsorbed amount n, T is the temperature, P is the pressure of the gas phase, and R_g the universal constant of gases (8.314 J mol^{-1} K^{-1}. Plotting (lnP) against (1/T) at constant adsorbed amounts (isosteric) yields a straight line, and its slope is equal to: -Qst/Rg (Figure 44). However, application of the Clausius-Clapeyron equation for calculating enthalpy is only valid for the evaporation of ideal gases from non-reactive systems, such as a mixture of hydrocarbons and has its limitations for reactive systems.

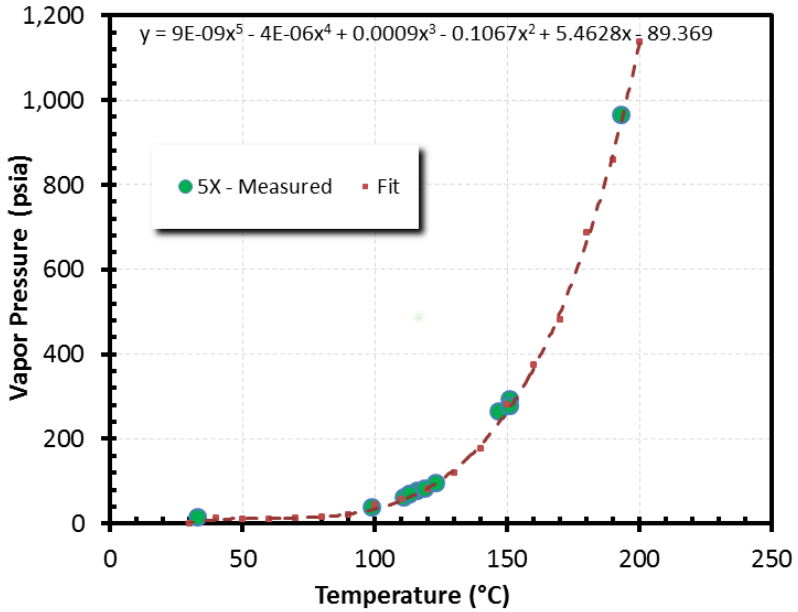

Figure 44. Vapor pressure with temperature curve for rich solution from absorber test series 1 (composition 5X).

Figures 45and 46 show the data for rich solution from absorber 1 testing (Test Series 1 with 20 wt.% mixed-salt (composition 5X, CO_2 loading at 0.5) and a rich solution prepared with composition 10X (20 wt.% mixed salt with 0.5 CO_2 loading). Analysis of data shown in

Figure 45 yielded a differential enthalpy of 45± 5 kJ/mol, while the data for composition 10X (Figure 46) yielded a differential enthalpy in the rage 39 to 47 kJ/mol (two distinctive regions were identified). The two regions seen in Figure 46 could be explained by considering changes to the hydrogen bonding. In general in hydrothermal systems, the hydrogen bonding network is diminished above 150° C.

This way of enthalpy estimation is very rudimentary for reactive systems; however, these estimated numbers are the upper limit and justify that the heat enthalpy for volatilization of gaseous species is 45± 5 kJ/mol.

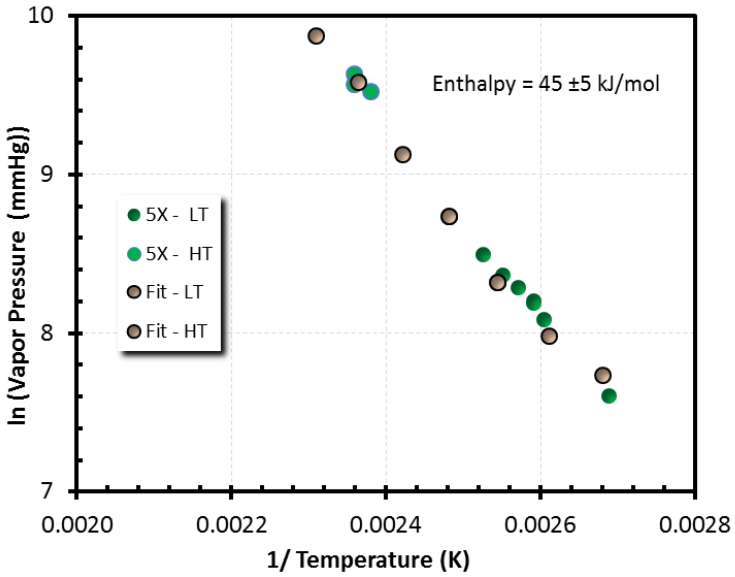

Figure 45. Logarithmic vapor pressure with temperature for data shown in Figure 41.

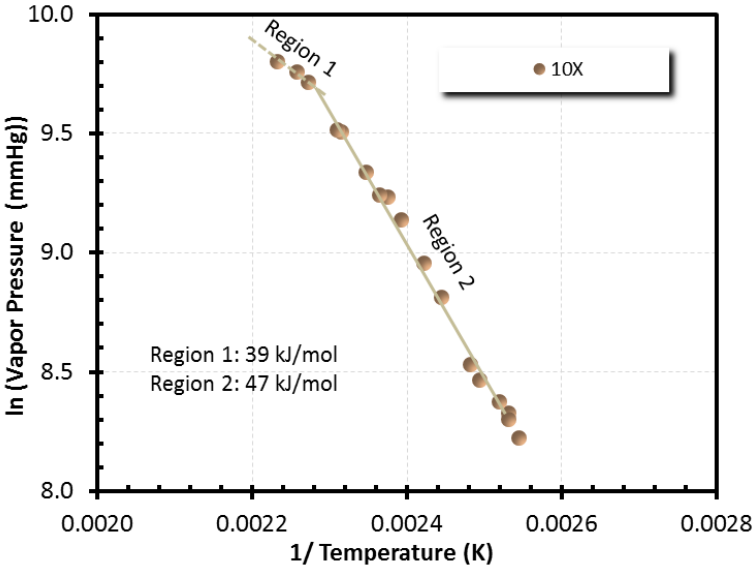

Figure 46. Test data for regeneration of 20 wt.% mixed solution (ammonia to K- ratio = 10X).

Our team member, Dr. Kaj Thomsen, suggested the calculation of the heat of absorption of CO_2 in the mixture using the "bubble-template" in the extended UNIQUAC model. The "differential enthalpy of absorption of each gas, kJ/mol" is equivalent to the enthalpy of evaporation. We made a comparison of predicted numbers from the UNIQAC model by assuming a Clausius-Clapeyron behavior and using the experimental numbers. For this testing, a known solution (CO_2 loading ~ 0.5) was loaded into the regenerator and the system was heated to about 175°C while registering the pressure generation. At 175° C, the pressure in the system was about 25 bar. Liquid samples from the bottom of the regenerator were collected during the heating when the regenerator pressure reached 5, 14, and 20 bar, respectively. The pressure and the temperature data for a selected run are given in Figure 47 (left side plot). Also presented in Figure 47 (right side plot) are the V-L-E modeling data showing the number of moles of ammonia expected to be in the vapor phase at 5, 10, and 20 bar at varying temperatures. The red arrows are drawn to indicate the corresponding moles of ammonia evaporated at a given temperature and pressure from both regenerator testing and V-L-E modeling. We find that the agreement of experimental data and the modeling is very good.

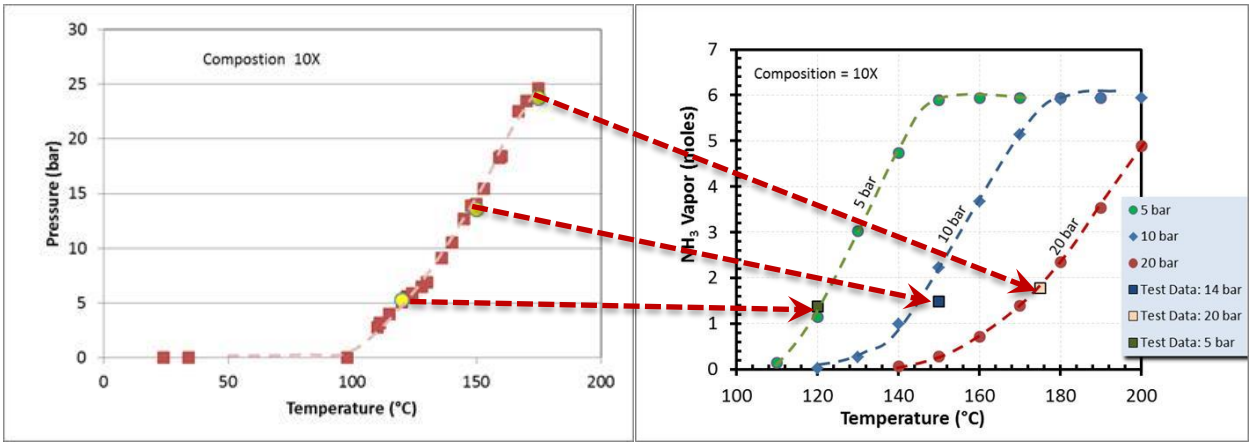

Figure 47. Comparison of regenerator test data with VLE modeling data.

The data shown on the left plot is from static regenerator testing. The data shown in the right plot is the data from VLE modeling. Test data at 5, 14, and 20 bar are also shown on the plot in the right with the modeled data for comparison. For modeling, a 38-wt% mixed-salt solution with 0.6 CO_2 loading was used.

Ammonia stripping in the bottom regenerator: To generate the K-rich stream, ammonia has to be stripped off from a portion of the lean solution from the regenerator. Figure 48 shows the number of moles of ammonia stripped from a 38-wt.% mixed-salt solution (0.6 CO_2 loading) at 5, 10, and 20 bar. This data show that almost all the ammonia can be stripped at 5 bar at 150 °C. Based on these results, a design point for bottom regenerator for a specific ammonia-stripping value can be selected for a given absorber operating condition (the K-rich absorber).

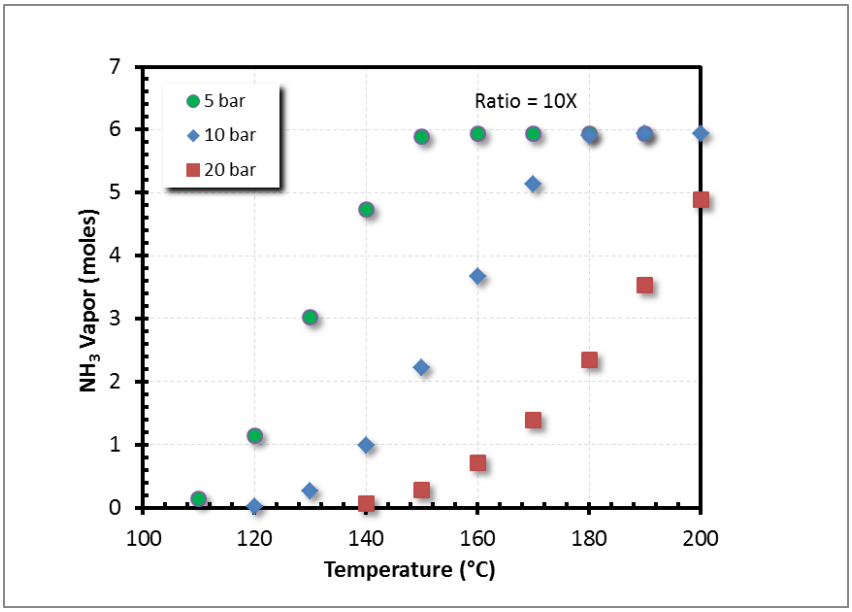

Figure 48. The NH_3 stripping potentials at various pressures and temperatures are shown for the 38-wt.% mixed-salt solution with a 0.6 loading.

Water stripping in the top regenerator. The dual regenerator system is designed to reduce water stripping. First, operation of the regenerator at a higher pressure reduces the water stripping from the solution. In addition, a temperature gradient is maintained to further reduce the water vapor pressure at the regenerator exit. Figure 49 shows the water and CO_2 vapor pressures for a 38 wt.% mixed-salt solution with varying CO_2 loadings at 20 bar.

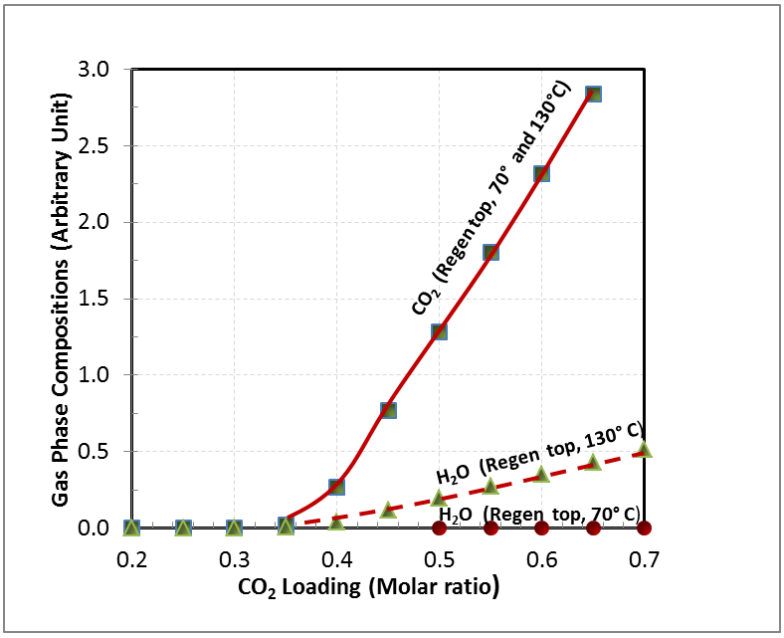

Figure 49. The CO_2 stripping at high pressure with reduced water stripping potential for various pressures and temperature CO_2 loadings are shown for 38-wt.% mixed-salt solution at 20 bar.

Continuous flow regenerator tests: The BP1 regenerator system (Figure 41 above) was operated with continuous rich-solvent feed into the regenerator. The regenerator has two liquid feed inlets: (1) one at the top section of the regenerator column, and (2) a second liquid feed inlet in the bottom section of the regenerator column. We ran the tests with a split flow scheme and used both inlets to feed the rich solution to control the ammonia emission and the temperature of the regenerator column. The rich solutions tested were 20-wt% mixed-salt (test ID: 5X) with 0.49 CO_2 loading. During the testing, the regenerator top section temperature was varied between 40 to 120° C, and the regenerator bottom section temperature was varied between 120 to 160 °C. The test pressure was varied between 5 to 12 bar. The liquid feed rate was 0.20 liters /min, and the measured CO_2 striping rate was 4 to 10 SLPM depending on the regenerator temperature and pressure. Table 5 shows results from the completed tests.

Table 5. Results from continuous flow testing of the regenerator with composition 5X.

Run Number	Regenerator Temperature °C	Regenrator Pressure bar	CO2 Stripped mole	NH3 Stripped mole	Rich Loading	Lean Loading
1--4	120	10.5	0.13	0.14	0.49	0.46
1--9	126	11.5	0.29	0.04	0.49	0.44
3--5	150	5.2	1.50	2.68	0.49	0.21
3--6	150	5.5	1.45	2.54	0.49	0.22
3--5	150	5.2	1.50	2.68	0.49	0.21
3--6	150	5.5	1.45	2.54	0.49	0.22
3--7	150	5.6	1.38	2.38	0.49	0.23
4--3	161	10.8	1.27	0.52	0.49	0.25
4--4	160	11.5	1.26	0.14	0.49	0.26
4--5	160	11.3	1.26	0.04	0.49	0.25

Rich solutions with 30-wt% mixed-salt (test ID: 2X) with 0.40 CO_2 loading were also tested. Those results are given in Table 6.

Table 6. Results from continuous flow testing of the regenerator with composition 2X.

Run Number	Regenerator Temperature °C	Regenrator Pressure bar	CO2 Stripped mole	NH3 Stripped mole	Rich Loading	Lean Loading
5--1	115	8.7	0.09	0.01	0.40	0.39
5--2	133	10.9	0.69	0.01	0.40	0.28
5--3	134	11.3	0.70	0.01	0.40	0.28
5--4	136	11.3	0.80	0.01	0.40	0.26
5--5	140	11.6	0.96	0.04	0.40	0.24
5--6	150	12.1	1.23	0.04	0.40	0.19
6--1	143	11.2	1.08	0.02	0.40	0.21
6--2	144	11.1	1.16	0.01	0.40	0.2
7--1	142	11.7	0.98	0.00	0.41	0.25
7--2	142	11.2	1.04	0.05	0.41	0.24

Figure 50 shows the number of moles of CO_2 stripped in each run in the pressure ranges of 6-7 and 11-12 bar in the temperature range of 120 to 160 °C for 20-wt% mixed salt solutions (Id-5X). As expected, CO_2 stripping increased with increasing temperature and decreasing pressure. Figure 51 shows the number of moles of NH_3 stripped at 150 °C in the pressure range of 5 to 12 bar.

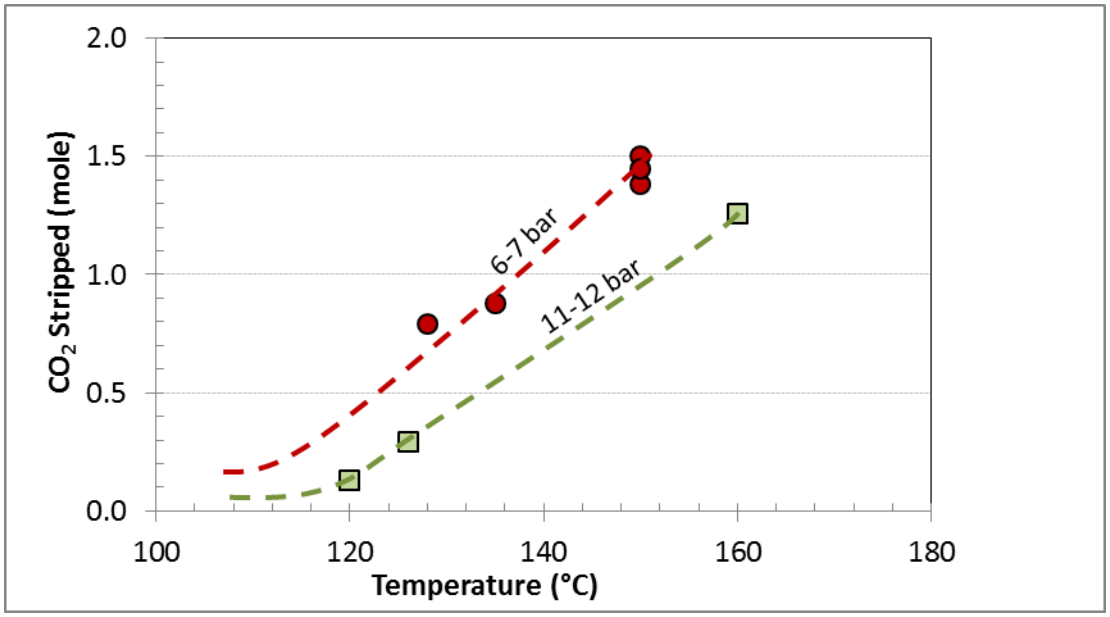

Figure 50. CO_2 stripping as a function of regenerator temperature and pressure.

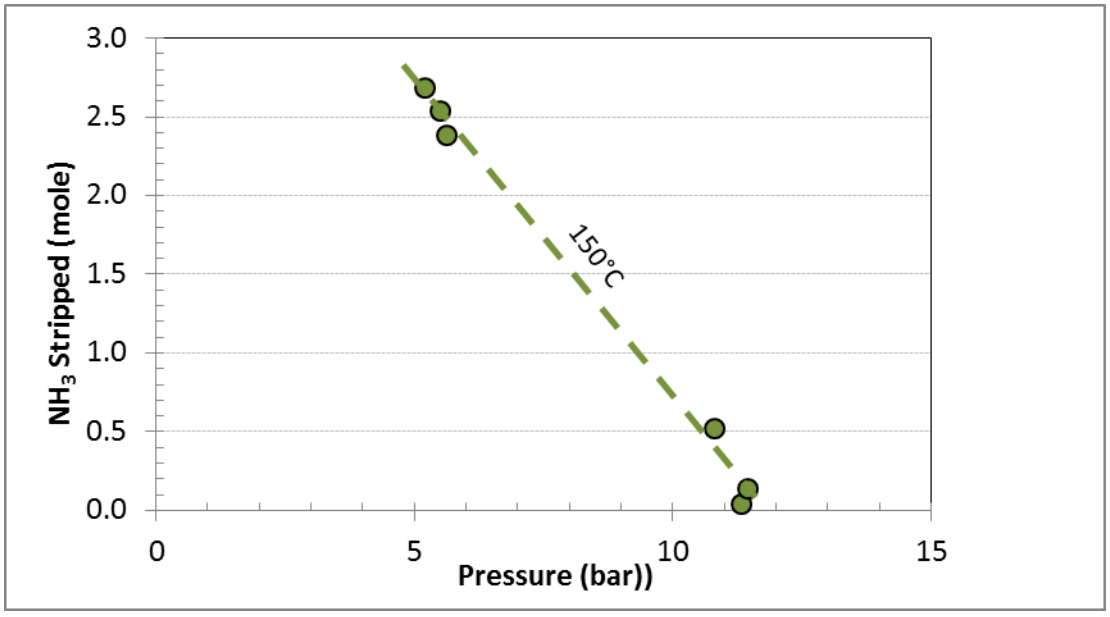

Figure 51. NH_3 stripping as a function of pressure at 150 °C.

It is important to note that the CO_2 stripping is highly temperature dependent, and the ammonia stripping is pressure dependent. Data from Figure 51 clearly indicate that a two-stage regenerator with a flash for removing ammonia to generate ammonia-lean absorption solution is possible.

Figure 52 shows the measured lean loading form each run conducted in the temperature range of 120 to 160 ºC. The data in Figure 52 shows that lean loadings less than 0.2 can be achieved.

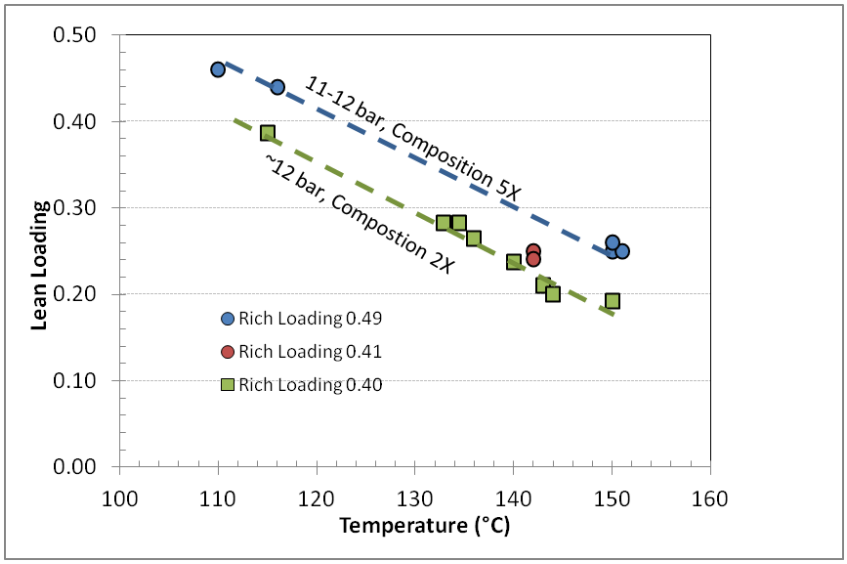

Figure 52. Measured values for CO_2 lean loading at 6-7 and 11-12 bar pressure in the temperature range 120 to 160°C.

During the regenerator testing, we also conducted tests to check the operability of the system with minimum ammonia and water evaporation. For such operation, the regenerator column top needs to be kept at a lower temperature to condense the ammonia and water vapor. Figures 53 and 54 show sample temperature profiles. There are 11 resistance temperature detectors (RTD, identified as RTD0 to RTD11) that measure the temperature. These figures show the recorded temperature at various time stamps (e.g., 3000 = 60 min run time). In the mode of operation shown in Figure 53, most of the ammonia is recovered in the lean solution (no stripping of ammonia). In the mode of operation shown in Figure 54, ammonia was stripped off from the lean solution (see the data in Figure 51). These types of tests helped (1) to collect information for the design of the regenerator in BP2, and (2) to gain experience to operate the integrated system in BP2.

The regenerator performed as designed without any process issues. The pressure, temperature, and stripped CO_2 flow were stable once the system reached steady state. Figure 55 shows the process pressure stability and CO_2 stripping rate during steady-state operation of the system at ~ 11.5 bar at 160 °C (Run 4-4 in Table 5).

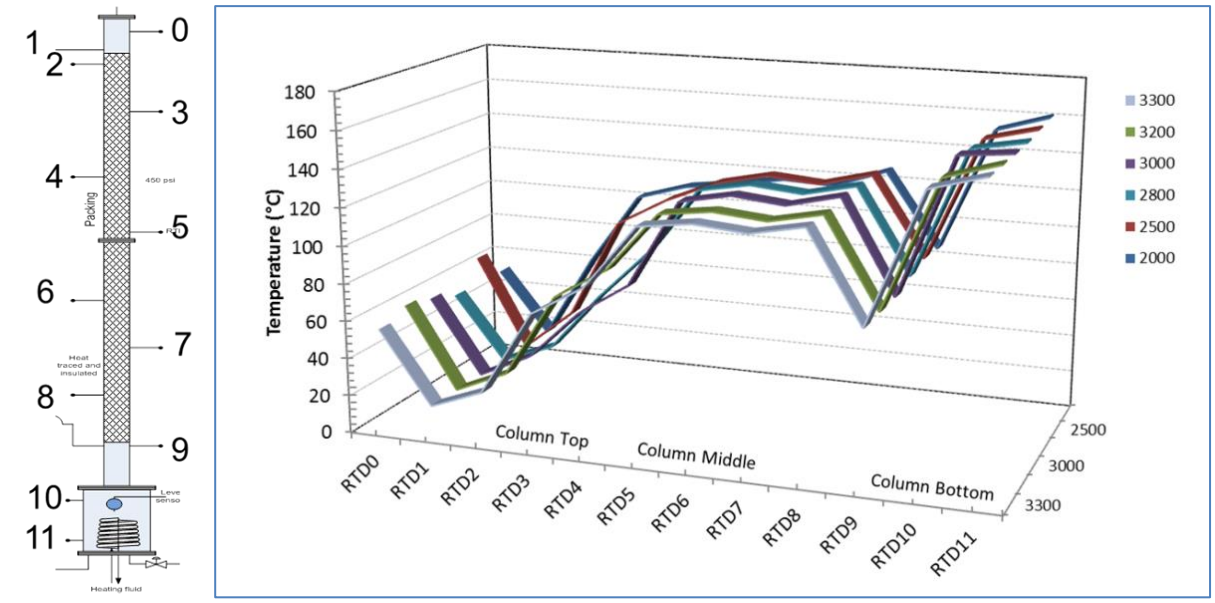

Figure 53. Temperature profile along the regenerator column; the column top (RTD 3) was kept at <º60 °C to condense ammonia.

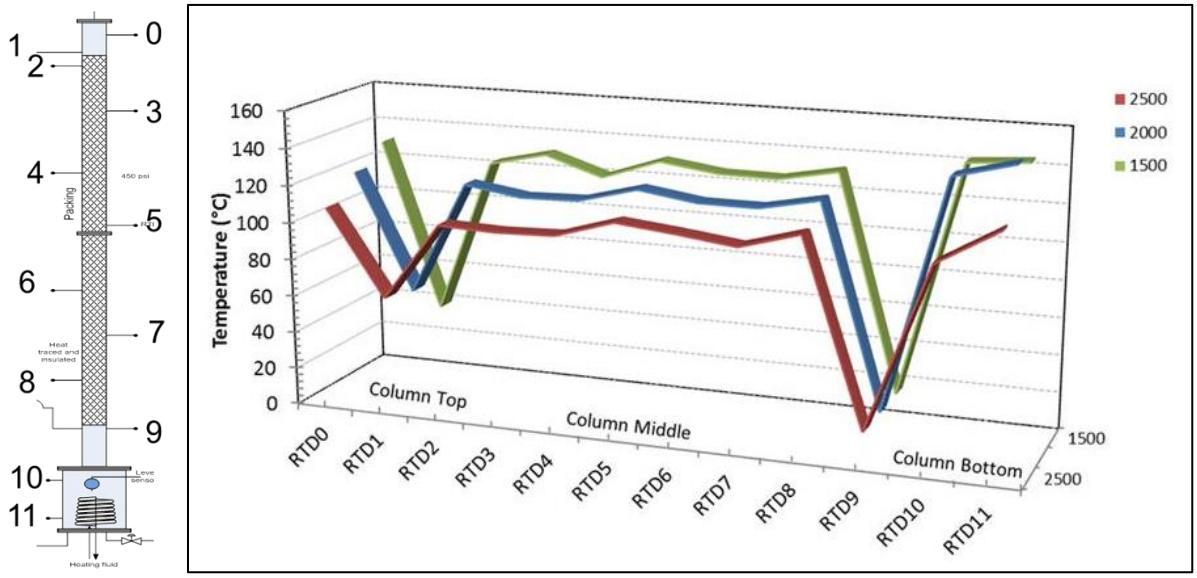

Figure 54. Temperature profile along the regenerator column; the column top (RTD 3) temperature was >120 ºC to strip ammonia.

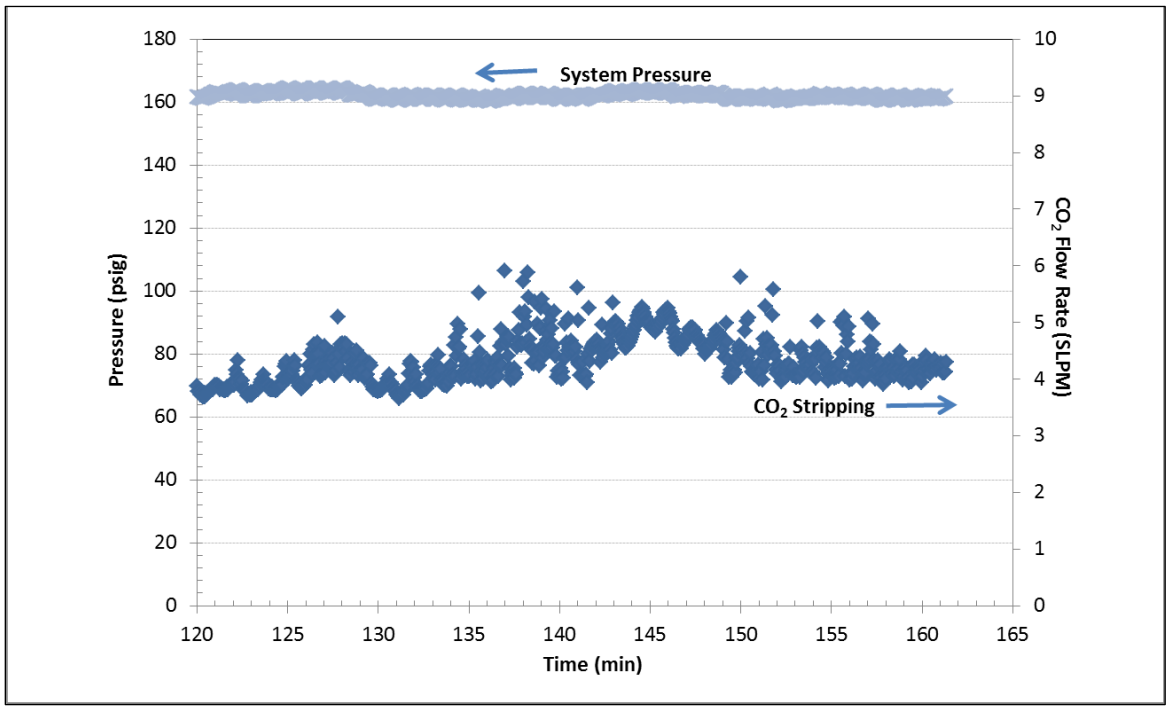

Figure 55. Process operating pressure and CO_2 stripping flow rate at 160 ºC.

Figure 56 shows the data for NH_3 and CO_2 stripping for 30-wt% mixed-salt solution in the regenerator, which was operated with the regenerator top ~ 60 °C, a much lower temperature than the bottom. Data from modeling is also shown in this plot. For modeling, an isothermal regenerator (warm regenerator top) was assumed. This data confirms that ammonia can easily be stripped off and condensed back in the cooler section of the regenerator.

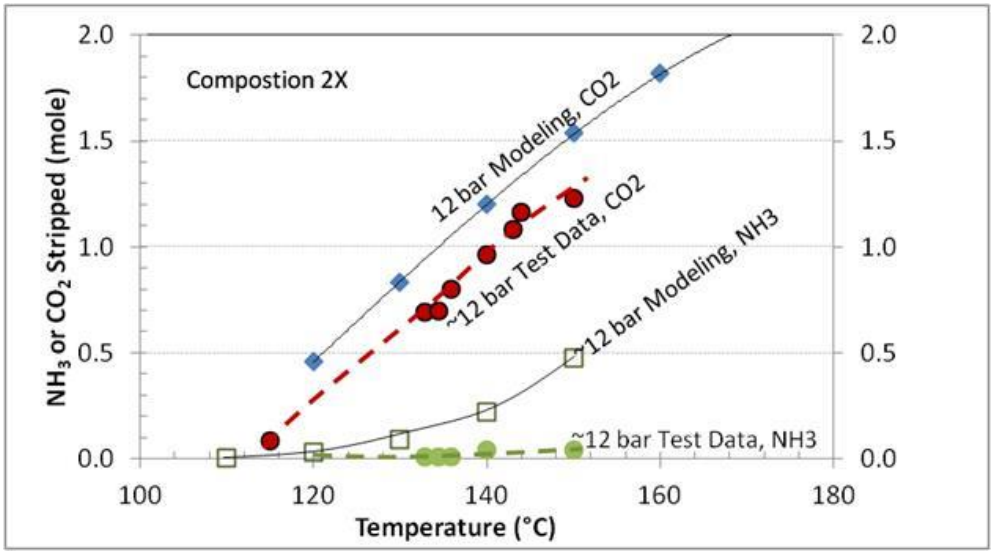

Figure 56. Comparison of data from modeling (warm regenerator top) with test data (cool regenerator top) for NH_3 and CO_2 stripping

5.3 Task 3: Preliminary Process Modeling and Techno-Economic Analysis

It is important that a process model for complex systems be validated by two or more agencies (or methods) to be used reliably for evaluating the process techno-economic report. The process flow chart for modeling work is shown in Figure 57. In step 1, speciation data were produced by a validated V-L-E model (e.g., UNIQUAC and OLI Analyzer). Then, these data were used generate heat and mass balances for DOE Case 12 using (1) ASPEN®, and (2) in an extended UNIQUAC model. However, to our knowledge, there was disagreement in data obtained from e-NRTL model built inside ASPEN for ammonia-based systems—especially for modeling the regenerator at high-temperature and high-pressure regions (120-150 °C and > 5 bar). Therefore, we selected ASApS and OLI Systems, two companies with experts in thermodynamic modeling of electrolytes at very high electrolyte concentrations to perform the modeling work (Dr. Kaj Thomsen, ASApS, and Dr. Andre Anderko, OLI Systems). PoliMi was then able to use the UNIQAC model developed by ASApS and show the energy and mass balance for the process using the preliminary layout.

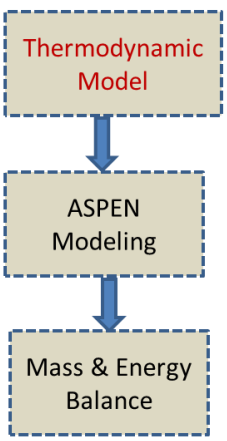

Figure 57. Process flow chart for modeling in BP1.

Work conducted by Aqueous Systems Aps (ASApS). The work conducted by ASApS included: (1) compilation of literature experimental data available for CO_2-K_2CO_3-H_2O system; and (2) combining the CO_2-K_2CO_3-H_2O system with NH_3-CO_2-H_2O system to generate an input file that is in a readable form of ASPEN® Plus so that it can be used by PoliMi to simulate the mixed-salt system in their power plant model. They completed their modeling task in BP1.

ASApS completed the compilation of experimental data in Q2 of BP1. This constitutes the first milestone in ASApS project work. The experimental data that has been compiled – in addition to the data available from earlier modeling of the CO_2-NH_3-H_2O system – is as follows:

- 3405 experimental data points for the NH_3-CO_2-KOH-H_2O system were found in 49 different papers, reports, and dissertations.

- 935 experimental data points relevant for the $CO_2 – K_2CO_3 – H_2O$ system were found in 14 different scientific papers.

ASApS also reported that the amount of data collected is very significant compared to the amount of data already available in the databases for these systems. The amount of experimental data that were available and used for determining parameters in previous models (Thomsen and Rasmussen, Chemical Engineering Science, 54, 1999, 1787-1802; Darde et al., Ind. Eng. Chem. Res., 49, 2010,12663-12674-24) was ~5000 points. The new data collected in this project almost doubles the amount of data available for determining parameters in the thermodynamic model. The new data include data for vapor—liquid equilibrium, solid-liquid equilibrium, and liquid-liquid equilibrium. In addition to the equilibrium data, there are significant amounts of data for the enthalpy of mixing and the heat capacity of the relevant systems.

All of the experimental data have been reviewed and transcribed into a format that make them ready to use for determining parameters in the model. The subsystem consisting of CO_2-K_2CO_3-H_2O has now been modeled. A large amount of new data was found in the first part of this project and was used for determining model parameters for the system. Many of the data points from different sources were not in very good agreement. The time required for modeling this system became much longer than expected because it was necessary to decipher which data sets were in agreement. In order to determine if data were in agreement with each other, data sets from new sources were added to the parameter determination process one by one so that it could be established if that source of data was in agreement with previous data sets. Some data had to be left out because they were obviously in disagreement with other data. After time-consuming iterations, a very precise model for the CO_2-K_2CO_3-H_2O system has been determined during this period. The model is valid from the freezing point of the solutions and up to 200 °C. Based on this milestone, it is expected that the addition of ammonia will take place smoothly.

The extended UNIQUAC thermodynamic model for gas solubility in salt solutions was developed in1999. It was derived from the original UNIQUAC expression developed in 1970s by adding a Debye-Hückel term to account for additional excess Gibbs energy from the electrostatic interactions between ionic species (see references in Appendix A). The model requires UNIQUAC volume and surface area parameters for each species, along with temperature-dependent binary interaction energy parameters for each pair of species. Phase equilibrium calculations are performed with the approach coupled with equilibrium speciation reactions with potential solid phase precipitation. The liquid-phase activity coefficients are calculated from the extended UNIQUAC model, while the gas-phase fugacity coefficients are from the Soave-Redlich-Kwong equation of state. Besides phase relations, the model also reproduces thermal properties, such as enthalpy and entropy, within the experimental accuracy.

The final project report from ASApS is attached as Appendix A. Dr. Kaj Thomsen also provided extended UNIQUAC program (2014 update) in Excel. ASApS updated the ammonia data in UNIQAC in 2012 and also in 2014.

In contrast to the equilibrium model being developed by ASApS, OLI developed a rate-based model using SRI's experimental data. SRI provided OLI with the data from the small bench-scale testing to start the development. They updated the model when data from SRI's large bench-scale testing became available. The optimized rate-based model using the data from SRI absorber and regenerator was provided to PoliMi for their update of the power plant modeling with the mixed-salt CO_2 capture system.

OLI's software is used in the oil and gas, chemical and power generation industries as well as in various DOE laboratories. The OLI software (in particular, the Electrolyte Simulation Program or ESP and the OLI Engine for ASPEN Plus) has been used at SRI for decades for predicting speciation in hydrothermal systems. This software has been extensively validated in industry and academia and is the de-facto industry standard for simulating systems that contain electrolytes. For the mixed-salt project OLI upgraded the ESP for the K_2CO_3-NH_3-CO_2-H_2O system by including available experimental data. They have conducted a material and heat-balance analysis for a mixed-salt system layout based on the data from SRI's current work. This layout is given in Figure 58. The project report from OLI Systems is attached as Appendix C.

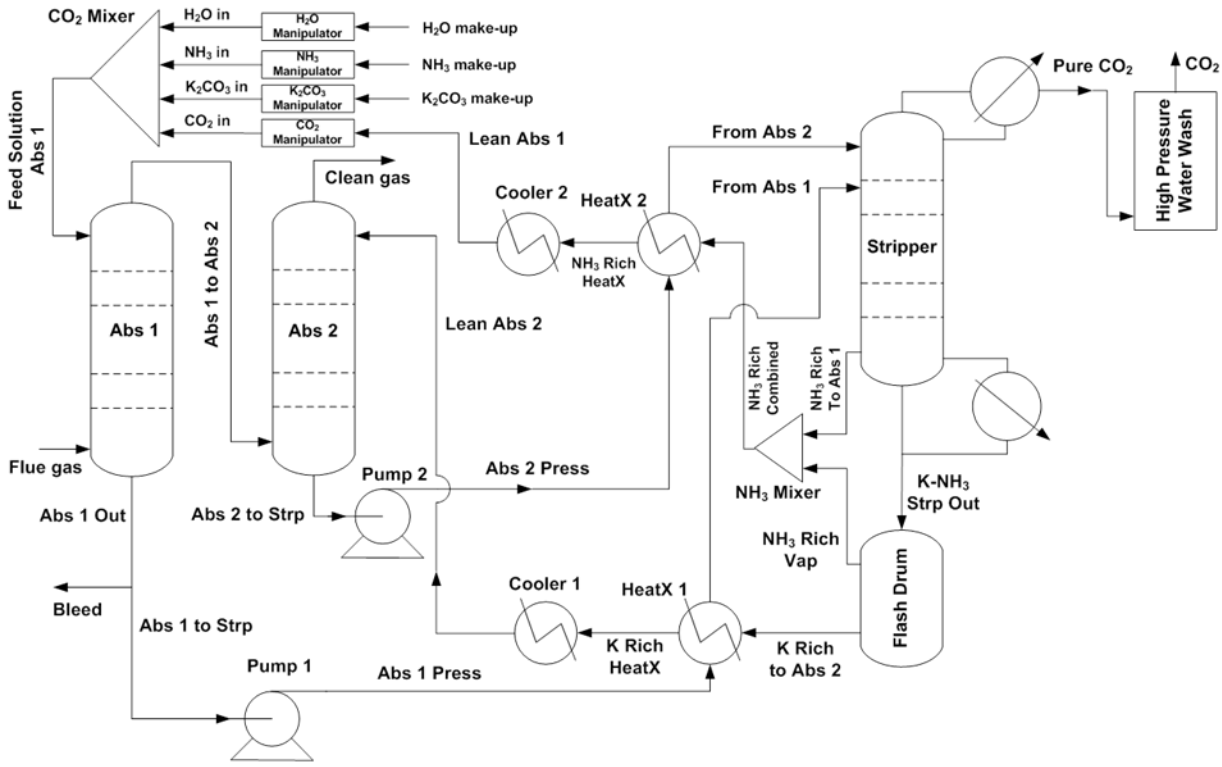

Figure 58. Mixed-salt layout used by OLI Systems.

Work conducted by Stanford University. The objective of the Stanford University work was to develop a modeling and optimization capability to determine optimal designs for CO_2 capture system-enabled fossil-fuel-fired power generation in varying economic and policy

environments. Because flexible response from thermal power stations is likely to increase in value with time as renewable energy penetration increases, a major objective of this work was to quantify the impact of variable operations on optimal plant design. For example, the modeling and optimization capability could be used to quantify the value of using CO_2 capture systems to modulate the output of a power station (e.g., export more power during certain hours and less during other hours by varying CO_2 capture rates) in response to changes in power demand and supply. The modeling and optimization capability would be useful for conducting technology and policy assessments. Ultimately, the modeling and optimization capability may be used to inform the high-level design of low-carbon power generation systems to reduce the cost of electricity.

Goal 1: Preliminary design of the process integration architecture between the mixed-salt process and the Stanford heat integration model (SRI to provide the preliminary test data and ASPEN data as needed).

Goal 1 milestone: Perform modeling runs of heat integration model using preliminary model of mixed-salt process.

Goal 2: Optimize and test the Stanford heat integration model using the mixed-salt process and compare it with the amine process.

Goal 2 milestone: Perform modeling runs of heat integration model using a thorough model of the mixed-salt process and compare it with results using the amine process.

Stanford project report is attached as Appendix B. A paper has been published from the Stanford project work [7].

Work conducted by Politecnico di Milano (PoliMi). During BP1, PoliMi completed the baseline study to calibrate the numerical models of two pulverized-coal steam supercritical power plants, one without and one with carbon dioxide capture. The models replicate the simulations executed by DOE-NETL and presented in two reports “Cost and Performance Baseline for Fossil Energy Plants – Volume 1: Bituminous Coal and Natural Gas to Electricity” (refer to Case 11 and Case 12) and “Quality Guidelines for Energy System Studies.”

PoliMi conducted the validation comparing for a number of case studies the vapor-liquid-solid equilibrium results obtained by ASApS with the original code and those by PoliMi with its implementation in Aspen Plus. The original code and its implementation in ASPEN Plus are not identical because the two programs adopt different formulations for the reaction constants and for the pressure term of the fugacity expression. The results from the two programs differ by relative errors generally below 2%. The agreement is better for low temperatures and pressures typical of absorber conditions than for the high temperatures and pressures that are typical of regeneration conditions. The errors above 2% usually refer to properties that have very low values, such as very small component concentration. We conducted the same comparison against the OLI data, and the results are shown in Table 7.

Table 7. Comparison of V-L-E data from UNIQUAC, OLI, and ASPEN.

Feed →	H2O	NH3	CO2	T
Concentration	1kg	5moles	3moles	120°C

Model	Vapor Presure (bar)							
	P_{total}	Abs. Error	P_{H2O}	Abs. Error	P_{NH3}	Abs. Error	P_{CO2}	Abs. Error
AspenPlus	22.38		2.02		0.57		19.80	
OLI Analyzer	22.44	-0.06	0.90	1.12	0.31	0.26	21.23	-1.43
ASApS Ex. UNIQUAC	21.04	1.34	2.00	0.02	0.59	-0.02	18.45	1.34

The numerical models were prepared and executed with the PoliMi in-house code named GS, which has been developed over a few decades of research to simulate power cycles and energy systems. The majority of the assumptions defined by DOE-NETL are transferred as is into the GS models. The results show no more than about 2% differences between DOE-NETL and PoliMi simulated flow rates and temperatures of relevant streams of the power cycle, both with and without CO_2 capture. Moreover, the compositions of the gaseous streams entering and leaving the FGD are closely matched. Finally, power balances and plant performances are also very accurately replicated. The developed models were adapted to be used in the next stages of the project to assess the integration of the mixed-salt technology with the power generation. Table 8 compares power balance and global performance of the power plant with and without CO_2 capture.

During the 3rd and 4th quarters of BP1, PoliMi, and ASApS worked together to integrate and validate the data from newly updated UNIQUAC in process modeling in ASPEN. Bi-weekly WebEx meeting were held between SRI, ASApS, and PoliMi to produce a preliminary layout for the mixed-salt process. PoliMi performed mass and heat balance analysis for the preliminary layout, and the report was submitted to DOE in 2017 January.

Table 8. Power balance and global performance power plant with and without CO_2 capture.

	Power plant without CO_2 capture [1, Case 11]		Power plant with CO_2 capture [1, Case 12]	
	DoE-NETL	PoliMi	DoE-NETL	PoliMi
Power balance, kW				
Steam turbine power	580,400	580,080	662,800	662,750
Coal Handling and Conveying	440		510	
Pulverizers	2780		3850	
Sorbent handling & reagent preparation	890		1250	
Ash handling	530		740	
Primary air fans	1300	1310	1800	1810
Forced draft fans	1660	1650	2300	2280
Induced draft fans	7050	7020	11,120	11,160
SCR	50		70	
Baghouse	70		100	
Wet FGD	2970		4110	
Econamine FG plus auxiliaries	-		20,600	
CO_2 compression	-		44,890	
Miscellaneous balance of plant	2000		2000	
Steam turbine auxiliaries	400		400	
Condensate pumps	800	710	560	800
Circulating water pumps	4730		10,100	
Ground water pumps	480		910	
Cooling tower fans	2440		5230	
Transformer losses	1820		2290	
Gross power, kW	580,400	580,080	662,800	662,750
Total auxiliaries, kW	30,410	30,290	112,830	112,670
Net power, kW	549,990	549,790	549,970	550,080
Heat input, kWLHV	1,349,384		1,864,357	
LHV efficiency, %	40.76	40.74	29.50	29.51
Heat input, MWHHV	1,399,023		1,932,940	
HHV efficiency, %	39.31	39.30	28.45	28.46

5.4 Task 4: Budget Period 2 Continuation Application

SRI prepared and submitted the continuation report at the end of BP1 documenting the results and project status, and the plans for the BP2. Project peer review meeting was held in Pittsburgh, PA on March 19, 2015. For this event, a presentation and a technology summary report was submitted. Indira Jayaweera participated the review meeting in person.

6. WORK PLAN FOR BUDGET PERIOD 2

In BP2, we designed and built a properly scaled high-pressure regenerator and integrated it with the absorber to demonstrate the complete CO_2 capture system with a low-cost production of CO_2 stream. We optimized the system operation and collected data to perform the detailed techno-economic analysis (TEA) of the CO_2 capture process integration to a full-scale power plant. The project objectives for BP2 are listed below followed by a detailed description of the tasks.

- Design and construct the bench-scale integrated test system
- Determine the optimal regenerating conditions including dual-stage regeneration.
- Perform integrated absorber/regenerator testing.
- Continue development of rate-based thermodynamic modeling database for potassium- and ammonium-based system heat and mass balance evaluations.
- Perform a TEA to determine the cost associated with integrating a CO_2 capture system based on the mixed-salt process for a > 550-MW PC power plant.
- Prepare a technology environmental health & safety (EH&S) risk assessment of the CO_2 capture system based on the mixed-salt process.
- Revise and maintain the Project Management Plan (PMP).

7. BUDGET PERIOD 2 TASKS

Below, we describe the BP2 tasks in detail and the worked performed in these tasks.

7.1 Task 5: Bench-Scale Integrated System Testing

The expected outcomes of this task were to identify a suitable process configuration capacity for commercial-scale operation and a description of the integrated absorption/desorption models that could be used to predict equipment performance and capacity for commercial-scale application. The identification of a process configuration would include preliminary concepts for absorption/desorption equipment, absorber/regenerator architectures, column-packing densities and estimated pressure drops, methods of heat removal and additions, steam requirements, and estimated cost of all equipment. This task consisted of several subtasks. The integrated system testing was conducted at SRI's high-bay test site.

Subtask 5.1 - Design of the Bench-Scale Integrated Test System

This subtask addressed activities related to design a bench-scale, continuous, integrated test system that was designed to run on a simulated gas stream. Relevant kinetic and heat-transfer test data were obtained from the test system. We made minimal changes to the absorber system used in BP1.

We completed the design of the regenerator system in Q1 of BP2. A simplified schematic of the integrated absorber-regenerator system is given in Figure 59. The design of the bench-scale system was based on a standard absorption process flow sheet that included a standard dual-absorber system and an advanced regenerator. We made a few changes to the absorber system used in BP1 such that it can be easily coupled to the regenerator for integrated system testing. We also performed Aspen® modeling of the designs to validate the flowsheet configurations and process conditions. Model data is discussed in detail under Task 6.

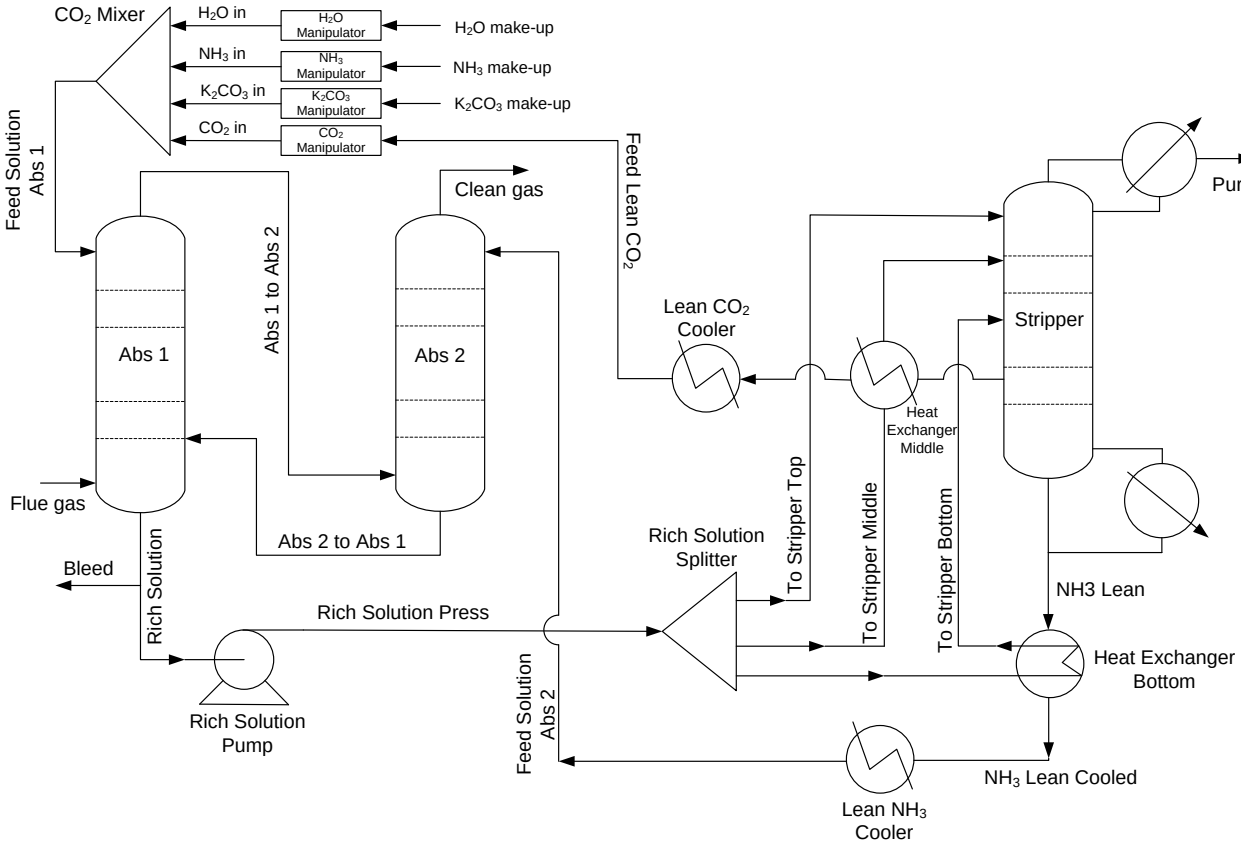

Figure 59. Preliminary schematic of the integrated system as modeled for testing the mixed-salt process in BP2.

Based on BP1 results, we have considered two arrangements for the regenerator system as shown in Figure 60. One configuration included the original design with isobaric operation of the system with CO_2 stripping in the top section of the regenerator column followed by NH_3

stripping in the bottom section. The second configuration included a flash to strip NH_3 at a lower temperature. OLI Systems and PoliMi modeled these options in the Q1 BP2 period. Details of modeling by OLI are given in the process modeling section (subtask 6.1). Based on the modeling and the experimental results, SRI selected the option 1 layout and completed the design of the regenerator. The design was submitted to the DOE Project Manager for approval before the construction. Figure 61 shows the simplified process flow diagram of the integrated mixed-salt process as built.

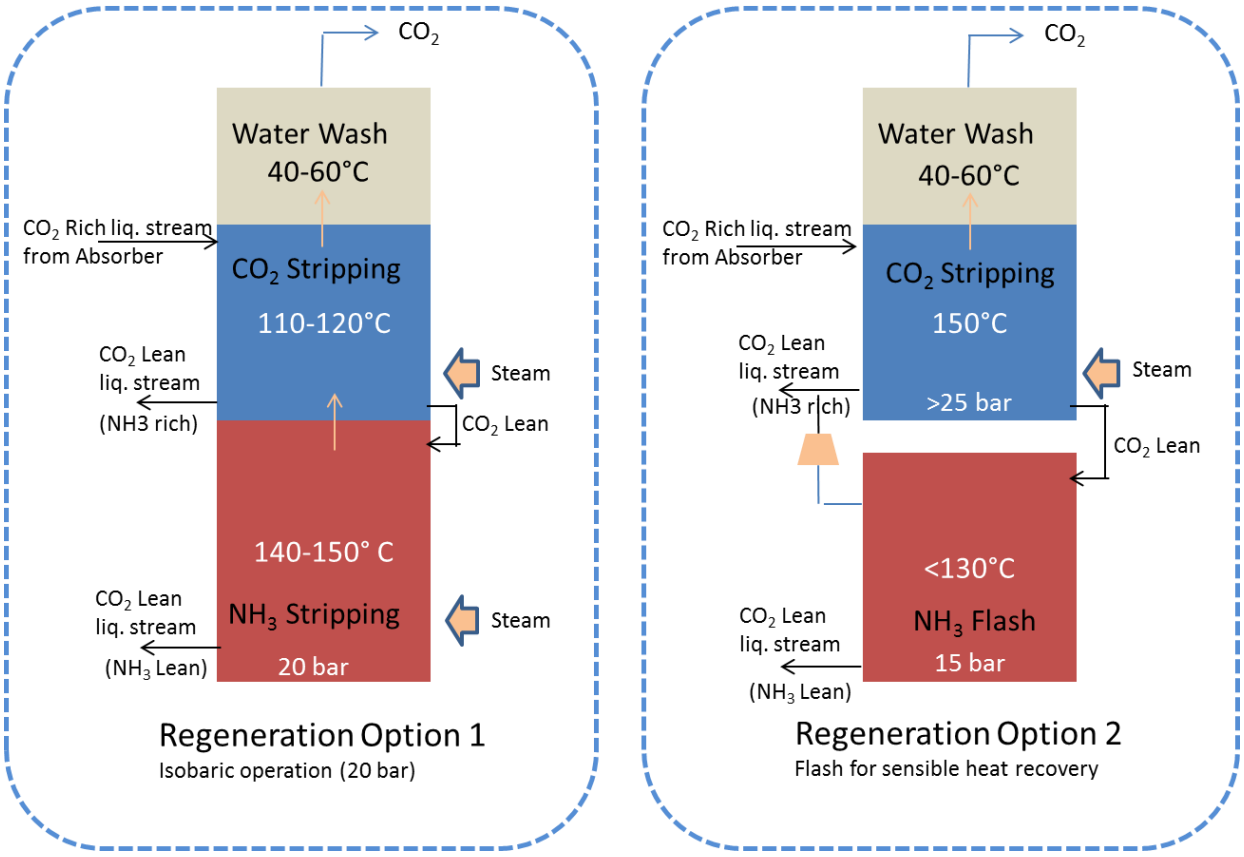

Figure 60. Regenerator options.

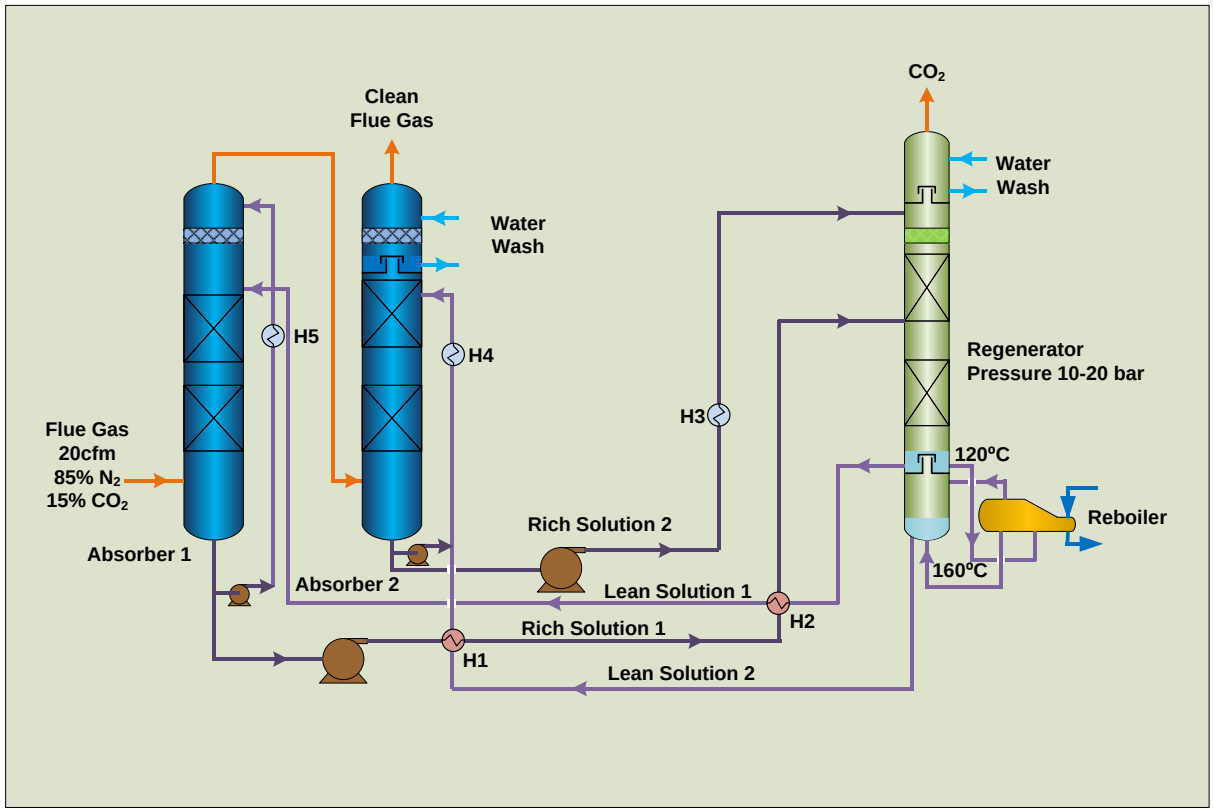

Figure 61. Schematic of the integrated system for testing the mixed-salt process in BP2 as built.

Subtask 5.2 - Construction of the Bench-Scale Integrated Test System

We initiated construction of regenerator and the integrated system during Q2 of BP2. Figure 62 shows the piping and instrumentation diagram (P&ID) for the mixed-salt regenerator. Figure 63 shows photographs of the regenerator column and heat exchangers during the installation. The reboiler is mounted behind and to the side of the lowest column section shown in the photograph to the side. We completed the installation and testing of the integrated system in Q3 BP2 and completed the system operation software and hardware about the same time. Figure 64 shows the completed regenerator system. The left picture shows the new two-stage regenerator, and the picture to the right shows the both two-stage regenerator and the previous single-stage regenerator.

The process operation of the regenerator section is as follows. The rich liquid from Absorber 1 (Rich Liquid 1) is split to 80:20 and pumped into the column at two stages as shown, with 20% going to the upper stage. The rich solution from Absorber 2 (Rich Liquid 2), which has a lower ammonia concentration than Absorber 1 Rich Liquid, is pumped to the top stage of the regenerator column. This rich liquid flow is cooled to 15 °C to further reduce the ammonia emission from the regenerator. As a polishing step, the high-pressure water wash is mounted at

the very top of the regenerator such that the emitted CO_2 gas has less than 10 ppm ammonia content. The regeneration energy is provided by steam (175°C). The vapor stream from the reboiler is passed through the bubble caps and the liquid hold in the lower middle stage of the regenerator column. The temperature of this solution is about 120 -140 °C, and the lean stream, for Absorber 1 is drawn from this stage of the regenerator column. The lean solution for Absorber 2 is drawn from the bottom stage of the regenerator column, and the temperature of this stage is about 160 °C. The regenerator is operated under isobaric conditions with a temperature gradient, ~30-50 °C at the top and 155-160 °C at the bottom. There are temperature sensors (as shown in the diagram) along the column to record the temperature profile of this test system. Two main heat exchangers recover the sensible heat from the regenerated solution to heat the incoming rich solution. The Aspen model indicates the outgoing lean streams from heat exchangers are ~ 40 °C, and thus they need to be cooled to about 15-20 °C before they are fed to the absorber columns. Therefore, two cooling coils are installed on the lean solution return lines.

For the continuous operation of the regenerator, the input rich-solution flows and exit lean-solution flows must be balanced, and the liquid levels of draw stages must be carefully controlled. There are flow meters and level sensors that are actively monitored by the control program, which controls pumps, valves, and steam flow to maintain the pressure, temperature, and flow rates to the operator-specified parameters. Hardware and software for integrated system operation were designed and built.

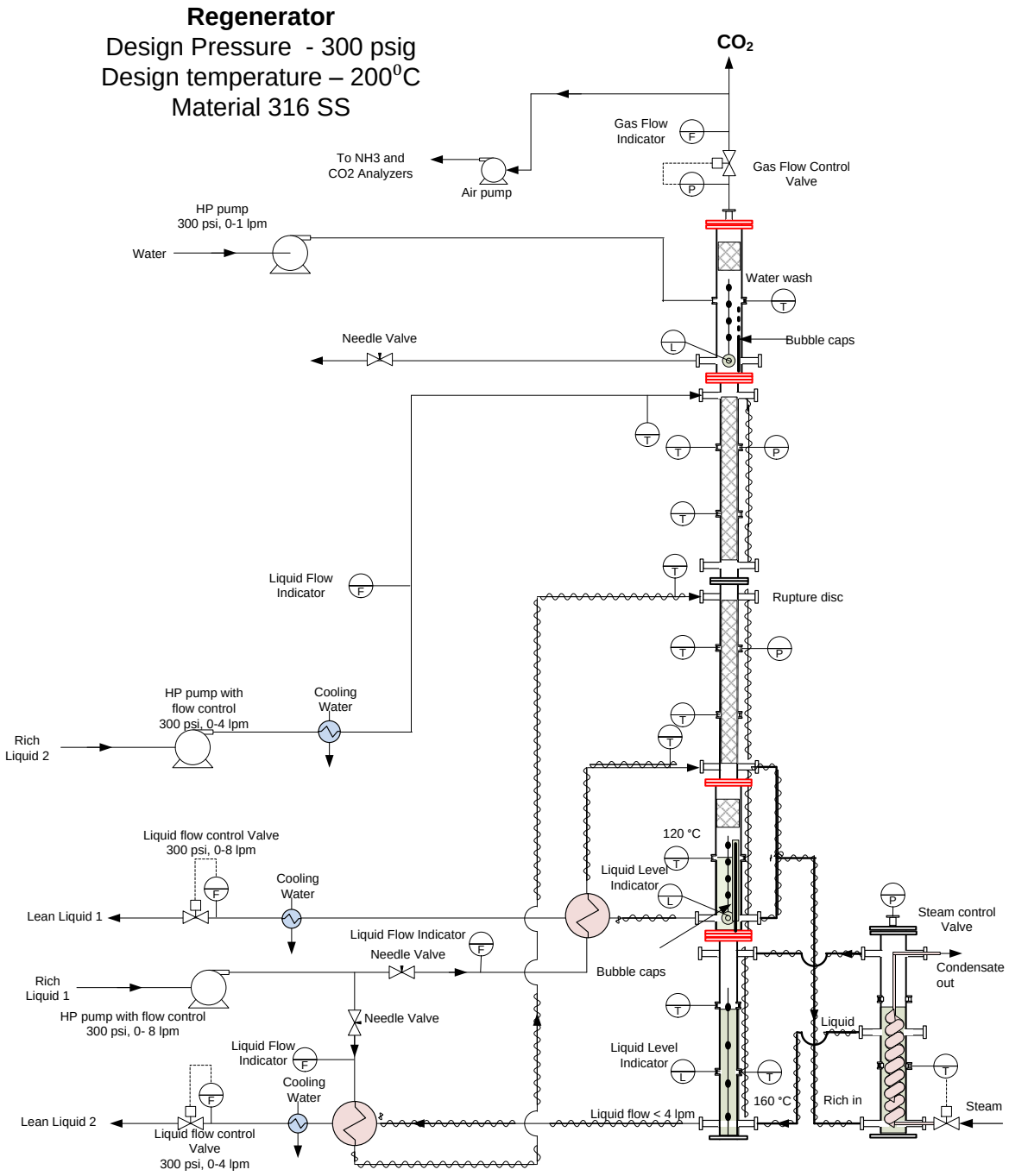

Figure 62. Schematic diagram of the regenerator.

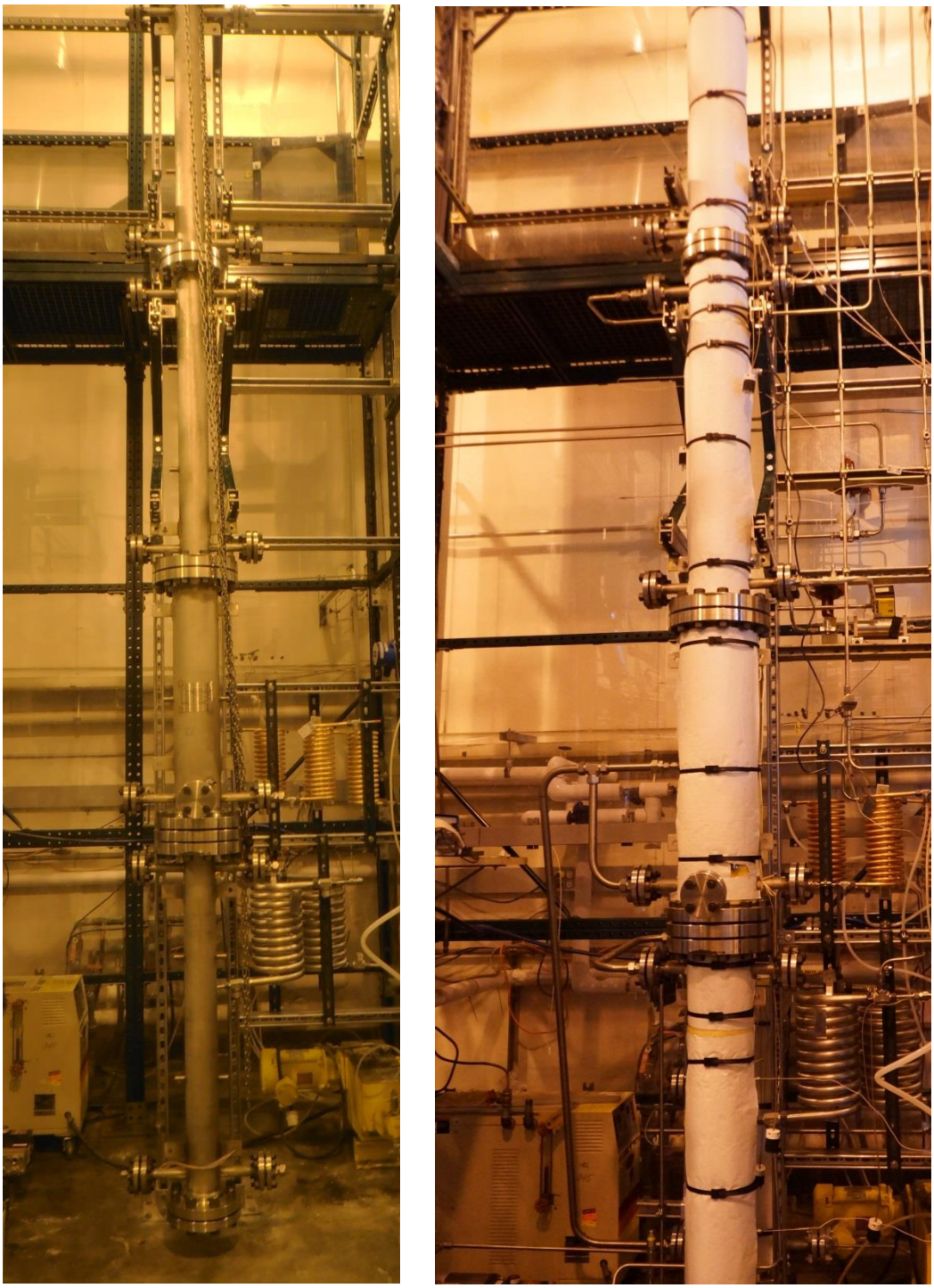

Figure 63. Photographs of the regenerator column and heat exchangers during installation (left) and near completion (right).

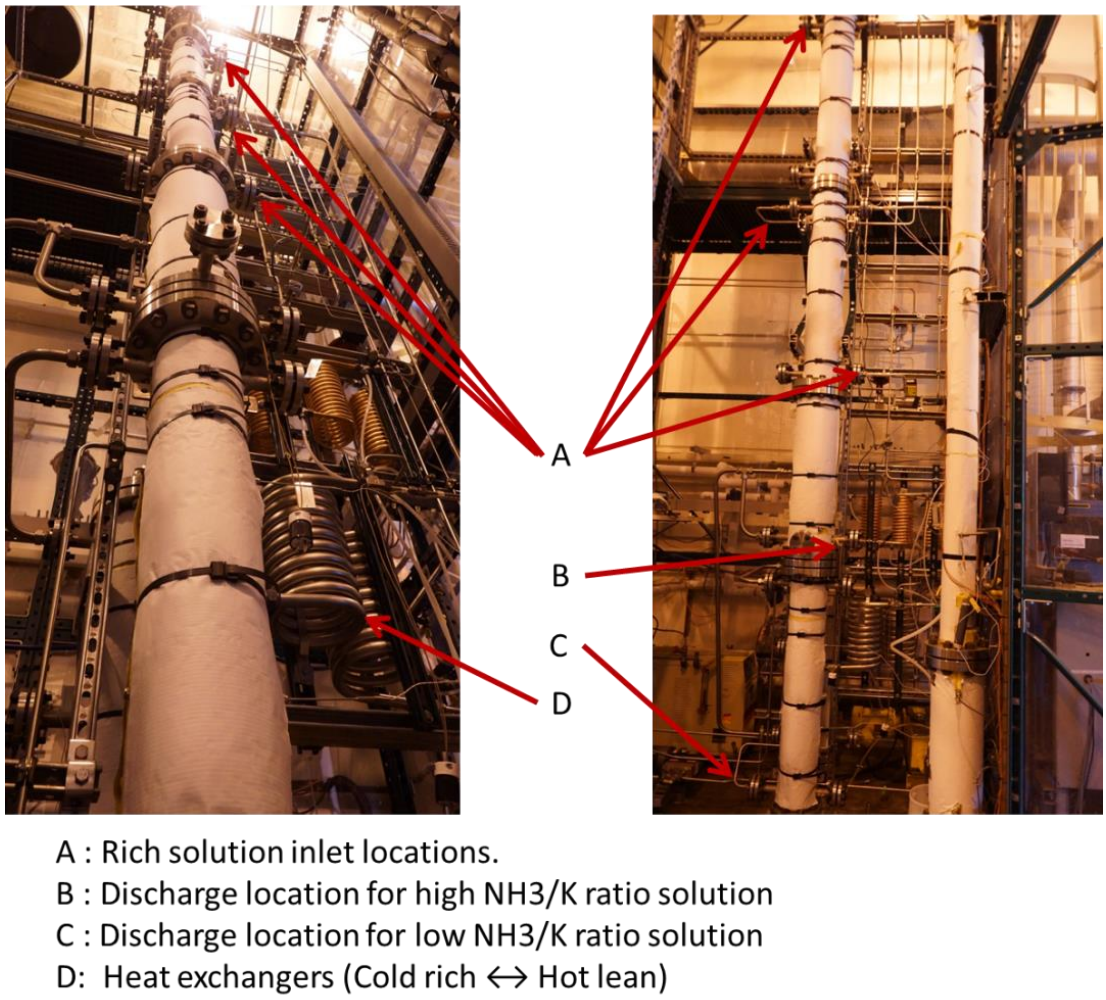

Figure 64. A photograph of the completed regenerator column. The picture to the right shows both the two-stage regenerator and the single-stage regenerator built in BP2, and BP1, respectively.

Figure 65 shows the control and data acquisition program windows for the mixed-salt regenerator. As in the absorber control program, all parameters can be displayed in graphical and numerical formats in the regenerator control program so the trends can be easily visualized. Although the regenerator and absorber are controlled with two independent programs, critical sensor information pertinent to system control is shared such that remedial action can be taken by either control program if conditions deviate outside the set limits. This arrangement gave us the flexibility for any changes needed to be made quickly. Software and hardware controls were tested, and they performed as designed.

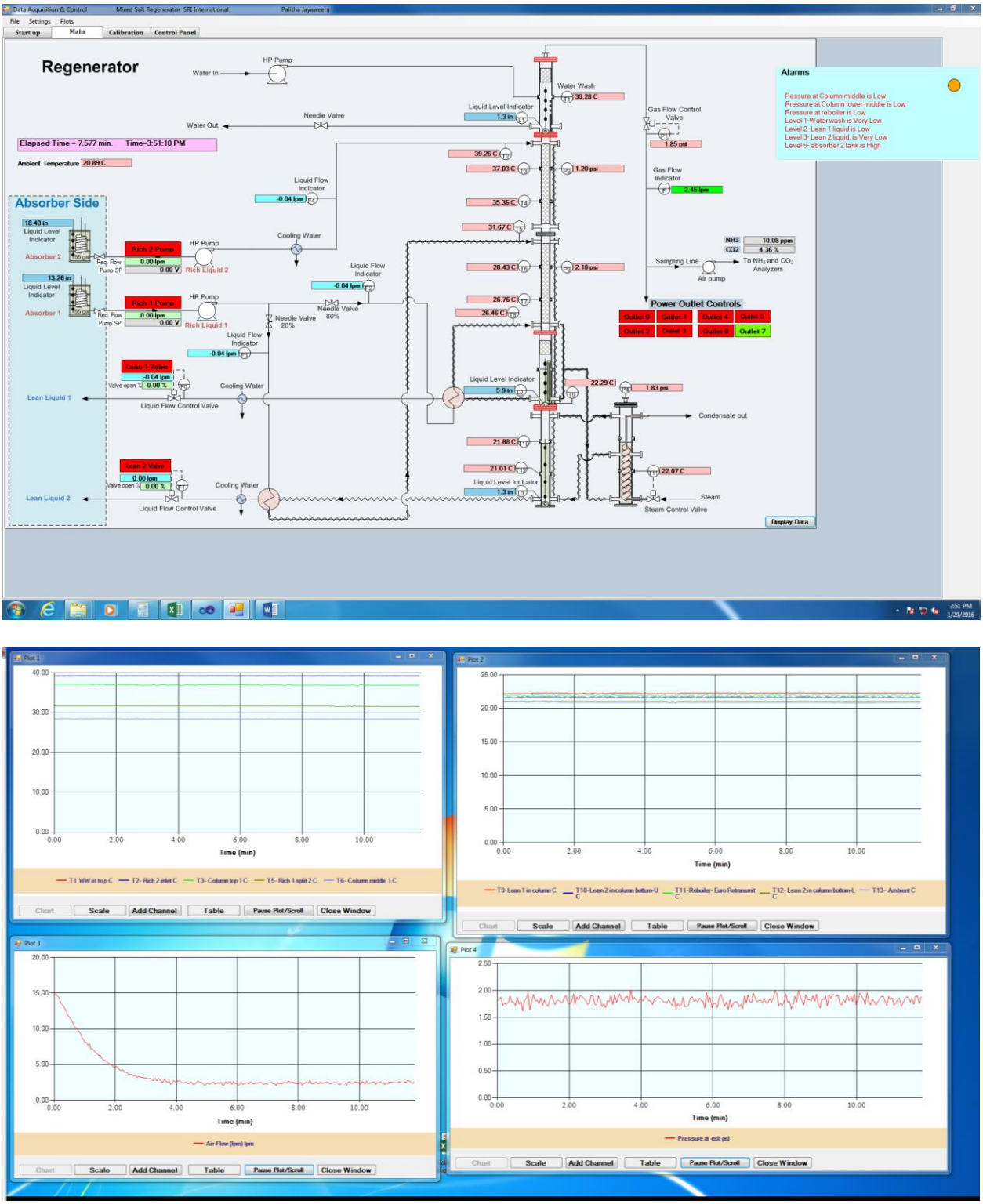

Figure 65. Control program windows of the regenerator.

We tested the regenerator as a stand-alone system to confirm the operation of both software and hardware components. For initial testing of the regenerator, we used rich solutions that we stocked from previous absorber runs. For shakedown tests, we used 50% diluted rich solutions as a precaution to avoid precipitation or line blockage. Figure 66 shows the temperature profile of lean solution draw stages during heat up and steady state operation in a preliminary test. The reboiler can be heated up rapidly as we have a generous supply of steam and small liquid hold volume. However, the heat-up rate was controlled to allow smooth operation and it reached the steady state quickly without fluctuations. Figure 67 shows the temperature profile of the regenerator column and temperatures of the inlet/outlet flow streams. Inlet streams recovered sensible heat from outgoing streams at the heat exchangers. The column temperature profile was as expected, and the regenerator performed as designed.

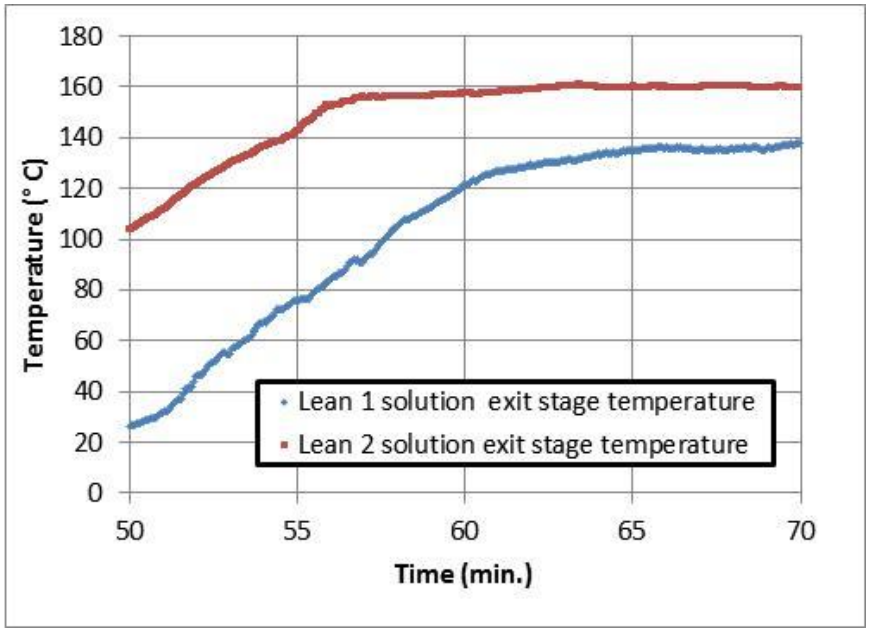

Figure 66. Temperature profile of Lean 1 and Lean 2 draw stages.

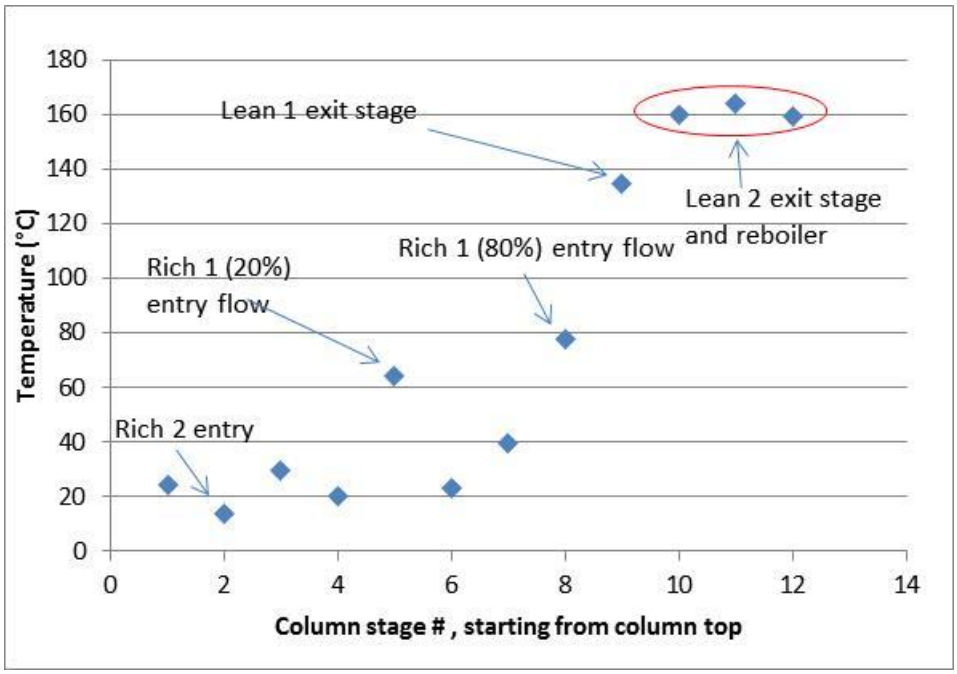

Figure 67. Temperature profile of column stages and solution inlets.

Additional absorber testing: While the regenerator was being built, we performed 3-hour continuous tests with the absorber using a stock lean solution that would be similar to that expected from the operating regenerator. These tests mimicked the integrated operation, and we gained valuable experience on the operation of the system with the actual regenerator. We used a 1.15 lpm lean solution feed rate with about 0.19 CO_2 loading. Figure 68 shows the results of the test, indicating 90% CO_2 capture in Absorber 1 with 0.19 to 0.40 cyclic loading. Capture efficiency was recorded continuously with inline CO_2 detectors, and rich- and lean-solution loading values were obtained from periodic sample analysis as shown by data points in the plot.

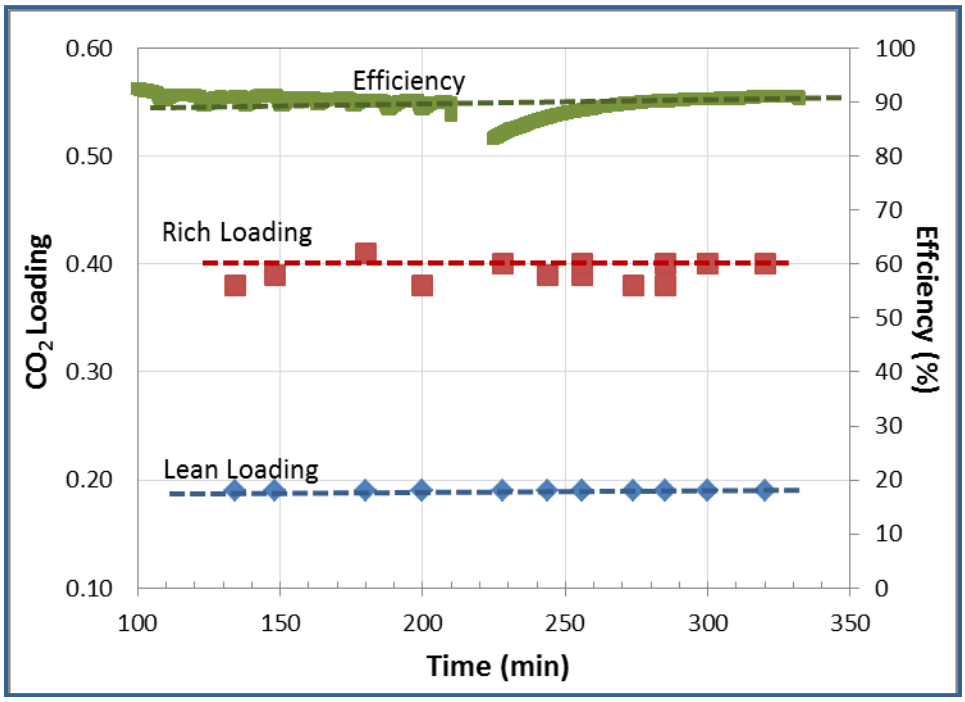

Figure 68. 90% CO_2 capture efficiency with 0.19 to 0.40 cyclic CO_2 loading in Absorber 1; Gas flow rate = 15 acfm.

Subtask 5.3 – Bench-Scale Test Plan for Integrated System Testing

This subtask addressed activities to develop a test plan for performing absorption and regeneration tests in the integrated bench-scale unit. The test plan defined test success goals to support the DOE program goals. Testing would determine process kinetics sufficient to scale-up the process to a commercially relevant demonstration scale as the next development step. The test plans were designed for continuous tests of sufficient duration to determine expected degradation, if any, of the solution for a commercially relevant period of time. The test plans were submitted to the DOE Project Manager for review and comment before initiation of tests. Table 9 shows the system test plan and schedule.

Table 9. Test plan.

Time Frame	Event
January 2016	Testing with 3 m solution; parametric testing, SOP development, HAZOP review.
February 2016	Testing with 6 m solution, parametric testing, system optimization.
March 2016	Long-term operation of absorber-regenerator integrated system.

Subtask 5.4 – Bench-Scale Tests

This subtask addressed activities to conduct bench-scale continuous integrated absorber-regenerator testing. Tests were conducted according the test plans developed in Subtask 5.3. Tests results are discussed below in detail.

Once we completed preparation of standard operating procedures and shakedown testing of the integrated system, we started parametric studies as planned in Subtask 5.3. We tested the system with simulated flue gas flow rates from 300 to 500 slpm with 15% CO_2 concentration in the simulated flue gas stream with absorption efficiencies ranging from 75 to 95%. Typical run times were 3 to 7 hours. Absorption efficiency, ammonia emission, temperature profiles in the absorber and the regenerator, and CO_2 regeneration were monitored as other parameters were varied.

Figure 69 shows the typical temperature profile of Absorber 1 and Absorber 2 during an integrated run. The Absorber 1 temperature profile shows elevated section in the middle of the column due to absorption reaction heat. Absorber solution reservoirs were cooled with building cooling water to remove the heat of reaction from the absorber solution. The Absorber 2 temperature profile is less prominent than that of Absorber 1 as most of the reaction is taking place at the Absorber 1 column.

Figure 70 shows a representative temperature profile of the regenerator during an integrated system test. The exit temperature of the regenerated CO_2 stream after the water wash was about 25°C. The drops and spikes in the temperature profile are due to rich solution inlet temperatures as cold inlet rich streams are heat-exchanged with hot outgoing lean streams to recover sensible heat (Figure 61, H1 and H2). Table 10 shows operating parameters of the integrated system during a typical experiment.

Figure 71shows the regenerated CO_2 flow output with the time for a total of 300 slpm simulated flue gas (15% CO_2) stream in the absorber. We demonstrated better than 90% capture and regeneration in this test. Most importantly, the integrated system was stable and performed well under the planned test conditions.

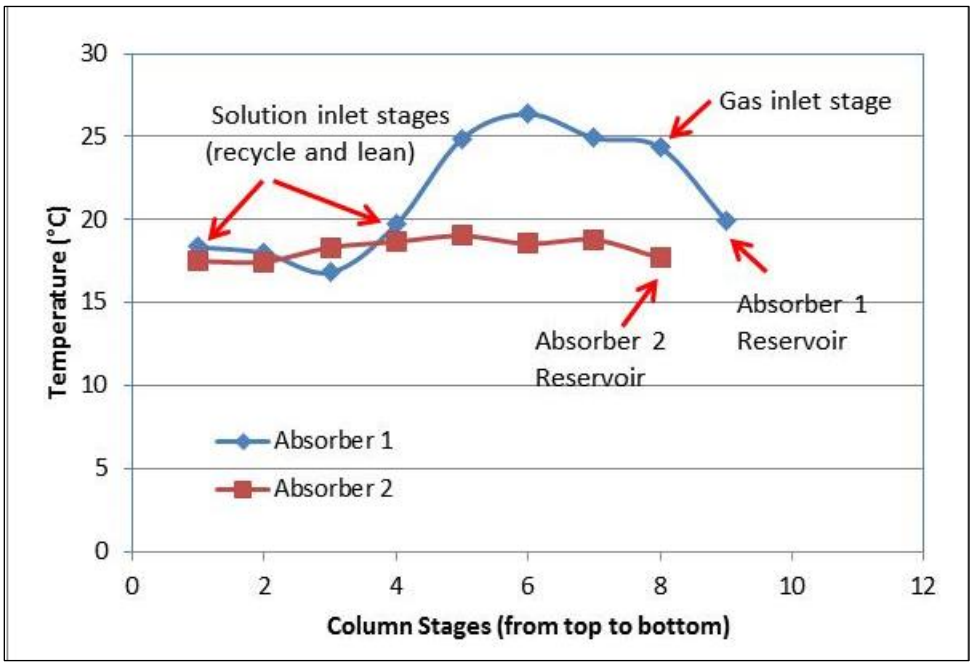

Figure 69. Temperature profile of the integrated absorber 1 during a typical run.

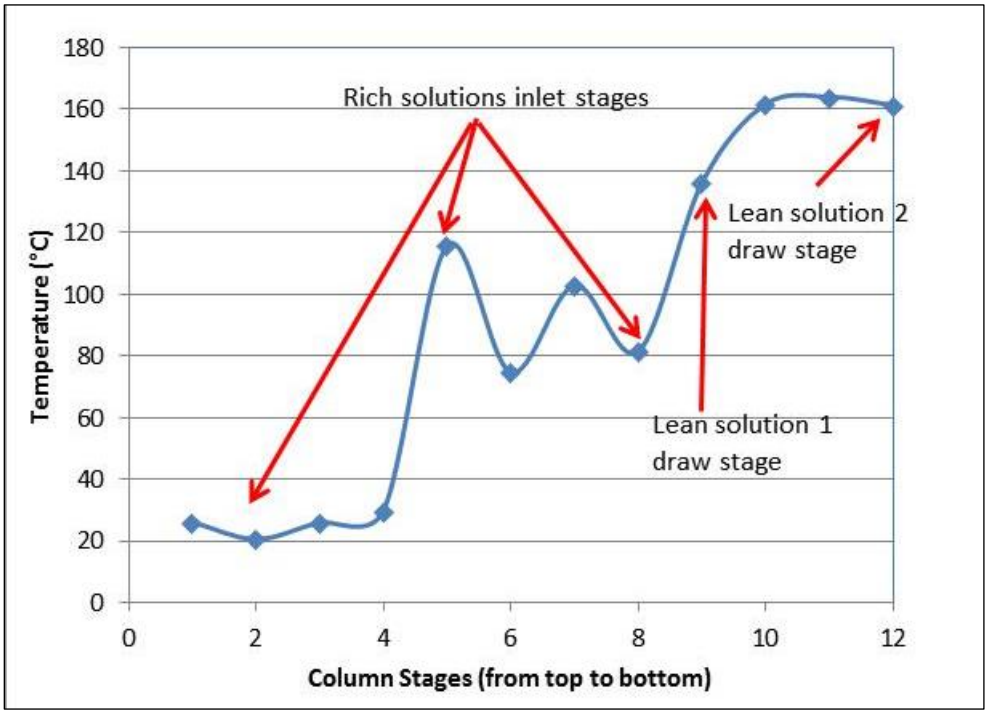

Figure 70. Temperature profile of the integrated regenerator during a typical run.

Table 10. An example of operating parameters of the integrated absorber-regenerator during a typical run.

CO2 flow (lpm)	**55.59**
Air Flow (lpm)	**347.24**
Total Gas flow (lpm)	**403**
Inlet CO2 (%)	**16.71**
ABS1 CO2 (%)	**4.35**
ABS1 CO2 (%)	**1.91**
Absorption Efficiency (%)	**88.6**
Regen CO2 flow (lpm)	**52.5**
Lean 1 Flow (lpm)	**1.92**
Recycle 1 flow -includes lean 1 (lpm)	**4.89**
Recycle 2 flow -to top (lpm)	**3.20**
Lean 2 Flow (lpm)	**1.02**
Recycle flow-includes lean2 (lpm)	**10.78**

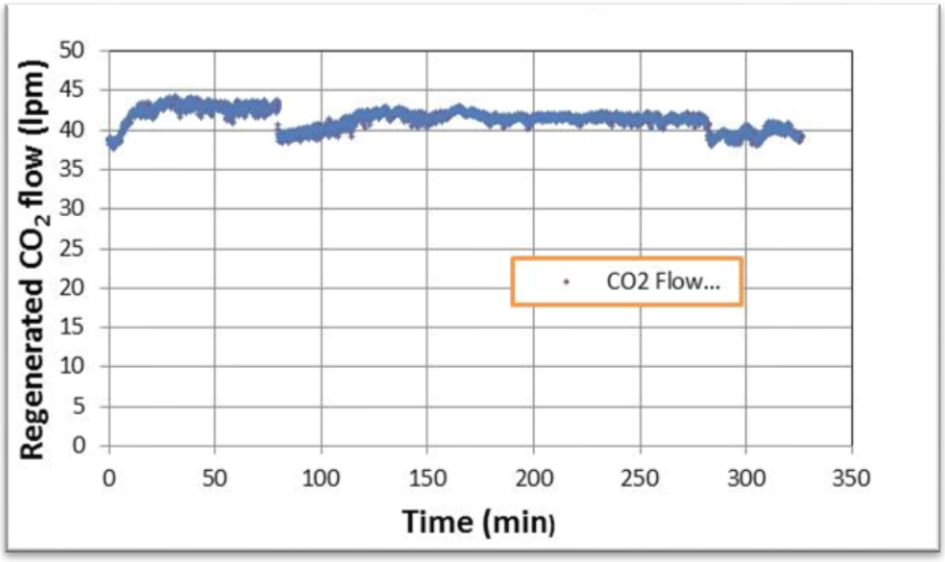

Figure 71. Observed 90% capture efficiency and regeneration with cyclic loading of ~0.7 M/M of ammonia.

We completed integrated system tests studying various parameters and their interdependencies that would be necessary for easy, reliable, and efficient operation of the system. We varied the ammonia-to-potassium ratio (N/K) from 1.6 to 2.2 during these runs. Figure 72 shows a plot of pH and CO_2 loadings of various rich and lean solution samples

collected throughout these tests. These measurements were made off-line as titrations were used to measure the amount of CO_2 loading. Clearly, measured pH and the CO_2 loading show an excellent linear relationship, indicating that an on-line pH sensor can be used for active process control. This is especially beneficial for large-scale systems because off-line sample analysis adds a significant lag time.

The observed N/K ratio for lean solution drawn from the bottom stage of the regenerator to the Absorber 2 was less than 0.2 for all runs. This observation validated the process capability of stripping ammonia in the bottom stage of the dual-stage regenerator to increase the N/K ratio of the lean solution in the upper draw stage that feeds the Absorber 1. Figure 73 shows the alkalinity of the rich and lean solutions circulating in the integrated system measured at various times during integrated tests. This clearly demonstrates the performance of the regenerator producing two mixed-salt compositions (high and low N/K) to use in the two absorbers.

Low N/K in the Absorber 2 helps to reduce the ammonia concentration in the cleaned flue gas stream exiting the absorber to the water wash section. Figure 74 shows the measured and modeled ammonia concentrations as a function of CO_2 loading for the mid-section of the Absorber 2. At the time of this testing, the last section of the Absorber 2 was used as a water wash. During the integrated testing, we successfully achieved less than 50 ppm of ammonia emission with a short water wash section and water recycle. We believe we could reduce the emissions further by changing the gas and liquid flow patterns. Our objective was to reduce the ammonia carry over from the Absorber 2 mid-section to the water wash section to below 2000 ppm, which would reduce the ammonia loss in the system, and greatly reduce the water usage in the water wash.

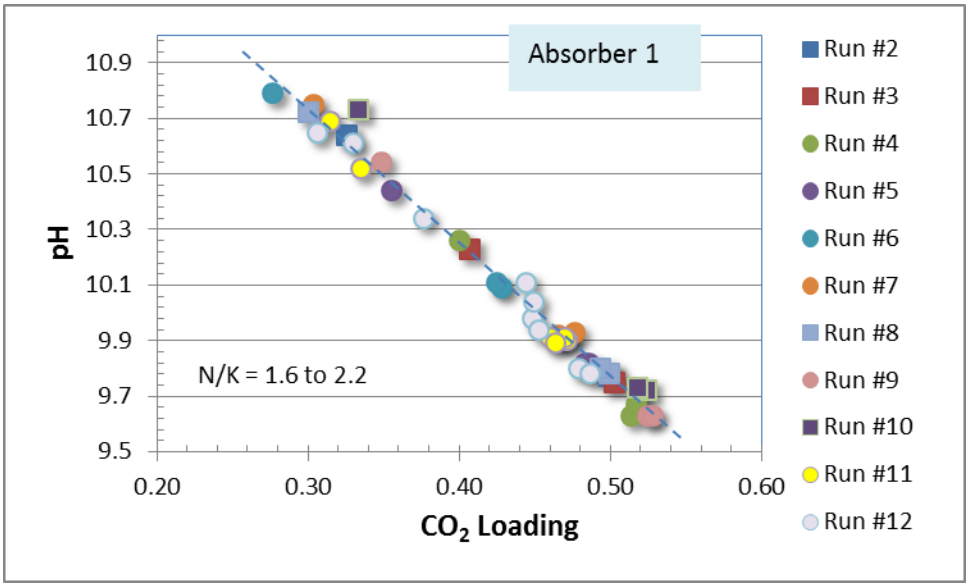

Figure 72. Data showing relationship of the measured pH of rich and lean solutions from absorber 1.

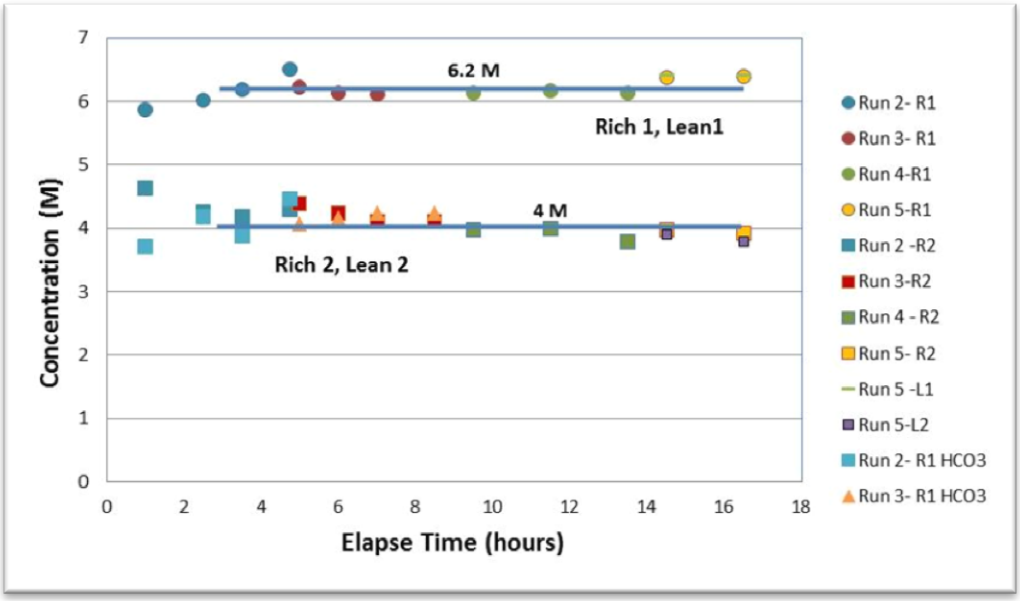

Figure 73. Alkalinity of rich and lean solutions circulating in the integrated system.

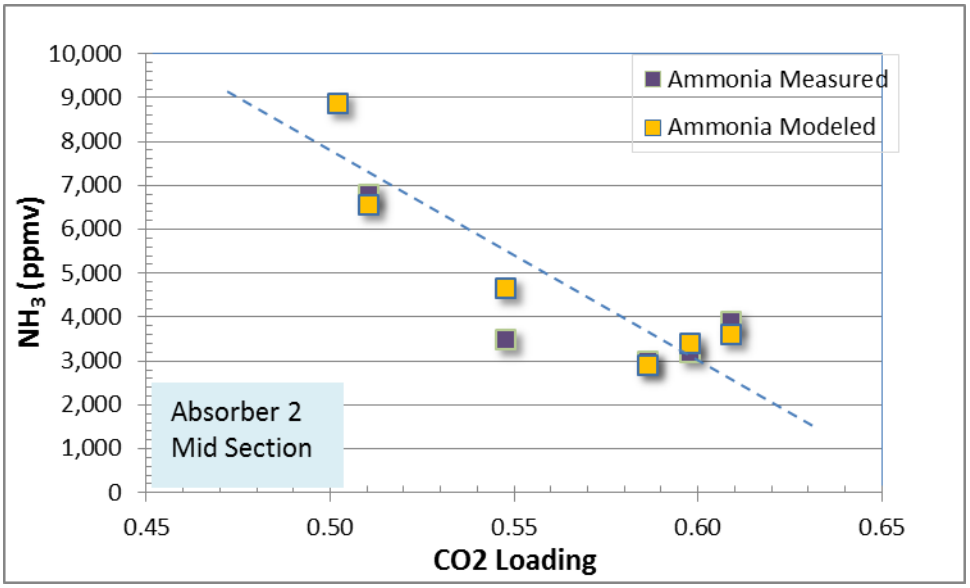

Figure 74. Measured and modeled ammonia values as a function of CO_2 loading for Absorber 2.

Figure 75 shows the variation of capture efficiency with time and inlet CO_2 flow for one of the integrated tests (Run #12) in which we changed the inlet gas flow rate while keeping other operating parameters the same. The capture efficiency was over 90% with the inlet flue gas flow of 400 slpm (60 lpm CO_2). The absorption efficiency was decreased to 80% when we increased the flue gas flow rate at the time marker 3500 min. to 500 slpm (60 to 75 slpm CO_2) without

changing any solvent flow rates. Although the system responds quickly to any changes in the inlet gas stream, it takes about 60-90 min to become stable to the new operating parameters as seen in the figure. This is due to the absorption solution volumes in reservoir tanks, which account for about 200 L of fluid. The total flow rate in and out of the regenerator is about 3 L, and thus one cycle through the system takes about 65 min. The x-axis of Figure 75 indicates the cumulative test time of the integrated system runs.

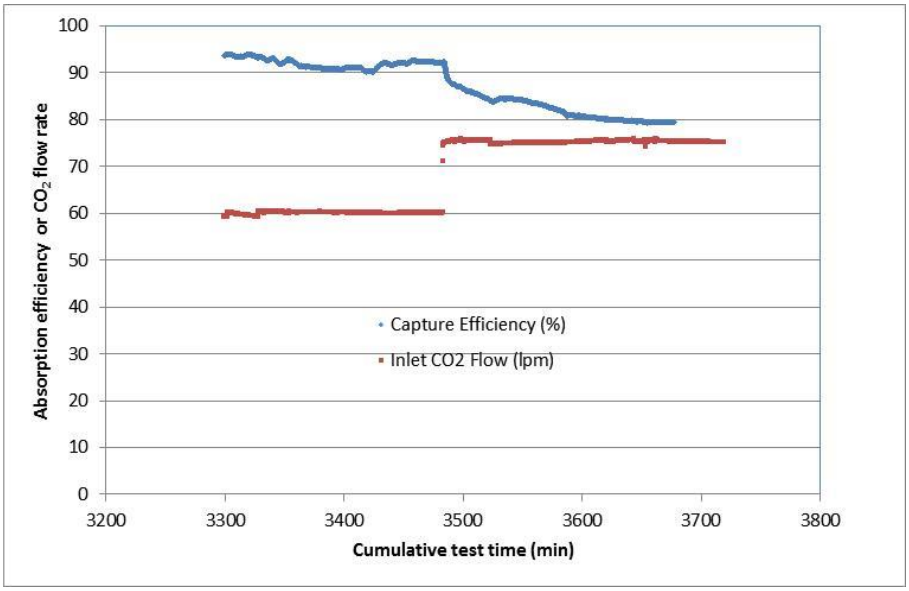

Figure 75. Absorption efficiency and CO_2 inlet flow rate with time.

Figure 76 shows the average total feed gas flow rate, CO_2 feed gas flow rate, and the generated CO_2 gas flow rates over the course of the test campaign (BP2 Run #4 through #12). The integrated system performed as designed with excellent absorption and regeneration cycles. The system controls autonomously maintained the flowrate balance in and out of regenerator such that it did not get flooded or dried up. Most of other system controls were also automated so that the integrated system could be operated by one person.

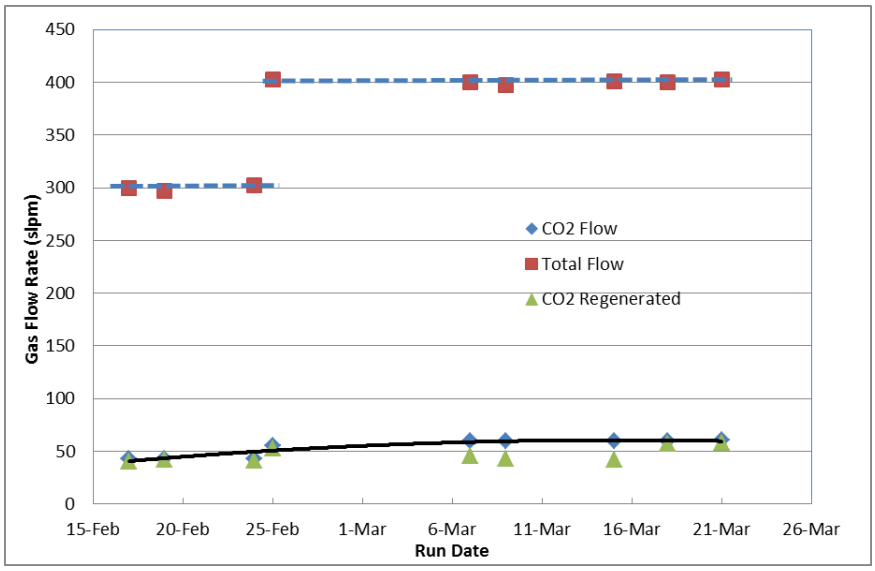

Figure 76. The average gas flow rates for the feed gas and the recovered CO_2 during the first 60 hour run campaign.

7.2 Task 6: Process Modeling, Techno-Economic Analysis, and Technology EH&S Risk Assessment

This task addressed activities to perform final process modeling, techno-economic analysis and technology EH&S risk assessment. The process modeling, material balance, and heat balance calculations were based on updated rate-based modeling, and design changes were based on the data from Task 5 testing.

The project team also conducted the TEA based on the final design configuration and operating conditions determined from test results. Details regarding the preparation of the TEA were provided by DOE. As described in the Task 5 of BP1, a fair amount of work has been done to produce a process layout. In addition, V-L-E data for the K_2CO_3-NH_3-CO_2-H_2O has been updated to estimate mass and heat balance information for the process with reduced uncertainties.

Subtask 6.1 – Process Modeling

This subtask addressed activities to utilize the bench-scale data to perform rate-based heat and mass-transfer modeling. A rate-based model for detailed mass-balance and heat-balance calculations for a flue gas feed equivalent to a 550-MWe flue gas stream was developed. This model was developed and validated in OLI's Environmental Simulation Program (ESP). A summary of the modeling and the results are discussed here. The details of modeling can be found in Appendix C and Appendix to TEA report.

OLI Modeling of the Regenerator

Initially, OLI conducted the mass and heat balance determination for various regenerator options similar to the schematic shown in Figure 77, which shows two examples of regenerator system layouts with flash options. The layout marked as [a] had a flash with the gaseous components mixing with stripped lean liquid from the regenerator, and layout [b] had the gaseous components from the flash returning back to the regenerator for heat recovery. Reboiler duty requirements for layouts [a] and [b] with 0.2 to 0.5 cyclic CO_2 loading operation are 2.2 and 1.8 MJ/kg-CO_2, respectively. The mass balance and the energy balance from OLI were confirmed by PoliMi as well. We performed the absorber-regenerator system optimization to reduce water use and operate the system with < 10 ppm NH_3 in the absorber exhaust gas and regenerated CO_2 stream.

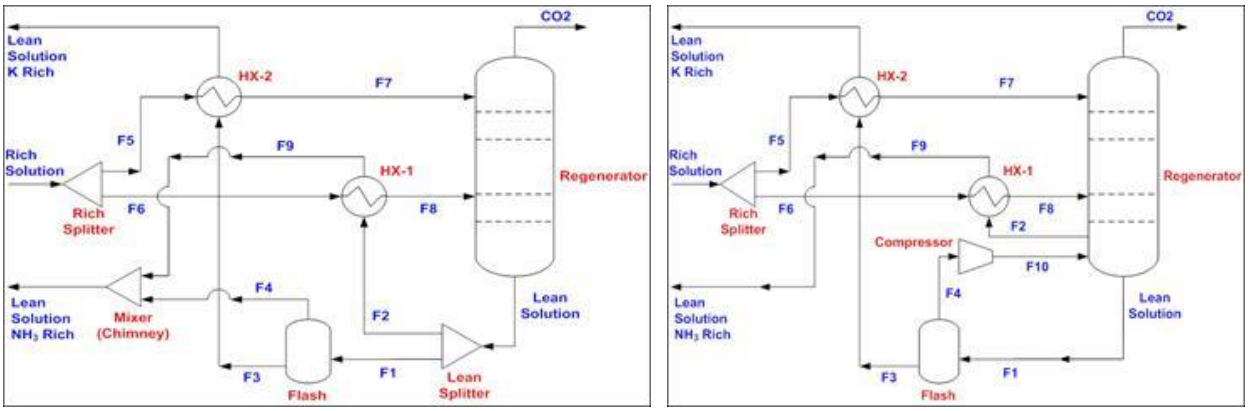

Figure 77. Regenerator layouts with flash options.

OLI completed the rate-based modeling using the ESP for the mixed-salt flowsheets. Using the updated rate-based model, they have determined the complete mass and energy balance for a full-scale system operating with the mixed-salt CO_2 capture system (a configuration similar to the current bench scale is used). The technology was modeled for the carbon dioxide recovery (CDR) facility, in which 90% percent of the CO_2 from the flue gas was captured from a supercritical PC plant with a nominal net output of 550 MW (DOE Case 11). The other fixed parameters were regeneration of high-pressure CO_2 at 99% purity and an ammonia release from the absorber that was less than 10 ppm. The mixed-salt technology was compared with Fluor Econamine FG Plus^{SM} technology (DOE Case 12). The Econamine FG Plus process uses a formulation of MEA and a proprietary corrosion inhibitor to recover CO_2 from the flue gas. The heat duty requirement at the reboiler stripper for the Fluor Econamine FG Plus^{SM} technology was reported as 3.56 MJ/kg (1,530 Btu/lb) of CO_2 recovered. The CO_2 capture and CO_2 pipeline purity specifications were met in all the process configurations investigated in this study. SRI's mixed-salt process can strip CO_2 at high pressure because the stripper for rich-solvent regeneration is operated at higher pressure than the Econamine FG Plus.

Thus, the electrical power required for compressing CO_2 to delivery pressures (> 130 atm) is greatly reduced in the mixed-salt process compared to other solvent-based technologies operating with lower-pressure regenerations. Ammonia-based technology requires absorber solvent cooling and treated gas washing to reduce ammonia emissions. The raw water consumption combines the water being used in the two water-wash sections. The Fluor Econamine FG Plus^{SM} technology requires a large water recycle in the CDR unit for cooling purposes (1,173,350-1,286,900 lpm or 310,000-340,000 gpm), which greatly exceeds the PC plant cooling water requirement (643,450-757,000 lpm or 170,000-200,000 gpm). The mixed-salt process requires a relatively smaller recycle for cooling purposes, and the overall cooling water recycled was 71% less in SRI's mixed-salt process compared to the baseline case. As such, the auxiliary power required for SRI's mixed-salt process CDR unit was 60% less than the baseline case. The heat duty for SRI's mixed-salt process was calculated to be 2.0 MJ/Kg of CO_2 recovered (in the stripper reboiler). This accounts for a 44% decrease in the heat duty requirement in the SRI's mixed-salt process compared to the baseline case.

In summary, SRI's mixed-salt technology can capture CO_2 at high pressure and can meet present DOE targets of CO_2 capture and pipeline purity requirements. The study showed the technology offers much lower energy penalty than Fluor Econamine FG Plus^{SM} technology and/or conventional MEA-based technology for post-combustion CO_2 capture. The technology can easily be scaled up with use of conventional process equipment

Aspen Plus® and OLI Modeling of SRI Bench-scale Absorber System

For direct comparison of model and test results from the SRI bench scale system, SRI performed process modeling using Aspen Plus®. SRI built the Aspen model with column geometry and packing that represent the SRI Absorber 1 as built. Figure 78 shows the simplified model flowsheet. We used 12 stages for the column and 70% Murphree efficiency in the stages. Input gas and solution flow rates and compositions were kept the same as the test run so that we could compare the results of the model directly with observed data. The recycle solution flow was split and fed to stage 1 and 3 of the column. Fresh lean solution was mixed with the recycle solution flow going into stage 3. Table 11 below summarizes input parameters and model results. The model showed 90% CO_2 absorption, indicating an excellent agreement with the test results obtained.

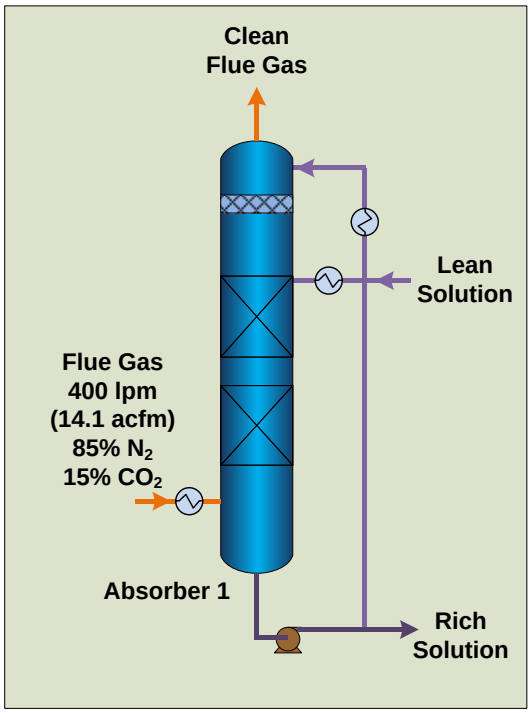

Figure 78. Simplified Aspen model flowsheet for SRI Absorber 1.

Table 11. Summary of Aspen model flow parameters and results.

Flue gas flow	400	lpm	32.98	kg/hr
CO_2 flow	60	lpm		
N_2 Flow	340	lpm		
Temperature	20	°C		
Lean solution in flow	1.15	lpm	75.94	kg/hr
L/G	2.30			
CO_2 Loading	0.18			
Recycle flow	1.28	lpm		
Rich solution flow	1.29	lpm		
CO_2 Loading	0.46			
Absorber 1 Absorption Efficiency	90%			

Figure 79 shows temperature profile of the column from the model and observed data. Both profiles show the same trend; however, the model predicted higher temperature than the observed data. The difference was highest in the midsection of the column, most likely due to

thermal losses of the column because it was not well insulated, and the model did not account for the losses.

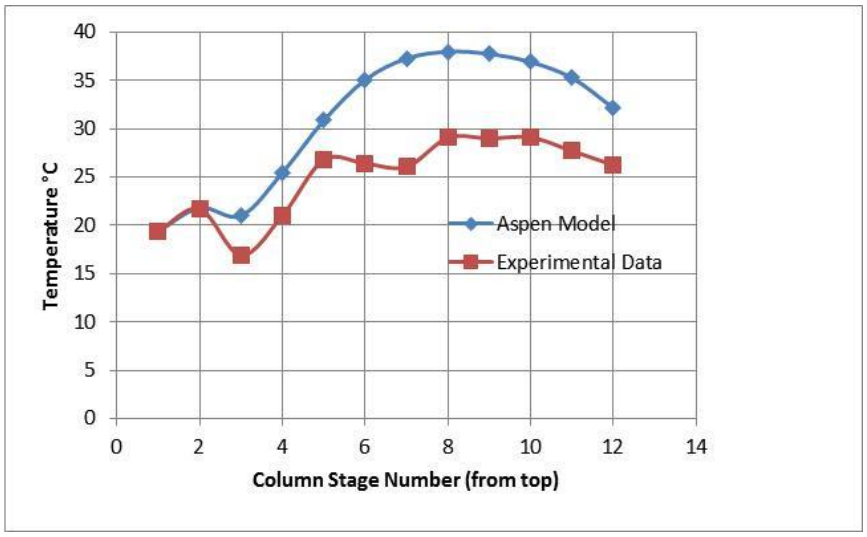

Figure 79. Comparison of modeled and observed Absorber 1 temperature profiles.

Figure 80 shows the vapor phase CO_2 mole fraction profile of the column from the Aspen model. We did not have the ability to measure the CO_2 mole fraction in individual stages of the column. However, the mole fraction at the exit stage (stage 1) was in excellent agreement with the observed data. The lowest mole fraction in stage 3 is due to incoming lean solution at that stage. The CO_2 level slightly increased from stage 3 to 1 as CO_2 rich solution was recycled to the top of the column to reduce the ammonia carryover from Absorber 1 to Absorber 2.

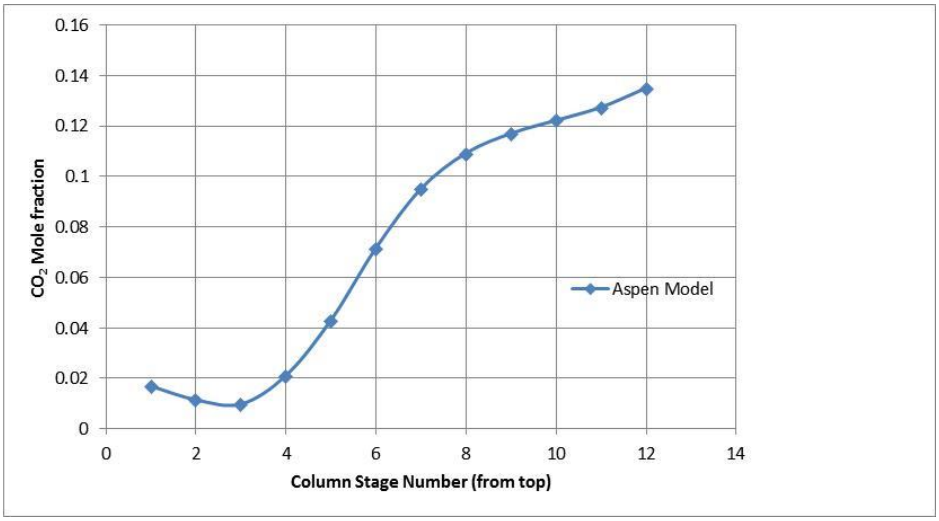

Figure 80. Vapor-phase CO_2 mole fraction profile of Absorber 1 from the Aspen model.

Figure 81 shows the simplified flowsheet diagram of the Aspen model for the complete absorber system. For model validation, we used absorber Run 24 flow rates conditions as described above in Table 11. The model and experimental results agreed well for both absorber efficiencies as shown in Figure 82. The measured ammonia emission 30 ppm also agreed well with the 23 ppm value predicted by the model.

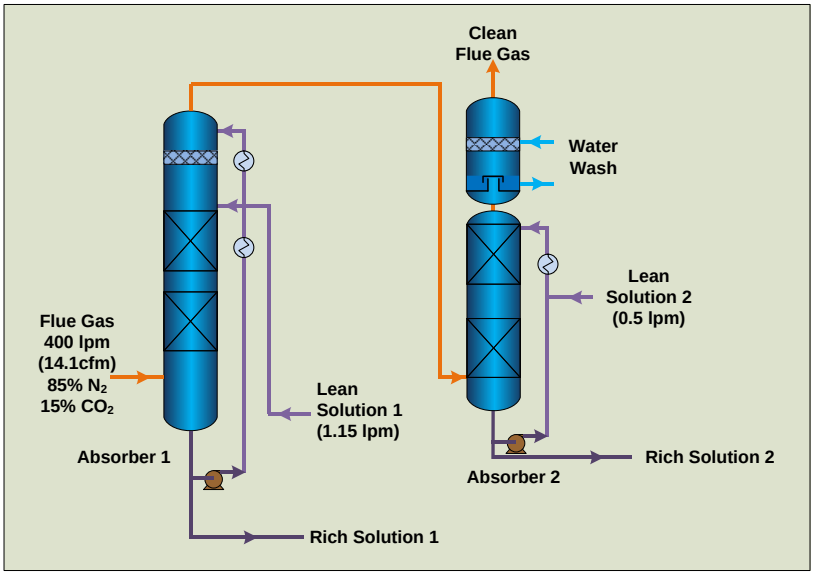

Figure 81. Complete absorber section flowsheet of the Aspen Plus® model.

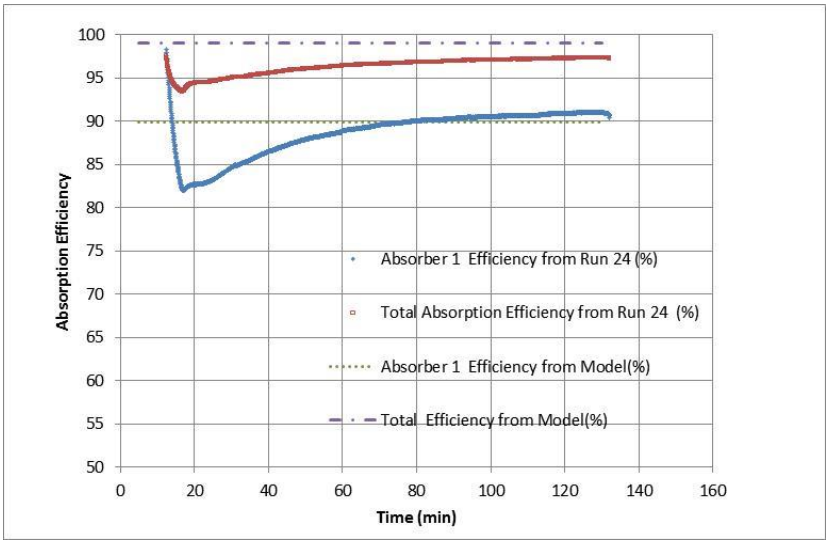

Figure 82. Comparison of absorber test results and Aspen Plus® model.

OLI Systems also independently modeled the complete mixed-salt absorber-regenerator system and conducted the mass and heat balance determination for the complete absorber-

regenerator similar to the schematic shown in Figure 81 with OLI's ESP simulation software. Figure 83 shows the temperature profile results from various models for Absorber 1. The differences in the profiles may be arising from the model convergence algorithms and tolerances employed. In SRI and OLI models, the reboiler duty requirements with 0.2 to 0.5 cyclic CO_2 loading operations are 2.0 and 1.8 MJ/kg-CO_2, respectively, showing good agreement between the models.

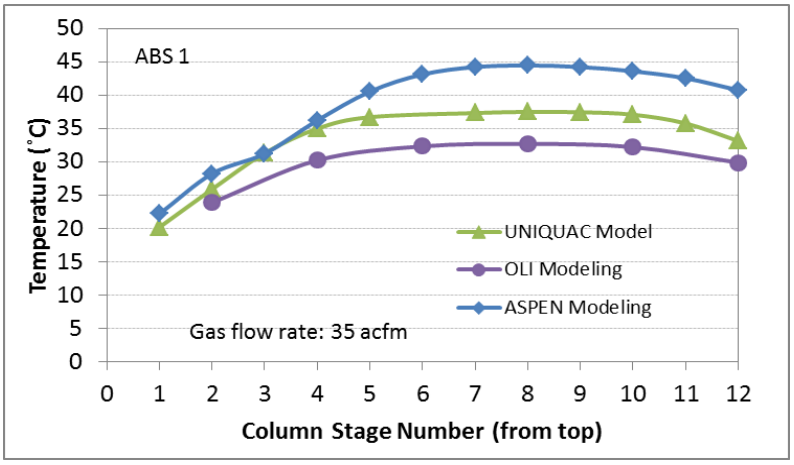

Figure 83. Comparison of observed and modeled temperature profiles for Absorber 1.

Subtask 6.2 – Techno-Economic Analysis

This subtask addressed activities to conduct a detailed TEA of the mixed-salt process in accordance with Attachment 1 – "Basis for Techno-Economic Analysis." Heat and mass balance data were updated based on Subtask 6.1 results. Available DOE economic analyses were used as a basis for this task to ensure the results could be more easily compared to other DOE efforts. For the techno-economic analysis and the updates as described in Subtask 9.4, the optimized flowsheet produced by OLI was used. The TEA report was submitted to DOE as a standalone document.

Subtask 6.3 – Technology EH&S Risk Assessment

This subtask addressed activities for preparation of the technology EH&S risk assessment of the mixed-salt process in accordance with the DOE document– "Basis for Technology EH&S Risk Assessment" included in the PMP for the project. The EH&S report was prepared for the optimized process configuration. A hazard and operability (HAZOP) analysis to review the P&IDs of the current system was conducted in January 2016. The technology EH&S Risk Assessment report is submitted along with this final report as a standalone document.

7.3 Task 7: Integrated System Testing with Variant 1 Flow Sheet.

In BP2, additional tasks were added to the project to study two new variants of the MSP flowsheet in order to optimize the process further and reduce the water use and reboiler duty. In our first configuration (Figure 84, left), solutions circulating in the top and bottom are kept separate, and thus the rich solutions from the top absorber do not go down through the bottom absorber. In Variant 1, absorbers are arranged to have the liquid flow directly from top absorber to the bottom absorber, shifting the ammonia vapor pressure profile downward in the absorber columns. The objective of this flow arrangement is to reduce the ammonia carry over from Absorber 1 to Absorber 2.

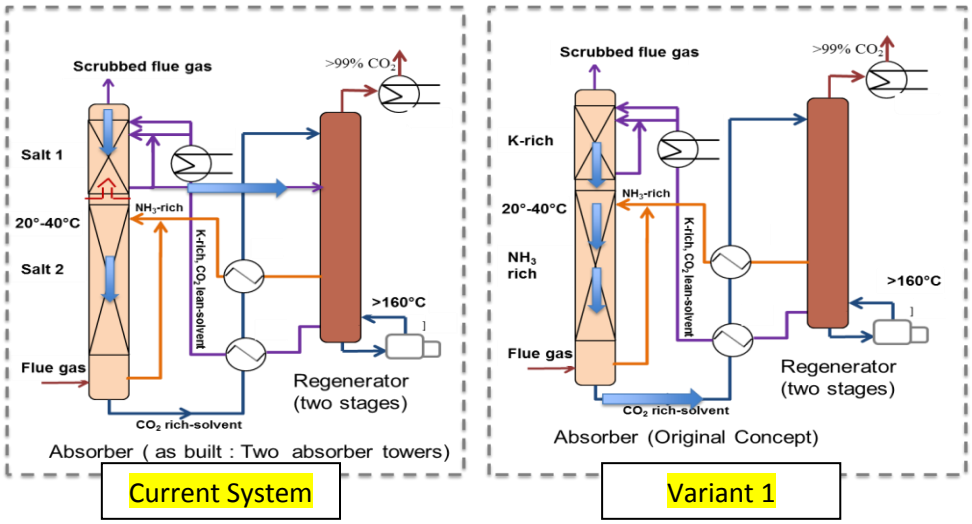

Figure 84. Absorber configuration options, current and Variant 1. No change to the regenerator side.

Subtask 7.1 – Variant 1 System Modification:

This subtask addressed activities related to modifying the bench-scale continuous test system according to the flow-sheet for Variant 1. The columns and the piping were designed to ensure DOE program goals were efficiently met. Figure 85 shows photographs of the absorber system taken during the system modification to include a new water-wash section, and a photograph of the completed absorber system with the new water wash. The water wash has a recirculation pump and bleed and inlet water ports. Water inlet to the absorber water wash is connected to the water exit from the regenerator high pressure water wash. Thus, in the integrated system, there is only one fresh water inlet and the water passes through regenerator high-pressure water wash first and then to the absorber water wash, minimizing the water demand of the system. The system solution flow was rearranged to represent the flowsheet in Variant 1.

Figure 85. Photographs of the absorber system taken during the water-wash installation (left) and the completed system (right).

Subtask 7.2 – System Operation with Variant 1

This subtask addressed activities related to conducting the bench-scale continuous integrated absorber-regenerator testing of the modified system. System operation parameters to be varied included system temperature, pressure, feed gas flow rate, CO_2 loading, and liquid recycle flow rates.

With the new flow sheet configuration, we performed a series of integrated runs to optimize the system operating parameter. Table 12 below shows the summary of runs and key experimental parameters and data. The all the test were performed with the same recirculating solution without replenishing ammonia. The ammonia loss of the system was significantly reduced; from ~3000-4000 ppm to ~1000 ppm with the new flowsheet design. Most importantly, we managed to maintain the high absorption efficiency under these test conditions.

Table 12. Summary key parameters and data of Integrated System test runs.

Run #	Total gas flow (lpm)	Inlet CO2 %	Exit CO2%	CO2 Capture Efficiency (%)	Ammonia before ww (ppm)	Ammonia after WW (ppm)	Regenerated CO2 (lpm)	NH3 after HPWW (PPM)	Run duration (hours)
Run #14	404	15.27	3.00	83	5300	270	59	31	3
Run #15	405	15.34	1.23	93	3800	261	59	38	4.6
Run #16	399	15.36	1.75	90	2886	179	53	38	5
Run #17	403	15.18	1.93	89	2293	85	54	63	6.6
Run #18	403	14.97	1.70	90	1769	97	51	0	3
Run #19	401	15.07	2.08	88	1151	25	54	0	6.6
Run #20	396	15.31	2.64	85	851	30	48	0	6
Run #21	398	15.28	2.14	88	1539	56	53	0	6
Run #22	400	15.13	2.54	85	1052	36	54	0	5.1
Run #23	397	15.18	2.40	86	964	1	52	0	7.1
Run #24	398	14.95	2.61	85	1018	3	49	0	5.7

Subtask 7.3 – Variant 1 Bench-Scale Test Data Analysis:

This task involved the analysis of data from the bench-scale tests in Subtask 7.2 to determine the best conditions suitable for cyclic operation of the absorber and regenerator with reduced ammonia emissions. Based on the analysis of Subtask 7.2 data, SRI determined if additional bench-scale tests would benefit the project.

Figure 86 shows a plot of absorber inlet CO_2 flow and regenerated CO_2 flow with time for a continuous 5-hour run. After an initial ~20 min, the system became very stable and continued to maintain the performance over the 5-hour test period. This test also demonstrates the rapid start capability of the mixed-salt process, which would be very useful for applications in which CO_2 output varies widely in a short time.

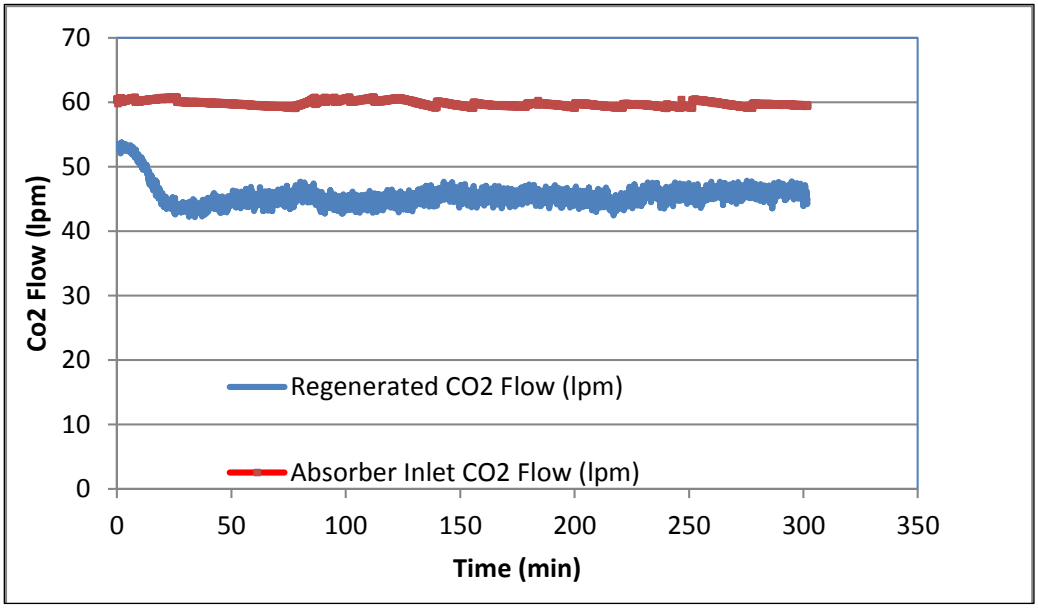

Figure 86. CO_2 absorption and regeneration in a typical integrated system test.

Figure 87 shows the ammonia emission from the absorber column. Once the system became stable, the ammonia loss from the absorber was about 1000 ppm, which was carried in the scrubbed flue gas stream to the water wash. The cleaned flue gas stream from the water was lower than 10 ppm, meeting the emission requirements of the absorption system. The ammonia in the regenerated CO_2 stream after the high-pressure water wash also meets the emission requirements for the CO_2 product.

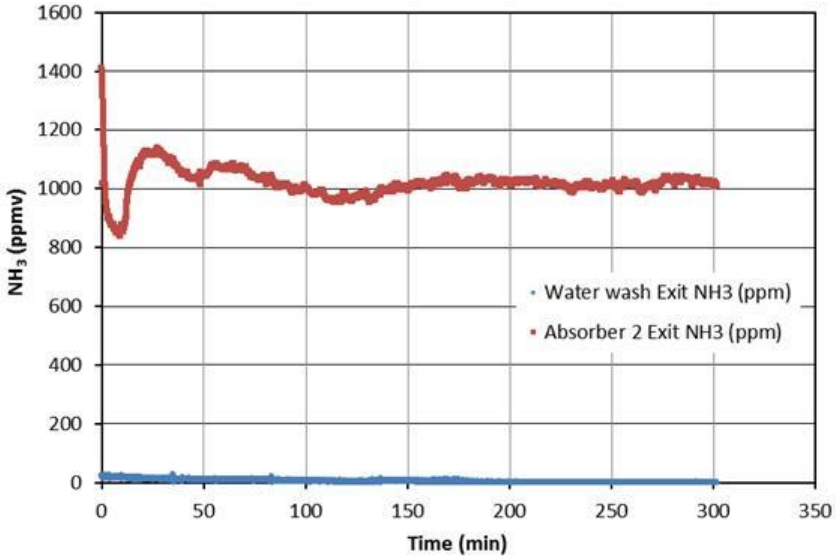

Figure 87. Ammonia emission from the absorber column in a typical integrated system test.

Figure 88 shows temperature profiles of the absorber stages starting from the top. The lower and middle sections of the Absorber1, which captures larger portion of CO_2 was operated at 20-25 °C range. Top of the absorber was operated slightly lower to minimize the ammonia carry over to Absorber 2. Absorber 2 was operated close to 20°C, which was optimized for highest CO_2 absorption and lowest ammonia loss. As mentioned earlier, mixed-salt absorbers can be operated in 20˚-40 ˚C range. For large-scale systems, the desired absorber temperature can be decided based on the available cooling water temperature.

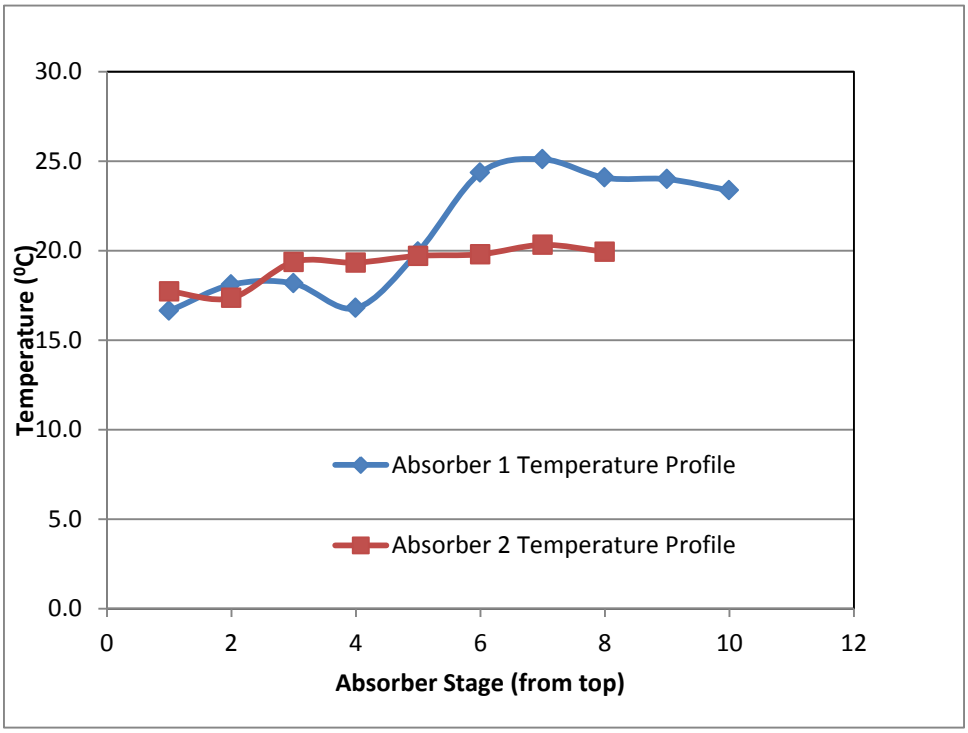

Figure 88. Temperature profile of the absorption columns in a typical integrated system test.

7.4 Task 8: Integrated System Testing with Variant 2.

In this variant as shown in Figure 89, the CO_2-rich solution is introduced at the exit of the second absorber in the current system to reduce the ammonia content in the gas stream leaving the absorbers. This arrangement was tested to reduce the ammonia loss and waste-water generation in the water-wash units. The IHI Corporation also was interested testing the Variant 2 configuration. Their activities are described in Task 10.2.

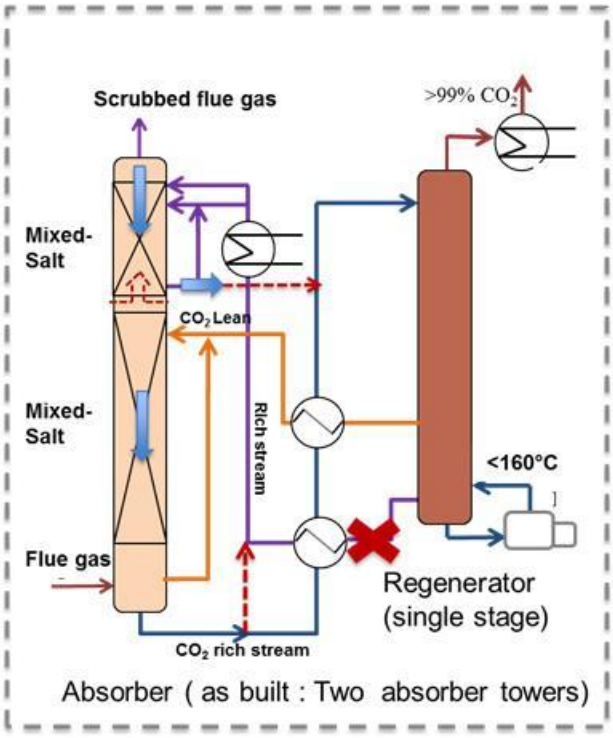

Figure 89. Absorber configuration options, Variant 2. Red-dashed lines show the new flow direction.

***Subtask 8.1 – Variant 2 System Modification*:**

This subtask addressed activities related to modifying the bench-scale continuous test system according to the flow-sheet for Variant 2. Because the mixed-salt system was designed with some flexibility of flow pattern changes, the Variant 2 option was demonstrated without major system modifications. We also added a setup for steam measurements so that we could obtain a preliminary estimate of steam use in the regenerator. The setup included a steam trap, condensate trap, and a condensate cooling system.

Subtask 8.2 – System Operation with Variant 2

This subtask addresses activities for conducting bench-scale continuous integrated absorber-regenerator testing of the modified system. System operation parameters to be varied include temperature, pressure, feed gas flow rate, CO_2 loading, and liquid recycle flow rates.

We operated the Variant 2 configuration with 90% CO_2 capture efficiency. However, we encountered difficulties with this configuration. The system took longer to reach steady state and needed higher flow rate of water in the water wash to reduce the ammonia emission than did Variant 1.

Subtask 8.3 – Variant 2 Bench-Scale Test Data Analysis:

This subtask involved the analysis of data from the bench-scale tests in Subtask 8.2 to determine the best conditions suitable for cyclic operation of the absorber and regenerator with reduced ammonia emissions. Based on the analysis of Subtask 7.2 data, SRI determined if additional bench-scale tests would benefit the project.

In the Variant 2 tests performed at SRI with 90% absorption efficiency, we noticed a higher ammonia carryover from the absorbers than with Variant 1and hence required a large volume of water in the water wash to control ammonia emission. Also, system had to be operated at high L/G to maintain the absorption efficiency. Therefore, we discontinued the Variant 2 option, as it was clearly inferior to Variant 1 flowsheet configuration.

7.5 Task 9: High-Capacity Runs and Modeling Update

In this task, SRI and the team performed equilibrium modeling to conduct a speciation analysis at high mixed-salt compositions and system testing, determine the system energy and mass balance, and update the TEA. The updated rate-based model developed in Subtask 3.1 and data from Task 7 and 8 testing were used in process modeling to estimate the heat and mass balance (for new flow sheets). The TEA prepared in Subtask 6.2 was also updated.

Subtask 9.1 – Modeling of High-Capacity Solvent:

This subtask addressed activities for SRI to utilize the UNIQUAC model developed in BP1 to model the speciation of highly concentrated mixed-salt systems. We modeled the system operational regimes for operation without solid formation as a function of the temperature, pressure, and CO_2 loading of the rich and lean solutions. The results of this modeling was incorporated to AsAPs report and the details can be found in the Appendix A

Subtask 9.2 – System Operation at High Capacity:

This subtask addressed activities related to conducting bench-scale continuous integrated absorber-regenerator testing of the modified system with conditions determined from Subtask 9.1 We performed several test runs with high loading conditions. The system operation was completely satisfactory under these conditions and we did not encounter any operational issues. The parametric tests were conducted with varying L/G ratios and the observed the corresponding CO_2 capture efficiencies. Figure 90 shows a sample test run with observed CO_2 capture efficiency in the range 85 to 90% and the regeneration with cyclic CO_2 loading of ~ 8-9 wt%. Figure 91 shows the observed alkalinities of circulating rich and lean solutions in the integrated system. In summary, the system operation can be easily adjusted dynamically to the required capture efficiency and/or energy demand of the integrated system.

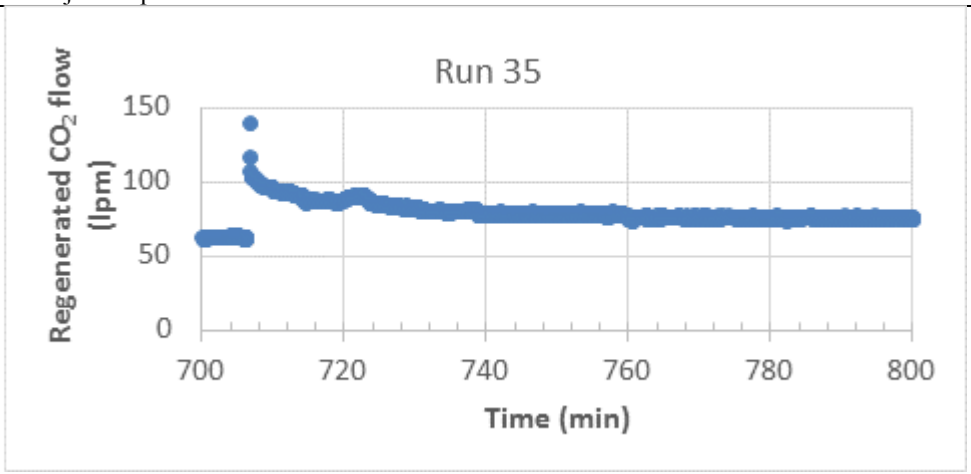

Figure 90. Observed 85-90% capture efficiency and regeneration with cyclic CO_2 loading of ~ 8 - 9 wt.%.

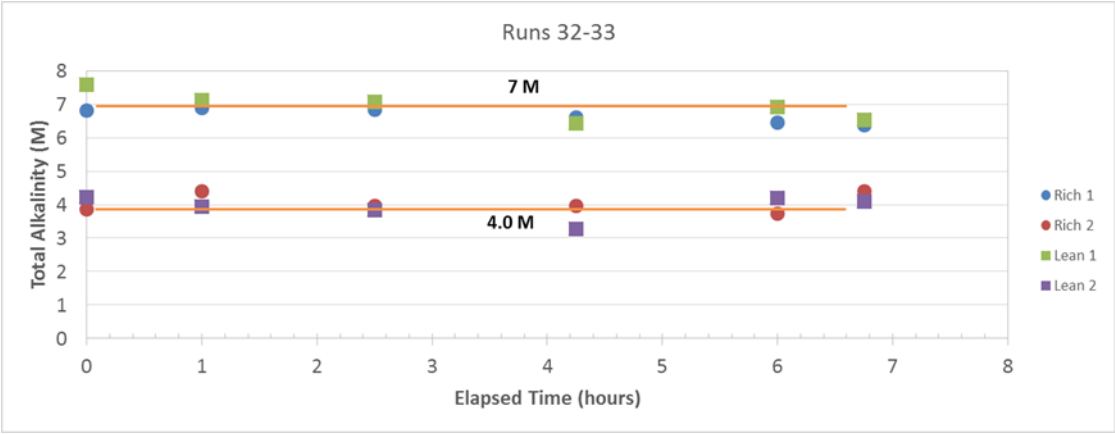

Figure 91. Alkalinity of rich and lean solutions circulating in the integrated system.

Subtask 9.3 – Mass Balance and Energy Update:

This subtask addressed activities for the team to work on updating and modeling the process to include the system modifications in Tasks 7 and 8. The team used the comprehensive thermodynamic model for predicting phase equilibria and thermophysical properties for the system K_2CO_3-CO_2-NH_3-H_2O and the rate-based model developed with data from Subtask 5.4 to determine the energy and mass balances for flowsheets Variants 1 and 2. The team analyzed the test data from SRI from Subtasks 7.2 and 8.2 to update the design boundaries (T and P) for thermodynamic and rate-based modeling. The team updated the process flow sheet developed in Subtask 6.1 to include the variations in Tasks 2, 7, and 8. OLI performed a process simulation using the ESP. The process simulation results were verified and fine-tuned on the basis of SRI's process data. The details of this analysis are included in the OLI report attached as Appendix A to the Techno-Economic Analysis report, which is submitted to DOE as a standalone document.

Subtask 9.4– Techno-Economic Analysis Update:

This subtask addressed activities for SRI to conduct an updated detailed TEA of the mixed-salt process to include the process flow sheet from Subtask 9.3 in accordance with Attachment 1 – "Basis for Techno-Economic Analysis." Heat and mass balance data were updated based on Subtask 9.3 results. As before, available DOE economic analyses were used as a basis for this task to ensure the results were easily compared to other DOE efforts.

In Task 6, we performed the TEA based on the mass and energy calculation for SRI's original concept (see Figure 1). Even for that concept, CO_2 capture and CO_2 pipeline purity specifications were met; they were also met in all other process configurations investigated in this study. OLI completed the preliminary evaluation of the mass and energy balance for Variant 1. Below, we provide the data for our original flow sheet and the Variant 1 flow sheet.

Summary for the original flow sheet: SRI's mixed-salt process can strip CO_2 at high pressure because the stripper for rich-solvent regeneration is operated at higher pressure than that for the Fluor Econamine FG Plus^{SM} process. The electrical power required for compressing CO_2 to delivery pressures (> 130 atm) is greatly reduced in the mixed-salt process compared to other solvent-based technologies operating with lower-pressure regenerations. Ammonia-based technology requires absorber solvent cooling and treated gas washing to reduce ammonia emissions [15]. The raw water consumption combines the water used in the two water-wash sections. The Fluor Econamine FG Plus^{SM} technology requires a large water recycle in the carbon dioxide recovery (CDR) unit for cooling purposes (1,173,350-1,286,900 lpm or 310,000-340,000 gpm), which greatly exceeds the PC plant cooling water requirement (643,450-757,000 lpm or 170,000-200,000 gpm). The mixed-salt process requires a relatively smaller recycle for cooling purposes, and the overall cooling water recycled was 71% less in SRI's mixed-salt process compared to the baseline case. As such, the auxiliary power required for SRI's mixed-salt process CDR unit was 60% less than the baseline case. The heat duty for SRI's mixed-salt process was calculated to be 2.0 MJ/Kg of CO_2 recovered (in the stripper reboiler). This accounts for a 44% decrease in the heat duty requirement in the SRI's mixed-salt process compared to the baseline case.

Table 13 summarizes the performance comparison between the original mixed-salt technology and a DOE baseline case.

Table 13. Comparison between mixed-salt original design and DOE baseline case.

Performance Factors	Econamine FG Plus Baseline	SRI's Mixed-Salt Technology*
CO_2 capture, %	90.2	90.1
CO_2 purity, %	99.8	99.3
Stripper pressure, atm	1	12
Raw water consumption, m^3/min (gpm)	0.1 (36)	2.54 (671)
Raw water recycle, m3/min (gpm)	1,173-1,287 (310,000-340,000)	341 (89,868)
Auxiliary power, KWe	20,600	3,472
Heat duty, MJ/Kg of CO_2	3.56	2

Summary for Variant 1. In our original system (Figure 84, left), solutions circulating in the top and bottom are kept separate, and thus the rich solutions from the top absorber do not go down through the bottom absorber. In Variant 1, absorbers are arranged to have the liquid flow directly from top absorber to the bottom absorber, shifting the ammonia vapor pressure profile downward in the absorber columns. Forcing the ammonia profile downward in the multistage absorber columns reduced the ammonia carryover with the exiting scrubbed gas. In addition to reducing ammonia emission, this design simplified the process control and required less equipment than the original MSP flowsheet since it combines ammonia-lean and ammonia-rich streams in the absorbers and delivers the combined stream to the regenerator via a single high-pressure pump. The potassium concentrations of both inlet CO_2-lean streams are the same as they are when returning from a dual-stage single regenerator, and potassium is non-volatile. This variant operated with the cooling coil in between Absorbers 1 and 2 for further control of ammonia carryover from Absorber 1 to 2. Since the raw water use (cooling water recycle from the cooling tower) in the original mixed-salt design is an order of magnitude lower than that for amine technology (see Table 14), there is room to use more cooling water for ammonia control if needed, which in turn will significantly reduce the water demand in the water wash and reduce the raw water use. In addition, a commercially available membrane system can be considered for ammonia and water recovery and recycling of water-wash effluent.

Table 14 summarizes preliminary data from the OLI evaluation and compares the performance of the mixed-salt technology (original process option) and the mixed-salt Variant 1. The preliminary data shows raw water consumption is reduced by factor of 6 in Variant 1 compared to the original design.

Table 14. Comparison between the original mixed-salt design and Variant 1.

Performance Factors	SRI's Mixed-Salt Technology*	SRI's Mixed-Salt Technology (Variant 1)*
CO_2 capture, %	90.1	90.1
CO_2 purity, %	99.3	> 99.0
Stripper pressure, atm	12	10
Raw water consumption, m^3/min (gpm)	2.54 (671)	0.41 (107.5)
Raw water recycle, m3/min (gpm)	341 (89,868)	305 (80,569)
Auxiliary power, KWe	3,472	3,581
Heat duty, MJ/Kg of CO_2	2	2
* Systems are given in Figure 1		

OLI modeled the regenerator at 180° C; this was an attempt to reduce the ammonia present in the lean stream to Absorber 2 (Case: Variant 1 HT option). The net result was the reduction of ammonia in the flue gas exit from the absorber 1 by about 50%. However, the reboiler energy requirement is increased by about 0.1 MJ/kg compared to the lower temperature regenerator option (160° C). The data for Variant 1 (high temperature [HT] option) is summarized in Table 15.

Table 15. Comparison of the mixed-salt Variant 1 (HT option) and DOE baseline case.

Performance Factors	Econamine FG Plus Baseline	Shell Cansolv Baseline	SRI's Mixed-Salt Technology*
			Variant 1 (BP2)
			Rate-based
CO_2 Capture, %	90.2	90.0	90.3
CO_2 Purity (before compression), %	99.8	98.24	99.6
CO_2 Product Compressor	Yes	Yes	No
Stripper Pressure, atm	1.0	1.98	10.0
Raw Water Consumption, m^3/min (gpm)	0.1 (36)	0.02 (5)	0.000 (0.000)
Raw Water Recycle, m^3/min (gpm)	1,173-1,287 (310,000-340,000)	Substantial amount (data not presented)	727 (178,995)
Auxiliary Power, KWe	20,600	16,000	3,221
Heat duty, MJ/Kg of CO_2	3.56	2.56	2.19

* Comparison with respect to CDR unit only

PoliMi completed the TEA update for the Variant 1 process and issued a report. The report was sent to project PM as a standalone document.

7.6 Task 10: Regenerator Steam Use Measurement and Modeling

This task addressed activities related to analysis of the complete data set from the SRI testing and information from OLI to optimize the process flow sheet for determining resource requirements for updating the TEA. The model and the experimentally determined energy data for the mixed-salt regeneration were compared for accuracy.

Subtask 10.1– Regenerator Steam Use Measurement:

This subtask addresses the activities to modify the regenerator reboiler steam feed inlet and the steam return to install necessary steam flow meters and values to evaluate the steam use. We installed condensate traps to ensure the steam was of good quality. We also performed additional temperature measurements to determine the overall heat use in the regenerator side of the integrated system.

We determined the steam usage by measuring the amount of condensate collected. Steam measurements were performed when the system was running under steady-state conditions. In a typical measurement, the condensate from the steam return line was collected over a predetermined period of time. The collected condensate weight was determined, and the amount of condensate was measured at two feed gas flow rates (17 and 28 acfm) and varying L/G ratios. The data from our measurements are given in Figure 92. The steam consumption (and corresponding reboiler duty) increased with L/G ratio as the recirculated solvent volume increased. This was expected as the sensible heat demand increased with the higher recirculation solvent volume. IHI has measured the reboiler duty under similar conditions and reported that at L/G of about 1.5 the reboiler duty is 2.3 MJ/kg CO_2. In SRI system, it was difficult to maintain the steady state operation at very low L/G (less than 1.5) due to the instability of the circulating pumps at very low flow rates.

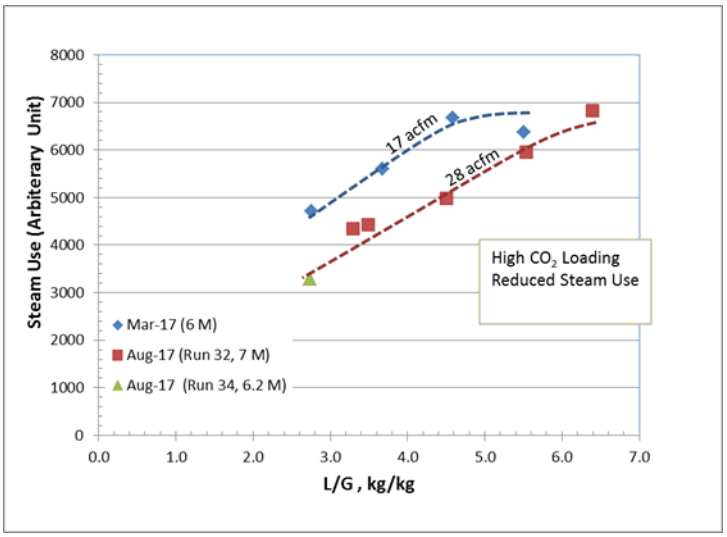

Figure 92. Steam use vs. L/G for integrated runs under steady-state conditions at 17 and 28 acfm gas flow rates.

Subtask 10.2– IHI System Testing and Modeling:

This subtask addressed activities that included IHI Corporation to conduct the small bench-scale test to aid the system modification relevant to Variant 2 in Subtask 8.1 and the Aspen Plus® modeling of the Variant 2 system. IHI made necessary modifications to their system to closely mimic the SRI mixed-salt system and collected the data to determine the conditions for reduced ammonia emissions. They also used the actual regenerator steam as measured at SRI in Subtask 10.1 to perform Aspen modeling of the process.

IHI has a small bench-scale test plant for the amine process at IHI Yokohama. IHI modified it to run the mixed-salt system (Variant 2) and conducted several tests to collect the data to determine the conditions for reduced ammonia emissions. Figure 93 shows a photograph of the bench-scale test plant for the mixed-salt process. In this plant, the absorber has two sections with heat exchangers to control the liquid temperature. The ammonia scrubbing system also has two sections. In the first section, a part of CO_2-rich solution from the bottom of absorber was used with recirculation to capture NH_3 in the outgoing gas stream. The second water-wash section is used to reduce NH_3 emission below 10 ppm. The regenerator was a single-stage system, producing a one lean solution concentration as required in Variant 2. The top section of the regenerator was the cooling and water wash to control the ammonia in the CO_2 product gas.

In IHI test of Variant 2, they observed ~6000 ppm NH_3 carryover from the absorber to the water wash, which required a large amount of water in the water wash. In addition, the reboiler duty showed no improvement over Variant 1. Therefore, the team concluded that the Variant 1 flow sheet was a better configuration for reduced ammonia emission and optimal reboiler duty and water use.

Figure 93. Bench scale test plant at IHI Yokohama

8. PRODUCTS

During the course of this 45-month mixed-salt process development project, the intellectual property (IP) listed below was generated. The overall objective of the project to advance and test a solvent-based CO_2 capture technology that can capture CO_2 from existing or new PC power plants at low cost was successfully demonstrated. SRI's newly developed ammonia-based mixed-salt technology (mixed-salt process) was tested successfully at the bench-scale level to validate the process can capture CO_2 at high efficiency (> 90%) with very high CO_2 loading (> 10 wt.%) and require less than 2 GJ/tonne for solvent regeneration. We advanced the technology from the laboratory scale to large bench-scale level, and the process is now ready for engineering scale testing.

Inventions, Patent Applications, and/or Licenses

The SRI patent (US Patent 9,339,757) on mixed-salt technology entitled, "Rate Enhancement in Aqueous Potassium Carbonate Solutions by an Ammonia-Based Catalyst," was issued on May 17, 2016.

Japanese Patent No. 5989916 "Ammonia-based mixed-salt CO_2 capture process for power plant and industrial applications" was granted in September 2016.

9. PARTICIPANTS & OTHER COLLABORATING ORGANIZATIONS

The following organizations participated in the program:

- OLI Systems (OLI), NJ
- Stanford University, CA (BP1 only)
- IHI Corporation, Japan
- Polytechnico De Milano (PoliMi), Italy
- Aqueous Systems Applications (ASApS), Denmark

10. OVERALL PROJECT SUMMARY

SRI has been developing ammonia-based processes for both post-combustion and pre-combustion applications for over a decade. Leveraging on this expert knowledge of current, state-of-the-art ammonia-based and potassium-based processes, we have demonstrated a novel, highly efficient MSP in a large bench-scale system. The MSP combines existing ammonia and potassium-carbonate technologies with improved absorption steps for rate enhancement and ammonia emission reduction, and a novel selective regeneration process with a high-pressure CO_2 product to introduce a new and advanced transformational solvent-based technology. The striking advantages of the SRI process include: low heat of reaction, high loading of CO2, high-pressure regeneration of > 99% pure dry CO2, low sensitivity to impurities, low process cost, use of a non-degradable low-cost solvent with a very low carbon footprint for its production, low emissions, and reduced water use compared to the state-of-the-art ammonia-based and amine technologies. Under the currently funded DOE program for MSP testing at large bench scale, the following research goals have been achieved.

10.1 Goals and Milestones Completed in BP1

During the BP1, SRI focused on system design, procurement, installation, and absorber testing-related activities. We also successfully completed the installation of the absorber and the modification to the regenerator systems. We tested the absorbers and the regenerator as individual subsystems and collected necessary data for system integration and large bench-scale regenerator design. OLI and PoliMI performed initial modeling of the MSP and reported that the modeling was in good agreement with the experimental data. PoliMi has successfully completed the establishment of baseline models (in-house power plant modeling) of the two PC steam supercritical power plants identified by NETL for the TEA study. Initial process modeling by IHI indicates that the mixed-salt process can significantly improve the efficiency loss compared to an amine-based CO_2 capture process as shown in Figure 94. The number for net power plant efficiency for the mixed-salt process as estimated by IHI is comparable to the finding by PoliMi, and the results of two models are compared in Figure 95. However, the detail power losses are varied due to the different process layouts considered. The PoliMi process layout evolved based on interactive discussions over two years, and the IHI layout is very preliminary.

The following is the list of goals and milestones completed during Budget Period 1.

- Optimized the bench-scale absorber and regenerator performance at the component stage to achieve > 90% CO_2 capture with reduced NH_3 emission, low water use, and high-pressure regeneration.
- Determined the independent relationships between solvent concentration, absorption and regeneration conditions, column packing, CO_2 capture efficiency, ammonia loss, and water usage.

- Established a rate-based thermodynamic modeling database for the potassium- and ammonium-based system heat and mass balance evaluations.
- Prepared a preliminary techno-economic analysis.
- Revised and maintained the Project Management Plan (PMP).
- Conducted overall project management reporting.
- Prepared and submitted the Budget Period 2 continuation application.

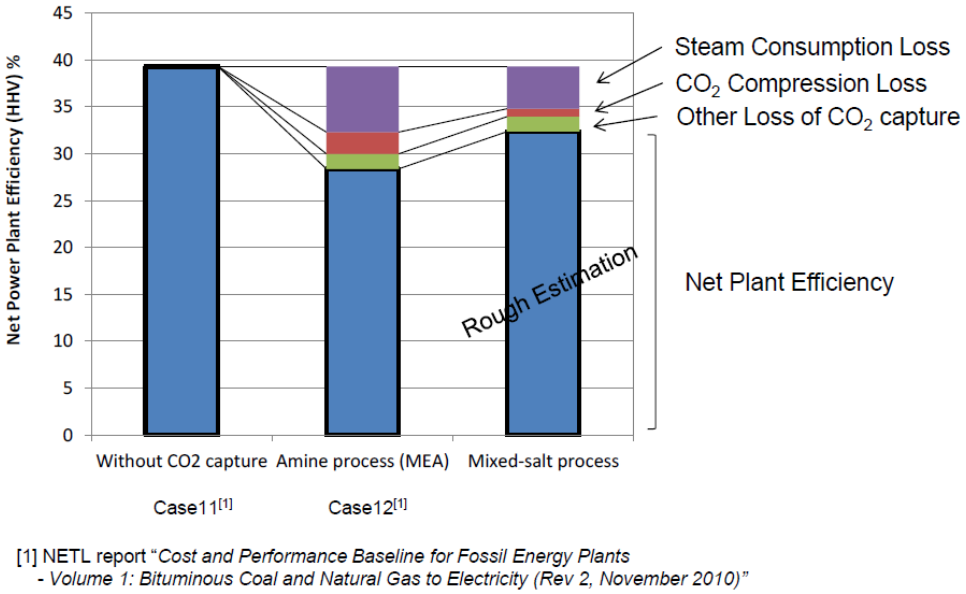

Figure 94. Net power plant efficiency comparison for mixed-salt and MEA for DOE Cases 11 and 12.

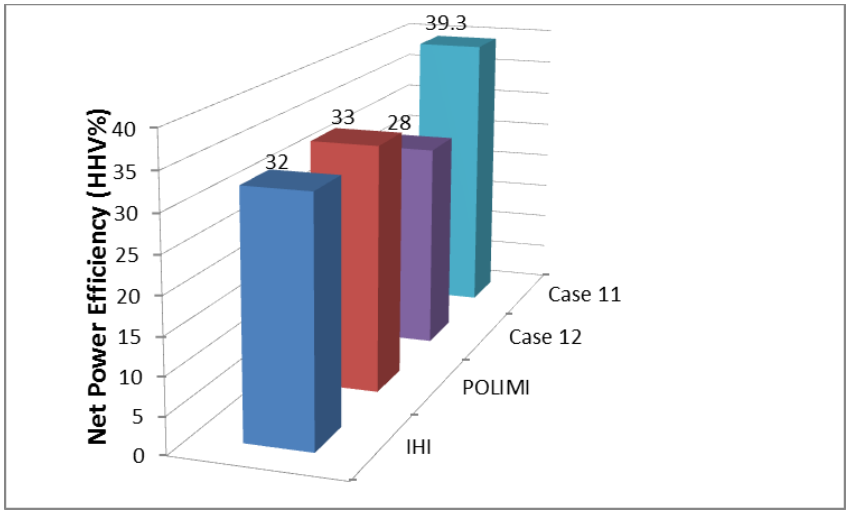

Figure 95. Net power plant efficiency comparison for mixed salt and MEA for DOE Cases 11 and 12. Comparison of IHI and PoliMi modeling results.

10.2 Goals and Milestones Completed in BP2

In budget period 2, SRI designed and built large bench-scale regenerator that was properly sized for the absorber system. We successfully integrated absorber and regenerator and performed continuous test campaigns. We demonstrated the performance of MSP in a continuous absorption-regeneration over long period of time and showed the operability of the process under dynamic conditions. We also explored two process flowsheet variants in order to further reduce the ammonia loss and water usage. We found that MSP process can be scaled well to the next level. Under a new project that we are planning to begin this year, we will be testing the MSP at 10 MW level at TCM, Norway.

The following is the list of goals and milestones completed during Budget Period 2.

- Collected experimental and modeling data available in the literature for the H_2O-CO_2-NH_3-K_2CO_3 system; developed a software package to determine speciation and compositions.
- Developed comprehensive data base for both equilibrium and rate-based modeling of the H_2O-CO_2-NH_3-K_2CO_3 system used in MSP. Modeled the MSP integration with a supercritical coal power plant (DOE case 11). Mass and energy balance were determined for a two-process layout to add a CO_2-capture system for DOE Case 11. The comparison was made between the MSP and DOE Cases 12 and 12B. Modeled and tested two process flowsheets to reduce both the process water use and NH_3 emissions (<10 ppmv) and demonstrated the capture cost is less than \$40/ton-CO_2.
- Demonstrated the operation of the MSP absorber at high temperature (20° – 40°C) without solvent chilling and reduction of ammonia emissions using the two-stage absorber approach.
- Demonstrated high cyclic CO_2 loading capacity (10 wt%) and high throughput using high-concentration solvent (~ 9 molal) without solid formation.
- Demonstrated system cyclic operation with cyclic loading between 0.2 and 0.59 with 90% efficiency at a bench-scale of ~ 0.3 ton/day CO_2 capture.
- Collected test data over a wide range of conditions. Parameters varied included feed gas flow rate, mixed-salt composition, CO_2 loading, and the L/G ratio.
- Demonstrated longer-term operation of the integrated system with 90% CO_2 capture and regeneration of the high NH_3/K and low NH_3/K lean solutions and > 99% purity CO_2 using a two-stage regenerator.
- Measured the process steam use and demonstrated the process regeneration energy ~2 MJ/kg-CO_2 by modeling and by testing at both SRI and IHI.
- Identified technology gaps to reduce the overall process energy requirements that can be addressed at the engineering-scale testing. The integrated system has been tested over last 2.5 years.

- Completed the TEA and EHS evaluation. Summary of the TEA is given below.

Comparison between MSP and DOE baseline case

Performance Factors	Econamine Baseline	SRI's Mixed-Salt Technology*
CO_2 capture, %	90.2	90.3
CO_2 purity (before compression), %	99.61	> 99.0
Stripper pressure, atm	1.0	10.0
Raw water recycle, gpm	~325,000	<100,000
Auxiliary power, KWe	20,600	3,581
Heat duty, MJ/kg of CO_2	3.56	2.0

Process Modeling: OLI, IHI and POLIMI
Cyclic loading: 0.18 to 0.58
Reboiler duty: 2.0 (OLI); 2.3 MJ/kg-CO_2 (POLIMI); 2.1 to 2.3 MJ/kg-CO_2 (IHI Measured)
Ammonia emission < 10 ppm
Cost of CO_2 Captured (Excluding T&S): ~$38/tonne-$CO_2$ for Mixed-Salt; $54/tonne-$CO_2$ for Case 12B

11. BIBLIOGRAPHY & REFERENCES CITED

[1] L. Melzer, "Carbon dioxide enhanced oil recovery: factor involved in adding carbon capture, utilization and storage (CCUS) to enhanced oil recovery," 2012. [Online]. Available: http://neori.org/Melzer_CO2EOR_CCUS_Feb2012.pdf.

[2] R. Williamson and J. Mathews, "Rate of Absorption and Equilibrium of Carbon Dioxide in Alkaline Solutions," *Industrial and Engineering Chemistry, Volume 16 (No. 11),* pp. 1157-1160, 1924.

[3] P. Kumar, A. Kalinichev and R. Kirkpatrick, "Hydrogen bonding structure and dynamics of aqueous species from car-parrinelo molecular dynamic simulations," *J. Phys. Chem. B, 113,* pp. 794-802, 2009.

[4] J. Cullinane, "DOE Report: DE-FC26-02NT41440," April 2005. [Online]. Available: http://www.osti.gov/bridge/servlets/purl/839556/839556.pdf.

[5] E. Sanchez-Fernandez, F. M. K. de Miguel Mercader, L. van der Ham, M. Linders and E. Goetheer, "New process concepts for CO2 capture based on precipitating amino acids (2013 GHGT-11)," *Energy Procedia ,* in press.

[6] P. Feron, "COAL21 Post Combustion CO2 Capture Meeting," 2008. [Online]. Available: http://www.learningace.com/doc/775969/304d25a0075a8aee4f042b49f9a40b79/feron-slides.

[7] C. Kang, A. Brandt, L. Durlofsky and I. Jayaweera, "Assessment of advanced solvent-based post-combustion CO2 capture process using bi-objective optimization technique," *Applied Energy, 179,* pp. 1209-1219, 2016.

[8] PoliMi, "TEA on Mixed Salt Technology submitted to NETL, DOE," June 2017.

[9] OLI Systems Inc., “Report on Mixed-Salt Technology for CO2 Capture: Equilibrium-based and Rate-based Model (BP2),” 19 June 2017.

[10] DOE/NETL, “Cost and Performace Baseline for Fossil Energy Plants – Volume 1a: Bituminous Coal and Natural Gas to Electricity (Rev 3)” 6 July 2015. Available: https://www.netl.doe.gov/File%20Library/Research/Energy%20Analysis/Publications/Rev3Vol1aPC_NGCC_final.pdf

[11] I. S. Jayaweera, P. Jayaweera, G. N. Krishnan and A. Sanjurjo, "Rate enhancement of CO2 absorption in aqueous potassium carbonate solutions by an ammonia-based catalyst". US Patent 9,339,757, 17 May 2016.

[12] I. Jayaweera, P. Jayaweera, R. Elmore, J. Bao and S. Bhamidi, "Update on Mixed-salt Technology Development for CO2 Capture from Post-combustion Power Stations," *Energy Procedia, 63 (12th International Conference on Greenhouse Gas Control Technologies, GHGT-12,* pp. 640-650, 2014.

[13] I. Jayaweera, P. Jayaweera, G. Krishnan and A. Sanjurjo, "The race for developing promising CO2 capture technologies ready for 2020 deployment: novel mixed-salt based solvent technology," *Pap. Am. Chem. Soc., Div. Energy Fuels (1),* p. 58, 2013.

[14] I. Jayaweera, P. Jayaweera, Y. Yamasaki and R. Elmore, "Mixed-Salt Solutions for CO2 Capture," in *Absorption-Based Post-combustion Capture of Carbon Dioxide*, Elsevier, 2016, pp. 167-200.

[15] S. Mills, "Coal-fired CCS demonstration plants," 2012. [Online]. Available: http://asertti.org/newsletter/documents/Coal-fired_CCS_demonstration_plants_2012-by_Stephen_Mills.pdf.

[16] D. Dillon, R. Chu, G. Choi, W. Harper and S. Sugita, "An engineering and economic assessment of post-combustion CO2 capture for 1100 F ultra-supercritical pulverized coal power plant application," *EPRI, PID 1017515,* 2010.

[17] U.S. Energy Information Administration, "International Energy Outlook 2016 with Projections to 2040, Report # DOE/EIA-0484, May 2016," 2016. Updated version, September 2017.

[18] U.S. Energy Information Administration, "Annual Energy Outlook 2017 with Projections to 2050, Report # DOE/EIA-0383, January 2017," 2017.

[19] G. Lombardo, R. Agarwal,J. Askander, “Chilled Ammonia Process at Technology Center Mongstad-First Results”, Energy Procedia **5**, 31-39, 2014.

[20] E. Rubin, H. Mantripragada, A. Marks, P. Versteeg and J. Kitchin, "The outlook for improved carbon capture technology," *Progress in Energy and Combustion Science 38 (5),* pp. 630-671, 2012.

[21] "EPA Fact Sheet: Proposed carbon pollution standard for new power plants," 2012. [Online]. Available: http://www.epa.gov/captrade/maps/co2.html.

[22] Global CCS Institute, "GETICA CCS demo project public report," 2012. [Online]. Available: http://www.globalccsinstitute.com/projects/12691.

[23] P. Versteeg and E. Rubin, "A technical and economic assessment of ammonia-based post-combustion CO2 capture at coal-fired power plants," International Journal of Greenhouse Gas Control 5, pp. 1596-1605, 2011.

[24] K. B. Y. Kim and J.-N. Kim, http://www.asiapacificpartnership.org/pdf/CFE/meeting_newcastle/JongNam_Kim.pdf, Korea Institute of Energy Research, 2008.

Appendices

12. APPENDIX A: AQUEOUS SYSTEMS APPLICATIONS (ASAPS) REPORT

Attached below are

(1) Statement of Work for ASAps (Dr. Kaj Thomsen) for BP1 and BP2
(2) Project Status Report for BP1

Statement of Work for BP1

ASAps Task 1: Upgrading the Extended UNIQUAC thermodynamic model based on existing data for the CO2 –NH3 – H2O system and the CO2 - K2CO3 – H2O system up to the highest temperatures available/relevant. Upgraded thermodynamic data files for CO2-H2O-NH3-K2CO3 to be transferred to SRI (DOE FUNDED)

ASAps Task 2: Validating the upgraded thermodynamic model by comparing experimental and calculated values. Writing of report on the upgrading of the model (COST SHARE HOURS 40% of Tasks 1 & 2 efforts)

Task milestones were completed on time.

Statement of Work for BP2

ASAps Task 3: Second upgrade of the extended UNIQUAC based on the results from BP1 to support the work at PoliMi.

Report on Upgrading the Extended UNIQUAC thermodynamic model based on existing data for the CO_2 – NH_3 – H_2O system and the CO_2 - K_2CO_3 – H_2O system up to 200°C/100 bar

Project carried out as SUBAGREEMENT NUMBER: 139-000011 with SRI based on funding from Department of Energy under (Grant No.DE FE0012959, Title: DEVELOPMENT OF MIXED-SALT TECHNOLOGY FOR CARBON DIOXIDE CAPTURE FROM COAL POWER PLANTS

Aqueous Solutions ApS, Snogegaardsvej 149, Soborg, Denmark,
Kaj Thomsen
May 15, 2014

Table of Contents

Introduction

Model parameters in the Extended UNIQUAC thermodynamic model for the $CO_2 – NH_3 – H_2O$ system and the CO_2 - $K_2CO_3 – H_2O$ system were determined in this work. The Extended UNIQUAC model was first applied to describing systems with CO_2 and NH_3 in the work published by Thomsen and Rasmussen in 1999 (Thomsen & Rasmussen, Modeling of Vapor-liquid-solid equilibrium in gas-aqueous electrolyte systems, 1999). This model also included the $CO_2 – NH_3 – H_2O$ system and the CO_2 - $K_2CO_3 – H_2O$ system but the model parameters were based on experimental data at temperatures below 110°C. Calculations and process simulations carried out with the model were therefore only accurate at temperatures below 110°C. Above this temperature, calculations represented extrapolations.

The model was later extended to higher temperatures by Darde *et al*. in 2010 (Darde, van Well, Stenby, & Thomsen, 2010). This extension was based on the same core parameters for H_2O, NH_4^+, H^+, CO_3^{2-}, and OH^- as were used in the model by Thomsen and Rasmussen (Thomsen & Rasmussen, Modeling of Vapor-liquid-solid equilibrium in gas-aqueous electrolyte systems, 1999). These parameters, which were determined based on experimental data from a limited temperature range, were combined with parameters for the CO_2-HCO_3^--H_2O system determined by Garcia et al. (Garcia, Thomsen, & Stenby, 2006). Experimental data for CO_2-NH_3-H_2O mixtures at temperatures up to 200°C were used for determining model parameters for NH_3 specific parameters. This model was limited to the CO_2-NH_3-H_2O system and could therefore not be used for the Mixed Salt Technology for Carbon Capture.

The current model is based on a completely new framework of model parameters. All the model parameters have been determined on the basis of experimental data in the temperature range from the freezing point of the solutions to 200°C. The model parameters for H_2O, H^+, OH^-, and K^+ were determined in a previous project (Thomsen, Working up phosphate from ashes, 2008). The model parameters for the remaining species were determined in this project.

Upgrading of model parameters

In this project, the required model parameters for the ammonium ion were first determined based on more than 6000 experimental data containing ammonium ions in addition to alkali and earth alkali ions and chloride, sulfate, and nitrate ions. Of these data, approximately 4000 experimental data were solid-liquid equilibrium data and 2000 were osmotic coefficient data and thermal property data. The validation of the model parameters for the ammonium ion will not be shown in this report, which primarily deals with the parameters for the $CO_2 – NH_3 – H_2O$ system and the CO_2 - $K_2CO_3 – H_2O$ system.

After the model parameters for the ammonium ion were determined, the model parameters for the CO_2 - $K_2CO_3 – H_2O$ system were determined. Finally the parameters for the $CO_2 – NH_3 – H_2O$ system were determined. In the end, all parameters were adjusted simultaneously. Experimental data at pressures up to 100 bar and temperatures up to 200°C were used for upgrading the parameters.

The CO_2 - K_2CO_3 – H_2O system

The model parameters for the CO_2 - K_2CO_3 – H_2O system were determined based on approximately 2700 experimental data. The sources of experimental data for the CO_2 - K_2CO_3 – H_2O system are given in Table 1 in the appendix. In the following, representative experimental data are plotted together with model calculations to show the good agreement between the model and the experimental data

About 700 of the experimental data were measurements of CO_2 in pure water at various temperatures and pressures. There are some scattering in the data, but the model is able to reproduce the data with an average deviation of 4.9%. A parity plot showing the agreement between pressures calculated with the model and experimental data is shown in Figure 1. In Figure 1, dashed lines are indicating 10% deviation between calculated and experimental pressures.

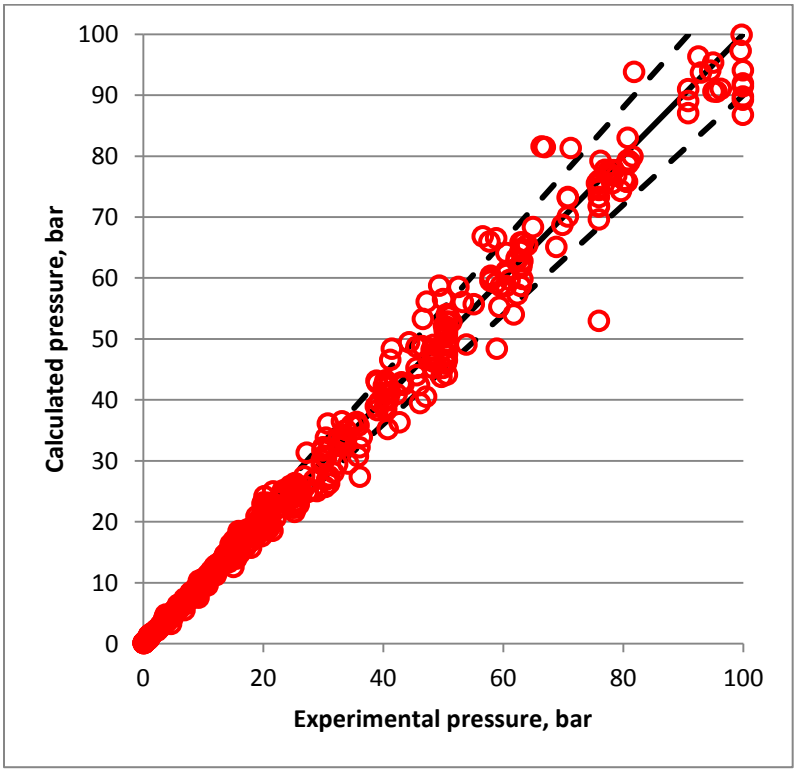

Figure 1: Parity plot showing the agreement between pressures calculated with the Extended UNIQUAC model and experimental data for the binary system CO_2-H_2O. The average deviation is 4.9 %. The two dashed lines indicate 10% deviation between calculated and experimental values.

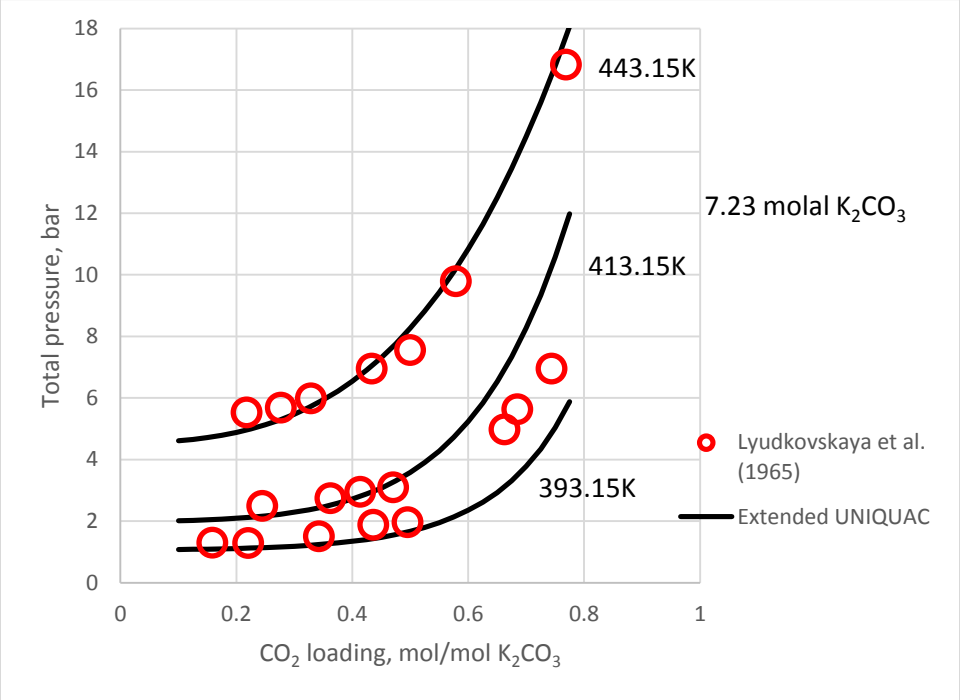

Figure 2: Total pressure at 393.15/413.15K/443.15K (120°C/140°C/170°C) over aqueous solutions of 7.23 molal K_2CO_3 loaded with CO_2. Model calculations are in good agreement with experimental data from Lyudkovskaya et al. (reference in Table 1). An average deviation of 13% was found for the 62 experimental data from this source.

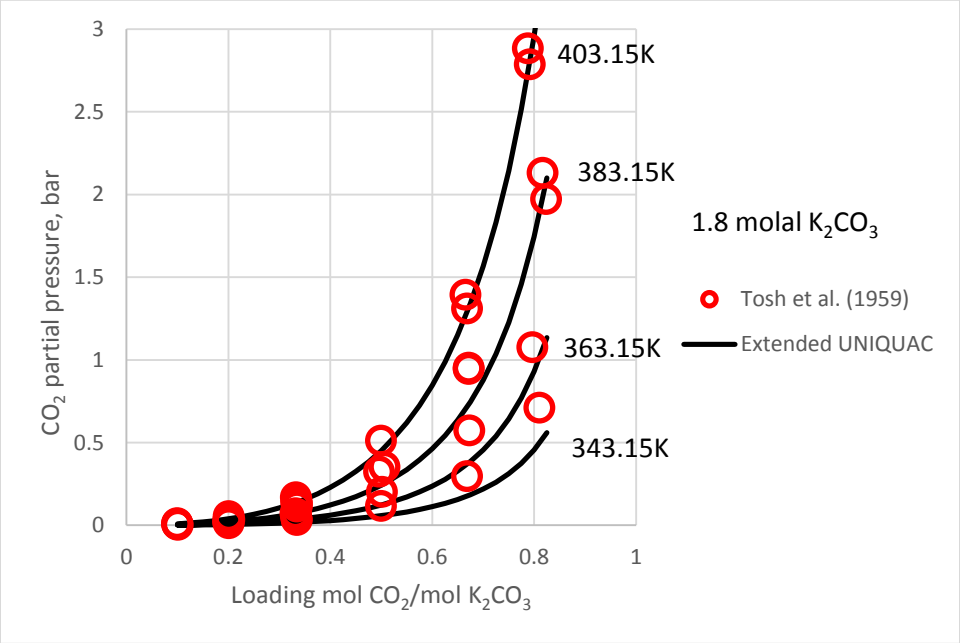

Figure 3: CO_2 partial pressure at 343.15/363.15/383.15/403.15 K (70/90/110/130°C) over aqueous solutions of 1.8 molal K_2CO_3 solutions loaded with CO2. Model calculations are in good agreement with experimental data from Tosh et al. (reference in Table 1). An average deviation of 17% was found for the 130 experimental data with CO_2 partial pressure from this source.

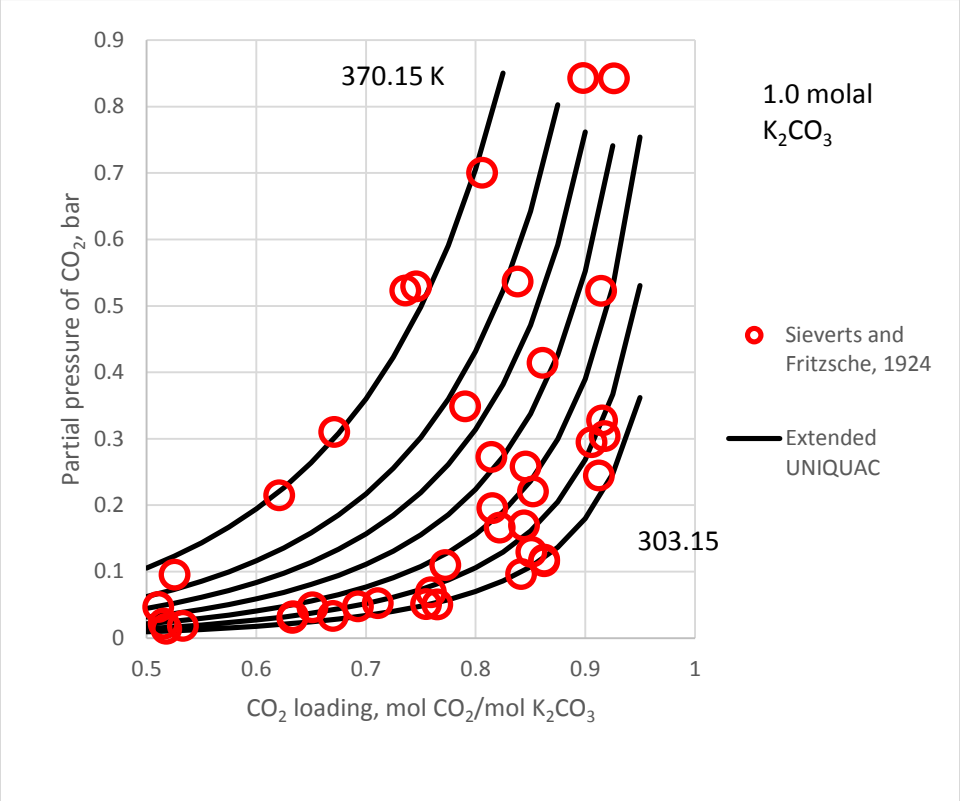

Figure 4: CO_2 partial pressure at 303.15/313.15/323.15/333.15/343.15/353.15/370.15 K (30/40/50/60/70/80/97°C) over aqueous solutions of 1 molal K_2CO_3 solutions loaded with CO_2. An average deviation of 19% was found for the 50 experimental data with CO_2 partial pressure from Sieverts and Fritzsche (reference in Table 1).

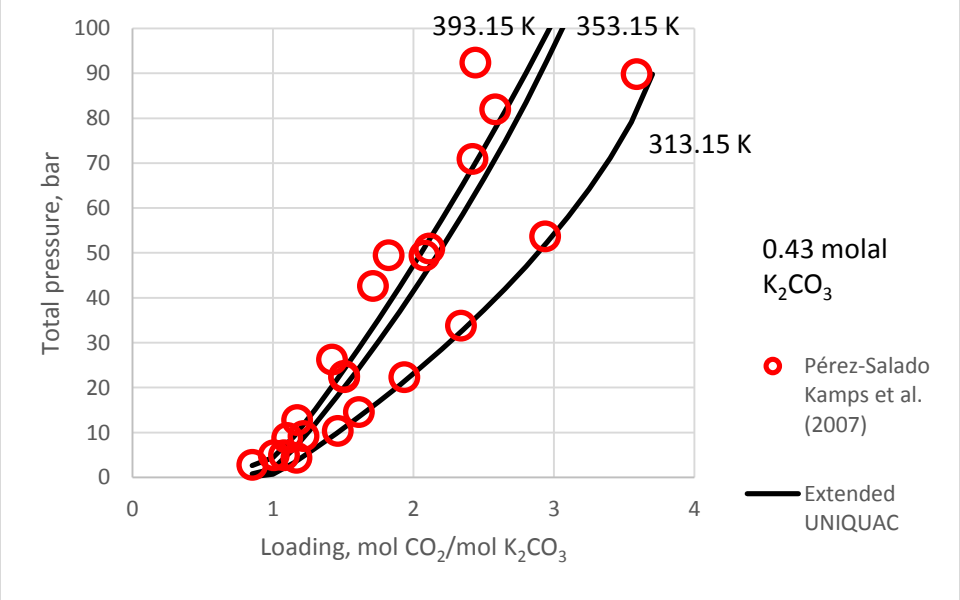

Figure 5: Total pressure at 313.15/353.15/393.15 K (40/80/120°C) over aqueous solutions of 0.43 molal K_2CO_3 solutions with high loadings of CO_2. An average deviation of 14% was found for the 40 experimental total pressure data from Pérez-Salado Kamps et al. (reference in Table 1).

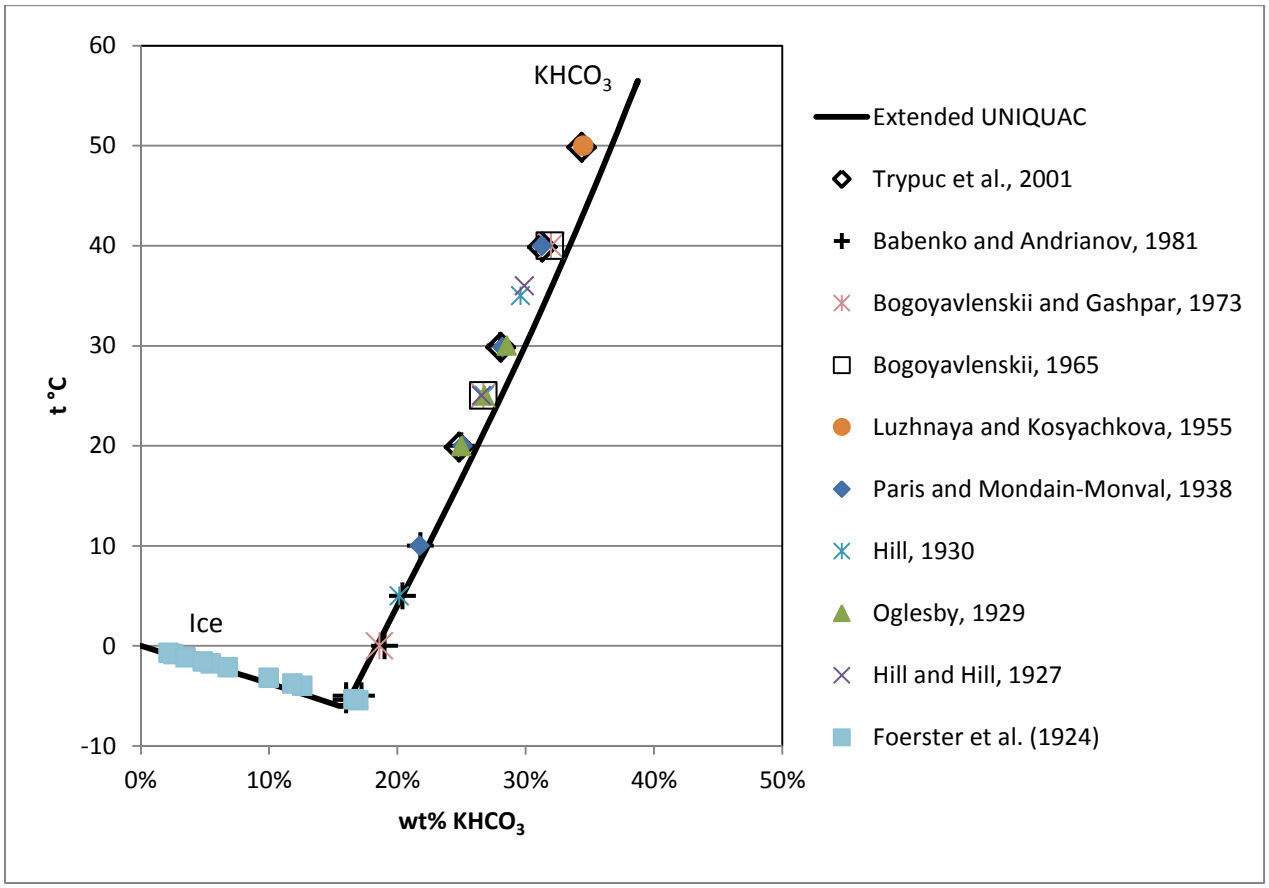

Figure 6: Solubility of $KHCO_3$ in water at 1.01325 bar CO_2 partial pressure. The references can be found in Table 1 in the appendix.

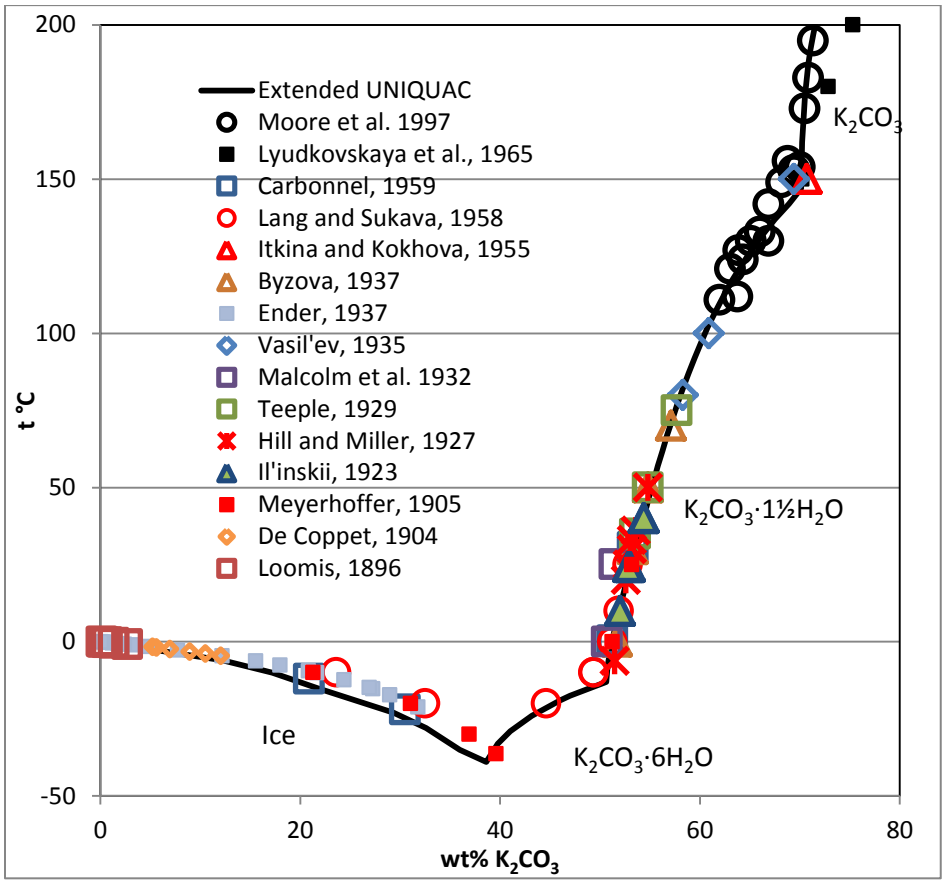

Figure 7: Solubility of K_2CO_3. The experimental data are from the marked sources, all listed in Table 1 in the appendix. Generally, there is a good agreement between experimental data and the calculated curve.

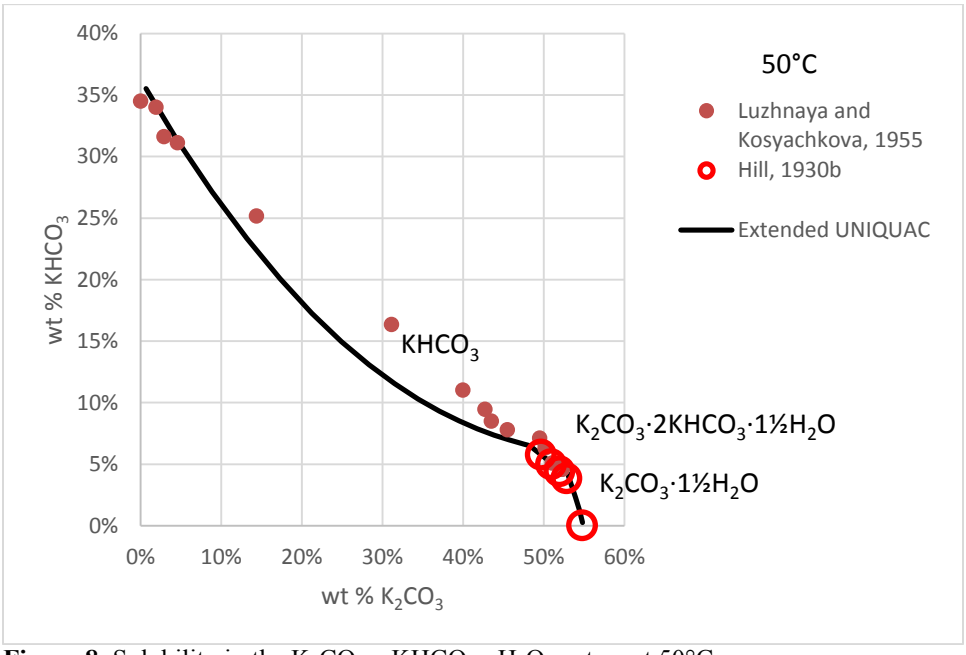

Figure 8: Solubility in the K_2CO_3 – $KHCO_3$ - H_2O system at 50°C.

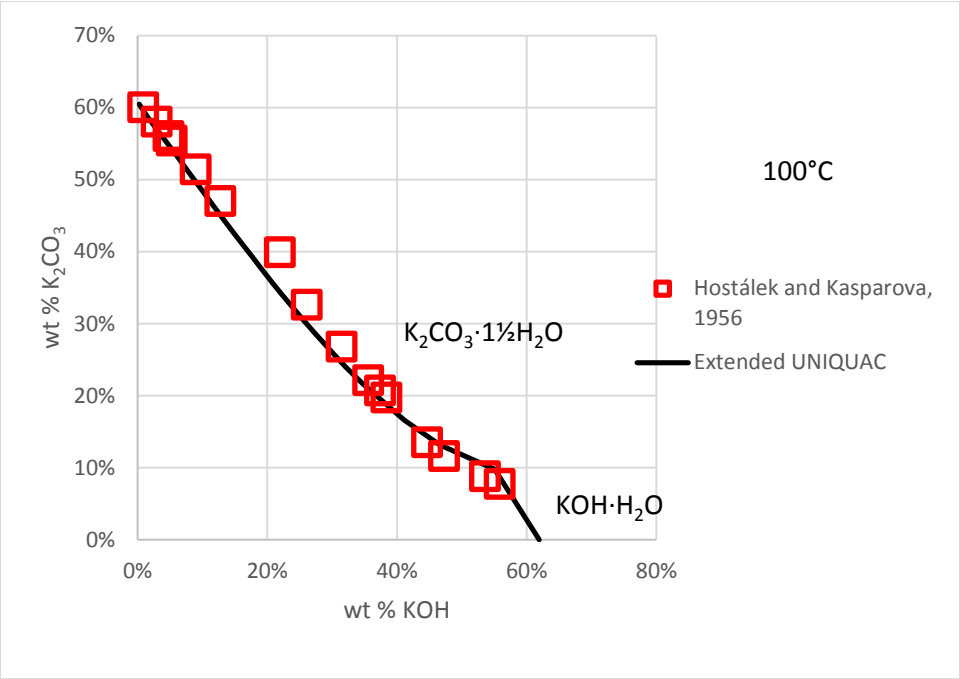

Figure 9: Solubility in the K_2CO_3 – KOH – H_2O system at 100°C.

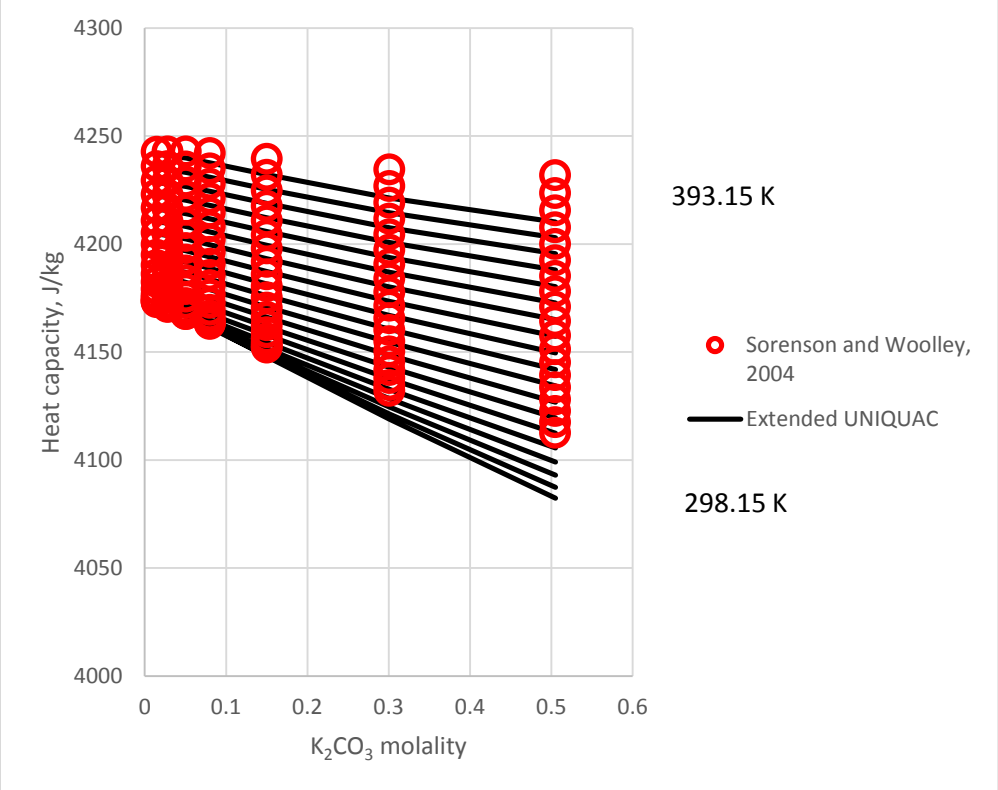

Figure 10: Heat capacity of K_2CO_3 solutions at temperatures between 298.15 K and 393.15 K. The average relative difference between model calculations and experimental data is only 0.15% for K_2CO_3 data and 0.05% for $KHCO_3$ data from the same source.

The CO_2-NH_3-H_2O system

The parameters for the CO_2 – NH_3 – H_2O system were determined on the basis of more than 5200 experimental data. Of these, more than 500 were solid-liquid equilibrium data. Some of these data also contained KOH/K_2CO_3 together with NH_3. The experimental data used are listed in Table 2.

All measurements of data in these systems are quite challenging due to the high volatility and reactivity of the components. As it was seen in the CO_2 – K_2CO_3 – H_2O systems, some scattering between the experimental data are seen, even for data from the same source.

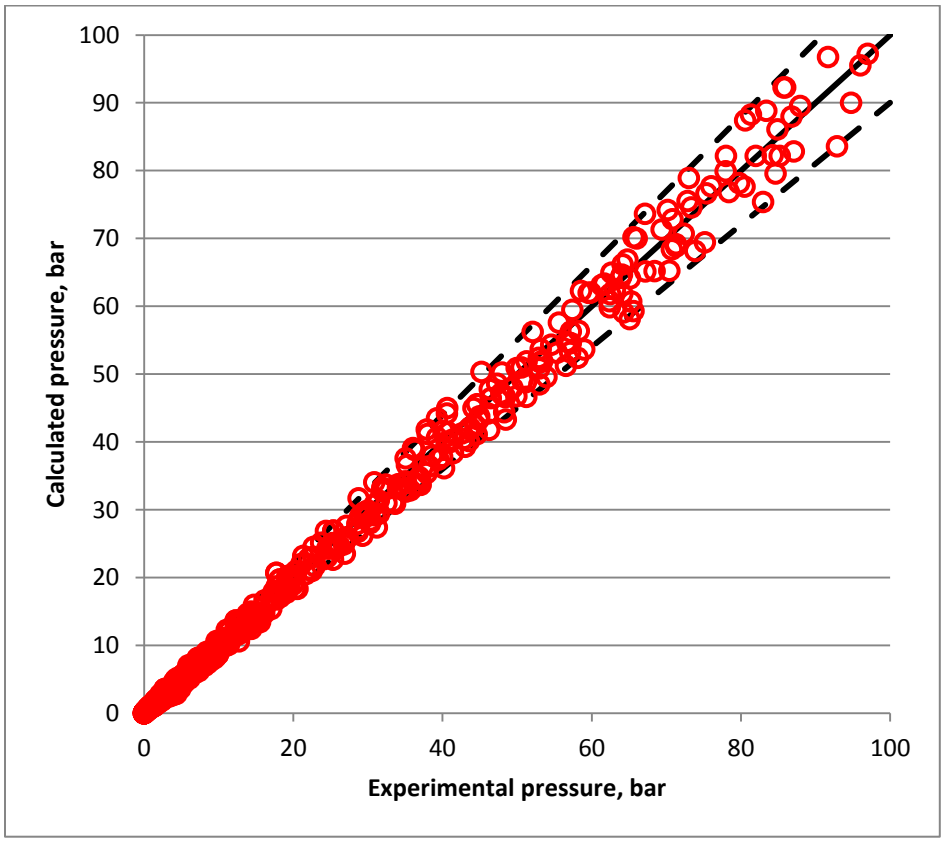

Figure 11: Parity plot of experimental and calculated pressures above NH_3-H_2O solutions. The average relative deviation between the approximately 1500 calculated and experimental data points is 7.9%. In the figure, dashed lines are indicating 10% deviation between calculated and experimental data.

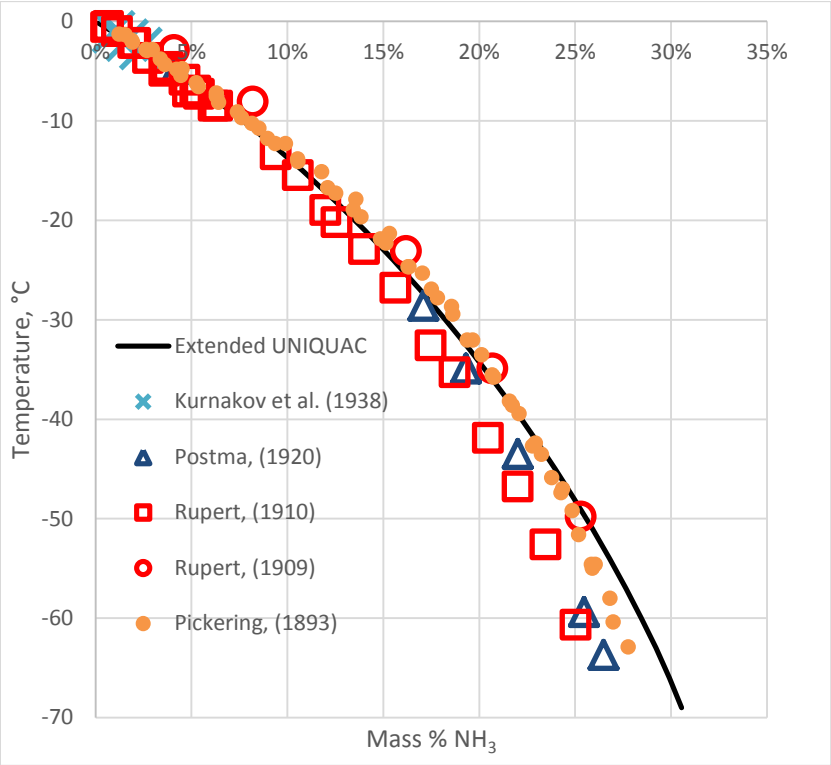

Figure 12: Solid-liquid equilibrium in the NH_3 – H_2O system. All the data refer to solutions in which ice is forming at the specified temperature.

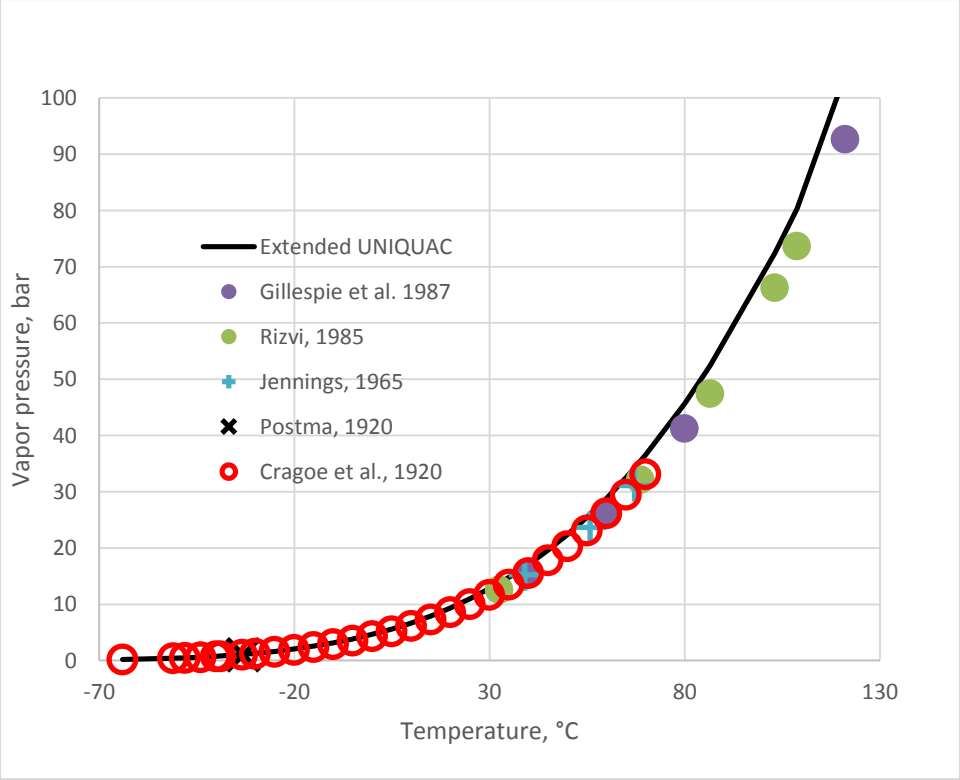

Figure 13: Vapor pressure of pure NH_3 as a function of temperature. Experimental and calculated values in bar.

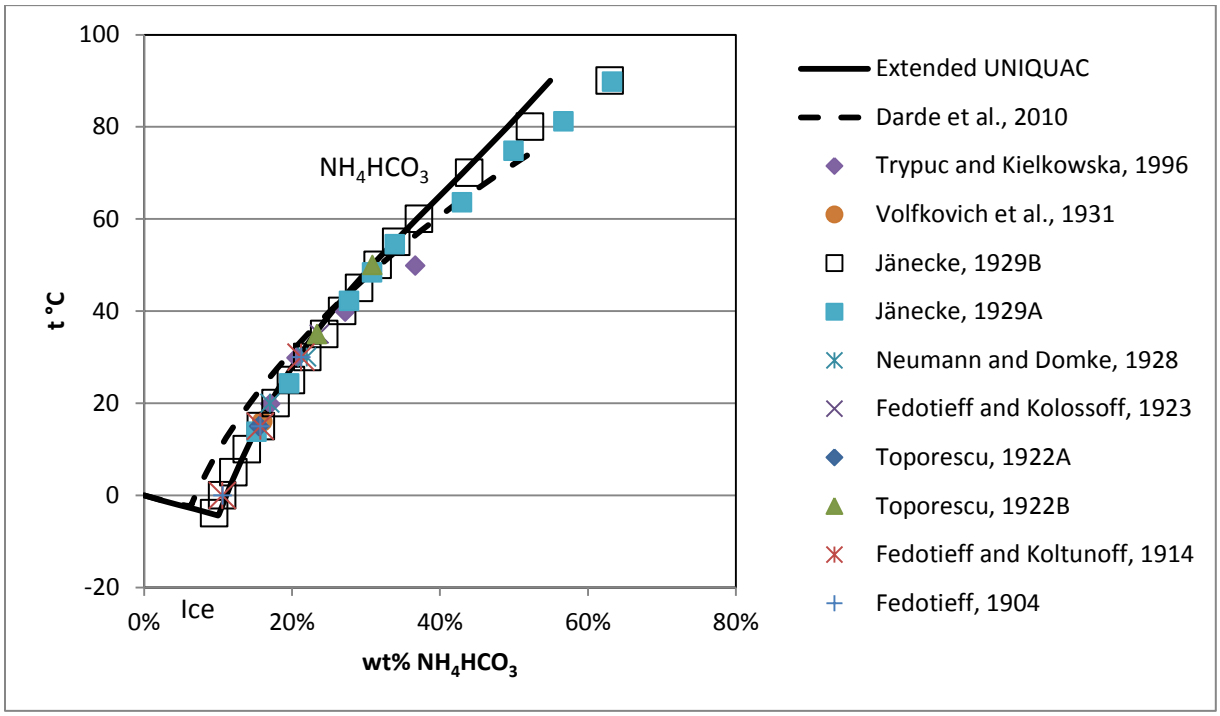

Figure 14: Solubility of NH_4HCO_3 at temperatures up to 90°C. Calculated and experimental values. The full line shows results obtained with this model. The dashed line shows values calculated by the model of Darde et al, 2010

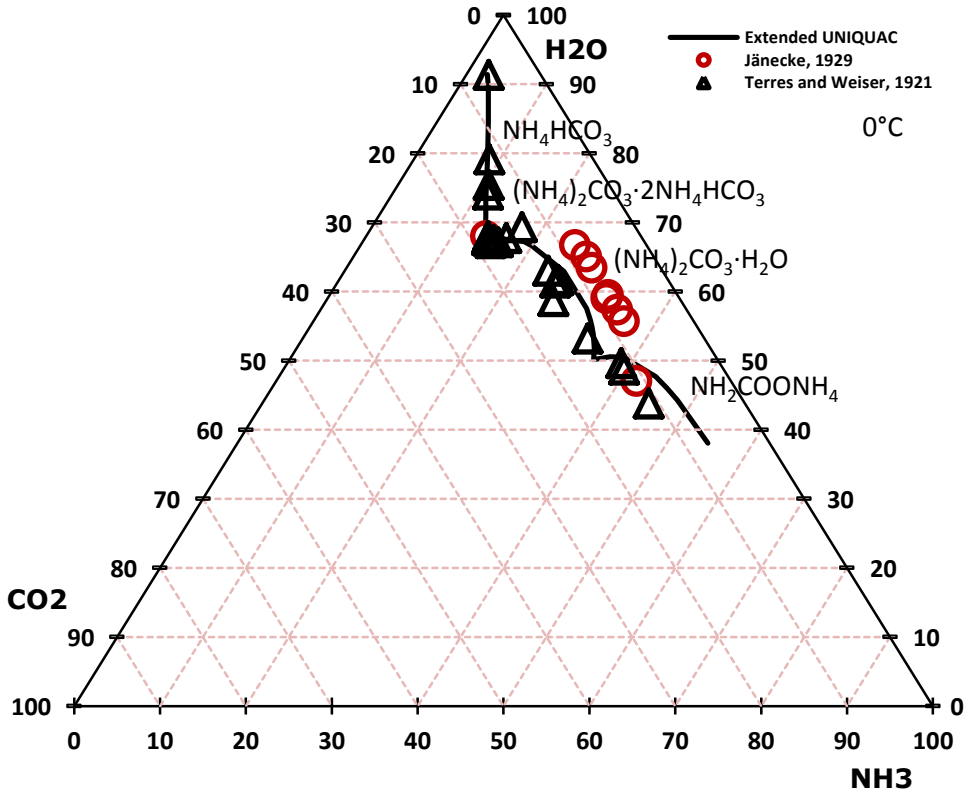

Figure 15: Calculated and experimental solubility in the CO_2-NH_3-H2O system at 0°C. There are significant differences in the data from different sources.

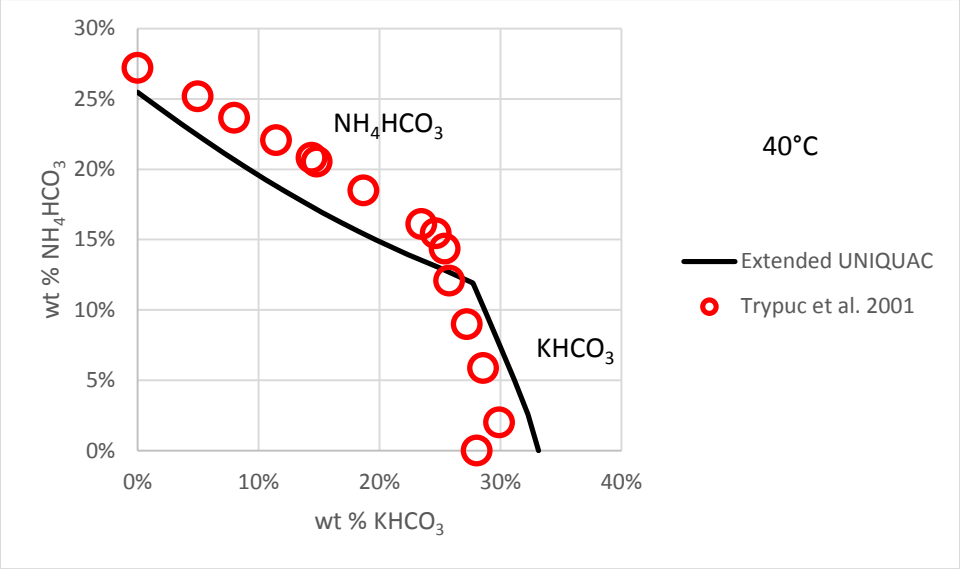

Figure 16: Solubility in the ternary $KHCO_3$-NH_4HCO_3-H_2O system. A few wt % difference between measured and calculated values is seen. This indicates the difficulty of measuring solubility in these volatile systems.

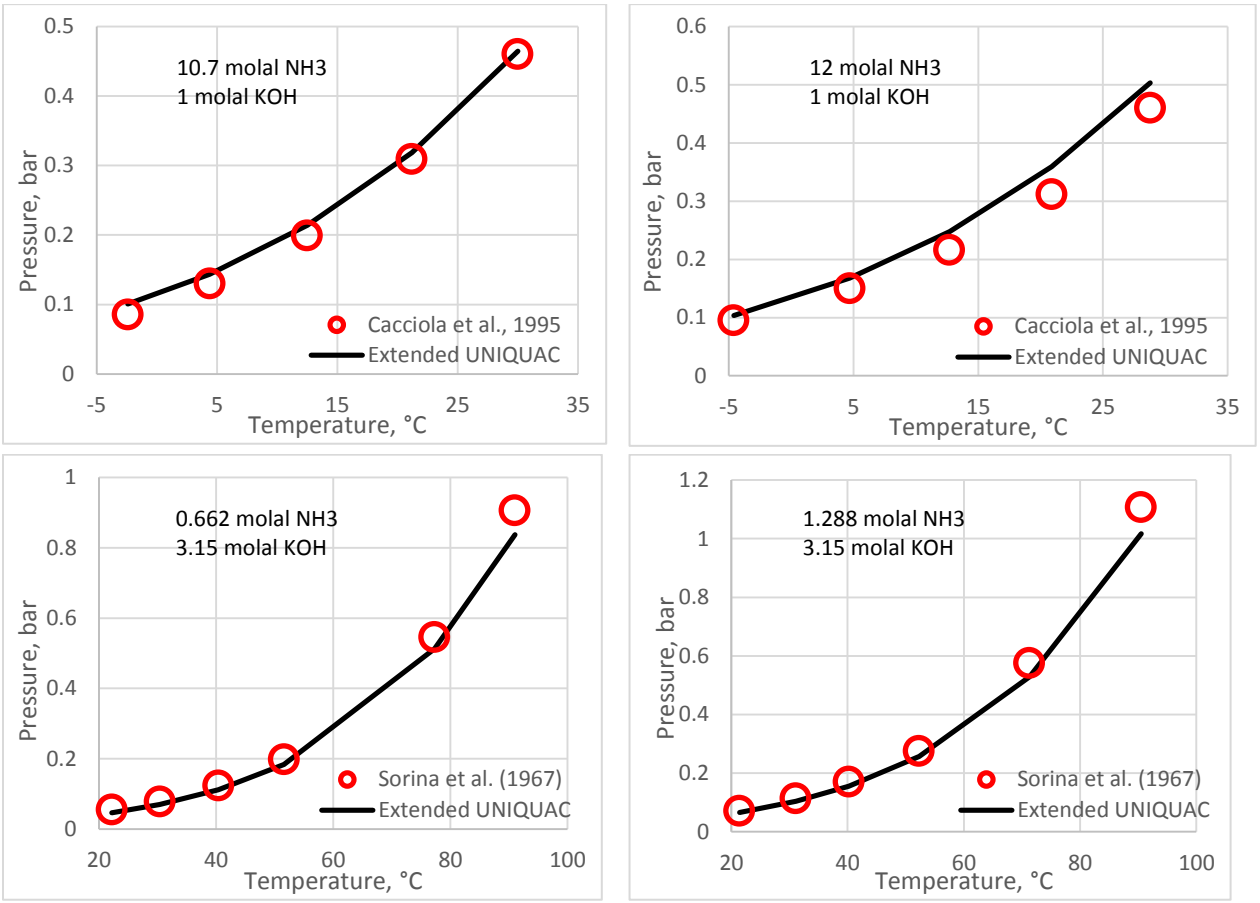

Figure 17: Vapor pressure above KOH solutions with different amounts of ammonia as a function of temperature. The average relative deviation for the 280 experimental data for this ternary system is 8%.

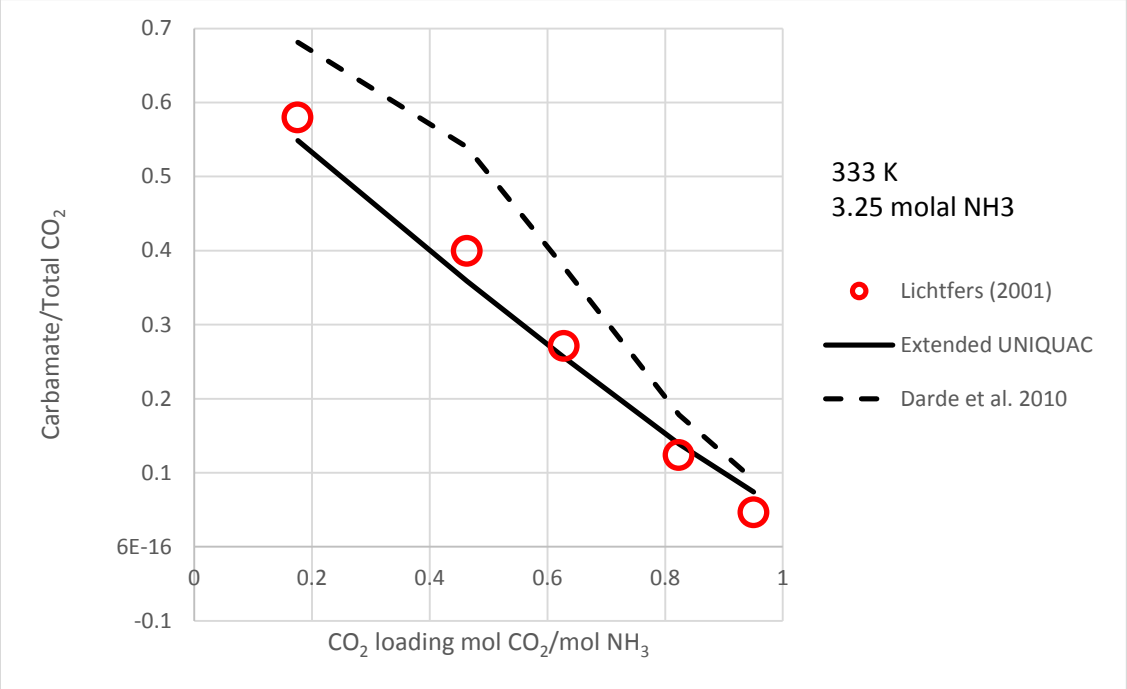

Figure 18: Speciation in the CO_2-NH_3-H_2O system. Full line: calculated with the updated model, dashed line: calculated with the model of Darde et al. Circles, Experimental data from Lichtfers, 2001. The relative deviation between calculated and the 81 experimental data from this source is 26 % with the new model and 25 % for the model by Darde et al, 2010.

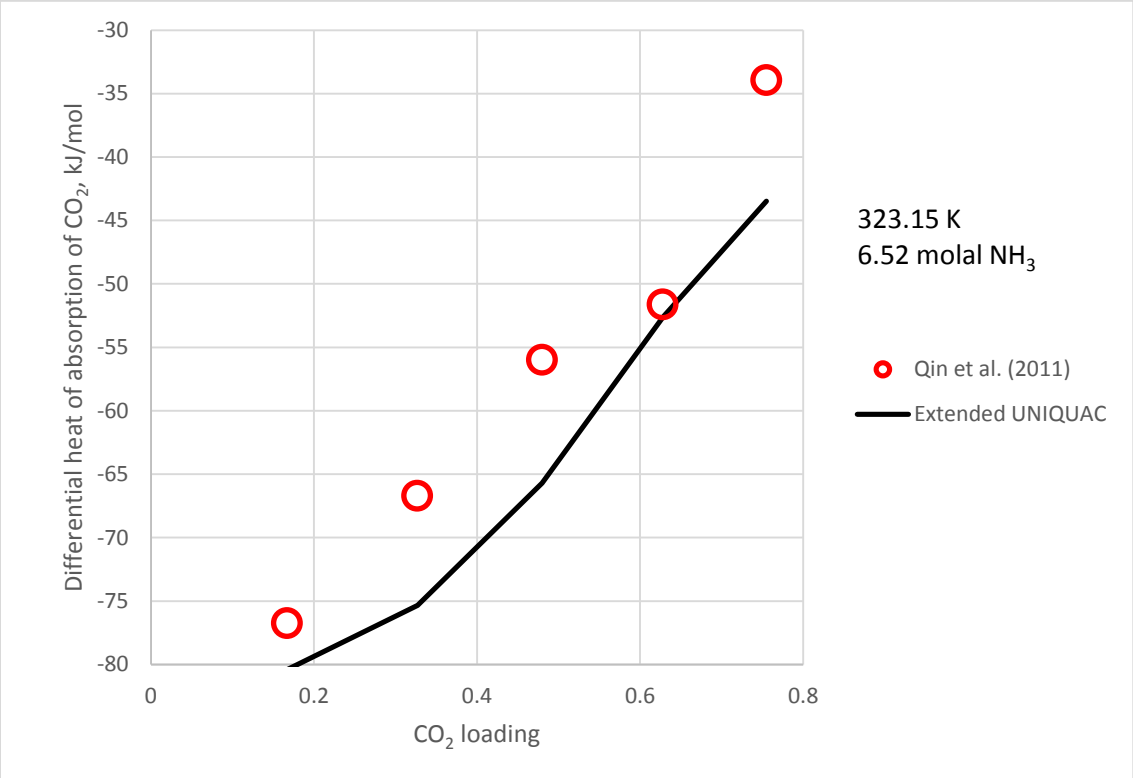

Figure 19: Differential heat of absorption of CO2 in loaded 6.52 molal NH3 solutions at 323.15 K / 50°C. The average relative deviation between the calculated values and the 149 experimental data from this source is 24%

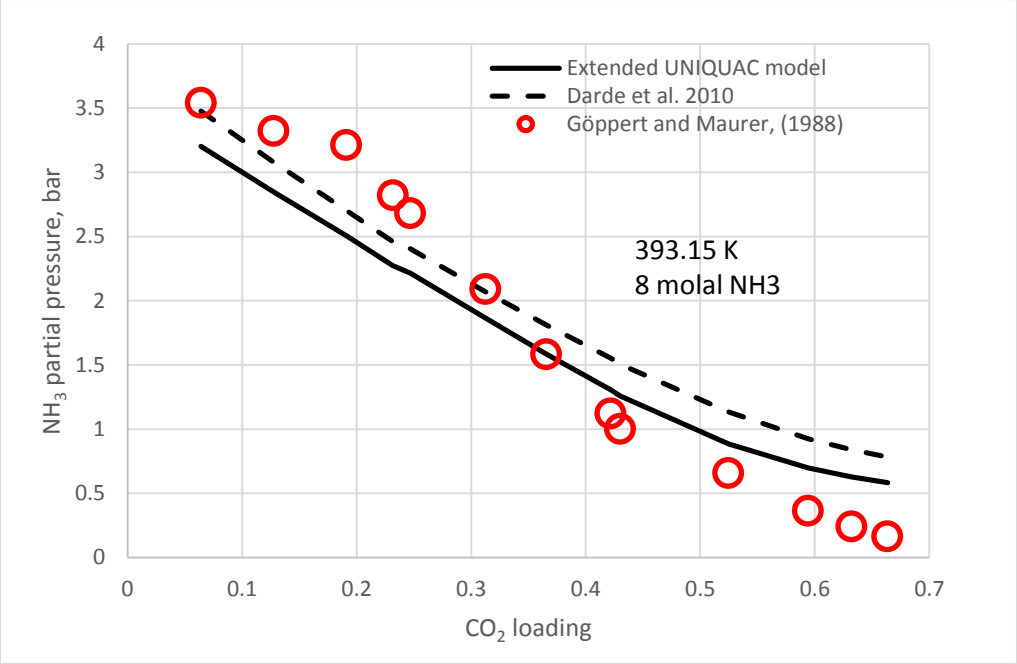

Figure 20: Partial pressure of ammonia in loaded 8 molal solutions of NH_3 at 393.15 K/120°C. The full line shows the calculated result in this work. The dashed line is calculated with the parameters of Darde et al. 2010. The circles indicate experimental data from Göppert and Maurer, 1988. The average relative deviation between experimental and calculated ammonia partial pressures from the 559 data from this source is 35%. The corresponding number for the model of Darde et al. is 43%.

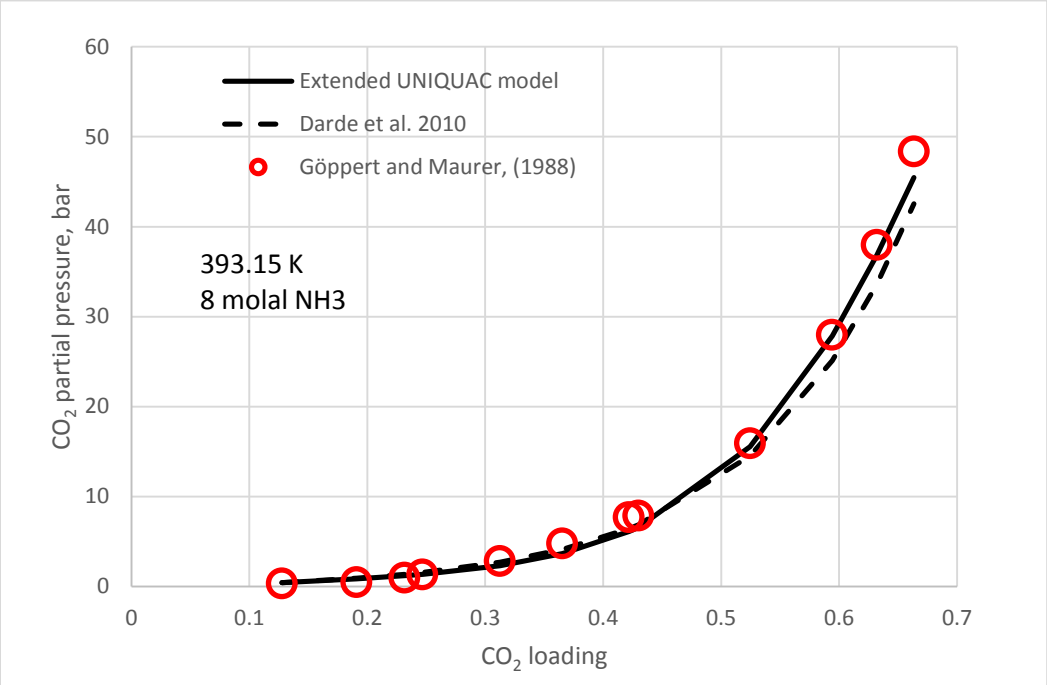

Figure 21: Partial pressure of carbon dioxide in loaded 8 molal solutions of NH_3 at 393.15 K/120°C. The full line shows the calculated result in this work. The dashed line is calculated with the parameters of Darde et al. 2010. The circles indicate experimental data from Göppert and Maurer, 1988. The average relative deviation between experimental and calculated carbon dioxide partial pressures from the 559 data from this source is 12%. The corresponding number for the model of Darde et al. is 11% even though in the particular graph shown here, the current model is slightly better than the model of Darde et al.

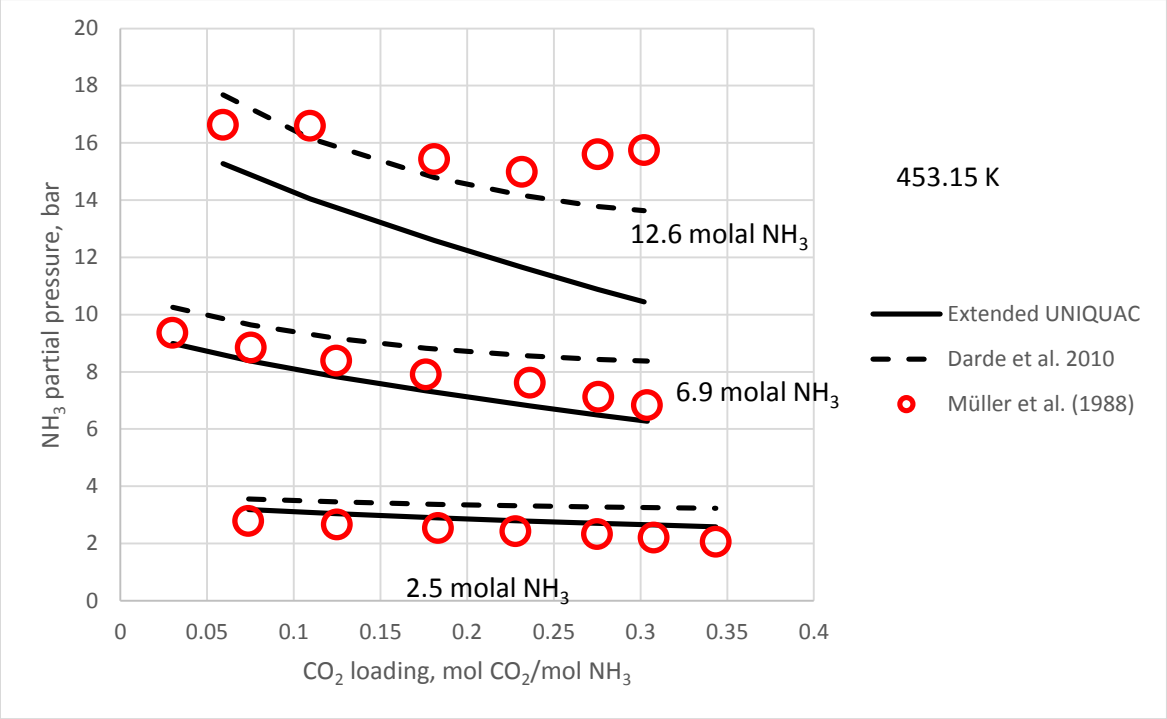

Figure 22: NH_3 partial pressure at three different NH_3 molalities at 453.15 K/180°C. The upgraded model gives slightly better results than the model of Darde et al, 2010. The average relative deviation between 586 experimental data from Müller et al, 1988 and calculated NH_3 partial pressures is 34% for the upgraded model and 44% for the model of Darde et al. 2010. For the case shown in this figure, the Darde model is actually performing better than the upgraded model at 12.6 molal NH3

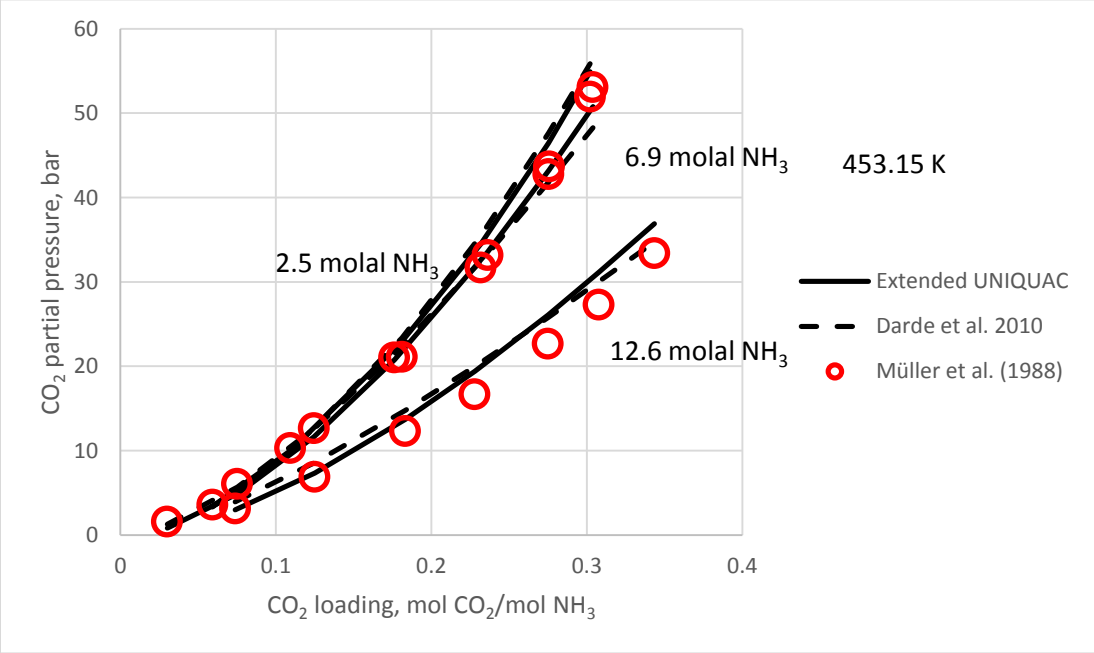

Figure 23: CO_2 partial pressures at three different NH_3 molalities at 453.15 K/180°C. The upgraded model and the model of Darde et al. 2010 give similar results. The average relative deviation between 586 experimental data from Müller et al, 1988 and calculated CO_2 partial pressures is 12% for both the upgraded model and the model of Darde et al. 2010.

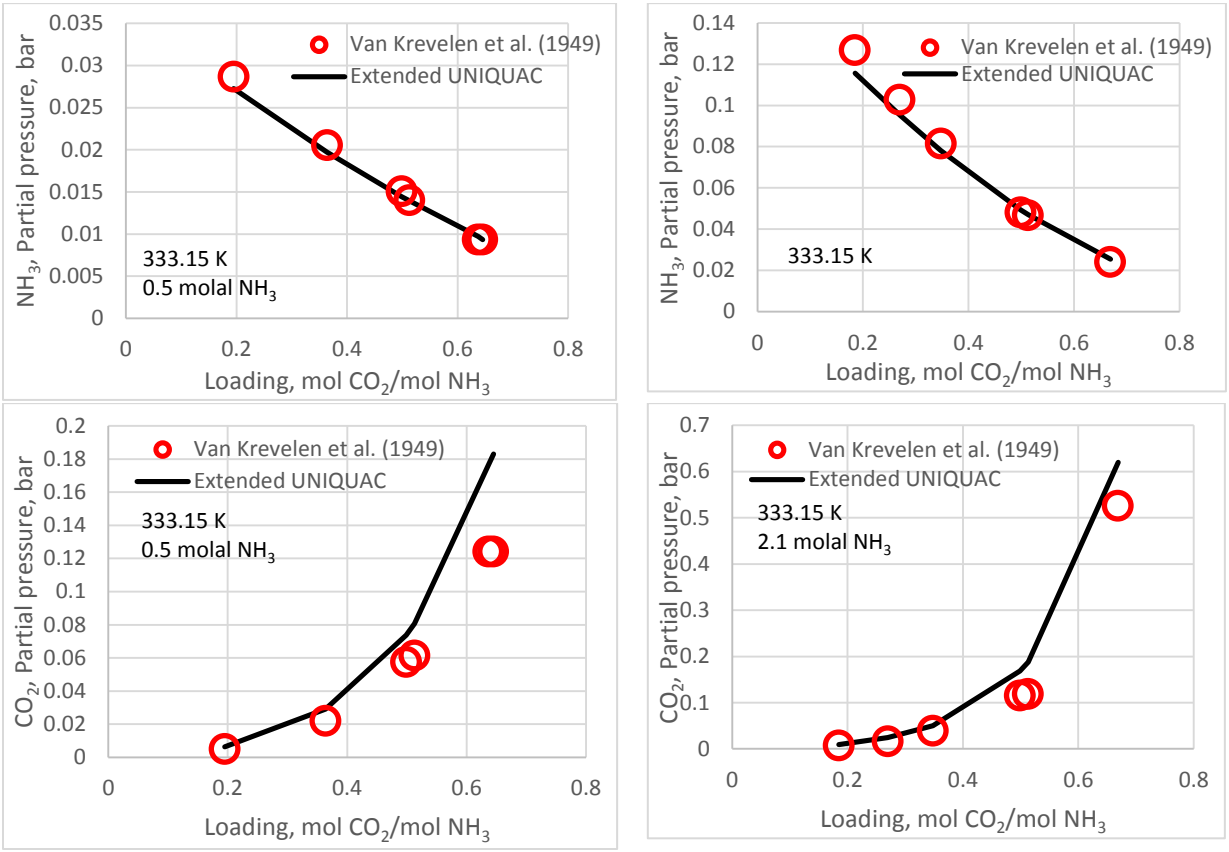

Figure 24: Low temperature/low pressure data: Ammonia partial pressure and carbon dioxide partial pressure in 0.5 and 2.1 molal NH_3 solutions at 333.15K/60°C. The average relative deviation between the 61 experimental data points from this source and the upgraded model is 2.3% for the ammonia partial pressures and 17% for the carbon dioxide partial pressures.

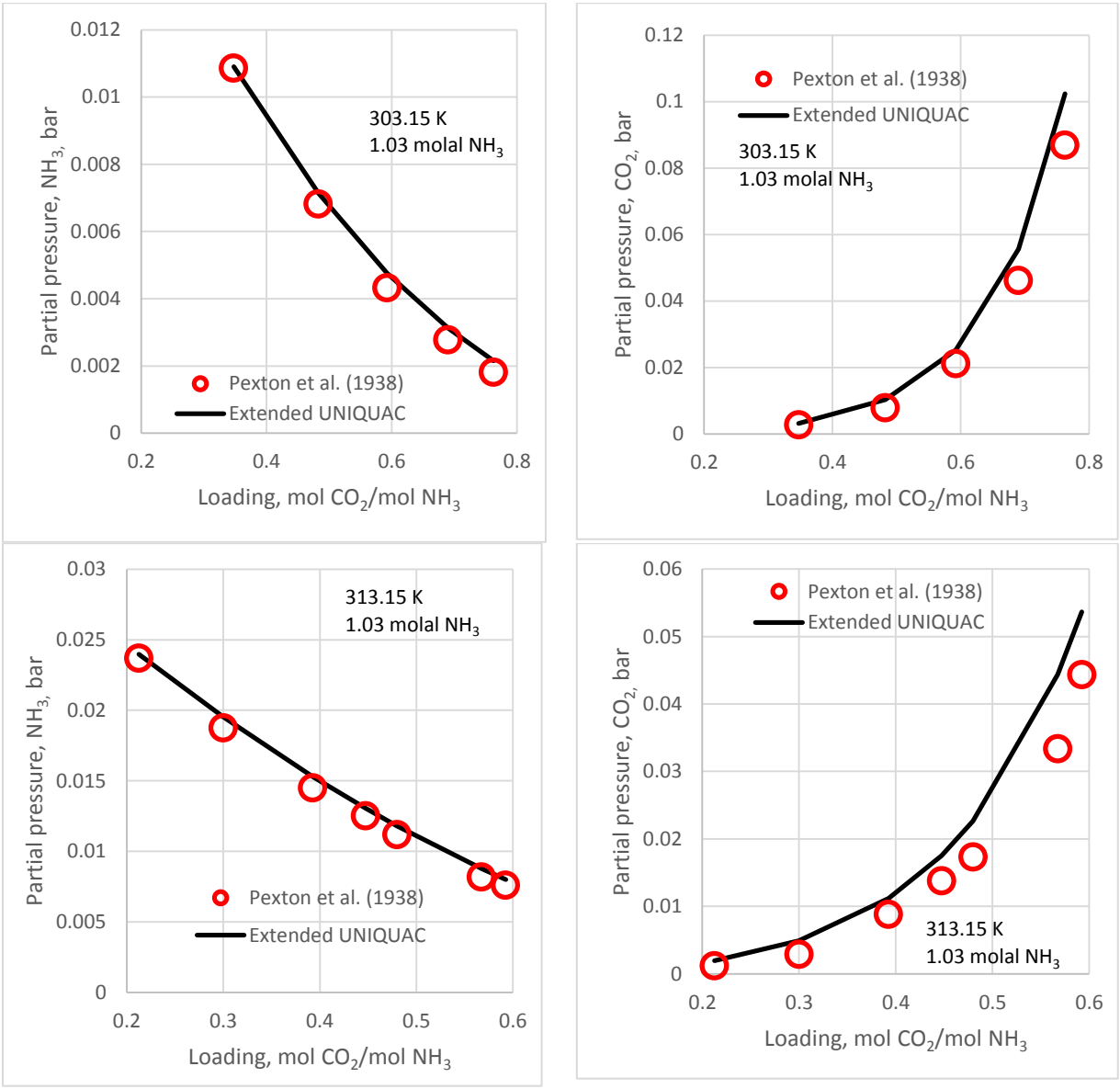

Figure 25: Low temperature/low pressure data: Ammonia partial pressure and carbon dioxide partial pressure in 1.03 molal NH_3 solutions at 303.15K/30°C and 313.15/40°C. The average relative deviation between the 91 experimental data points from this source and the upgraded model is 0.5% for the ammonia partial pressures and 5.7% for the carbon dioxide partial pressures.

Conclusion

Extended UNIQUAC model parameters have been determined for the CO_2-NH_3-KOH-H_2O system. The parameters are based on approximately 8000 experimental data. The experimental data cover the temperature range from the freezing points of the solutions and up to 200°C and the pressure range up to 100 bar. Experimental data for these systems are quite scattered, which makes the modeling work quite challenging.

The determination of the new parameters presented here was carried out in a 400 hour project. If more time had been available, the model could probably have been improved further.

The new model parameters give results similar to or better than the model of Darde et al. (Darde, van Well, Stenby, & Thomsen, 2010) for the CO_2-NH_3-H_2O system. In addition, the new model describes phase equilibria in systems with KOH/K_2CO_3 with high accuracy.

References

Darde, V., van Well, W. J., Stenby, E. H., & Thomsen, K. (2010). Modeling of Carbon Dioxide Absorption by Aqueous Ammonia Solutions Using the Extended UNIQUAC Model. *Ind. Eng. Chem. Res., 49*, 12663-12674.

Garcia, A. V., Thomsen, K., & Stenby, E. H. (2006). Prediction of mineral scale formation in geothermal and oilfield operations using the extended UNIQUAC model Part II. Carbonate scaling minerals. *Geothermics, 35*, 239-284.

Thomsen, K. (2008). *Working up phosphate from ashes.* Soborg, Denmark: Aqueous Solutions ApS.

Thomsen, K., & Rasmussen, P. (1999). Modeling of Vapor-liquid-solid equilibrium in gas-aqueous electrolyte systems. *Chemical Engineering Science, 54*, 1787-1802.

Appendix for Aqueous Solutions Aps Report: Data sources
Data for the CO_2 - K_2CO_3 – H_2O system

The sources of data used for determining model parameters related to ammonia are given in Table 1. The sources in the table are first sorted according to the type of data written in column 2 and next sorted according to the name of the first author given in column 1. In column 3, the number of data from each source used for the parameter estimation is given. In the fourth column, a number indicates how many of these data were added/typed in this project.

Table1: Sources of experimental data used for determining model parameters in the CO_2 - K_2CO_3 – H_2O system

Source	Type of data	Number of data points	Added in this project
Walker A.C.; Bray U.B.; Johnston J.; Equilibrium in solutions of alkali carbonates; J. Am. Chem. Soc.; 49(1927)1235-1256	CO_2 partial pressure over aqueous $KHCO_3$-K_2CO_3	35	35
Álvaro Pérez-Salado Kamps; Eckehard Meyer; Bernd Rumpf; and Gerd Maurer; Solubility of CO2 in Aqueous Solutions of KCl and in Aqueous Solutions of K2CO3; J. Chem. Eng. Data; 52(2007)817-832(3)	CO_2 solubility in aqueous K_2CO_3	41	
Cullinane; J. Tim; Rochelle; Gary T.; Carbon dioxide absorption with aqueous potassium carbonate promoted by piperazine; Chem. Eng. Sci.; 59(2004)3619-3630	CO_2 solubility in aqueous K_2CO_3	2	
Cullinane; J. Tim; Rochelle; Gary T.; Thermodynamics of aqueous potassium carbonate; piperazine; and carbon dioxide; Fluid Phase Equilibria; 227(2005)197-213(2)	CO_2 solubility in aqueous K_2CO_3	2	
Korbutova Z.V.; Karpova Y.G.; Solubility of CO2 in aq. K2CO3; The Soviet Chemical Industry ; (1980)1401-1407	CO_2 solubility in aqueous K_2CO_3	65	65
Lyudkovskaya; M. A.; Fridman; S. D.; Klevke; V. A.; Purification of gases from CO2 by a "hot" solution of K2CO3. Phase equilibriums in the system K2CO3-KHCO3-H2O; Khimicheskaya Promyshlennost (St. Petersburg; Russian Federation) ; 41(1965)339-343(5)	CO_2 solubility in aqueous K_2CO_3	62	
Park S-B.; Shim C-S.; Lee H.; Lee K-H.; Solubilities of carbon dioxide in the aqueous potassium carbonate and potassium carbonate-poly(ethylene glycol) solutions ; Fluid Phase Equilibria ; 134(1997)141-149	CO_2 solubility in aqueous K_2CO_3	28	
Sieverts A.; Fritzsche A.; Kaliumcarbonatlösungen und Kohlendioxyd I.+II. ; Z. anorganische und allgemeine	CO_2 solubility	50	

Chemie ; 133(1924)1-16 and 17-25	in aqueous K_2CO_3		
Tosh J.S.; Field J.H.; Benson H.E.; Haynes W.P.; Equilibrium study of the system potassium carbonate; potassium bicarbonate; carbon dioxide; and water; Bureau of Mines (1959); Report of Investigations 5484	CO_2 solubility in aqueous K_2CO_3	148	
Bamberger; A.; Sieder;G.; Maurer; G. ; J. Supercritical Fluids ; 17(2000)97-110	CO_2 solubility in water	29	
Bartholomé E.; Friz Hans; Löslichkeit von Kohlendioxyd in Wasser bei höheren Drucken; Chemie Ingenieur Technik; 28(1956) 706-708	CO_2 solubility in water	15	
Cramer; S.D.; The solubility of methane; carbon dioxide; and oxygen in brines from 0° to 300°C; US Bureau of Mines Report of Investigations; 8706(1982)1-17	CO_2 solubility in water	7	
Curry; J.; Hazelton; C.L.; The Solubility of Carbon Dioxide in Deuterium Oxide at 25°C; J. Am. Chem. Soc.; 60(1938)2771-2773	CO_2 solubility in water	4	
Diana Koschel; Jean-Yves Coxam; Laurence Rodier; Vladimir Majer; Enthalpy and solubility data of CO2 in water and NaCl(aq) at conditions of interest for geological sequestration; Fluid Phase Equilibria; 247(2006)107-120	CO_2 solubility in water	8	
Ellis A.J.; Golding R.M.; "The solubility of CO2 above 100°C in water and in NaCl solutions"; American Journal of Science; 261(1963)47-60	CO_2 solubility in water	1	
Ellis, A.J.; The solubility of carbon dioxide in water at high temperatures; American Journal of Science; 257(1959)217-234	CO_2 solubility in water	36	
Fei; W.; Chen; J.; Ai; N.; Solubility of Carbon Dioxide in Four Mixed Solvents; J. Chem. Eng. Data; 50(2005)492-496	CO_2 solubility in water	4	
Floriane Lucile; Pierre Ceìzac; Francois Contamine; Jean-Paul Serin; Deborah Houssin; and Philippe Arpentinier; Solubility of Carbon Dioxide in Water and Aqueous Solution Containing Sodium Hydroxide at Temperatures from (293.15 to 393.15) K and Pressure up to 5 MPa: Experimental Measurements; J. Chem. Eng. Data; 57(2012)784-789	CO_2 solubility in water	30	
Geffcken G.; Beiträge zur kenntnis der löslichkeitsbeeinflussung ; Z. Physik. Chem.; Stoechiom. Verwandtschaftsl. ; 49(1904)257-302	CO_2 solubility in water	2	
Gillespie; P.C.; Wilson; G.M.; Vapor-Liquid and liquid-liquid equilibria: Water-methane; water-Carbon dioxide; water - Hydrogen Sulfide; Water - nPentane; water - methane - npentane; Gas Processor Association; Tulsa;	CO_2 solubility in water	18	

Research Report 48; 48(1982)			
Golutvin; Yu. M.; Malysheva; T. V.; Skorobogatova; V. I.; On the solubility of hydrogen sulfide and carbon dioxide in water; aqueous ammonia and phenols; Izv. Sib. Otdel. Akad. Nauk SSSR; (1958)83-87	CO_2 solubility in water	1	
Graydon K. Anderson; Solubility of Carbon Dioxide in Water under Incipient Clathrate Formation Conditions; J. Chem. Eng. Data; 47(2002)219-222	CO_2 solubility in water	52	
Harned H.S.; Davis R.; The ionization constant of Carbonic Acid in water and the solubility of CO2; J. Am. Chem. Soc.; 65(1943)2030-37	CO_2 solubility in water	18	
Kiepe; Joern; Horstmann; Sven; Fischer; Kai; Gmehling; Juergen; Experimental Determination and Prediction of Gas Solubility Data for CO2 + H2O Mixtures Containing NaCl or KCl at Temperatures between 313 and 393 K and Pressures up to 10 MPa; Industrial & Engineering Chemistry Research; 41(2002)4393-4398 (17)	CO_2 solubility in water	37	
Kiss A.v.; Lajtai I.; Thury G.; Über die Löslichkeit von Gasen in Wasser-Nichtelektrolytgemischen; Z. anorg. allg. Chemie; 233(1937)346-352	CO_2 solubility in water	3	
Kunerth; W.; Solubility of CO2 and N2O in certain solvents; Phys. Rev.; 2(1922)512-524	CO_2 solubility in water	8	
Malegaonkar M.B.; Dholabhai P.D.; Bishnoi P.R.; Kinetics of Carbon Dioxide and Methane Hydrate formation; The Canadian Journal of Chemical Engineering; 75(1997)1090-1099	CO_2 solubility in water	9	
Markham A.E.; Kobe K.A.; The solubility of Carbon dioxide and Nitrous oxide in aqueous Salt Solutions; J. Am. Chem. Soc.; 63(1941)449-454	CO_2 solubility in water	3	
Matous J.; Sobr J.; Novák J.P.; Pick J.; Solubility of Carbon Dioxide in Water at Pressures up to 40 atm; Collection Czechoslav. Chem. Commun. ; 34(1969)3982-3985	CO_2 solubility in water	13	13
Morgan O.M.; Maass O.; An investigation of the equilibria existing in gas-water systems forming electrolytes; Canadian Journal of Research; 5(1931)162-199	CO_2 solubility in water	19	
Morrison T.J. and Billett F.; The salting out of non-electrolytes. Part II: The effect of variation in non-electrolytes; J. Chem. Soc.; (1952)3819-3822	CO_2 solubility in water	19	
Müller G.; Bender E.; Maurer G.; Das Dampf-Flüssigkeitsgleichgewicht des ternären Systems Ammoniak - Kohlendioxid - Wasser bei hohen Wassergehalten im Bereich zwischen 373 und 473 Kelvin; Ber. Bunsenges. Phys. Chem.; 92(1988)148-160	CO_2 solubility in water	49	
Murray C.N.; Riley J.P.; The solubility of gases in distilled	CO_2	8	

water and sea water - IV. Carbon dioxide; Deep-Sea Research; 18(1971)533-541	solubility in water		
Nighswander J.A.; Kalogerakis N.; Mehrota A.K.; "Solubilities of carbon dioxide in water and 1 wt% NaCl; J. Chem. Eng. Data; 34(1989)355-360	CO_2 solubility in water	33	
Novak; J.; Fried; V.; Pick; J.; Löslichkeit des Kohlendiosyds in Wasser bei Verschiedenen Drücken und Temperaturen; Collect. Czech. Chem. Commun.; 26(1961)2266-2270	CO_2 solubility in water	24	
Postigo M.A.; Pedrosa G.; Katz M.; Nueva metodo experimental para la determinacion de solubilidad de gases en liquidos ; Anales Asoc. Quim. Argentina; 66(1978)25-30	CO_2 solubility in water	4	
Prutton C.F.; Savage R.L.; The solubility of Carbon Dioxide in Calcium Chloride-Water Solutions at 75; 100; 120° and high pressures; J. Am. Chem. Soc.; 67(1945)1550-4	CO_2 solubility in water	5	
Rumpf B.; Nicolaisen H.; Öcal C; Maurer G.; Solubility of Carbon Dioxide in Aqueous Solutions of Sodium Chloride: Experimental Results and Correlation; J. Solution Chemistry 23(1994)431-448(3)	CO_2 solubility in water	7	
Stewart P.B.; Munjal P.; Solubility of carbon dioxide in pure water; synthetic sea water and Synthetic Sea Water Concentrates at -50 to 250 C. and 10- to 45-Atm. Pressure; Journal of Chemical and Engineering Data ; 15(1970)67-71	CO_2 solubility in water	12	
Takenouchi S.; Kennedy G. C.; The binary system H2O-CO2 at high temperatures and pressures; American Journal of Science; 262(1964)1055-1074	CO_2 solubility in water	15	
Takenouchi S.; Kennedy G.C.; The Solubility of Carbon Dioxide in NaCl solutions at high temperatures and pressures; American Journal of Science; 263(1965)445-454	CO_2 solubility in water	2	
Van Slyke; D.D.; Determination of Solubilities of Gases in Liquids with Use of the Van Slyke-Neill Manometric Apparatus for both Saturation and Analysis; J. Biol. Chem.; 130(1939)545-554	CO_2 solubility in water	6	
Wasmund R.; Bultmann H.; Einfluss des Saccharosegehalts auf die CO2-Absorption wässriger Lösungen; Zuckerind.; 105(1980)1085-1087, Gas solubility	CO_2 solubility in water	65	
Wei Yan; Shengli Huang; Erling H. Stenby; Measurement and modeling of CO2 solubility in NaCl brine and CO2-saturated NaCl brine density; International Journal of Greenhouse Gas Control; 5(2011)1460-1477	CO_2 solubility in water	6	
Wiebe R; Gaddy V.L.; The solubility in water of carbon dioxide at 50; 75 and 100°; at pressures to 700 Atmospheres; J. Am. Chem. Soc.; 61(1939)315-318	CO_2 solubility in water	9	
Wiebe R; Gaddy V.L.; The solubility of Carbon Dioxide in	CO_2	16	

Water at Various Temperatures from 12 to 40°C and at pressures to 500 atm.; J. Am. Chem. Soc.; 62(1940)815-817	solubility in water		
Xiaoying Han; Zhihui Yu; Jingkui Qu; Tao Qi; Wei Guo; and Guoqing Zhang; Measurement and Correlation of Solubility Data for CO2 in NaHCO3 Aqueous Solution; J. Chem. Eng. Data; 56(2011)1213-1219(4)	CO_2 solubility in water	15	15
Yeh S.-Y.; Peterson R.E.; Solubility of Carbon Dioxide; Krypton; and Xenon in Aqueous Solutions; Journal of pharmaceutical sciences; 53(1964)822-824	CO_2 solubility in water	4	
Zawisza A.; Malesinska B.; "Solubility of Carbon Dioxide in Liquid Water."; J. Chem. Eng. Data; 26(1981)388-391	CO_2 solubility in water	33	
Zelvenskii; Y.D.; The Solubility of Carbon Dioxide under Pressure; Jour. Chem. Industry; 14(1937)1250-1257	CO_2 solubility in water	95	
Zheng; D-Q.; Tain-Min; G.; Knapp; H.; Experimental and modeling studies on the solubility of CO2; CHClF2; CHF3; C2H2F4 and C2H4F2 in water and aqueous NaCl solutions under low pressures; Fluid Phase Equilibria; 129(1997)197-209	CO_2 solubility in water	28	
Barbero J.A.; Hepler L.G.; McCurdy K.G.; Tremaine P.R; Thermodynamics of aqueous carbon dioxide and sulfur dioxide: heat capacities; volumes; and the temperature dependence of ionization; Can. J. Chem.; 61(1983)2509-2519	Heat capacity	10	
Chernen'kaya E.I.; Experimental determination of the specific heats of aqueous solutions of NH4HCO3; NaHCO3; Na2CO3; NH3; and of liquors of the soda industry at 25°c; J. Applied Chem. USSR; 44(1971)1562	Heat capacity	6	
Chernen'kaya E.I.; Bratash E.G.; Experimental determination of the specific heats of aqueous solutions of Na2CO3; NaHCO3; NH4HCO3 and of liquors o; J.Applied Chem. USSR; 45(1972)2325	Heat capacity	2	
E. C. Sorenson and E. M. Woolley; Thermodynamics of proton dissociation from aqueous bicarbonate: apparent molar volumes and apparent molar heat capacities of potassium carbonate and potassium bicarbonate at T=(278.15 to 393.15) K and at the pressure 0.3; The Journal of Chemical Thermodynamics ; 36(2004)289-298	Heat capacity	336	336
Ginzburg D.M.; Kochkalda V.E.; Enthalpies and specific heats in the potassium carbonate-water system; Russ. J. Phys. Chem.; 46(1972)1535(10)	Heat capacity	34	34
Hnedkowsky L.; Wood R.H.; "Apparent molar heat capacities of aq. sol. of CH4, CO2, H2S, NH3 at 28MPa; J. Chem. Thermodynamics; 29(1997)731-747	Heat capacity	4	

Rümelin G.; Über die verdünnungswärme konzentrierter Lösungen ; Z.Phys.Chem.(Leipzig); 58(1907)449	Heat capacity	2	
Thomsen J.; Wässrige lösung und hydratbildung; Thermochemische Untersuchungen; Band 3; Leipzig 1883 p. 34-39	Heat of dilution	4	
Benjamin L.; Heat of Solution of Potassium Carbonate.; J Chem. Eng. Data ; 7(1962)239-240	Heat of solution	11	11
Apelblat A.; The vapour pressures of water over saturated aqueous sulutions; J. Chem. Thermodynamics; 24(1992)619-626	Osmotic coefficient	7	
Roy R.N.; Gibbons J.J.; Williams R.; Godwin L.; Baker G.;Simonson J.M;Pitzer K.S; The Thermodynamics of Aqueous Carbonate Solutions; J. Chem. Thermodynamics ; 16(1984)303-315	Osmotic coefficient	46	
Roy R.N.; Gibbons J.J.; Wood M.D.; Williams R.W.; Peiper J.C.; Pitzer K.S.; The first ionization of carbonic acid in aqueous solutions of potassium chloride including the activity coefficients of potassium bicarbonate; J. Chem. Thermodynamics; 15(1983)37-47	Osmotic coefficient	48	
Sarbar M.; Covington A.K.; Nutall R.L.; Goldberg R.N.; Activity and osmotic coefficients of aqueous potassium carbonate; J. Chem. Thermodynamics; 14(1982)695-702	Osmotic coefficient	57	
Puchkov L.V.; Kurochkina V.V.; Saturated vapor pressure over aqueous solutions of potassium carbonate; J. Appl. Chem. USSR; 43(1970)175	Water activity	42	
Babenko A.M.; Andrianov A.M.; The KHCO3-KNO3-H2O system; Russian Journal Inorganic Chemistry; 26(1981)261-4 (2)	Solid-liquid equilibrium	8	
Bain; H.W.; The system potassium carbonate; sodium carbonate and water at 40°C and the trihydrate of sodium carbonate; J. Am. Chem. Soc.; 49(1927)2734-8	Solid-liquid equilibrium	1	
Blasdale; W.C.; Equilibria in Solutions Containing Mixtures of Salts III. The System; Water and the Chlorides and Carbonates of Sodium and Potassium at 25° IV. The System; Water and the Sulfates and Carbonates of Sodium and Potassium at; J. Am. Chem. Soc.; 45(1923)2935-2946	Solid-liquid equilibrium	1	
Bogoyavlenskii P.S.; Gashpar E.D.; The Potassium bicarbonate-nitrate-water system at 0°; 25°; and 40°C; Russ. J. Inorg. Chem.; 18(1973)1662-3	Solid-liquid equilibrium	3	
Bogoyavlenskii P.S.; Manannikova; A.S.; Sb.Nauch.Tr.L'vov.Gos.Vet.-Zootekhn.Inst. ; 6(1954)376	Solid-liquid equilibrium	1	
Bogoyavlenskii P.S.; Ni Shih-Ching; Solubility relation in the system NaHCO3-KHCO3-H2O and its dependence on some peculiarities of the structure of the salts; Scientia Sinica (English Edition) ; 8(1959)580-590 (6)	Solid-liquid equilibrium	1	

Bogoyavlenskii P.S.; Solubility and salting out in the KCl-KHCO3-K2SO4-H2O system at 25°C and 40°C; Russ. J. Inorg. Chem.; 10(1965)929-932	Solid-liquid equilibrium	2	
Byzova E.A.; Uch.Zap.Leningrad.Gos.Pedagog.Inst.im.; 6(1937)154 (3)	Solid-liquid equilibrium	4	
Byzova E.A.; Solubility of salts in the system K2CO3-K2SO4-KCl-H2O at 0; 30; 50; and 70°; Russ. J. Inorg. Chem.; 8(1963)1014-1017	Solid-liquid equilibrium	4	
Carbonnel L.; The ternary system H2O-KOH-K2CO3 in the temperature interval -22° to 30.7°; Bull. Soc. Chim. France; (1959)1990-6	Solid-liquid equilibrium	107	
De Coppet L.C.; On the molecular depression of the freezing point of water produced by some very concentrated saline solutions; J. Phys. Chem.; 8(1904)531-538	Solid-liquid equilibrium	6	
Ender F.; Zur individualität des osmotischen verhaltens der alkalicarbonate ; Z.Elektrochem. ; 43(1937)234-238	Solid-liquid equilibrium	20	
Ervin; G.J.; Giorgi; A.L.; McCarthy; C.E.; The system Potassium Carbonate-Sodium Carbonate-Water at 100 and 150°C; J. Am. Chem. Soc.; 66(1944)384-7	Solid-liquid equilibrium	2	
Foerster F.; Brosche A. and Norberg-Schulz Chr.; Über die schwefligsauren Salze des Natriums und des Kaliums.; Z. Phys. Chem.; 110(1924)435-496	Solid-liquid equilibrium	11	
Ginzburg D.M.; Markel C.A.; Solubility in the system 2Na+; 2K+/CO3--;2(OH-) - H2O at 75°C; Z. Neorg. Khim.; 17(1972)1439-43	Solid-liquid equilibrium	1	
Hill A.E.; and Hill D.G.; Ternary systems. V. potassium bicarbonate; potassium carbonate and water; J. Am. Chem. Soc.; 49(1927)967-969 (4)	Solid-liquid equilibrium	12	
Hill A.E.; Hydrated Potassium Sesquicarbonate K2CO3·2KHCO3·3/2H2O; J. Am. Chem. Soc.; 52(1930)3817-3825	Solid-liquid equilibrium	27	
Hill A.E.; Moskowitz S. Ternary systems VIII; Potassium carbonate; potassium sulfate and water at 25°C ; J. Am. Chem. Soc. ; 51(1929)2396-8	Solid-liquid equilibrium	10	
Hill; A.; Double salt formation among the carbonates and bicarbonates of sodium and potassium; J. Am. Chem. Soc. ; 52(1930)3813-3817	Solid-liquid equilibrium	14	
Hill; A.; Smith S.; Equilibrium between the carbonates and bicarbonates of sodium and potassium in aqueous solution at 25°C; J. Am. Chem. Soc.; 51(1929)1626-1636	Solid-liquid equilibrium	1	
Hill; A.E.; Miller; F.W.; Ternary Systems IV. Potassium Carbonate; Sodium Carbonate and Water; J. Am. Chem. Soc.; 49(1927)669-686	Solid-liquid equilibrium	7	
Hostálek Z.; Kasparova I.; Ternarni soustava voda-uhlicitan draselny-hydroxyd draselny; Chem. Listy; 50(1956)979-	Solid-liquid equilibrium	56	

981 (6)			
Il'inskii; V.P.; The influence of the formation of hydrates and double salts on the reaction of double decomposition of salts in aqueous solution; in the case of the system sodium chlorate-potassium carbonate; Zh. Russ. Fiz.-Khim. Obshchest.; 54(1923)29-59	Solid-liquid equilibrium	6	
Itkina L.S.; Kokhova V.F.; Solubility isotherm at 150° of the systems Na2SO4-Na2CO3-H2O and K2SO4-K2CO3-H2O.; Izv.Sektora Fiz.-Khim.Anal.;Inst.Obshch.Neorgan.Khim.Akad.Nauk ; 26(1955)242-7	Solid-liquid equilibrium	1	
Itkina; L. S.; Kokhova; V. F.; Isotherm at 150° of solubility in the system 2Na+; 2K+||CO3--; SO4-- + H2O.; Zhurnal Neorganicheskoi Khimii (1956); 1(1956)1665-71	Solid-liquid equilibrium	1	1
Krat V.N.; Isotherm of the ternary system sodium carbonate potassium carbonate/water at 0°; Tr. Gos. Inst. Prikl. Khim.; 23(1935)117-118	Solid-liquid equilibrium	1	
Kremann; K. and Zitek; A.; Die bildung von konversionssalpeter aus natronsalpeter ; Monatshefte für Chemie ; 30(1909)311-340 (4)	Solid-liquid equilibrium	2	
Lang A.A.; Sukava A.J.; The system KOH-K2CO3-H2O at low temperatures; Can. J. Chem.; 36(1958)1064-9 (7)	Solid-liquid equilibrium	80	
Loomis; E.H.; On the Freezing-points of Dilute Aqueous Solutions; Physical Review; 3(1896)270-292	Solid-liquid equilibrium	5	
Luzhnaya N.P.; Kosyachkova S.N.; Solubility isotherms of systems K2CO3-K2SO4-H2O and KHCO3-K2SO4-H2O at 50°; Izvest. Sektora Fiz.-Khim. Anal.; Inst. Obshchei i Neorg. Khim.; Akad. Nauk S.S.S.R.; 25(1954)345-9	Solid-liquid equilibrium	2	
Luzhnaya N.P.; Kosyachkova S.N.; Solubility isotherm at 50° of the quaternary system K2CO3-K2SO4-KHCO3-H2O.; Izv. Sektora Fiz.-Khim. Anal.;Inst. Obshch. Neorgan. Khim. Akad. Nauk; 26(1955)259-65	Solid-liquid equilibrium	18	18
Luzhnaya N.P.; Kosyachkova S.N.; The solubility isotherm of the aqueous system 2NaHCO3 + K2SO4 <-> 2KHCO3 + Na2SO4 at 50°; Izv.Sektora Fiz.-Khim.Anal.; Inst.Obshch.Neorgan.Khim.Akad.Nauk ; 27(1956)358-66	Solid-liquid equilibrium	1	
Lyudkovskaya; M. A.; Fridman; S. D.; Klevke; V. A.; Purification of gases from CO2 by a "hot" solution of K2CO3. Phase equilibriums in the system K2CO3-KHCO3-H2O; Khimicheskaya Promyshlennost (St. Petersburg; Russian Federation); 41(1965)339-343(5)	Solid-liquid equilibrium	21	
Malcolm P. Applebey; Margaret A. Leishman; The system Potassium Carbonate- Ammonia - Water; J. Chem. Soc.; (1932)1603-1608	Solid-liquid equilibrium	2	
Meyerhoffer W.; Reciprocal pairs of salts. IV. An affinity	Solid-liquid	6	

problem; Zeitschrift fur Physikalische Chemie; 53(1905)513-603	equilibrium		
Moore R.C.; Mesmer R.E.; Simonson J.M.; Solubility of Potassium carbonate in water between 384 and 529 K measured using the synthetic method; J. Chem. Eng. Data; 42(1997)1078-1081	Solid-liquid equilibrium	17	17
Ni Shi-Shen; Bogoyavlenskii; P.S.; Acta Chim Sinica ; 26(1958)274 (3)	Solid-liquid equilibrium	2	
Oglesby N.E.; A Study of The System Sodium Bicarbonate-Potassium Bicarbonate-Water; J. Am. Chem. Soc.; 51(1929)2352-2362	Solid-liquid equilibrium	3	
Osaka; J.; On Sodium Potassium Carbonates; Mem. Coll. Sci. Eng. (Kyoto) ; 3(1911)55-61	Solid-liquid equilibrium	1	
Paris R.; Mondain-Monval P.; Etude du système ClK-CO3HK-H2O entre 10 and 40°C; Bull. Soc. Chim. France; 5(1938)1142-7	Solid-liquid equilibrium	4	
Rashkovskaya E.A.; Averbakh R.A.; Danilevskaya M.F.; Nisengol'ts F.S.; Solubility isotherms in the systems Na || (HCO3)2; SO4 + H2O; K2 || (HCO3)2; SO4 + H2O; and K2 || (HCO3)2; CO3; SO4 + H2O at 35°; Ukr. Khim. Zh.; 24(1958)510-20 (4)	Solid-liquid equilibrium	2	
Ravich; M.I.; Itkina L.S; Kokhova V.F.; Existence of an equilibrium solid phase K2CO3·Na2CO3 in the system K2CO3-Na2CO3-H2O at temperatures above 100°; Izv. Sektora Fiz.-Khim. Anal.; Akad. Nauk SSSR; 25(1954)350-60	Solid-liquid equilibrium	2	2
Sedel'nikov; G.S.; Trofimovich A.A.; The reciprocal system 2K+; 2Na+; 2HCO3-; CO32-; H2O at 75°C; Russ. J. Inorg. Chem.; 4(1959)649-652 (6)	Solid-liquid equilibrium	5	
Slivko T. A.; Shakhno I. V.; Plyushchev V. E.; The 2K; 2Li; CO3; 2Cl-H2O System at 25°C; Russ. J. Inorg. Chem.; 15(1970)287-9	Solid-liquid equilibrium	1	
Slivko; T. A.; Shakhno; I. V.; Plyushchev; V. E.; Malyshko; L. F.; The K+; Li+//CO3(2-); NO3(-)-H2O system at 25°C; Russ. J. Inorg. Chem.; 13(1968)1047-1049 (7)	Solid-liquid equilibrium	1	
Starkova Z.P.; The system K2CO3-KHCO3-H2O at 42°; Zh. Obsch. Khim.; 1(1931)747-9 (6)	Solid-liquid equilibrium	16	
Takahashi G.; Bull. Imp. Hyg. Lab. (Tokyo); 29(1927)165	Solid-liquid equilibrium	8	
Teeple; J.E.; The Industrial Development of Searles Lake Brines; The Industrial Development of Searles Lake Brines; (1929)	Solid-liquid equilibrium	5	
Trypuc M.; Kielkowska U. and Stefanowicz D.; Solubility Investigations in the KHCO3 + NH4HCO3 + H2O System;	Solid-liquid equilibrium	4	

J. Chem. Eng. Data; 46(2001)800-804			
Urazov G.G; Lifatova Z.I.; Combined solubility of Li2CO3 with Na or K carbonate in water; Zh. Prikl. Khim.; 17(1944)16-21 (1)	Solid-liquid equilibrium	1	
Vasil'ev; B.B.; System sodium carbonate potassium carbonate-water at elevated temperatures; Tr. Gos. Inst. Prikl. Khim; 23(1935)110-117	Solid-liquid equilibrium	3	
Waal A.J.C.; Dissertation; Leyden; "Tables Annuelles"; (1910)	Solid-liquid equilibrium	2	
Yin Ching-chin; Shen Yuan-lung; Shen Jien-king; Chen Hsiang-chuan; Liu Tung; Acta Chim. Sinica; 30(6)(1964)572	Solid-liquid equilibrium	1	

Data for the CO_2 - NH_3 – H_2O system, some also containing KOH/K_2CO_3

The sources of data used for determining model parameters related to ammonia are given in Table 2. The sources in the table are first sorted according to the type of data written in column 2 and next sorted according to the name of the first author given in column 1. In column 3, the number of data from each source used for the parameter estimation is given. In the fourth column, a number indicates how many of these data were added/typed in this project.

Table 2: Sources of experimental data used for determining model parameters in the CO_2 - NH_3 – H_2O system. Some of the systems also contain KOH/K_2CO_3.

Source	Type of data	Number of data points	Added in this project
Lichtfers U.; Spektroskopische Untersuchungen zur ermittlung von Speziesverteilungen im System Ammoniak-Kohlendioxid-Wasser; Dissertation; (2001) Aachen; Shaker Verlag	Dissociation/ Speciation	82	82
Staudt H.J.; Experimentelle Bestimmung und Korrelation der excessenthalpie und des excessvolumens binärer wässriger amin- und a; Dissertation; Universität Kaiserslautern; (1984)	Excess enthalpy	92	
Chan J.P.; Giauque W.F.; The entropy of NH3·2H2O. Heat capacity from 15 to 300K; J. Phys. Chem.; 68(1964)3053-3057	Heat capacity	13	13
Gawlick H.; Dissertation; Dissertation; Braunschweig; (1934) ,	Heat capacity	8	
Hildenbrand D.L.; Giauque W.F.; Ammonium Oxide and Ammonium Hydroxide. Heat Capacities and Thermodynamic Properties from 15 to 300K; J. Am. Chem. Soc.; 75(1953)2811-2818 (12)	Heat capacity	21	21
Hnedkowsky L.; Wood R.H.; "Apparent molar heat capacities of aq. sol. of; J. Chem. Thermodynamics; 29(1997)731-747	Heat capacity	19	
Salavera D.; Libotean S.; Patil K.R.; Esteve X.; and Coronas A.; Densities and Heat Capacities of the Ammonia + Water + NaOH and Ammonia + Water + KOH Solutions; J. Chem. Eng. Data; 51(2006)1020-1025	Heat capacity	54	54
Wrewsky M.; Kaigorodoff; Wärmekapazität wässeriger Lösungen von Chlorwasserstoff und Ammoniak bei Verschiedenen Temperaturen; Z. Physik. Chemie; 112(1924)83-89	Heat capacity	23	
Baud E.; Gay L.; Determination des hydrates; en solution; par la methode thermique. Application au système eau-ammoniac liquide; Ann. Chim. Phys.; 17(1909)398-418	Heat of dilution	24	
Berthelot M.; Dissolution des Acides et des Alcalis; Ann. Chim. Phys.; 4(1875)445-536	Heat of dilution	10	

Macriss R.A.; Eakin B.E.; Ellington R.T.; Huebler J.; Physical and thermodynamic properties of ammonia-water mixtures; Research Bulletin No. 34; Institute of gas technology; Chicago IL; 1964	Heat of dilution	80	80
Rumpf B.; Weyrich F. and Maurer G.; Enthalpy of dilution in aqueous systems of single solutes ammonia; sodium sulfate and ammonium sulfate: Experimental results and modeling; Thermochimica Acta; 303(1997)77-91	Heat of dilution	27	
Thomsen J.; Wässrige lösung und hydratbildung; Thermochemische Untersuchungen ; Band 3; Leipzig 1883 p. 34-39	Heat of dilution	3	
Wrewsky M; Sawaritzky N.; Die Bildungswärmen wässeriger Lösungen von HCl und NH3 bei verschiedenen Temperaturen ; Z. Physik. Chemie; 112(1924)90-96	Heat of dilution	67	
Zinner K.; Wärmetönung beim Mischen von Ammoniak und Wasser in Abhängigkeit von Zusammensetzung und Temperatur; Z. gesamte Kälte-Industrie ; 41(1934)21-29	Heat of dilution	457	457
Liu; Jinzhao • Wang; Shujuan • Svendsen; Hallvard F. • Idrees; Muhammad Usman • Kim; Inna • Chen; Changhe; Heat of absorption of CO2 in aqueous ammonia; piperazine solutions and their mixtures; International Journal of Greenhouse Gas Control ; 9(2012)148-159	Heat of solution	60	
Mollier H.; Lösungswärme von Ammoniak in Wasser; Forschungsarbeiten auf Dem Gebiete des Ingenieurwesens; 63/64(1909)107-113	Heat of solution	12	12
Qin; Feng • Wang; Shujuan • Kim; Inna • Svendsen; Hallvard F. • Chen; Changhe; Heat of absorption of CO2 in aqueous ammonia and ammonium carbonate/carbamate solutions; International Journal of Greenhouse Gas Control ; 5(2011)405-412(5)	Heat of solution	149	149
Ramstetter H.; Hantke G.; Eine neue Methode zur Messung von Wärmetönungen; Z. phys. Chem. ; Bodenstein-Festband(1931)662-668	Heat of solution	5	
Clifford I.L.; Hunter E.; The System Ammonia-Water at Temperatures up to 150°C and at Pressures up to twenty atmospheres; Journal of physical Chemistry ; 37(1933)101-118	NH_3 solubility in water	52	
Gaus W.; Über den Einfluss von Neutralsalzen auf die Tension des Ammoniaks aus wässeriger Lösung ; Zeitschrift für anorganische und allgemeine Chemie ; 25(1900)236-264	NH_3 solubility in water	6	
Gillespie P.C.; Wilding V.W.; Wilson G.M.; Vapor-liquid equilibrium measurements on the ammonia-water system from 313 to 589 K; AIChE symposium series ; 83(256)(1987)97-127	NH_3 solubility in water	183	
Ginzburg; D. M.; Markel; S. A.; Sirenko; M. A.; Sodium	NH_3	24	

sulfate-ammonia-water system at 600 and 760 torr.; Tr. N.-i. i Proekt. In-t Osnovn. Khimii (1975); (40); 40(1975)85-96	solubility in water		
Guillevic J-L.; Richon D.; Renon H.; Vapor-Liquid Equilibrium Data for the Binary System Water-Ammonia at 403.1; 453.1; 503.1 K up to 7.0 MPa; J. Chem. Eng. Data; 30(1985)332-335	NH_3 solubility in water	18	
Hales J.M.; Drewes D.R.; Solubility of ammonia in water at low concentrations; Atmospheric environment. A; General topics; 13(1979)1133-1147	NH_3 solubility in water	30	
Harms-Watzenberg F; Messung und Korrelation der thermodynamischen Eigenschaften von Wasser-Ammoniak-Gemischen; Fortschrittberichte VDI; reihe 3; 380(1995)	NH_3 solubility in water	30	
Ikemizu K. Sasaki K.; Morooka S.; Kato Y.; Shinohara H.; Diffusivities and solubilities of NH3 gas in aqueous solutions of ammonium salts; Kagaku Kogaku Rombunshu ; 4(1978)(3)273-276	NH_3 solubility in water	12	12
Inomata; H.; Ikawa; N.; Arai; K.; Saito; S.; Vapor-Liquid Equilibria for the ammonia-methanol-water system; J. Chem. Eng. Data ; 33(1988)26-29	NH_3 solubility in water	6	
Iseli M.; Experimentelle und thermodynamische untersuchung des siedegleichgewichtes des systems NH3-H2O bei hohen drucken; Dissertation; Eidgenössischen technischen hochschule ; Zürich; 1985	NH_3 solubility in water	44	
Jennings B.H.; Ammonia-Water Properties; Transactions of the american society of heating and refrigeration engineers ; 71(1965)21-29 (1)	NH_3 solubility in water	75	
Jones Merle E; Ammonia equilibrium between vapor and liquid aqueous phases at elevated temperatures.; J. Phys. Chem.; 67(1963)1113-1115	NH_3 solubility in water	17	
Kurz F.; Untersuchungen zur silmultanene Lösung von Ammoniak und Kohlendioxid in Wasser und salzhaltigen wässrigen Lösungen; Dissertation; Universität Kaiserslautern; (1994)	NH_3 solubility in water	156	
Mallet J.W.; On the solubility of ammonia in water at temperatures below 0°C; American Chemical Journal; 19(1897)804-809	NH_3 solubility in water	4	
Mezger R.; Payer T.; Kohlensaure Ammoniumverbindungen ; Das Gas- und Wasserfach ; 68(1925)651-5	NH_3 solubility in water	120	120
Mittasch A.; Kuss E.; Schlueter H.; Dichten und Dampfdrucke von wässrigen Ammoniaklösungen und von flüssigem Stickstofftetroxyd für das Temperaturgebiet 0° bis 60°.; Zeitschrift für anorganische und allgemeine Chemie; 159(1926)1-36	NH_3 solubility in water	49	28
Mollier H.; Dampfdruck von wässrigen	NH_3	35	

Ammoniaklösungen; Zeitschrift des Vereinigung deutsche Ingeniören ; 52(1908)1315-1320	solubility in water		
Morgan O.M.; Maass O.; An investigation of the equilibria existing in gas-water systems forming electrolytes; Canadian Journal of Research; 5(1931)162-199	NH_3 solubility in water	19	
Neuhausen B.S.; Patrick W.A.; A Study of the System Ammonia-Water as a Basis for a Theory of the Solution of Gases in Liquids; Journal of physical Chemistry ; 25(1921)693-720	NH_3 solubility in water	31	
Polak J; Lu B. C-Y; Vapor-Liquid Equilibria in System Ammonia-Water at 14.69 and 65 psia; J. Chem. Eng. Data ; 20(1975)182-3	NH_3 solubility in water	23	
Postma S.; Le systéme ammoniaque - eau; Recueils des travaux chimiques des Pays-Bas ; 39(1920)515-536	NH_3 solubility in water	24	
Rizvi S.S.H.; Measurement and correlation of ammonia water equilibrium data; Dissertation; Department of Chemical and Petroleum Engineering; University of Calgary; Alberta; Canada; 1985	NH_3 solubility in water	177	
Rumpf B.; Weyrich F. and Maurer G.; Simultaneous Solubility of NH3 and SO2 in H2O at temperatures from 313.15 to 373.15 amd Pressures up to 2.2 MPa; Fluid Phase Equilibria; 83(1993)253-260	NH_3 solubility in water	9	
Rumpf; B.; Kamps; A. P. S.; Maurer; G.; Simultaneous solubility of ammonia and hydrogen sulfide in water at temperatures from 313 K to 393 K; Fluid Phase Equilibria ; 158-160(1999)923-932	NH_3 solubility in water	6	
Salavera D.; Chaudhari S.K.; Esteve X.; and Coronas A.; Vapor-Liquid Equilibria of Ammonia + Water + Potassium Hydroxide and Ammonia + Water + Sodium Hydroxide Solutions at Temperatures from (293.15 to 353.15) K; J. Chem. Eng. Data; 50(2005)471-476	NH_3 solubility in water	35	35
Sassen C.L.; van Kwartel R.A.C.; van der Kool H.J.; de Swan Arons J.; Vapor-Liquid Equilibria for the system Ammonia + Water up to the Critical Region.; J. Chem. Eng. Data; 35(1990)140-144	NH_3 solubility in water	39	
Schultz J.F.; Elmore G.V.; The System Ammonium Nitrate-Ammonia-Water; Industrial and Engineering Chemistry; 38(1946)296-298	NH_3 solubility in water	34	
Shokin I.N.; Krasheninnikov S.A.; Binh L.V.; Determination of equilibrium pressures of ammonia over the systems NaCl-NH3-H2O; NH4Cl-NH3-H2O; and NaCl-NH4Cl-NH; The Soviet Chemical Industry; 2(1971)140-1	NH_3 solubility in water	6	6
Smolen T.M.; Manley D.B.; Poling B.E.; Vapor-Liquid Equilibrium data for the NH3-H2O System and Its	NH_3 solubility in	198	

Description with a modified cubic equation of state; J. Chem. Eng. Data; 36(1991)202-208	water		
Wilson Grant M.; Owens Richard S.; Roe Marshall W.; Sour Water Equilibria; ACS Symposium Series 133; Thermodynamics of Aqueous Systems with Industrial Applications; Newman SA; Editor; (1980)187-226	NH_3 solubility in water	10	
Cacciola G.; Restuccia G.; Aristov Yu; Vapor Pressure of KOH+NH3+H2O solutions; J. Chem. Eng. Data.; 40(1995)267-270	NH_3 solubility in water, KOH	59	
Salavera D.; Chaudhari S.K.; Esteve X.; and Coronas A.; Vapor-Liquid Equilibria of Ammonia + Water + Potassium Hydroxide and Ammonia + Water + Sodium Hydroxide Solutions at Temperatures from (293.15 to 353.15) K; J. Chem. Eng. Data; 51(2006)773-774 (2)	NH_3 solubility in water, KOH	175	175
Sorina G.A.; Miniovich V.M.; Efremova G.D.; Solubility of ammonia in aqueous solutions of KOH; Zhurnal Obshchei Khimii ; 37(1967)2150-2154	NH_3 solubility in water, KOH	64	
Abegg R.; Riesenfeld H.; Über das Lösungsvermögen von Salzlösungen für Ammoniak nach Messungen seines Partialdrucks; Zeitschrift für Physikalische Chemie; Stöchiometrie und Verwandschaftslehre ; 40(1902)84-108	NH_3 solubility in water, KOH, K_2CO_3	8	8
Cragoe C.S.; Meyers C.H.; Taylor C.S.; The vapor pressure of ammonia ; J. Am. Chem. Soc. ; 42(1920)206-229	NH_3 vapor pressure	29	29
Ginzburg; D. M.; Markel; S. A.; Detinich; L. P.; Sodium chloride-ammonium chloride-ammonia-carbon dioxide-water system at 1 atm.; Zhurnal Prikladnoi Khimii ; 45(1972)1687-90 (8)	NH_3-CO_2-H_2O vapor-liquid equilibrium	36	
Göppert U.; Maurer G.; Vapor-liquid equilibria in aqueous solutions of Ammonia and Carbon Dioxide at Temperatures Between 333 and 393K and Pressures up to 7 MPa ; Fluid Phase Equilibria ; 41(1988)153-185	NH_3-CO_2-H_2O vapor-liquid equilibrium	559	
Koren J.G. and Andreatch A.J.; Near Infrared Spectrophotometric Determination of Ammonia; Carbon Dioxide; and Water at Elevated Temperatures and Pressures.; Anal. Chem.; 37(1965)256-258(2)	NH_3-CO_2-H_2O vapor-liquid equilibrium	14	14
Kurz F.; Rumpf B.; Maurer G.; Vapor-liquid-solid equilibria in the system NH3-CO2-H2O from around 320 to 470K: New experimental data and modeling; Fluid Phase Equilibria; 104(1995)261-275	NH_3-CO_2-H_2O vapor-liquid equilibrium	63	
Müller G.; Bender E.; Maurer G.; Das Dampf-Flüssigkeitsgleichgewicht des ternären Systems Ammoniak - Kohlendioxid - Wasser bei hohen Wassergehalten im Bereich zwischen 373 und 473 Kelvin; Ber. Bunsenges. Phys. Chem.; 92(1988)148-160	NH_3-CO_2-H_2O vapor-liquid equilibrium	586	
Otsuka E.; Yoshimura S.; Yakabe M.; Inoue S.; Equilibrium	NH_3-CO_2-	71	

of the NH3-CO2-H2O system; Kogyo Kagaku Zasshi; 62(1960)1214-8	H_2O vapor-liquid equilibrium		
Pawlikowski E.M.; Newmann J.; Prausnitz J.M.; Phase Equilibria for aqueous solutions of Ammonia and Carbon Dioxide; Ind. Eng. Chem. Process. Des. Dev.; 21(1982)764-770	NH_3-CO_2-H_2O vapor-liquid equilibrium	33	
Pexton S.; Badger E.H.M.; and L. Silver; Vapour pressures of ammonia and carbon dioxide in equilibrium with aqueous solutions.; Journal of the society of chemical industry; 57(1938)106-110(4)	NH_3-CO_2-H_2O vapor-liquid equilibrium	91	
Ramasamy K.; A study of the vapour-liquid equilibria of the system ammonia-carbon dioxyde-water in relation to the synthesis of urea; TU Delft; Delft University of Technology; Doctoral thesis; (1988)	NH_3-CO_2-H_2O vapor-liquid equilibrium	47	47
Takahashi T.; Equilibrium pressure for the NH3-CO2-H2O system; Kogyo Kagaku Zasshi; 65(1962)743-745	NH_3-CO_2-H_2O vapor-liquid equilibrium	8	8
Van Krevelen D.W.; Hoftijzer P.J.; Huntjens F.J.; Composition and Vapour Pressures of Aqueous Solutions of Ammonia; Carbon Dioxide and Hydrogen Sulphide; Recueil des travaux chimiques des Pays-Bas; 68(1949)191-216	NH_3-CO_2-H_2O vapor-liquid equilibrium	61	
Verbrugge P.; Vapour-Liquid Equilibria of the Ammonia-Carbon Dioxide-Water System; Dissertation Delft University Press; (1979)	NH_3-CO_2-H_2O vapor-liquid equilibrium	97	
Yanagisawa; Y.; Harano Y.; Imoto T; Vapour-liquid equilibrium for the ternary system of Ammonia-Carbon dioxide-Water; J. Chem. Soc. Japan; (1973)917-923(5)	NH_3-CO_2-H_2O vapor-liquid equilibrium	18	18
Yanagisawa; Y.; Harano Y.; Imoto T; Vapour-liquid equilibrium for the ternary system of Ammonia-Carbon dioxide-Water at 70-99°C; J.Chem.Soc.Japan; (1975)271-274(2)	NH_3-CO_2-H_2O vapor-liquid equilibrium	21	21
Yanagisawa; Y.; Yano M; Harano Y.; Imoto T; Vapor-liquid-equilibrium for quaternary system of urea-ammonia-carbon dioxide-water; J. Chem. Soc. Japan; (1975)976-979(6)	NH_3-CO_2-H_2O vapor-liquid equilibrium	16	16
Rumpf B., Weyrich F., Maurer G.; Enthalpy changes upon Partial Evaporation of Aqueous Solutions containing Ammonia and Carbon Dioxide; Ind. Eng. Chem. Res.; 37(1998)2983-2995	NH_3-CO_2-H_2O partial evaporation	89	
Allamuratova; A. Zh.; Erkaev; A. U.; Kucharov; B. Kh.; Solubility in NH4NO3-(NH4)2CO3-H2O system;	Solid-liquid equilibrium	1	

O'zbekiston Kimyo Jurnali ; (2009)53-56(5)			
Belyaev I. N.; Lesnykh D. S.; and Grigor' eva E. A.; Urea-ammonium carbonate-water system; Zhur. Neorg. Khim.; 11(1966)1472	Solid-liquid equilibrium	11	11
Belyaev I.N.; Gregor'eva E.A.; The Ammonium-Carbonate-Sulfate system at 15°C; Russ. J. Inorg. Chem.; 24(1979)1588	Solid-liquid equilibrium	1	
Belyaev I.N.; Grigoreva E.A.; Berdyukova V.A.; Solubility and Physiochemical properties of saturated solutions in sodium carbonate-sodium chloride (ammonia+water); Izv. Vyssh. Ucheb. Zaved.; Khim.; Khim.; Teknol.; 20(1977)639-641	Solid-liquid equilibrium	1	
Belyaev I.N.; Grigor'eva E.A.; Berdyukova V.A.; The Na2CO3- (NH4)2CO3 - NH3 - H2O system at 10°C; Russ. J. Inorg. Chem ; 26(1981)753-755	Solid-liquid equilibrium	1	
Belyaev I.N.; Grigor'eva E.A.; Physicochemical Investigation of the (NH4)2CO3 - Li2CO3 - H2O System at 15°C; Russ. J. Inorg. Chem.; 13(1968)899-900	Solid-liquid equilibrium	1	
Belyaev I.N.; Grigor'eva E.A.; The (NH4)2CO3 - Na2CO3 - H2O System at 25°C; Russ. J. Inorg. Chem.; 13(1968)292-294(2)	Solid-liquid equilibrium	1	
Belyaev I.N.; Grigor'eva E.A.; The Potassium-ammonium carbonate - water system at 15°; Russ. J. Inorg. Chem.; 12(1967)889-891 (6)	Solid-liquid equilibrium	19	
Belyaev; I. N.; Grigor'eva; E. A.; Berdyukova; V. A.; Study of the sodium; ammonium||chloride; carbonate solubility diagram in an (ammonia + water) mixed solvent at 20°. 1. Sodium carbonate-ammonium carbonate-ammonia-water system; Izvestiya Severo-Kavkazskogo Nauchnogo Tsentra Vysshei Shkoly; Estestvennye Nauki ; (1980)52-53(3)	Solid-liquid equilibrium	1	1
Belyaev; I. N.; Grigor'eva; E. A.; Berdyukova; V. A.; Study of the sodium; ammonium||chloride; carbonate solubility diagram in the ammonia-water mixed solvent at 20°. II. Ammonium chloride-ammonium carbonate-ammonia-water system; Izvestiya Severo-Kavkazskogo Nauchnogo Tsentra Vysshei Shkoly; Estestvennye Nauki ; (1981)57-8(2)	Solid-liquid equilibrium	1	1
Belyaev; I. N.; Grigor'eva; E. A.; Spuskanyuk; Zh. F.; Physicochemical study of ammonium carbonate-ammonium halide-water systems; Zhurnal Neorganicheskoi Khimii; 15(1970)796-800(3)	Solid-liquid equilibrium	3	3
Berdyukova; V. A.; Grigor'eva; E. A.; Lopatin; S. S.; Khutsistova; F. M.; Denisenko; L. E.; Potassium carbonate-potassium chloride-ammonia-water and potassium chloride-ammonium chloride-ammonia-water systems at 25°C; Zhurnal Neorganicheskoi Khimii ; 31(1986)1062-7(4)	Solid-liquid equilibrium	1	1

Fedotieff P.P; Der Ammoniaksodaprozes vom standpunkte der phasenlehre; Z. Physikalische Chemie; 49(1904)162-188	Solid-liquid equilibrium	3	
Fedotieff P.P.; Koltunoff J.; Eine andere Form des Ammoniaksodaverfahrens ; Z. anorg. allg. Chemie; 85(1914)247-260	Solid-liquid equilibrium	3	
Fedotieff P.P; Kolossoff A.; Die dritte form des ammoniaksodaverfahren ; Z. Anorg. Allg. ; 130(1923)39-46	Solid-liquid equilibrium	1	
Grigor'eva; E. A.; Solubility in the ammonium carbonate-potassium carbonate-water system; Mater. Nauch. Konf. Aspir.; Rostov.-na-Donu Gos. Univ.; 7th 8th; (1968)188-90	Solid-liquid equilibrium	3	3
Jänecke; E; Über das system H2O; CO2; NH3; Zeitschrift für Electrochemie ; 35(1929)716-728	Solid-liquid equilibrium	259	77
Jänecke; E.; Über die Löslickeit von ammonbicarbonat in wasser bis zum schmeltzpunkt; Zeitschrift für Electrochemie ; 35(1929)332-334	Solid-liquid equilibrium	19	
Kurnakov; N.S.; Ravich M.I.; Troitskaya N.V.; The ice fields of the ternary systems: base-acid-water. Formation of phosphates; chromates and borates; Izv. Sektora Fiz.-Khim. Anal.; Akad. Nauk SSSR (Ann. secteur anal. phys.-chim.; Inst. chim. gen. (U. S. S. R.); 10(1938)275-304	Solid-liquid equilibrium	3	
Kurz F.; Untersuchungen zur silmultanene Lösung von Ammoniak und Kohlendioxid in Wasser und salzhaltigen wässrigen Lösungen; Dissertation; Universität Kaiserslautern; (1994)	Solid-liquid equilibrium	3	
Malcolm P. Applebey; Margaret A. Leishman; "The system Potassium Carbonate- Ammonia - Water; J. Chem. Soc.; (1932)1603-1608	Solid-liquid equilibrium	10	
Mondain-Monval; P.; Sur la préparation du chlorure d'ammonium ; Compt. Rend. ; 174(1922)1014-1017	Solid-liquid equilibrium	1	
Mondain-Monval; P.; Sur la préparation du chlorure d'ammonium à basse temperature; Comptes Rendus hebdomadaires des séances de l'Academie des Sciences; 175(1922)162-164	Solid-liquid equilibrium	1	
Neumann B.; Domke R.; Die Gleichgewichtsverhältnisse beim ammoniaksodaprozesse unter druck; Z. Elektrochem. ; 34(1928)136-153	Solid-liquid equilibrium	4	4
Pickering S.U.; The hydrate theory of solutions. Some compounds of the alkyl-amines and ammonia with water; J. Chem. Soc.; 63(1893)141	Solid-liquid equilibrium	68	68
Postma S.; Le systéme ammoniaque - eau; Recueils des travaux chimiques des Pays-Bas; 39(1920)515-536	Solid-liquid equilibrium	6	
Rupert F.F.; The solid hydrates of ammonia; J. Am. Chem. Soc.; 31(1909)866-8	Solid-liquid equilibrium	5	
Rupert F.F.; The solid hydrates of ammonia II; J. Am. Chem. Soc.; 32(1910)748-749	Solid-liquid equilibrium	26	

Schütze H.; Piechowicz T.; Lösungsgleichgewichte in wässrigen Systemen (3. Mitteilung.) Das System NH4CO2NH2-(NH4)2SO4-NH3-H2O; Helv. Chim. Acta.; 26(1943)242-245 (1)	Solid-liquid equilibrium	4	
Terres E.; Behrens H.; Zur Kenntnis der physikalisch-chemischen Grundlagen der Harnstoft synthese aus Ammoniak; Koblensäure und Wasser; Zeitschrift für physikalische Chemie ; 139(1928)695-716	Solid-liquid equilibrium	49	15
Terres E.; Weiser H.; Beitrag zur kenntnis der ammoniak-kohlensäureverbindungen im gleichgewicht mit ihren wässerigen lösungen ; Z. Elektrochemie ; 27(1921)177-193	Solid-liquid equilibrium	107	
Toporescu; E.; Sur la preparation du bicarbonate du sodium; Compt. Rend. ; 175(1922)268-270	Solid-liquid equilibrium	2	
Toporescu; E.; Sur la preparation du bicarbonate du sodium; Compt. Rend. ; 174(1922)870-873	Solid-liquid equilibrium	1	
Trypuc M.; Kielkowska U.; "Solubility in the NH4HCO3+NH4VO3+H2O System"; J. Chem. Eng. Data; 41(1996)1005-1007	Solid-liquid equilibrium	4	
Trypuc M.; Kielkowska U.; Solubility in the NH4HCO3 + NaHCO3 + H2O System; J. Chem. Eng. Data; 43(1998)201-204	Solid-liquid equilibrium	4	
Trypuc M.; Kielkowska U. and Stefanowicz D.; "Solubility Investigations in the KHCO3 + NH4HCO3 + H2O System"; J. Chem. Eng. Data; 46(2001)800-804	Solid-liquid equilibrium	4	
Volfkovich; S. I.; Belopolskii; A. P.; Lebedev; B. A.; Utilization of natural sodium sulfate for manufacturing soda ash and ammonium sulfate.; Z. Prikladnoi Khimii; 4(1931)582-606	Solid-liquid equilibrium	1	

Model parameters and standard state properties

Properties of aqueous species

In Table 3, the standard thermodynamic properties for the aqueous species in the model are listed. The properties for the hydrogen ion are zero by convention, while the remaining, un-marked properties and parameters were determined in this work.

Table 3: Standard thermodynamic properties of aqueous species used in the upgraded model. Properties marked with an asterisk *, are from NIST (Wagman, et al., 1982). Properties marked with # were determined by Thomsen and Rasmussen (Thomsen & Rasmussen, Modeling of Vapor-liquid-solid equilibrium in gas-aqueous electrolyte systems, 1999). Parameters a, b, and c are used for calculating the temperature dependent heat capacity of the aqueous species according to the equation: Cp = a+bT+c/(T-200) J/(mol·K). Heat capacity parameters marked with & were determined by Thomsen, 2008 (Thomsen, Working up phosphate from ashes, 2008). The remaining heat capacity parameters were determined in this work.

Species	$\Delta_f G$, kJ/mol	$\Delta_f H$, kJ/mol	Cp, a	Cp, b	Cp, c
H2O	-237.129*	-285.83*	58.36952&	0.038961&	523.8794&
NH3(aq)	-26.5*	-80.29*	74.113	-0.00694	0
CO2(aq)	-385.98*	-413.8*	318.67	-0.35016	2333.7
O2(aq)	16.53822&	-10.5753&	404.1234&	0	0
N2	17.772&	-11.1515&	209&	0	0
K+	-283.27*	-252.38*	-36.0205&	0.135547&	590.6&
NH4+	-79.31*	-132.51*	79.9	0	0
H+	0	0	0	0	0
OH-	-157.248*	-230.243*	1418.157&	-3.44577&	-51473&
CO3--	-527.81*	-677.14*	780	-2.036	-47290
HCO3-	-586.77*	-691.99*	672	-1.385	-31300
NH2COO-	-378#	-497#	687.7435	-1.43091	-31823.9

Properties of solid species

The standard thermodynamic properties used in this project and determined in this project are given in Table 4.

Table 4: Standard thermodynamic properties of the solid phases appearing in the modeled system. The properties were determined in this project, except those marked with & which were determined by (Thomsen, Working up phosphate from ashes, 2008)

Salt	Δ_fG, kJ/mol	Δ_fH, kJ/mol	Cp, J/(mol·K)
KOH	-392.633[&]	-424.764[&]	64.9[&]
KOH·H2O	-650.165[&]	-747.548[&]	105[&]
KOH·2H2O	-893.463[&]	-1046.42[&]	145[&]
K2CO3	-1046.7	-1124.2	114.43
2K2CO3·3H2O	-2843.7	-3202.2	350
K2CO3·6H2O	-2492.6	-2927.7	354
KHCO3	-865.97	-971.94	88
2K2CO3·4KHCO3·3H2O	-6309.7	-7070.7	704
(NH4)2CO3·K2CO3	-1776.5	-2096.4	227
(NH4)2CO3	-586.43	-942.16	113
(NH4)2CO3·H2O	-927.25	-1231.9	153
NH4HCO3	-665.24	-844.55	85
(NH4)2CO3·2NH4HCO3	-2021.9	-2625.9	283
NH2COONH4	-449.42	-649.16	121
Ice	-236.521[&]	-292.788[&]	48[&]

Properties of gases

The properties of gases used in this project are given in Table 5.

Table 5: Properties of gases used in this project. The properties marked with * are from (Wagman, et al., 1982).

Gas	Δ_fG, kJ/mol	Δ_fH, kJ/mol	Cp, J/(mol·K)	Tc	Pc, bar	ω
CO2	-394.359*	-393.509*	37.11*	304.1282	73.773	0.225
NH3	-16.45*	-46.11*	35.06*	405.4	113.6	0.25
H2O	-228.572*	-241.818*	33.577*	647.096	220.64	0.344
O2	0	0	31.825	154.58	50.43	0.0222
N2	0	0	29	126.2	34	0.0377

Model parameters

The parameters in the Extended UNIQUAC model are the volume and surface area parameters, usually termed R and Q parameters, and the interaction parameters. The volume and surface area parameters used in this model are listed in Table 6. The interaction parameters are given in Table 7.

Table 6: Extended UNIQUAC volume and surface parameters. The parameters marked with ° are from (Abrams & Prausnitz, 1975). Those marked with & are from (Thomsen, Working up phosphate from ashes, 2008). The remaining R, and Q parameters were determined in this work.

Aqueous species	R	Q
H2O	0.92°	1.4°
NH3(aq)	1.39	2.267
CO2(aq)	2.368	3.143
O2(aq)	0.13779&	1E-16&
N2(aq)	3.0831&	3.881&
K+	1.86&	1.71&
NH4+	1.279	0.8545
H+	0.13779&	1E-16&
OH-	10.06&	9.01&
CO3--	4.035	6.445
HCO3-	8.59	9.897
NH2COO-	5.57	9.762

Table 7: Interaction parameters used in this project. Parameters for CO2 species and NH3 species were determined in this work. The remaining parameters were determined in (Thomsen, Working up phosphate from ashes, 2008).

Species 1	Species 2	u0	uT
H2O	H2O	0	0
H2O	NH3	56.764	0.557
H2O	CO2	408.63	-1.728
H2O	O2	10000000000	0
H2O	N2	-507.8001	-0.6865
H2O	K+	333.3512	0.33781
H2O	NH4+	-201.78	-0.8983
H2O	H+	10000	0
H2O	OH-	205.3527	0.80532
H2O	CO3--	-178.25	0.3414
H2O	HCO3-	274.63	-0.4826
H2O	NH2COO-	321	-8.379
NH3	NH3	409.16	-0.1587
NH3	CO2	10000000000	0
NH3	O2	10000000000	0
NH3	N2	10000000000	0
NH3	K+	429.53	-2.009

NH3	NH4+	328.81	2.443
NH3	H+	1000000000	0
NH3	OH-	488.79	-0.2533
NH3	CO3--	103.56	2.185
NH3	HCO3-	238.09	-0.9939
NH3	NH2COO-	375.4	-8.087
CO2	CO2	1413.8	0
CO2	O2	10000000000	0
CO2	N2	10000000000	0
CO2	K+	810.06	-9.333
CO2	NH4+	4.9967	-1.23
CO2	H+	1000000000	0
CO2	OH-	10000000000	0
CO2	CO3--	10000000000	0
CO2	HCO3-	517.54	0.04489
CO2	NH2COO-	10000000000	0
O2	O2	0	0
O2	N2	10000000000	0
O2	K+	10000000000	0
O2	NH4+	10000000000	0
O2	H+	10000000000	0
O2	OH-	10000000000	0
O2	CO3--	10000000000	0
O2	HCO3-	10000000000	0
O2	NH2COO-	10000000000	0
N2	N2	244.5326	13.69
N2	K+	10000000000	0
N2	NH4+	10000000000	0
N2	H+	1000000000	0
N2	OH-	10000000000	0
N2	CO3--	10000000000	0
N2	HCO3-	10000000000	0
N2	NH2COO-	10000000000	0
K+	K+	0	0
K+	NH4+	311.41	7.54
K+	H+	1000000000	0
K+	OH-	871.1804	0.71619
K+	CO3--	1087.3	16.22
K+	HCO3-	539.16	-0.01327
K+	NH2COO-	918.43	-1.46
NH4+	NH4+	0	0

NH4+	H+	1000000000	0
NH4+	OH-	1065.9	1.116
NH4+	CO3--	-771.36	0.3281
NH4+	HCO3-	-18.736	-3.878
NH4+	NH2COO-	-0.29841	-5.692
H+	H+	0	0
H+	OH-	1000000000	0
H+	CO3--	1000000000	0
H+	HCO3-	1000000000	0
H+	NH2COO-	1000000000	0
OH-	OH-	947.2529	0.063389
OH-	CO3--	766.66	-1.249
OH-	HCO3-	10000000000	0
OH-	NH2COO-	475.18	0.2241
CO3--	CO3--	588.32	-3.396
CO3--	HCO3-	238.89	-0.0164
CO3--	NH2COO-	4.4048	-14.17
HCO3-	HCO3-	403.66	0
HCO3-	NH2COO-	330.95	-6.589
NH2COO-	NH2COO-	1000	0

13. APPENDIX B: STANFORD UNIVERSITY REPORT

Attached below are

(1) Statement for work for Stanford University
(2) Project Status Report

STATEMENT OF WORK for BP1

Task 1: Preliminary design of the process integration architecture between Mixed-Salt and the Stanford heat integration Model (SRI to provide the preliminary test data and ASPEN data as needed).

Task 2: Stanford to provide results to SRI to use in quarterly reports and the continuation report to DOE.

Project Report

Report for Stanford portion of Mixed Salt project

September 21, 2014

Charles A. Kang

charlesakang@gmail.com, cakcak@stanford.edu

+1 650 479 6189, +1 650 387 3768

Summary

The Stanford heat integration model for auxiliary gas-fired CCS retrofits of coal-fired power stations has been modified to accommodate a simplified representation of the Mixed Salt process. Our modeling and optimization approach, which was originally developed for amine-based CO_2 capture processes, operates successfully with the Mixed Salt process. Preliminary optimization results indicate that the Mixed Salt process has superior performance in terms of both minimum capital investment and maximum net present value as compared to a reference amine system.

Objective

The objective of this work is to develop a modeling and optimization capability to determine optimal designs for CCS-enabled fossil-fuel-fired power generation in varying economic and policy environments. Because flexible response from thermal power stations is likely increase in value with time as renewable penetration increases, a major objective of this work will be to quantify the impact of variable operations on optimal plant design. For example, the modeling and optimization capability could be used to quantify the value of using CCS to modulate the output of a power station (e.g., export more power during certain hours and less during other hours by varying CO_2 capture rates) in response to changes in power demand and supply. The modeling and optimization capability will be useful for conducting technology and policy assessments. Ultimately the modeling and optimization capability may be used to inform the high-level design of low-carbon power generation systems to reduce the cost of electricity.

Background

Our work is principally concerned with modeling and optimization of CCS-enabled power generation from a systems perspective at the scale of a single power station. Our model represents the power station by sub-models for major system components, which in turn are based upon mass and energy balances with appropriate representation of thermodynamics and transport phenomena. The facility we have focused, shown in Figure 1, consists of an existing coal power station being retrofitted with CO_2 capture capability. In this system, CO_2 capture is powered by an integrated combined cycle gas turbine (CCGT) system. In this `auxiliary' concept, net electricity generation from the facility is increased instead of reduced as in `parasitic' configurations in which CO_2 capture is powered by steam diversion from the coal plant. One

effect of using the CCGT to supply heat for the CO_2 capture process is that we obtain operational flexibility that may not be achievable with many existing coal-fired power plants.
A major consideration in the design of such a facility is the interplay between capital cost and operating economics. Facility design and operations are inherently coupled: the valuation of a candidate facility design depends upon the way the facility is operated. This is particularly important for systems such as ours which have the ability to operate flexibly, because flexibility can be quite valuable. Therefore, we solve for optimal facility design and operations jointly. The specific objectives considered are the minimization of total capital requirement (TCR) and the maximization of net present value (NPV). Other objectives could be specified, but these objectives allow us to quantify the tradeoffs between systems with low upfront investment (which are generally simple and inflexible) and systems with high NPV (generally more complex and flexible). Through use of a bi-objective optimization procedure we generate the Pareto frontier, which consists of system designs and operating profiles that are

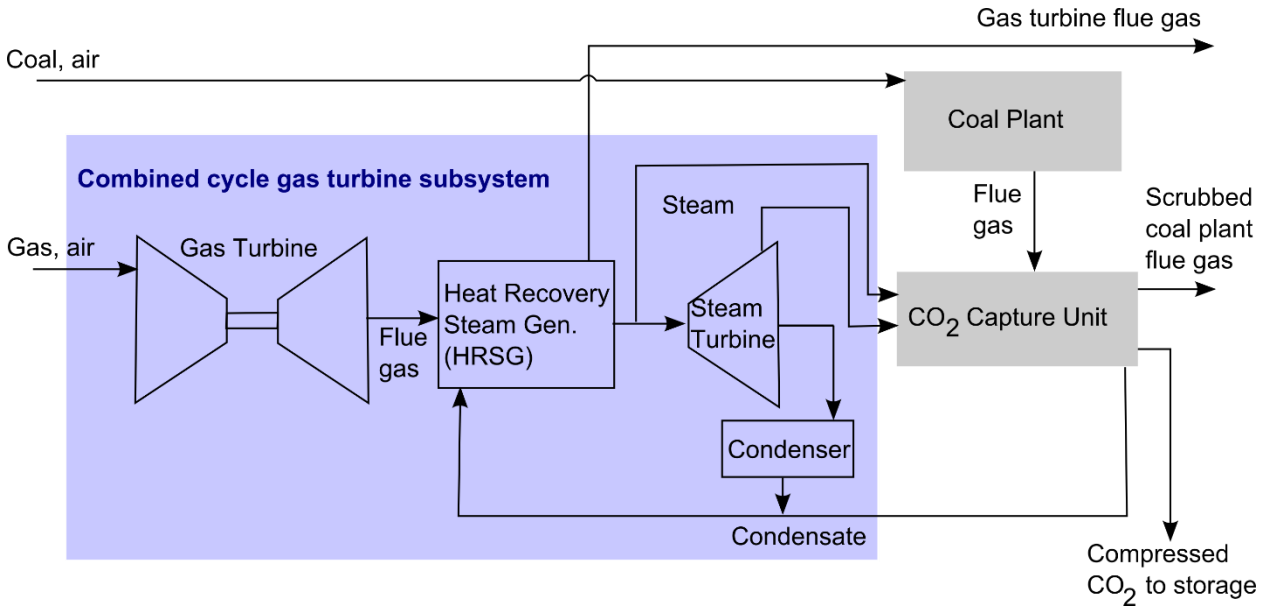

Figure 1: Schematic of overall CCS-enabled facility

The modeling component of our work includes economic considerations and has a major focus on engineering heat integration. Our facility burns coal and natural gas and produces (among other outputs) electric power and CO_2, some of which is captured. For a given system, the costs include capital investment, fuel, operations and maintenance, and corporate income tax. The revenue from a planned operating profile is calculated by evaluating system power sales over time with a given time-varying electricity price profile. The modeling effort has a major focus on heat integration because of the large demand for process heat in solvent-based CO_2 capture processes. Thus, a key component of this work is the optimization of the design and operation of the heat recovery steam generator (HRSG), which is a major CCGT component.
In our formulation we model and optimize the HRSG configuration, including the number, size, and arrangement of HRSG elements. This results in a challenging mixed-integer nonlinear

programming (MINLP) problem. We apply a bi-objective optimization framework to minimize the TCR and maximize the NPV of the overall system. The optimization algorithm evaluates many (~10^6) possible facility designs and operating profiles, systematically moving toward optimal solutions. The development of this modeling and optimization capability summarized in Kang et al. [1], and its companion Supplemental Material document [2].

We have extended this work to accommodate the Mixed Salt process by modifying the steam cycle model to produce process steam at multiple pressures. In its present state, the model represents CO_2 capture at a high level of abstraction. The energy demand is represented by specific heat duties for each steam temperature (e.g., 1.763 MJ at 130°C and 0.441 MJ steam at 160°C per kg CO_2 captured) and specific work duties (e.g., 175 kJ/kg CO_2 for compression). A single design decision variable is used for CO_2 capture capacity, and the capital cost of CO_2 capture is a function only of this one variable. Future work will include a more thorough representation of the process, depending upon data availability and quality.

Goals and milestones

Goal 1: Preliminary design of the process integration architecture between Mixed Salt and the Stanford heat integration model (SRI to provide the preliminary test data and ASPEN data as needed).

Goal 1 milestone: Perform modeling runs of heat integration model using preliminary model of Mixed Salt process. Milestone partially complete.

Goal 2: Optimization and testing of the Stanford heat integration model using richer representation of Mixed Salt process, subject to data availability and quality.

Goal 2 milestone: Perform modeling runs of heat integration model using rich model of Mixed Salt process and compare with results using amine process.

Preliminary Results

This section presents preliminary modeling and optimization results for auxiliary CCS retrofits of coal fired power plants using the Mixed Salt process. The primary focus is on the Pareto frontiers that indicate the optimal tradeoff between minimum total capital requirement (TCR) and maximum net present value (NPV). Results for the base case amine system are also presented for comparison purposes. We emphasize that these results are highly preliminary, and include large assumptions that have not yet been validated and may include subtle modeling discrepancies. As such, the results should be taken as indicative of general trends, but should not be quoted as robust conclusions.

The optimization is performed under the following assumptions and conditions:

- Capital cost of Mixed Salt system is the same as for amine system of same capacity (kg CO_2/s captured)
- All other economic parameters such as discount rates and escalation rates are the same between the two technologies (the mixed salt system does not have a higher cost of capital as might be associated with a newer, “riskier” technology)
    - Nominal discount rate is 11%
    - Escalation rate is 3.3%
- 2011 electricity, natural gas, and coal prices for West Texas were used
- Mixed salt energy requirements:
    - Regeneration steam high T: 0.441 MJ/kg CO_2 (steam at 6.18 bar, T_{sat} = 160°C)

  - Regeneration steam low T: 1.763 MJ/kg CO_2 (steam at 2.70 bar, T_{sat} = 130°C)
  - Pump and blower work: 40 kJ/kg CO_2
  - CO_2 compression work: 176 kJ/kg CO_2
- Amine energy requirements:
  - Regeneration steam: 3.68 MJ/kg CO_2 (steam at 3.00 bar, T_{sat} = 133.5°C)
  - Pump and blower work: 40 kJ/kg CO_2
  - CO_2 compression work: 335 kJ/kg CO_2

We note that the steam specifications for both processes assume a 10°C approach temperature within the reboiler. Further modeling assumptions and general background on the work are presented in references Kang et al. [1] and [2].

Figure 2 shows the Pareto frontiers of the Mixed Salt and amine processes together for comparison, while Figure 3 and Figure 4 show details on the Mixed Salt and amine Pareto frontiers separately. Each point on a Pareto frontier represents a system design, and the Pareto frontier taken as a whole identifies the optimal tradeoff between the two objectives of maximum NPV and minimum TCR – a decision maker deciding what facility to invest in would choose one point on the Pareto frontier, depending on the relative importance of the different objectives. In Figure 2 the best systems are "up" (maximum NPV) and "to the left" (minimum TCR). The Mixed Salt process performs better than amines in the domain studied here, as its Pareto frontier is uniformly above and to the left of the amine Pareto frontier. This means that, for any given capital investment level (TCR), greater NPV can be achieved by using a Mixed Salt system than by using an amine system, and conversely that any NPV level can be achieved using a Mixed Salt system for lower capital investment than by using an amine system.

The Mixed Salt system has lower minimum TCR because its lower parasitic energy requirement enables the construction of smaller CCGT system than is needed for an amine system. The Mixed Salt system has higher maximum NPV because its lower energy requirement enables more electricity sales from the auxiliary CCGT than for an amine system.

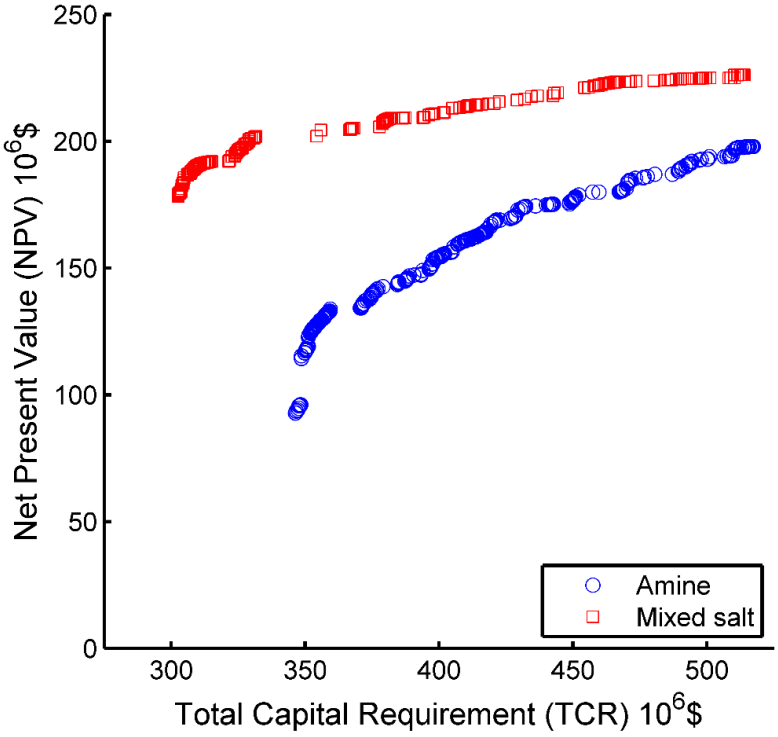

Figure 2: Preliminary comparison of Pareto-optimal mixed salt and amine systems

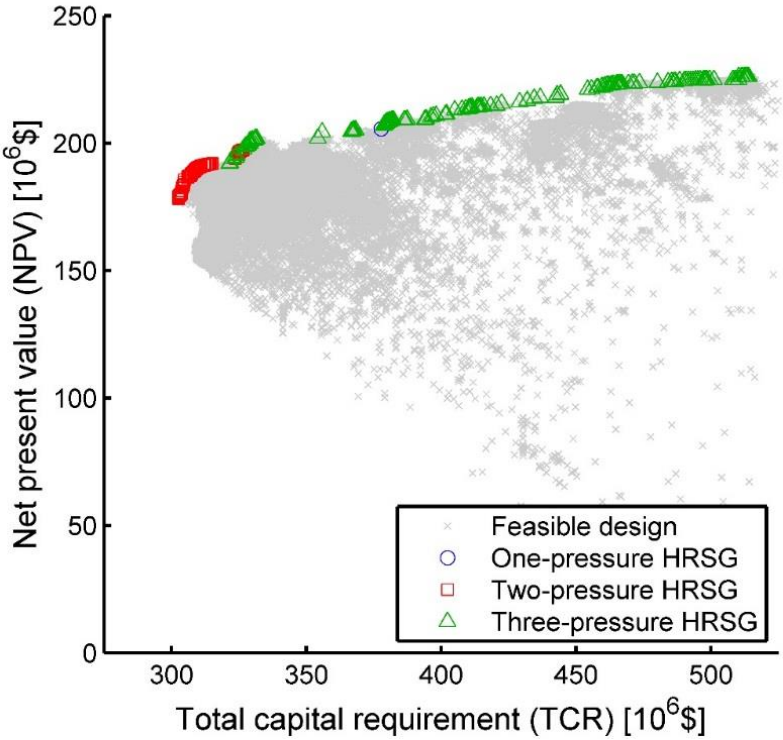

Figure 3: Detail of the mixed salt system Pareto frontier

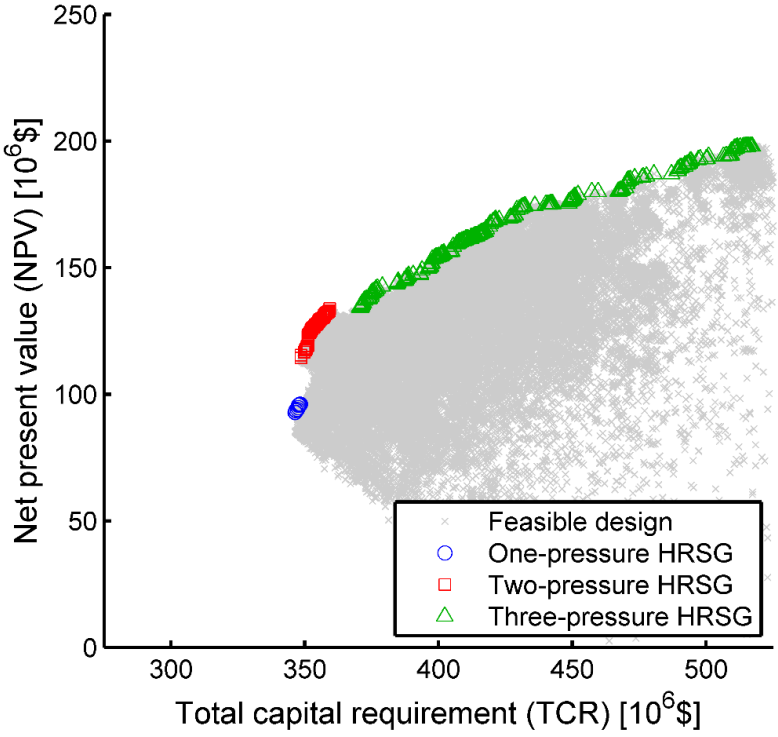

Figure 4: Detail of the amine system Pareto frontier

One major difference between the Mixed Salt and amine Pareto frontiers is that the mixed salt Pareto frontier has a shallower slope than the amine Pareto frontier. This indicates that there is lower economic improvement for increased capital investment with Mixed Salt than with amines; there is less "bang for the buck" of additional investment. This is a consequence of the lower energy requirement for the Mixed Salt process.

Another apparent difference between the optimal Mixed Salt and amine systems is that the minimum TCR mixed salt system appears to use a two-pressure HRSG as seen in Figure 2, not a one-pressure HRSG as seen in the amine system in Figure 3. This may indicate that high CCGT efficiency is more important for the Mixed Salt process than for the amine process, or may be a modeling artefact resulting from details of the way the steam cycle is modeled. Further investigation of this result is currently under way, and so this result may change or be made more robust with future modeling improvements.

References

[1] Kang, C.A., Brandt, A.R., Durlofsky, L.J. 2014. Optimizing heat integration in a flexible coal-natural gas power station with CO2 capture. Accepted pending minor revisions by *International Journal of Greenhouse Gas Control*.

[2] Kang, C.A., Brandt, A.R., Durlofsky, L.J. 2014. Supplemental Material (SM) for 'Optimizing heat integration in a flexible coal-natural gas power station with CO2 capture'. Supplementary material to be made available online with [1] in *International Journal of Greenhouse Gas Control*.

14. APPENDIX C: OLI SYSTEMS REPORT FOR BP1

Attached below are

(1) Statement for work for OLI Systems
(2) Project Status Report

Statement of Work_BP1

Task 1: Development of a comprehensive thermodynamic model for predicting phase equilibria and thermophysical properties for the system $K_2CO_3 – CO_2 – NH_3 – H_2O$. The model will be based on OLI Systems' Mixed-Solvent Electrolyte (MSE) framework. Appropriate parameters are already available for two key subsystems, i.e., $K_2CO_3 – CO_2– H_2O$ and $NH_3 – CO_2 – H_2O$. However, it will be necessary to analyze the behavior of the mixed system and develop appropriate parameters. (DOE funded).

Task 2: Analysis of test data from SRI to design the boundaries (T and P) for thermodynamic modeling and the preliminary process simulation design (OLI cost share).

Task 3: Based on the thermophysical properties obtained from the MSE model, a process flowsheet will be developed and process simulation will be performed using the Electrolyte Simulation Program (ESP). The process simulation with performed in two steps. In the first step, the absorber and regenerator will be modeled as equilibrium unit operations. In the second step, mass transfer effects will be introduced. For this purpose, OLI's mass transfer-based column algorithm will be used. The mass-transfer algorithm predicts the mass transfer coefficients on the basis of thermophysical properties obtained from the MSE model. The process simulation results will be verified and fine-tuned on the basis of SRI's process data (DOE funded).

Task 4: The process flow sheet will be transferred to Aspen+ (including the OLI Engine) so that other team members can conveniently perform the simulations in the future (OLI cost share).

Statement of Work_BP2

Task 5: Use SRI bench scale data to perform rate-based heat and mass transfer modeling (DOE funded)

Task 6: Optimize the model with field data to perform full scale plant heat and mass transfer modeling (DOE funded)

Task 7: Develop rate-based model for detailed mass balance and heat balance calculation for flue gas feed equivalent to a flue gas stream. The model will be developed and validated in ESP and then transferred to Aspen+ for use by other members of the team (OLI cost share).

Project report

Ronald D. Springer, Prodip Kundu and Andre Anderko
OLI Systems Inc.
September 20, 2014

Task 1. Thermodynamic model for the system $K_2CO_3 – CO_2 – NH_3 – H_2O$

Work was completed on the development of thermodynamic parameters for the system $K_2CO_3 – CO_2 – NH_3 – H_2O$. The thermodynamic modeling was performed using the Mixed-Solvent Electrolyte model (Wang et al., 2002, 2006, Springer et al., 2012). The thermodynamic model will be further used for the simulation of SRI's process.

First, the work was focused on revising existing parameters for the constituent subsystems NH_3-H_2O and NH_3-CO_2-H_2O. The reason for this revision was threefold:

(1) For the binary system NH_3 - H_2O, the previously developed model parameters did not reproduce derivative properties (especially caloric properties) as accurately as phase equilibria;

(2) For the ternary system $CO_2 – NH_3 – H_2O$, the phase behavior (in particular, the vapor pressures) was obscured by the effects of urea formation. While the formation of urea is important at appropriately high temperatures and pressures, it is kinetically inhibited at lower temperatures. Therefore, a model that treats the formation of urea on a purely thermodynamic basis deviates from experimental vapor pressure data at low temperatures.

(3) For the ternary system $CO_2 – NH_3 – H_2O$, not all relevant solid phases were originally included. In particular, the ammonium sesquicarbonate phase was missing.

There was no need to revise parameters for the subsystem $K_2CO_3 – CO_2 – H_2O$ because they were sufficiently accurate before the start of the project. After completing the revision of the NH_3-H_2O and NH_3-CO_2-H_2O subsystems, parameters were determined for the mixed system $K_2CO_3 – CO_2 – NH_3 – H_2O$. In the following section, we briefly describe the work on these systems.

$NH_3 – H_2O$ binary

In the first step, the MSE model parameters have been revised for the $NH_3 – H_2O$ binary. The parameter regressions were based on vapor-liquid equilibrium, caloric, density, and acid-base equilibrium data. The references to the literature sources are collected in the attached Excel file RefNH3CO2UreaK2CO3.xlsx. There is a large amount data in 159 sources (cf. the references labeled "NH3" in the attached spreadsheet). The speciation in this system has been reexamined and it has been determined that the model should include both the anhydrous form of ammonia, $NH_{3(aq)}$, and the hydrated form, NH_4OH, in addition to the NH_4^+ and OH^- ions. The hydrated form was not included in the previous version of the model. The hydration equilibrium between $NH_{3(aq)}$ and NH_4OH is important for maximizing the accuracy of the model at high concentrations of ammonia. Very good agreement with experimental data was obtained for temperatures ranging from -80°C to 300°C.

CO_2 - $NH_3 – H_2O$ ternary

After determining the parameters for the $NH_3 – H_2O$ binary system, experimental data for the $CO_2 – NH_3 – H_2O$ ternary have been regressed. Data from 158 literature sources have been collected (cf. the references labeled "NH3-CO2" in the attached spreadsheet). Due to its inherent chemical complexity, there are diverse and interrelated data sets for this system. They include:

(a) Solubility of ammonium bicarbonate in water
(b) Vapor pressure of ammonium carbamate. It should be noted that ammonium carbamate forms as a result of reaction between aqueous carbon dioxide and ammonia.
(c) Ammonium carbamate solubility in water
(d) Ammonium carbamate solubility in anhydrous ammonia
(e) Ionic equilibria in solution between aqueous NH_3 and CO_2, which leads to the formation of bicarbonate (HCO_3^-), carbonate (CO_3^{2-}), and carbamate ($NH_2CO_2^-$) ions.
(f) Ternary solubilities in the system $CO_2 – NH_3 – H_2O$, which include the precipitation of ammonium carbonate (both in its hydrated and anhydrous forms), ammonium bicarbonate, ammonium sesquicarbonate, and ammonium carbamate, which depends on the overall composition and temperature.
(g) Vapor-liquid equilibria in the system $CO_2 – NH_3 – H_2O$, which are influenced by the ionic equilibria. The vapor-liquid equilibrium data include both the total pressure and the partial pressures of ammonia and carbon dioxide.

All these data have been reproduced by the revised model.

Effects of urea

At appropriately high temperatures and pressures, conversion of ammonia and carbon dioxide to urea is observed. At such conditions, it is necessary to include the formation of urea together with all other ionic equilibria that are present in the $CO_2 – NH_3 – H_2O$ system. There are abundant experimental data in the literature for urea (cf. 135 references in the spreadsheet labeled "Urea") and for phase and chemical equilibria between urea, ammonia and carbon dioxide (cf. 160 references in the spreadsheet labeled "Urea-NH3-CO2".

To establish the parameters for urea and to ascertain the effect of urea on the phase behavior of the $CO_2 – NH_3 – H_2O$ system, the following data have been regressed:

(a) Vapor pressure of pure urea
(b) Solubility of urea in water
(c) Urea solubility in anhydrous ammonia
(d) Equilibrium conversion factors of CO_2 and NH_3 into urea as a function of NH_3 and CO_2 composition and temperature
(e) Equilibrium pressure that corresponds to the conversion of CO_2 and NH_3 into urea.

After regressing the urea parameters, they have been placed in a separate databank, which can be used for applications when the formation of urea can be anticipated. Thus, unlike in the previous version of the model, undue interference from urea formation will not be predicted at conditions at which the formation of urea is kinetically limited. Because of the inherent complexity of the $NH_3 – CO_2 – H_2O$ chemistry, the separate databank will also incorporate side products that accompany the formation of urea (i.e., isocyanic acid, cyanuric acid, and biuret).

The attached spreadsheet PredNH3CO2Urea.xlsx compares the results of thermodynamic modeling with experimental data for the subsystems described above.

Mixed system $K_2CO_3 – CO_2 – NH_3 – H_2O$

Data for the mixed system are less abundant than for the subsystems described above. 12 literature sources have been identified (cf. the references in the attached spreadsheet labeled as "NH3-K2CO3"). The main sources are listed in the following table, together with their ranges of conditions:

Reference	Data type	T range C	Concentration ranges, wt%			
			H_2O	K_2CO_3	$(NH_4)_2CO_3$	NH_3
Applebey and Leishman (1932)	LLE	0 - 25	49.55 – 72.14	2.72 - 47.13		2.52 – 32.07
Applebey and Leishman (1932)	SLE	0 - 25	0 - 65.21	0.16 - 51.72		0 - 99.84
Orelli (1940)	SLE	-30 - 19	1.5 - 83.14	0.3 - 34.1		1.7 - 98.2
Guyer et al. (1940)	SLE	-30 - 19	19.42 - 77.67	0.99 - 34.21		1.97 - 79.21
Belyaev and Grigoreva (1967)	SLE	15	41.16 - 54.88	0 - 52	0 - 44	0.84 - 1.12

Although multiple sources of data are available, they are limited to low temperatures. Thus, the empirical database for the mixed system is not nearly as comprehensive as for the subsystems containing NH_3, CO_2, and H_2O as independent components. Still, the available data reveal unusual phase behavior of the mixed system. Specifically, this system shows liquid-liquid phase splitting over a limited range of concentrations. Although neither the K_2CO_3-H_2O nor the NH_3-H_2O binaries show phase splitting, the addition of ammonia to aqueous K_2CO_3 induces the formation of two liquid phases over a relatively narrow range of NH_3 concentrations. This is illustrated in Figure 1, which shows the solubility of K_2CO_3 as a function of ammonia in the solvent. The gap in the solubility curves corresponds to the location of the liquid-liquid miscibility gap. It is clear that the miscibility gap is due to the presence of ammonia and not ammonium ions. This is demonstrated in Figure 2, which shows solid-liquid equilibria in the system $K_2CO_3 – (NH_4)_2SO_4 – H_2O$. In this case, the solubility curve has a "normal" shape with double salt phases but without phase splitting. The calculated and experimental compositions of the two liquid phases in the $K_2CO_3 – NH_3 – H_2O$ system are compared in Figure 3 using a parity plot. While there is a noticeable scattering, the calculations are consistent with the data. The scattering is mostly due to the fact that most of the data are quite old and are not always consistent with the more precise data for various subsystems of the NH_3-CO_2-H_2O system (e.g., for the solubility of $(NH_4)_2CO_3$).

While the agreement with the experimental data is generally satisfactory for the mixed system, it would be beneficial to verify the model at higher temperatures, at which no experimental data are available.

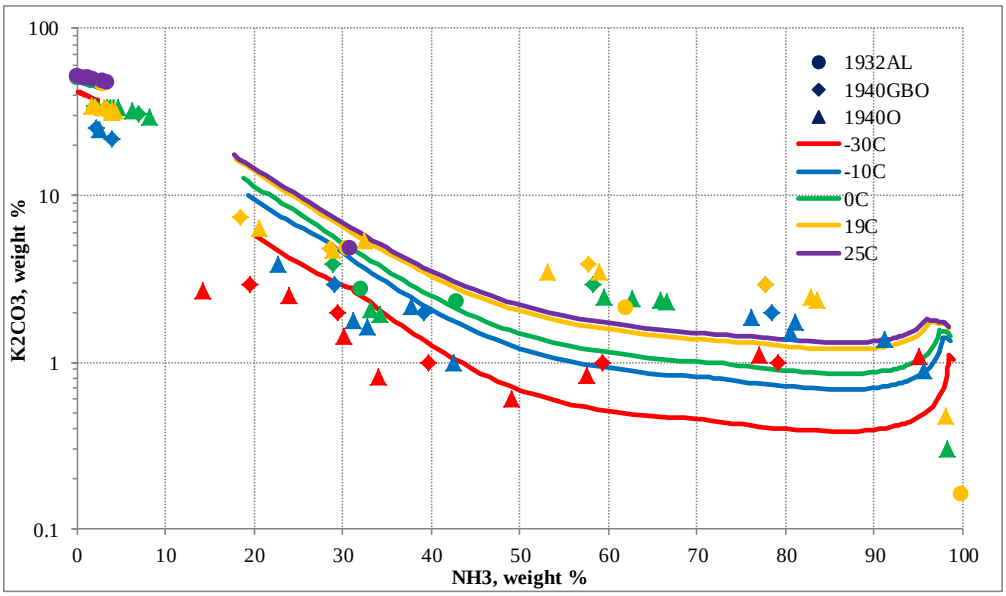

Figure 1. Calculated and experimental solid-liquid equilibria in the mixed system K_2CO_3 – NH_3 – H_2O.

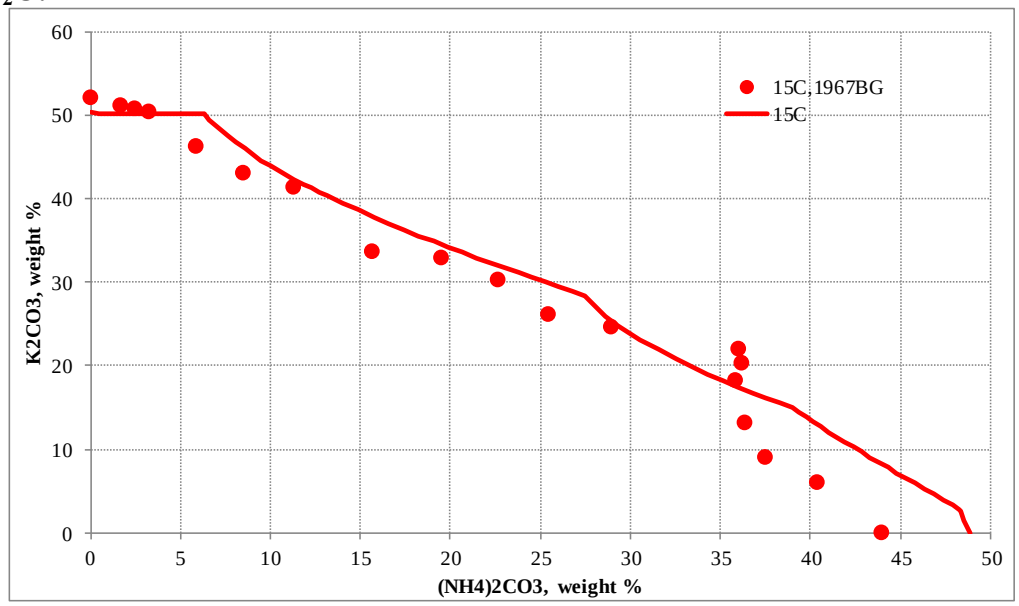

Figure 2. Calculated and experimental solid-liquid equilibria in the system K_2CO_3 – $(NH_4)_2CO_3$ – H_2O

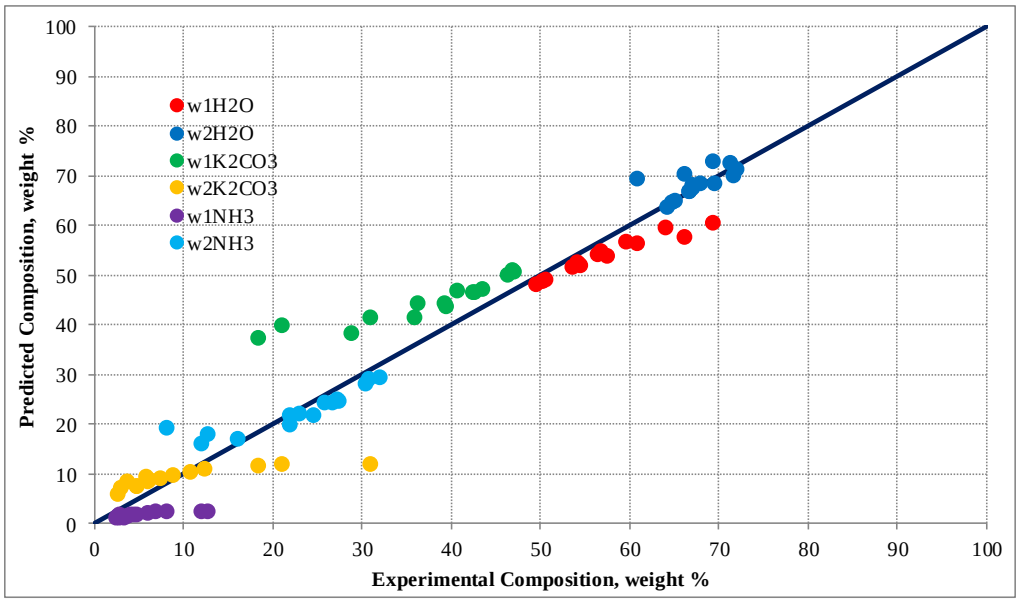

Figure 3. Comparison of calculated and experimental compositions of coexisting liquid phases in the system K_2CO_3 – NH_3 – H_2O.

The attached spreadsheet PredNH3KCO3.xlsx compares the calculated results with experimental data for the system K_2CO_3 – CO_2 – NH_3 – H_2O.
This completes Task 1, i.e., the thermodynamic analysis of the system K_2CO_3 – CO_2 – NH_3 – H_2O. In the next reporting period, the new thermodynamic parameters will be integrated with the OLI software and used for process simulation (Task 3).

Task 2. Analysis of test data from SRI
A document with process data has been obtained from SRI and has been analyzed as a foundation for creating a process flowsheet model.

Task 3. Process flowsheet model using the Electrolyte Simulation Program (ESP)
A process flowsheet was developed based on the preliminary information provided by SRI, and process simulation was performed using the Electrolyte Simulation Program (ESP). The current version of OLI Systems' Mixed-Solvent Electrolyte (MSE) model was used for the simulation while awaiting the completion of Task 1. The chemistry model for K_2CO_3-NH_3-H_2O-CO_2 system shows existence of urea, isocyanic acid, cyanuric acid, and biuret in the equilibrium equations, which were selectively removed from the chemistry model for preliminary study. The process flowsheet mainly consists of a dual-absorber section to selectively absorb CO_2 from the flue gas and a regenerator unit to desorb CO_2 and recycle the lean solution back to absorber. In the first step, the absorber and regenerator was modeled as equilibrium unit operations. A flue gas flow rate of 200 scfm with CO_2 concentration of 15% was used. Most of the process parameters were taken from SRI report to OLI and personal communications, however, assumptions were made wherever limited data were available (for example, pump around flows). The process flow diagram is shown in Figure 4. This simulation study will be continued after completion of the thermodynamic model of K_2CO_3-NH_3-H_2O-CO_2 system and followed by the validation of the process flowsheet against the process data provided by SRI.

Supplementary Information

The following spreadsheets are provided as attachments to this report:

RefNH3CO2UreaK2CO3.xlsx – the full collection of literature sources that were used in the thermodynamic analysis

PredNH3CO2Urea.xlsx – comparison of calculated results and experimental data for the subsystems that do not involve K_2CO_3

PredNH3KCO3.xlsx – comparison of calculated results and experimental data for the mixed system K_2CO_3-NH_3-H_2O-CO_2

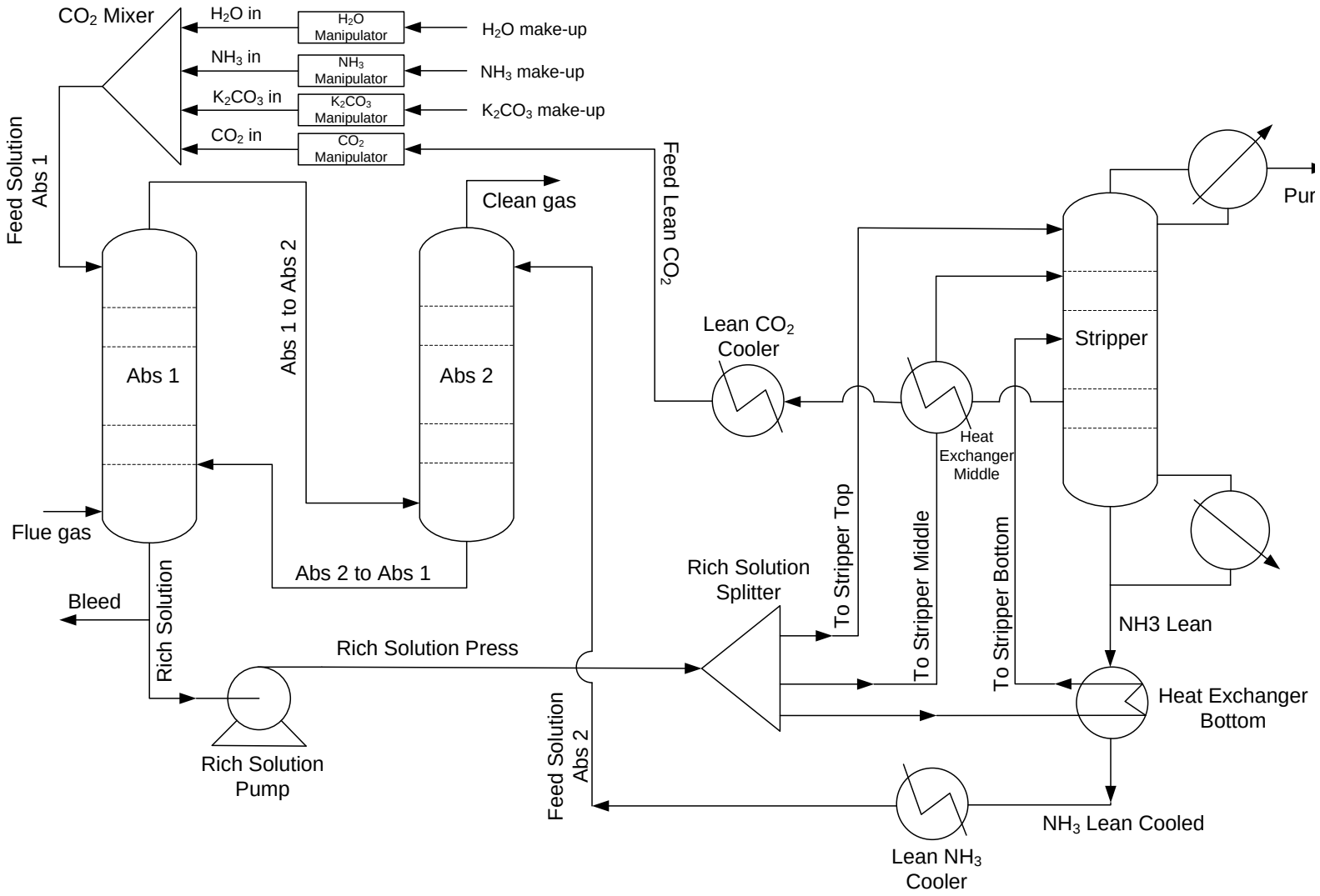

Figure 4: Process flow diagram for SRI Mixed-Salt Technology

References to the model

Wang, P.; Anderko, A.; Young, R. D., A Speciation-Based Model for Mixed-Solvent Electrolyte Systems. *Fluid Phase Equilibria* **2002,** 203, (1-2), 141-176.

Wang, P.; Anderko, A.; Springer, R. D.; Young, R. D., Modeling Phase Equilibria and Speciation in Mixed-Solvent Electrolyte Systems: II. Liquid-Liquid Equilibria and Properties of Associating Electrolyte Solutions. *Journal of Molecular Liquids* **2006,** 125, (1), 37-44.

Springer, R. D.; Wang, Z.; Anderko, A.; Wang, P.; Felmy, A. R., A Thermodynamic Model for Predicting Mineral Reactivity in Supercritical Carbon Dioxide: I. Phase Behavior of Carbon Dioxide – Water – Chloride Salt Systems Across the H_2O-Rich to the CO_2-Rich Regions *Chemical Geology* **2012,** 322-323, 151-171.